CORROSION PROCESSES AND MECHANISMS IN THE PRESENCE OF MONOETHYLENE GLYCOL (MEG)

Ikechukwu Cyril Ivonye

Submitted in accordance with the requirements for the degree of

Doctor of Philosophy

The University of Leeds

Institute of Engineering, Thermofluids, Surfaces and Interfaces

School of Mechanical Engineering

July, 2014

The candidate confirms that the work submitted is his/her own, except where work which has formed part of jointly-authored publications has been included. The contribution of the candidate and the other authors to this work has been explicitly indicated below. The candidate confirms that appropriate credit has been given within the thesis where reference has been made to the work of others.

In all the papers and presentations listed below, the primary author completed all the experimental data, paper drafting and presentation slide. All authors contributed to proof reading of the papers and presentation with advised before publication and presentation.

This copy has been supplied on the understanding that it is copyright material and that no quotation from the thesis may be published without proper acknowledgement.

THESIS RELATED PUBLICATIONS AND PRESENTATIONS

Journal Paper:

Ikechukwu Ivonye, Chun Wang, Xinming Hu, Anne Neville, *The effect of Monoethylene Glycol (MEG) and Corrosion Inhibitors in the corrosion of Carbon steel, Corrosion Journal (Accepted)*

Conference Paper:

Ikechukwu Ivonye, Chun Wang, Xinming Hu, Anne Neville, (2013) *Corrosion Study of Carbon Steel in presence of Monoethylene Glycol (MEG) and Corrosion Inhibitors in Acid.* NACE International Conference, Orlando Florida, USA, March 17-21, 2013, Paper No. 2349.

DEDICATION

I dedicate this work in loving memory of my late father Ezechiel Michael Ivonye who encouraged and supported me in this work from the beginning but could not see it through to the end.

ACKNOWLEDGEMENTS

thank my two boys Michael Uchenna Ivonye and Melvyn Nnamdi Ivonye for all their own contribution.

ABSTRACT

Carbon steel pipelines are employed in the oil and gas industry for long distance multiphase transportation. The integrity of these pipelines is critical to oil and gas production. Transportation of wet natural gas using carbon steel pipelines from source to processing plant may lead to corrosion, hydrate formation and even scale formation. To prevent hydrate formation MonoEthylene Glycol (MEG) is pumped through the pipeline. Corrosion inhibitors and other corrosion prevention methods may be employed to reduce corrosion to manageable and acceptable levels.

In this study the corrosion inhibition properties of MEG were investigated at both low and high temperature conditions. The reduction of carbon steel X65 corrosion in the presence of MEG alone and 1% NaCl alone at low temperature of 20°C was in line with previous studies. At high temperature of 80°C, the corrosion rate of the carbon steel in the presence of MEG tends to increase. Thus the reduction of the corrosion rate of carbon steel in the presence of MEG can be underestimated.

The increase in the corrosion rate of carbon steel in the presence of MEG at high temperature led to the search for the mechanism by which MEG reduces corrosion. The adsorption process was studied using Fourier transform infra-red spectroscopy (FTIR). Further determination of the adsorption isotherm properties and behaviour of MEG on the corrosion of carbon steel was recorded through experimentation. The results were used to determine the type of adsorption that occurs in the presence of MEG.

The corrosion rate of carbon steel in the presence of MEG is improved by deployment of chemical inhibitors to reach a minimal acceptable rate. This study investigated the use of two types of commercially-available inhibitors green (inhibitor 2) and non-green inhibitor (inhibitor 1) for reduction of the corrosion rate. The effects of the two inhibitors alone on the corrosion of carbon steel at both high and low temperatures were first examined. This enabled an assessment of the inhibitor in the presence of MEG.

A combination of the MEG and inhibitor was tested at both low and high concentrations. The influence on MEG on the inhibitor performance was determined.

Conditions necessary for the formation of protective iron carbonate were determined and used for pre-corrosion. The influence of iron carbonate on the corrosion of carbon steel was determined.

Pre-corroded carbon steel was used to assess the influence of MEG in the presence of iron carbonate. Further test on the pre-corroded carbon steel in the presence of MEG and inhibitor was performed to assess the influence of the inhibitor and MEG on iron carbonate scale.

TABLE OF CONTENTS

Contents

LIST OF FIGURES

LIST OF TABLES

Chapter 1. INTRODUCTION AND RESEARCH BACKGROUND

1.1. Research background

The demand for oil and gas as a source of energy has risen with more offshore wells being explored and developed. The consumption of oil and gas has been predicted to increase by a combined total of 2.7% per year from 2012 to 2035 [1]. Most of the oil and gas needs to be transported from the source to the processing plant onshore. Figure 1-1 shows the actual and predicted global energy demand and consumption from 1965 to 2035.
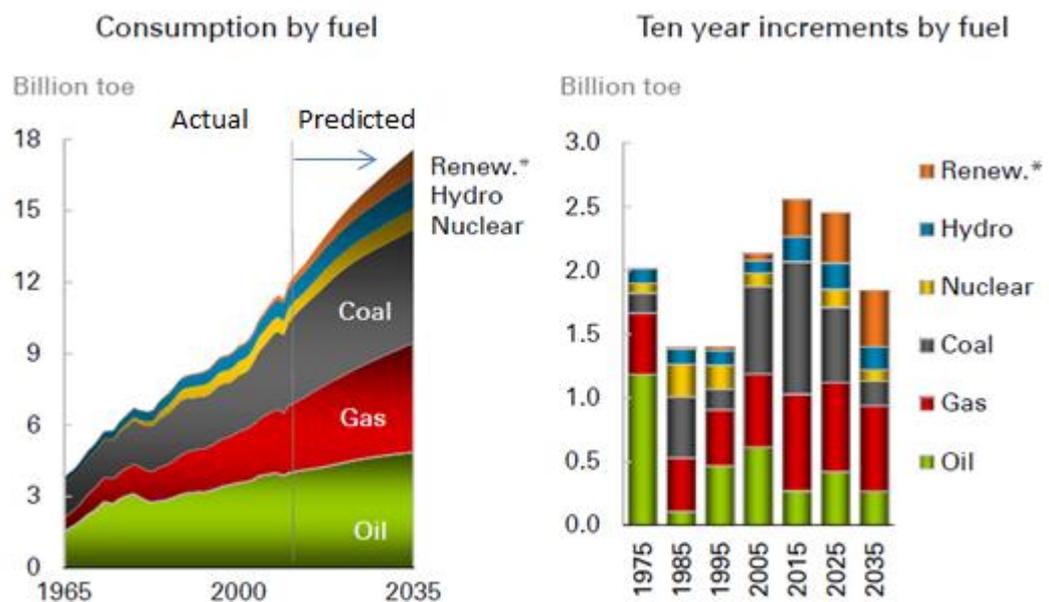
Figure 1-1: Actual and predicted growth rate for global energy demand/consumption from 1965 to 2035 [1].

The oil and gas industry is dependent on the use of carbon steel pipelines in the transportation of their products from the deep sea to onshore. The use of carbon steel is common due to their mechanical properties, cost and availability. Carbon steels require management strategies to prevent corrosion. They do not have high resistance to corrosion as compared to their counter parts Corrosion Resistant Alloys

(CRA). The CRAs on the other hand are often prohibitively expensive for long distance pipelines due to high cost and availability. The use of carbon steel implies that corrosion has to be prevented to maintain the integrity of the pipeline.

The natural gas produced from offshore oil and gas wells at high temperature and pressure may contain CO_2 and salt water in the form of produced water, condensed water or/and formation water. Due to cost and space, the process of removal of water and CO_2 are often done at an onshore processing plant away from the offshore production platform. This involves multiphase transportation using long carbon steel pipelines under high pressures. The transported natural gas may release some of the water content by condensation as the temperature drops along the pipeline. This may lead to the formation of hydrates along the pipeline which can possibly reduce the flow pressure or block the pipeline. Corrosion may also occur along the pipeline due to the water content. Prevention and mitigation of hydrates and corrosion become necessary in order to maintain the integrity of the pipeline. Most natural gas pipelines employ MonoEthylene Glycol (MEG) for the prevention of hydrates. It is a thermodynamic hydrate inhibitor compared to the kinetic hydrate inhibitor (KHI). Thermodynamic hydrate inhibitor works by reducing the minimum temperature at which hydrates can form along the pipeline while KHI works by reducing the time for hydrates to form and to grow which may not be suitable for very long distance pipeline[2].

MEG does have an effect in reducing corrosion on carbon steel but needs to be supplemented for most application. Corrosion of the carbon steel pipeline can be controlled by the use of the pH stabilization method or by the use of organic corrosion inhibitor. pH stabilization involves the addition of NaOH, $NaHCO_3$ or any other pH buffer to increase the pH of the pipeline system from 6.5 to 7.5 [3]. This will reduce the corrosion rate in the presence of MEG to the required minimum rate. Corrosion products, mainly iron carbonate, may also form at this pH level and conditions to reduce the corrosion rate further. A schematic description of multiphase transportation of natural gas pipeline is described in Figure 1-2.

In some situations, the formation of iron carbonate or any other scale for example where there is formation water passing through the pipeline may make it unfavourable for the use of the pH stabilization method. This makes it necessary to

find an alternative way to control the corrosion of the pipeline without the formation of undesirable scale. The use of organic corrosion inhibitors becomes necessary to avoid the formation of undesirable scaling. Organic corrosion inhibitors must be compatible with MEG in order to function effectively and efficiently in the presence of MEG. This is one of the focuses of this study.
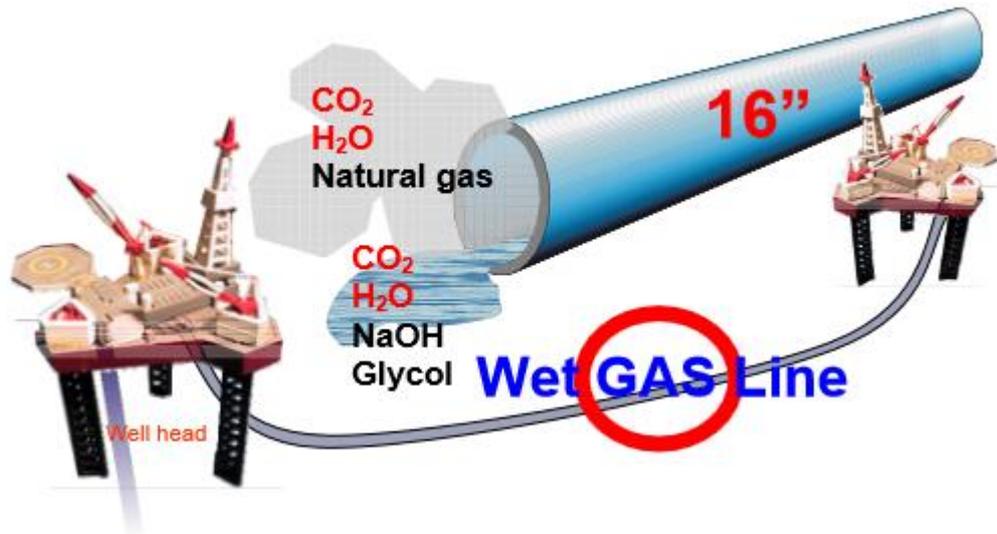
Figure 1-2 : Schematic description of multiphase transportation of natural gas pipeline [3].

The study is therefore aimed to assess the corrosion of carbon steel in the presence of MonoEthylene Glycol at different concentrations and the possible effect that may occur at both high and low temperature.

The study will also explore the use of MEG further to determine the mechanisms involved in the prevention of corrosion. This will be used to improve the corrosion management process in the presence of MEG effectively.

1.2. The important and impact of corrosion

The significant and importance of corrosion can be view from three main directions namely safety, conservation and economies [4]. Safety issues are one reason why corrosion is very important. Corrosion can compromise the integrity of the equipment and facility which can lead to failures and collapse. This situation will

3

put the lives and safety of people working with the equipment and even those living or doing business around the place in danger. Conservation is also important in the study of corrosion as corrosion tend to destroy oil and gas facilities and also the surrounding environment. For example damage to the sea may change the natural state of some wide life living in the sea and may lead to their death.

Economics is one of the major reasons why corrosion is very important. Corrosion widely leads to material loss and degradation which can cause massive damage to equipment and facilities. This will lead to economic losses that have direct and indirect impacts. Direct impacts are usually the cost of replacing the corroded equipment or parts such as replacing of corroded oil and gas carbon steel pipeline and repainting of offshore production platforms.

Results released by Koch et al [5] showed that the total loss due to corrosion in the USA is estimated to be approximately $276 billion annually in the USA. It has also been estimated that about a quarter of the cost could be reduced if new corrosion technology was available previously. Analysis of the direct losses due to corrosion based on five major sectors is given in Figure 1-3
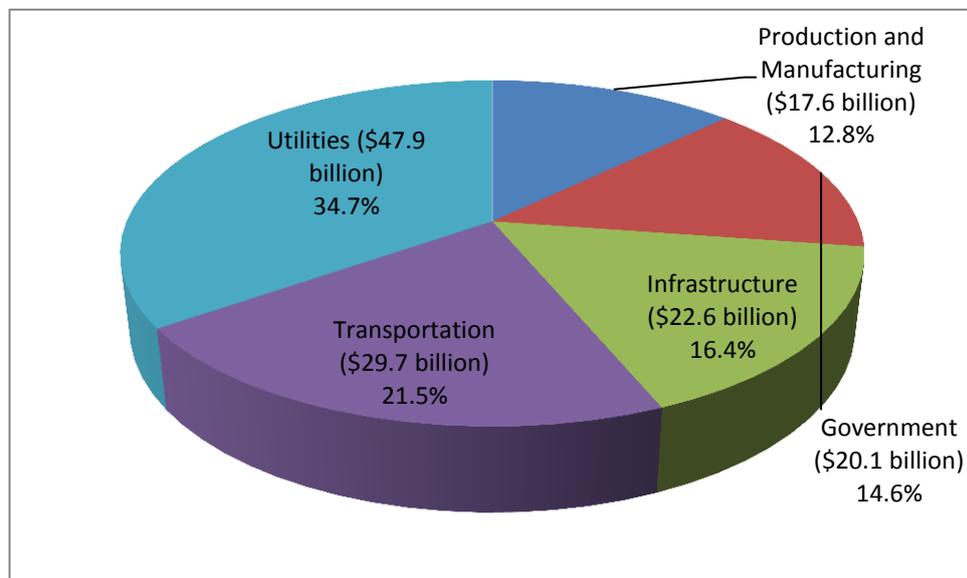
Figure 1-3 : Analysis of the direct losses due to corrosion based on five major sectors [5].

Indirect losses includes plant shutdown which normally lead to the loss of revenue from the plant while repairs are going on. This cost in some situations may be much higher than the direct cost of replacing the corroded part. An example is seen in the replacement of a corroded natural gas carbon steel transmission pipeline requiring shutdown which may cost less than the actual money loss during shutdown of the transmission line. Other indirect losses are loss of efficiency, contamination of product from corrosion products and overdesign of equipment to accommodate material loss due to corrosion of pipeline. This overdesign is common in carbon steel pipeline where pipeline with larger pipe thickness is used to avoid unexpected or worst case corrosion damage which may not be case for real field operations.

In the oil and gas industry corrosion is very significant as most of the oil and gas are sourced from remote and offshore areas and transported to process plant and consumers using numerous oil and gas equipment and facilities. The production process and multiphase transportation of the oil and gas can lead to corrosion on the metallic parts of the equipment and facilities. The annual cost of corrosion in major sectors of USA oil and gas industry is shown in Table 1-1

Table 1-1 : Annual corrosion costs in major sectors of USA oil and gas industry [5, 6].

Sector	Annual cost of corrosion in US (Billion US Dollars)
Production*	1,372
Transmission-pipeline	6,973
Transportation-Tanker**	2,734
Storage	7,000
Refining	3,692
Distribution	5,000
Special	Not Known
* Only for cost of corrosion for production from conventional sources	
** World Total	

In Alberta, Canada the cause of production pipeline failures has been given in Figure 1-4. The analysis shows that internal corrosion and external corrosion were the major cause of production pipeline failure. Internal corrosion was the major cause of failure in all. This makes it necessary to research into the mechanisms of internal corrosion to identify newer and better ways to prevent and reduce internal corrosion.
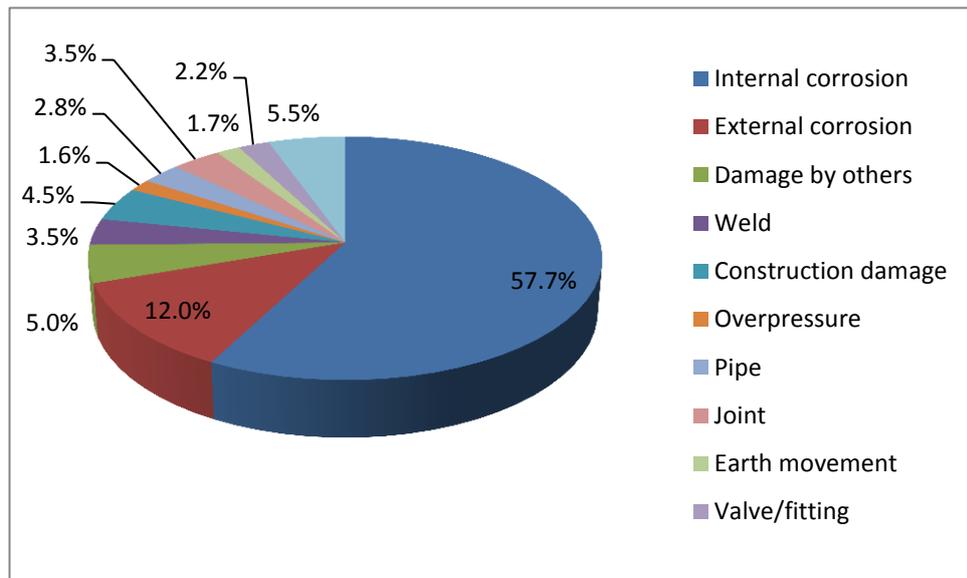
Figure 1-4 : Alberta, Canada production pipeline failure data for 1980-2005 [6, 7]

1.3. Objectives

The use of Monoethylene glycol (MEG) in the prevention of hydrate formation is a common practice in most offshore natural gas pipelines. This is mainly due to the fact that MEG is a thermodynamic hydrate inhibitor and stops the initiation of hydrate formation even at the very lowest temperatures encountered in the oil and gas sector. The use of MEG also helps prevent corrosion of the pipeline. This additional role of MEG has been studied at low temperature with little study at high temperature. MEG is normally introduced at high temperature where the carbon steel pipeline temperature may be up to 80°C in some cases. The exact mechanisms need to be established further to determine ways of improving the corrosion inhibition of MEG. Studies have shown reduction in efficiency of organic corrosion inhibitors in a MEG system. The effect and role of pH stabilizers also needs to be

studied further to determine their function as a sole mechanism of reducing corrosion in the presence of MEG and formation of the iron carbonate film. The role of iron carbonate films in further prevention of corrosion with or without MEG needs to be understood.

The objectives of this project are described briefly as follows

1. To determine the corrosion rates and mechanism of carbon steel in the presence of MonoEthylene Glycol (MEG) in both high and low temperatures taking into consideration the effect of concentration.

2. To evaluate the performance of two organic corrosion inhibitors to serve as the control experiment for the study.

3. To evaluate the compatibility of the organic corrosion inhibitor and MEG; how much does MEG affect corrosion inhibitor performance?

4. To assess the role of iron carbonate films in the presence of MEG; to understand how the films affect corrosion rates and mechanisms

5. To evaluate the effect of MEG and organic corrosion inhibitors on the reduction of corrosion rate in the presence of iron carbonate scale (i.e. pre-corroded carbon steel).

1.4. Statement of contribution to literature

The thesis contributes to the existing literature by determining the rates and mechanisms of corrosion in the presence of MEG at high temperature. The work studies the mechanisms of MEG in reducing the corrosion rate in carbon steel and presents novel aspects to add to the current understanding. Determination of the adsorption properties of MEG in this study showed physisorption as the mechanism by which MEG interacts with the carbon steel surface

The study also contributes to the understanding of how inhibitors can have synergistic effects associated with MEG in preventing corrosion. The synergistic and antagonistic effects of using different types of inhibitor with MEG are

highlighted. The study identifies possible issues that may occur in the use of newly formulated inhibitors at very high temperature.

The study also contributes to the knowledge of iron carbonate scale formation and its protectiveness against general corrosion of the carbon steel. The formation of under-scale corrosion which may form under the corrosion product is highlighted.

Finally the contribution of MEG in the formation and growth of iron carbonate scale on the carbon steel is presented with evidence that MEG does not encourage the formation of iron carbonate crystals at low temperature but rather encourages it at high temperature. It also demonstrates the effect of iron carbonate scale on the performance of MEG and inhibitor with possible contribution from each.

1.5. Structure of thesis

The structure layout of this thesis is divided as follows

- Chapter 1 gave the research background and the reasons and objective of the studies. It also highlights the contribution of the thesis to literature.
- Chapter 2 presented the fundamental principles of corrosion. This includes definition of corrosion and the thermodynamics of corrosion. It also identified the electrochemical reactions of corrosion. The electrochemical techniques employed in the test such as Direct current (DC) measurement and Alternating Current (AC) measurement was also described.
- Chapter 3 reviewed the literature of studies on relevant oil field corrosion in CO_2 environments. It also assessed the literature on MEG and corrosion inhibitors and possible problem that may have occurred with the use of MEG in details.
- Chapter 4, the experimental set up which described the experimental methods, test materials and test composition. It also showed the test procedures for all the experiments performed on this test. The surface analysis employed in this test was described in this chapter. The test equipment used in test was also described.

- Chapter 5 presented the results of corrosion assessment in the presence of MEG alone. Surface analysis to augment the electrochemical information was employed in this the post-analysis of the test. The determination of the adsorption properties of MEG and its mechanism in reduction of corrosion of carbon steel was also presented here.

- Chapter 6, presented results for experiments involving the two organic corrosion inhibitors employed in this study. The corrosion rate of the carbon steel in the presence of the corrosion inhibitors was determined. Here the comparison of the two inhibitors was made. Post surface analysis results to characterize the inhibitors were also described.

- Chapter 7 presented the result of the tests in the presence of MEG and the inhibitors. The result described the compatibility of MEG and the inhibitor. Surface analysis was also employed to support the result of the electrochemical test.

- Chapter 8 described the results on formation of iron carbonate on carbon steel surface (pre-corrosion). The conditions for a protective film to form were also described. Surface analysis was used to describe the corrosion of carbon steel in the presence of the iron carbonate scale.

- Chapter 9 described the result of pre-corroded carbon steel in the presence of MEG and in the presence of MEG and inhibitor. The compatibility of the MEG and MEG plus inhibitor was presented. Some corrosion aspects were described fully by the surface analysis.

- Chapter 10 is the general discussion with regard to the results from all the experiment.

- Chapter 11 gave the conclusion of the results and studies of this work. It also highlighted other area for further studies.

Chapter 2. PRINCIPLES AND THEORY OF CORROSION

2.1. Definition of corrosion

Corrosion may simply be defined a as chemical or electrochemical reaction of a metal with its environment which in most cases causes a deterioration or destruction of the material e.g. the rusting of iron [4]. In defining corrosion, the definition technically restricts corrosion to metals only. Non-metals do not corrode e.g. plastics are said to be degraded and not corroded. In most cases corrosion may be accompanied by physical process such as erosion as erosion-corrosion [4, 8]. Figure 2-1 shows an example of a metal that has corroded.

Figure 2-1 : Image of an offshore oil and gas pipe showing degradation due to corrosion [9].

There are two major types of corrosion namely wet/aqueous corrosion and dry corrosion. Wet/aqueous corrosion involves the corrosion process that occurs in the presence of moisture. This moisture could be in the form of water, steam or condensed water. Dry corrosion on the other hand involves the degradation of the metal when it comes in contact with an oxidizing gas at a very high temperature where moisture is likely not present. The process occurs like the wet/aqueous

corrosion but does not involve moisture. In the downstream oil and gas sector, most of the corrosion problems involve metal corrosion in the presence of moisture. Bearing this in mind, this project will deal with corrosion processes in the presence of moisture (i.e. Wet/Aqueous corrosion).

2.1.1. The corrosion cell and electrode definition

Wet/aqueous corrosion is an electrochemical reaction that involves a corrosion cell. The principal behind the electrochemistry was described by Michael Faraday in the early nineteenth century. Corrosion cell consist of four parts [10]. The parts are made up of two different electrodes called anode and cathode. The two electrodes are both inserted or are in contact with an electrolyte or an aqueous medium which serves as a conductive path for the ions from the electrochemical reaction. The corrosion cell is complete when there is an electrical connection between the two electrodes [10]. This can be achieved using a low resistance metal or wire to connect from one electrode to another. The removal of any of the parts from the corrosion cell will make corrosion not to occur. However local corrosion may still occur on the anode if the anode has some impurities. This impurities will establish a local-action cells that will lead to a slow corrosion reaction on the surface of the anode [4]. A schematic diagram showing the four parts of a corrosion cell is shown in Figure 2-2. When the cell is closed, the anode corrodes and Cations migrate to the cathode while the Anions migrate to the anode to complete the corrosion reaction.
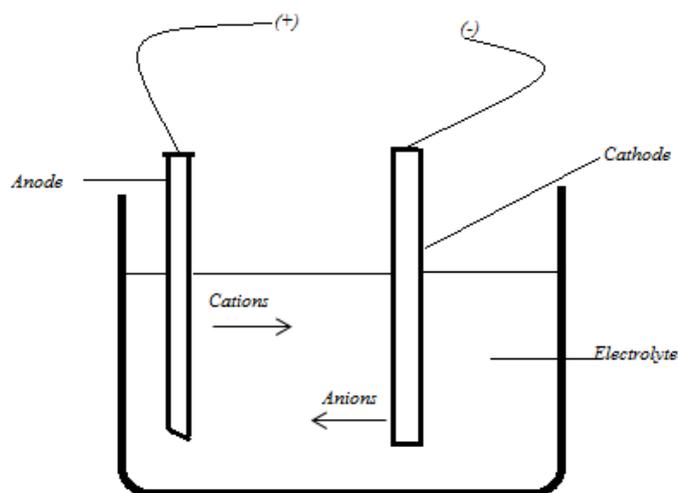
Figure 2-2 : Schematic example of an electrochemical corrosion cell.

The anode is the positive electrode where electrons move away from the cell. This is also where the oxidation reactions take place. Anions which are negative charge ions drift from the cathode towards the anode.

The cathode is the negative electrode where electrons enter the cells. This is also where the reduction reactions take place. Cations which are positive charge ions moves from the anode to the cathode.

2.1.2. Electrochemistry of aqueous corrosion

In our environment, water is always available naturally. The existence of water in our environment makes metals such as iron susceptible to corrosion. Aqueous corrosion involves the production and consumption of electron from the anodic and cathodic reactions. It is a chemical and electrochemical process that involves charge and mass transfer. The dissolution of metals in an aqueous medium causes corrosion. The corrosion can also be form by the production of solid, liquid, or gaseous non-metallic film on the surface of the metal.

If a metal is in contact with a solution, there exist on the surface local sites which are opposite in polarity. These sites forms local anodic and cathodic region at the surface of the metal and liquid that results in the flow of electrons. This normally happens instantaneously in most metals and will result in corrosion of the metal. The flow of electron occurs by the dissolution of the metal in the solution. In process where the local anodic and cathodic site does not happen instantaneously, corrosion does not occur. The process of metal dissolution due to the loss of electron on the metal surfaces is illustrated in Figure 2-3.
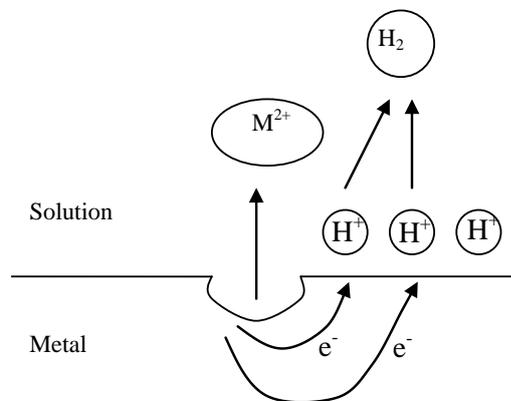
Figure 2-3 : Diagram showing metal dissolution in a solution liberating electron[8].

The process of metal dissolution involves the metal reacting with the species in its environment. This normally produces electrons that need to be consumed to maintain the neutrality of the process. The metal itself forms positive ions. The process is described below

$$M \rightarrow M^{n+} + ne^-$$
<div align="right">2-1</div>

The above process is an oxidation process and needs a reduction process to establish neutrality of the whole process. The reduction process involves one of the following processes which are dependent on the environment and species concentration. This reduction process is the cathodic process which consumes the electron produced at the anodic sites.

The types of reduction process that can follow are

- The liberation of hydrogen at the surface of the metal

$$2H^+ + 2e^- \rightarrow H_2$$
<div align="right">2-2</div>

(This occurs in an acid environment where the pH is less than 7)

$$2H_2O + 2e^- \rightarrow H_2 + 2OH^-$$
<div align="right">2-3</div>

(This occurs in environment with the pH 7 or more that is neutral or alkaline medium.)

- The displacement reaction

$$M^{n+} + ne^- \rightarrow M$$
<div align="right">2-4</div>

Or

$$M^{n+} + ne^- \rightarrow M^{(n-1)+}$$
<div align="right">2-5</div>

- The reduction of dissolved oxygen in the solution

$$O_2 + 4H^+ + 4e^- \rightarrow 2H_2O \qquad\qquad 2\text{-}6$$

(For acidic environment with pH less than 7)

$$2H_2O + O_2 + 4e^- \rightarrow 4OH^- \qquad\qquad 2\text{-}7$$

(For neutral and alkaline environment with pH 7 and above)

The reduction of dissolved oxygen depends on the amount of oxygen in that environment and in most cases; oxygen content of 5-10ppm will be enough for the reduction reaction of dissolve oxygen. This occurs in well aerated environment where there is enough oxygen to dissolve in the solution.

The formed anodic and cathodic sites are distributed based on the environmental condition, crystal lattices imperfection and the surface contamination. In areas where there are imperfections, there is a likelihood of the anodic sites developing in this area [11]. Other factors include the microscopic defects such as surface roughness, cut edges, scratches, imperfections in protective surface films formed, bimetallic couples and dissimilar surfaces. All this can encourage the development of micro anodic and cathodic sites for the corrosion reactions to proceed.

The process of corrosion in aqueous solutions involves the production of electrons. These electrons need to be consumed by other processes which are the reduction processes. The electron produced at the anodic site transport by diffusion convection and migration to the cathodic site to be consumed. The number of electrons produced always equal the number electron consume to maintain the charge neutrality of the electrochemical process. This is achieved by the two half electrochemical reaction of the anode and cathode. The net value of anodic and cathodic reactions gives the value of the potential of the cell.

2.2. Thermodynamics and kinetics of wet/aqueous corrosion

2.2.1. Gibbs free energy

The study of corrosion involves the knowledge of Gibbs free energy. The Gibbs free energy gives an idea of tendency of a chemical reaction to occur. A corrosion process is a chemical/electrochemical reaction and will involve the use of Gibbs free energy to determine whether a corrosion reaction will occur spontaneously or not. Generally the more negative in Gibbs free energy change (ΔG) value is, the more likely a reaction to move in that direction [12]. For example

$$Mg + H_2O(l) + \frac{1}{2}O_2(g) \rightarrow Mg(OH)_2(s) \qquad \Delta G° = -596.6 KJ \qquad \text{2-8}$$
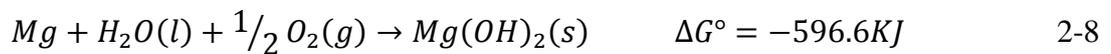
Where $\Delta G°$ is the standard Gibbs free-energy change for the above reaction.

The large negative value of the Gibbs free energy shows the tendency of Mg to corrode in aerated aqueous medium is high. Lower negative value of $\Delta G°$ means that the tendency for the reaction is lower.

Thermodynamic studies suggest that all metals tend to exist at low energy level. This tendency makes most of the metals naturally to exist combined with other elements since they have a stable low energy at this state. Iron for instance exists mostly as ore in nature. This is because the ores which are mostly oxides of iron itself are of low energy. To separate iron from its ore, energy is normally applied in form of heat to reduce the iron from its oxide. Some noble metals like gold (Au) will exist on its own and this is seen from its Gibbs free energy value

$$Au + \frac{3}{2}H_2O(l) + \frac{3}{4}O_2(g) \rightarrow Au(OH)_3(s) \; \Delta G° = +65.7 KJ \qquad \text{2-9}$$
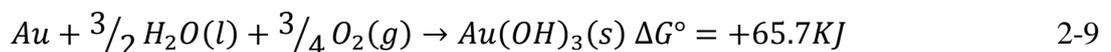
Here the Gibbs free energy for gold to react in aerated aqueous solution is positive. This from Gibbs free energy concept shows that the reaction cannot happen spontaneously. This is the reason gold does not corrode in normal conditions. A zero value of ΔG indicates that the reaction is in its equilibrium state. The high value of

$\Delta G°$ does not mean that the corrosion rate will be high it just implies that the reaction can occur easily. The rate may or may not be high. For this reason, aluminum which has a high negative $\Delta G°$ does corrode at lower rate compare to iron with a lower negative $\Delta G°$ value.

The tendency for a metal material to corrode can also be measured using its electromotive force (emf) denoted as (*E*). The emf itself relates to the Gibbs free energy as follows

$$\Delta G = -nFE \qquad\qquad 2\text{-}10$$

Where n represent the number of electron taking part in the reaction also known as electrochemical equivalents (EC). F is the Faraday's constant with its usual value of 96,500C/eq. From the equation it will be seen that a cell with a high emf is likely to have the overall reaction going in the direction of the product.

2.2.2. The Nernst equation and half-cell potential

The electromotive force (emf) is the voltage developed by any source of electric energy such as the electrochemical cell. The emf of a cell is of importance to the study of corrosion and can be measured or calculated. In measuring the emf of a cell, the potentiometer/potentiostat is employed in the measurement by opposing the unknown emf with a known one such as SHE (standard hydrogen electrode) or Ag/AgCl in saturated KCl. It can also be measured by the use of a high impedance voltammeter. For the calculation of the emf in terms of the concentration of the reactants and products, we can derive the Nernst equation.

Considering a cell reaction with w moles of W substance, z moles of Z substance reacting to form x moles of X substance and y moles of Y substance in the manner below,

$$wW + zZ \rightarrow xX + yY \qquad\qquad 2\text{-}11$$

The Gibbs free energy change is given by the different between the molar free energy of the products and reactants.

$$\Delta G = (xG_X + yG_Y) - (wG_W + zG_Z) \qquad \text{2-12}$$

In a standard form the standard change in the Gibbs free energy is

$$\Delta G° = (xG°_X + yG°_Y) - (wG°_W + zG°_Z) \qquad \text{2-13}$$

If the activities (a) of each of the reactants and products are taken as their corrected pressure (for gases) or concentration (for liquid and solid), then the difference in Gibbs free energy at any state with the standard state can be given as

$$\Delta G - \Delta G° = RTln\left(\frac{a_X^x.a_Y^y}{a_W^w.a_Z^z}\right) \qquad \text{2-14}$$

Where R is the gas constant (8.314J/K-mole)

     T is the absolute temperature in Kelvin (i.e. degree Celsius + 273)

     a_X^x = the activity of substance X

     a_Y^y = the activity of substance Y

     a_W^w = the activity of substance W

     a_Z^z = the activity of substance Z.

In an equilibrium state, the reaction has no tendency to occur and this makes the ΔG to become zero. The equation is then reduced to

$$\Delta G° = -RTInK \qquad \text{2-15}$$

Where K = $\left(\frac{a_X^x.a_Y^y}{a_W^w.a_Z^z}\right)$

For an occasion where the activities of the reactants and products (i.e. a_X^x, a_Y^y and a_W^w, a_Z^z) equate to 1, the value of lnK will then be 0. This will then make ΔG and $\Delta G°$ equal.

Relating the above $\Delta G°$ above with emf (E), and given that the standard state for $\Delta G°$ is

$$\Delta G° = -nFE°$$ 2-16

Equating the value of EMF (E) from equation 2-10 and the value of standard EMF $(E°)$ from equation 2-16 into equation 2-14 and simplifying, the equation becomes

$$E = E° - \frac{RT}{nF} ln(\frac{a_X^x.a_Y^y}{a_W^w.a_Z^z})$$ (Nernst equation) 2-17

Equation 2-17 is known as the Nernst equation and can be used to calculate the emf of a cell at any given state when the standard emf is known. The activity of the substance in liquid form is the equal to the concentration of in moles per 1kg of water (molarity) multiply by a correction factor called the activity coefficient. For gases the activity is the fugacity of the gas at normal pressure while for solid and water the activities are set at 1.

To calculate the emf of a cell, it is always convenient to calculate the potential of each cell and then add them together to get the correct emf.

Example for the reaction

$$Fe^{2+} + 2e^- \rightarrow Fe$$ 2-18
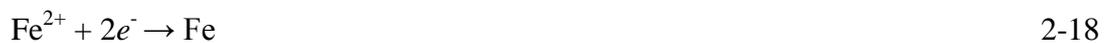
$$\emptyset_{Fe} = \emptyset°_{Fe} - \frac{RT}{nF} ln(\frac{Fe}{Fe^{2+}})$$ 2-19

Where, (Fe) is the activity of iron which is unity because it is solid. (Fe^{2+}) is the activity of iron ions. $\emptyset_{Fe}$ and $\emptyset°_{Fe}$ are potential and standard potential of iron (Fe) respectively.

Substituting the values of RT /F which is 0.02569 at room temperature (i.e. 298K) and since 2 electron are involved n=2

$$\emptyset_{Fe} = \emptyset°_{Fe} - \frac{0.02569}{2} \ln(\frac{1}{Fe^{2+}}) \qquad\qquad 2\text{-}20$$

2.2.3. The standard hydrogen potential

The measuring of the emf of a cell is based on a known standard emf. This is because the absolute potential of electrodes is unknown hence the cells are unknown. The hydrogen potential has been taken as the standard potential from which other potential can be compared and measured. The potential of hydrogen is therefore taken to be zero at all temperature.

To determine the hydrogen potential, a platinized platinum piece is dipped inside a solution saturated with hydrogen gas at atmospheric pressure of 1atm as shown in

Figure 2-4. When the pressure of the gas in the atmosphere is equal to the activity of the hydrogen ion, it then means that the value of the potential is zero. This can be represented in the equation as

$$\emptyset_{H_2} = \emptyset°_{H_2} - \frac{RT}{2F} \ln(\frac{pH}{(H^+)^2}) \qquad\qquad 2\text{-}21$$

Where $\emptyset_{H_2}$ and $\emptyset°_{H_2}$ are the potential of hydrogen and the standard potential of hydrogen respectively. pH is the fugacity of hydrogen.

$$\emptyset_{H_2} = 0 - \frac{0.02569}{2} \ln(\frac{pH}{(H^+)^2}) \qquad\qquad 2\text{-}22$$

When pH and $(H^+)^2$ are equal we have $\ln 1$ which gives 0 then $\emptyset_{H_2} = 0$.
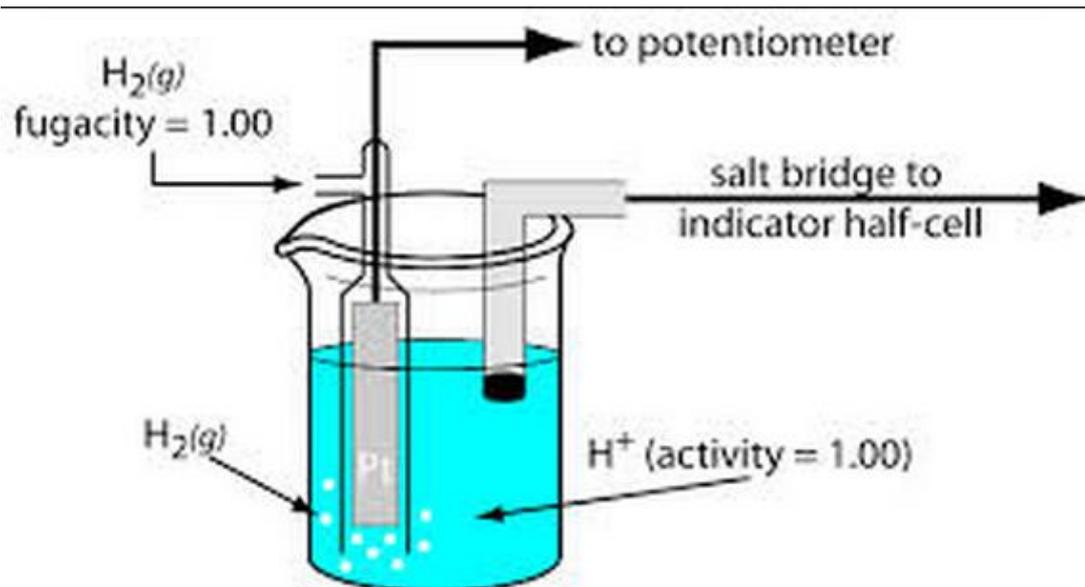
Figure 2-4 : Schematic of hydrogen electrode [4, 13]

The half-life potential of any other electrode/metal is measured against that of hydrogen. It is taken that hydrogen is part of the other cell of the half-life of the cell that is measured. It should be noted that the standard hydrogen electrode is not a convenient reference electrode and other type of electrode are used for electrochemical measurements. The establishment of convenient reference electrode is necessary in determination of the corrosion rate in a corrosion cell. Examples of common reference electrodes are

Hg/solid Hg_2Cl_2 in 0.1N KCl   +0.334 V to $\emptyset_{H_2}$ (Saturated Calomel electrode)

Ag/solid AgCl in 0.1N KCl   +0.288V to $\emptyset_{H_2}$

Cu/saturated $CuSO_4$ +0.316V to $\emptyset_{H_2}$

2.2.4. Emf series

The knowledge of the emf series can be very useful in understanding corrosion. The emf series arranges the standard potential of all metals base on hydrogen potential in an ascending or descending order. A typical emf series is shown in Table 2-1

Table 2-1: The Emf series [4]Table 1-1

Electrode Reaction	Standard Potential, $\phi°$, in volts at 25 °C
$Au^{3+} + 3e^- = Au$	1.50
$Pt^{2+} + 2e^- = Pt$	~1.2
$Pd^{2+} + 2e^- = Pd$	0.987
$Hg^{2+} + 2e^- = Hg$	0.854
$Ag^+ + e^- = Ag$	0.800
$Hg_2^{2+} + 2e^- = 2Hg$	0.789
$Cu^+ + e^- = Cu$	0.521
$Cu^{2+} + 2e^- = Cu$	0.342
$2H^+ + 2e^- = H_2$	0.000
$Pb^{2+} + 2e^- = Pb$	−0.126
$Sn^{2+} + 2e^- = Sn$	−0.136
$Mo^{3+} + 3e^- = Mo$	—0.2
$Ni^{2+} + 2e^- = Ni$	−0.250
$Co^{2+} + 2e^- = Co$	−0.277
$Tl^+ + e^- = Tl$	−0.336
$In^{3+} + 3e^- = In$	−0.342
$Cd^{2+} + 2e^- = Cd$	−0.403
$Fe^{2+} + 2e^- = Fe$	−0.440
$Ga^{3+} + 3e^- = Ga$	−0.53
$Cr^{3+} + 3e^- = Cr$	−0.74
$Zn^{2+} + 2e^- = Zn$	−0.763
$Cr^{2+} + 2e^- = Cr$	−0.91
$Nb^{3+} + 3e^- = Nb$	—1.1
$Mn^{2+} + 2e^- = Mn$	−1.18
$Zr^{4+} + 4e^- = Zr$	−1.53
$Ti^{2+} + 2e^- = Ti$	−1.63
$Al^{3+} + 3e^- = Al$	−1.66
$Hf^{4+} + 4e^- = Hf$	−1.70
$U^{3+} + 3e^- = U$	−1.80
$Be^{2+} + 2e^- = Be$	−1.85
$Mg^{2+} + 2e^- = Mg$	−2.37
$Na^+ + e^- = Na$	−2.71
$Ca^{2+} + 2e^- = Ca$	−2.87
$K^+ + e^- = K$	−2.93
$Li^+ + e^- = Li$	−3.05

The standard potentials with a negative signs are those who potential to oxidized is more than that of hydrogen while the standard potentials with a positive signs are those whose potential to oxidized are less than that of hydrogen. This arrangement can easily be used to predict which metal is anodic in an electrochemical cell. For example iron is anodic to platinum when both are part of an electrochemical corrosion cell. It should however be noted that emf series has a limited use as the

potential of two electrodes can change due to the type of electrolyte they are in contact [4, 14].

The measurement of the emf of cell can be done using a reference electrode connected across to the anode electrode. This reference electrode such as the one previously described can easily measure the potential of the anode in any environment since its own potential is relative stable at most environment. Using this method the corrosion rate of an electrochemical cell can be derived. The arrangement of this kind of cell used in determination of the corrosion rate is known as three electrode cell. Figure 2-5 shows the schematic description of a three electrode cell. The cell includes the working electrode e.g. carbon steel which is the anode. When the circuit is complete by connecting it to an EMF source like a potentiostat, the anode corrodes though oxidation reaction and produces electrons which are consumed at the cathode. A typical cathode can be a platinum cylinder which is nobler than the carbon steel (anode). A convenient reference electrode such as Ag/solid AgCl in 0.1N is connected to the anode and used to measure the potential/voltage across the anode as it corrodes.
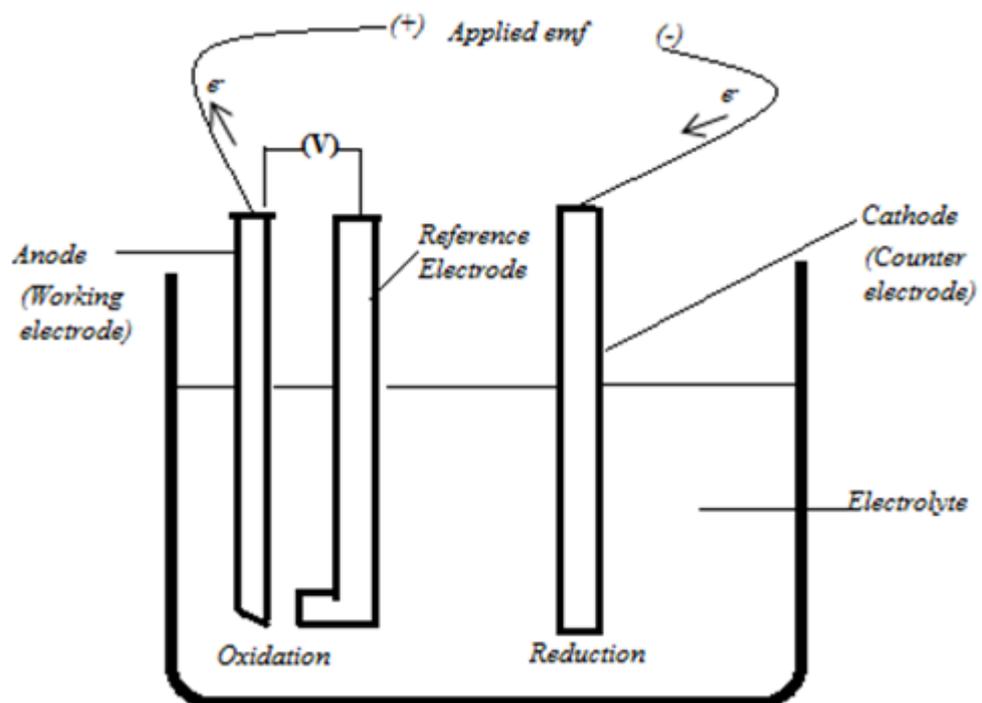
Figure 2-5 : A schematic description of a three electrode cell set up.

2.2.5. Pourbaix diagram

The Pourbaix diagram also known as the E-pH is a convenient and compact summary of the thermodynamic data which is used to determine the way metal and related species behave in a given environmental condition [15]. The Pourbaix diagram is described in the form of potential-pH diagrams which will relate the corrosion and electrochemical behavior of most metal in its given environment (i.e. water). The diagrams are based on the Nernst equation

In the Pourbaix diagram the potential and pH is taken to be the most important and influential variables that governs the behavior of metals in its environment. In designing a Pourbaix diagram, the potential is always plotted on the Y axis with pH on the X axis.

The Pourbaix diagram is good in the sense that it gives an idea of how most metals will behave in a particular potential and pH condition. The immunity state, oxides or complex ion formation of a metal at any particular potential and pH state can be viewed at a glance using a Pourbaix diagram [4]. The corrosion engineer uses the Pourbaix diagrams to identify where corrosion can occur in a particular domain and the possible corrosion product that will be formed. Practical environments always differ from the ideal situation of a potential-pH diagram and so Pourbaix diagram should be treated with caution [15].

The Pourbaix diagram has been produced for most metals that are used in industry. The Pourbaix diagram of iron is shown Figure 2-6. It shows in a glance what reaction will occur for iron and the products that will form during any reaction at the potential-pH condition. It also shows the region where iron is stable. In this diagram a horizontal line means that the reaction is independent of the pH and only involves electrons. The vertical line means that the reaction only involves pH (i.e. OH^- and H^+) with no electron taken part in the reaction.

The diagonal lines represent the reaction that involves both potential and pH of the environment. This means that the reaction at these points is influence by the pH of the solution and the flow of electrons.
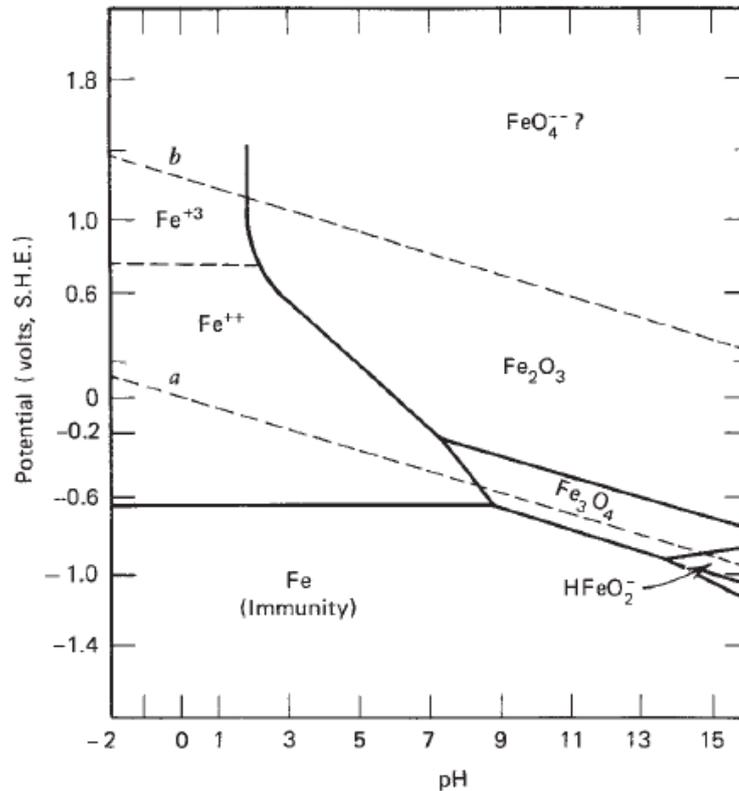
Figure 2-6 : The Pourbaix diagram of iron [16].

The Pourbaix diagrams are useful;

- For determining the corrosion product and composition that will be form at any given potential and pH.
- Predicting of direction of a reaction and its spontaneous nature.
- Predicting the changes that may occur with potential, pH and solution composition and how it will affect the corrosion of the metal.
- Identifying the boundaries of potential and pH that shows the equilibrium stability of the metal, where it will not corrode (immune area), where corrosion soluble products will form and the passive region where the protective corrosion films are formed.
- It gives ideas of the cathodic reaction product. This will identify if oxygen or hydrogen will be evolved from the cathodic reaction.

2.2.6. The Electric Double Layer (EDL)

The EDL is a spatial region of a metal –electrolyte surface which contains a negative charge of electron and positive charge ions separated by water molecules from the electrolyte in a metal electrochemical reaction [11].

In an electrochemical set up where metals are immersed in a solution /electrolyte, the metal in a solution/electrolyte leaves their metal lattices as metal ions and leave behind their electron. At this surface of the metal and electrolyte, water molecules surround the metal ions and make the metal ions to diffuse freely away from the metal surface. The electron causes some of the metal ions to be attracted back towards the surface of the metal. The water molecules on the other hand prevent the metal ion from being reduced back to metal. The positive ions which are already in the solution/electrolyte are also attracted towards the electron layer on the metal surface. The surface of the metal then consists of a region with electron on the metal surface with sheath of water molecules and adjacent metal ion and any positive ion from the electrolyte. There exist a charge separation at the metal and solution /electrolyte surfaces which are describe as the electric double layer (EDL) [8, 11].
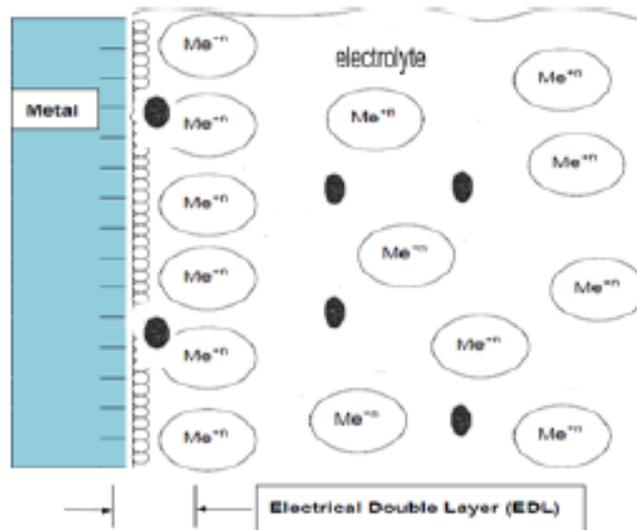
Figure 2-7 : A description of the electric double layer (EDL) [11]

There are a lot of models of the EDL. In a particular model where the corrosion reaction is in equilibrium, the oxidation and reduction reactions occur at equal rates.

In this case the surface of the metal will be made up of electrons adjacent to a sheet of water molecules and another layer of metal ions. The number of metal ions leaving the surface of metal is equal to the number of metal ions being reduces to the metal.

Corrosion of metals always occurs immediately in most corrosive environment and as such makes the metal ions not to be in equilibrium. The situation where the metal ions continue to leave the metal surface gives rise to steady state corrosion. The Gouy-Chapman-Stern model is one of the most popular models used in describing the EDL [8]. This model consist of two layers namely the Stern layer (SL) and the diffuse layer (DL). A sheet of charge exists due to adsorbed ions and Coulomb interactions which make up the Stern layer. The sheet of charge is a product of excess and deficiency electrons and forms on the metal-electrolyte surface. The SL is made up of two layers namely the inner Helmholtz (IHP) and the outer Helmholtz plane (OHP). The DL is the region just beside the SL and has ions which can move freely with no restriction to its direction. Unlike the DL, the specifically adsorbed ions and molecules, and solvated molecules (In most cases water molecules) are contained in the IHP and have some movement restrictions. The solvated ions cannot touch the electrode but approach it to a distance with the locus of centers as OHP. The charge metal and solvated ions interaction consists of electrostatic forces independent of the properties of the ions [17]. Figure 2-88 shows the electric double layer Gouy-Chapman-Stern model with metal attaining a net negative charge.
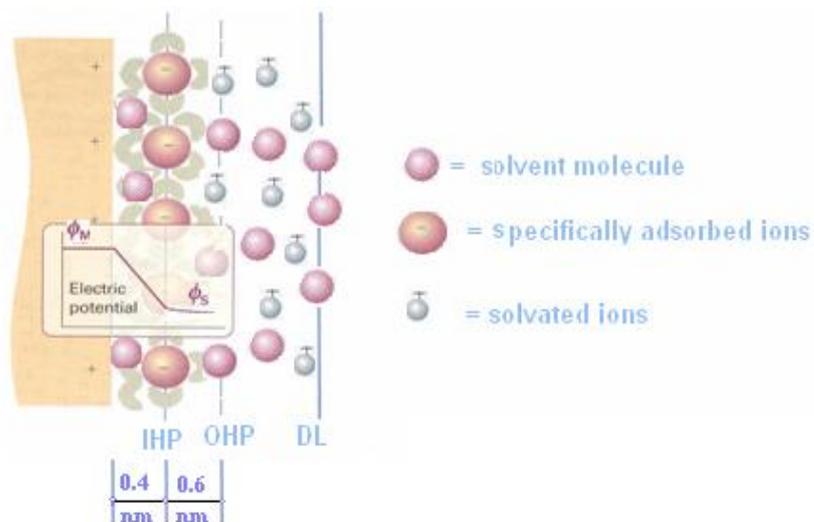
Figure 2-8: The electric double layer with metal attaining net negative charge [8, 17]

A capacitor is made up two planes of opposing charges separated by an insulator. The EDL itself acts like a capacitor in the sense that it is made up of two opposing charge on the metal and electrolyte surface separated by the solvent molecule (mostly water molecules) that physically act as the opposing charges separator. The capacitance of the EDL is much dependent on the composition of the metal and the electrolyte. The behavior of the EDL is not restricted to its capacitive ability. The EDL also behaved like a resistor. This behavior is shown in the ability of the metal to resist transferring their electron to the positive species available in the electrolyte. The EDL can also be represented in a circuit form known as the Equivalent Electric Circuit Model (EECM). This is shown below in Figure 2-9
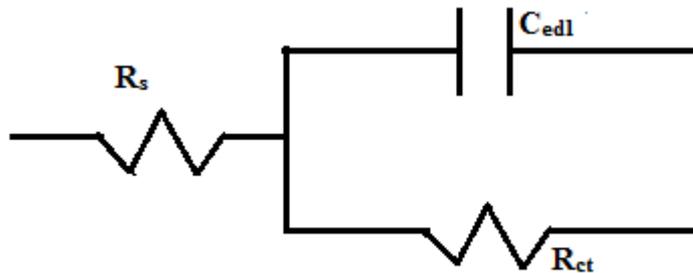
Figure 2-9 : EECM representing similar properties to the EDLThe C_{edl} represent the capacitance due to the EDL while R_{ct} represent the resistance due to the EDL and R_s represent the solution resistance .

The existence of charge separation in an EDL makes it to generate a potential difference. This potential difference can be measured between a metal electrode and a reference electrode or more still a metal electrode and another metal electrode.[11].

2.2.7. The relationship between the voltage, electric current and EDL chemistry

There exist a relationship between the voltage, electric current and EDL chemistry. This is so because there are measurable electric potential at the EDL with an electron transfer in the electrochemical process (corrosion process). When the net current flowing within a corrosion cell is zero, the potential at that point is known as

the Open Circuit Potential (OCP) represented as (E_{corr}). This occurs when the anodic reaction is in equilibrium with the cathodic reaction. The corresponding current at that point is referred to as the corrosion current density known as (i_{corr}) [4, 11]. The Nernst equation can be used to mathematically relate the EDL composition to potential difference. As previously described, the EDL is composed of the charge of the ions in the solution and the charge on the surface of the metal. This can be loosely determined by the concentration of the solution. Using equation 2-17 previously described as the Nernst equation the chemical activities of both the products and reactants are replaced with activity coefficient (γ_p) and (γ_r) multiply with the concentration of the product species and reactants species represented by an the element symbol in brackets. This can then be rewritten as:

$$E = E° - RTln(\frac{\gamma_p[Products]}{\gamma_r[reactants]}) \qquad\qquad 2\text{-}23$$

Where, (γ_p) and (γ_r) represent the activity coefficients for products and reactants respectively.

From equation 2-23, it shows that the measured potential depends on the concentration of active species and also the metal ions. If there is a change in the concentration, the measured potential will be affected. The OCP (i.e. E_{corr}) will then change and this will also change the EDL composition.

The relationship between the EDL and the electric current can be found using the Butler Volmer (BV) equation. Here the change in the potential of metal with the electric current caused by an external source is shown by BV equation below [17]

$$i = i_{corr}\left[exp - \left(\frac{\alpha\eta nF}{RT}\right) - exp\left(\frac{(1-\alpha)\eta nF}{RT}\right)\right] \qquad\qquad 2\text{-}24$$

Where (n, F, R, and T) has their usual values and meaning as previously defined for equation 2-10 and equation 2-14.

i is the external current density in amps/cm^2 passing to or from the electrode due to the voltage applied on it.

i_{corr} is the corrosion current density in amps/cm^2 that occurs when no voltage is applied through the electrode (i.e. at OCP).

α is a coefficient with values that can range from 0 to 1

η is the overpotential which is the difference between the applied potential and the OCP value (i.e. V$_{applied}$ − OCP)

The cathodic current is represented by the term $exp - \left(\frac{\alpha \eta n F}{RT}\right)$ while the anodic current is represented by the term $exp \left(\frac{(1-\alpha) \eta n F}{RT}\right)$.

At the OCP where the applied voltage is zero, the η = 0. This makes the value of the anodic and cathodic current to be equal and hence the net current i is equal to zero. This proves that at OCP there is no current flow in the system.

2.3. Electrochemical techniques

The assessment of corrosion rate is done using different corrosion techniques. The use of methods like gravimetric-based mass loss, quartz crystal microbalance-based mass loss can be used to determine the corrosion rate of a metal [18, 19]. In this thesis the techniques that are common and relevant to this project are considered. The electrochemical techniques that will be discussed here are the Direct Current (DC) method of potential-time measurement, Linear Polarization Resistance (LPR), Tafel slope and Alternating Current (AC) method of Electrochemical Impedance Spectroscopy (EIS).

2.3.1. Potential-Time measurement - (DC method)

The potential-time measurement is one of the simplest methods used in assessment of corrosion and corrosion rate. When a metal such as iron is immersed in a solution/electrolyte, a potential difference on the metal-electrolyte surface is established. This potential occurs without the application of any current on the metal. The potential will vary and come to a constant value at some point in time.

This value known as the Open Circuit Potential (OCP) will give quickest idea of how a metal will behave.

The potential-time measurement is easy and quick to determine. It gives an idea of the thermodynamic stability of a metal in its environment and also determines the domain the metal lies in its pourbaix diagram [11]. It also gives an idea of the galvanic relationship the metal has with its environment. The potential-time measurement on the other hand is good starting point for other DC measurement because it will give an idea of the potential which can be used to compare existing potential before other measurement is done. The manner in which a metal can react in that environment can be then understood.
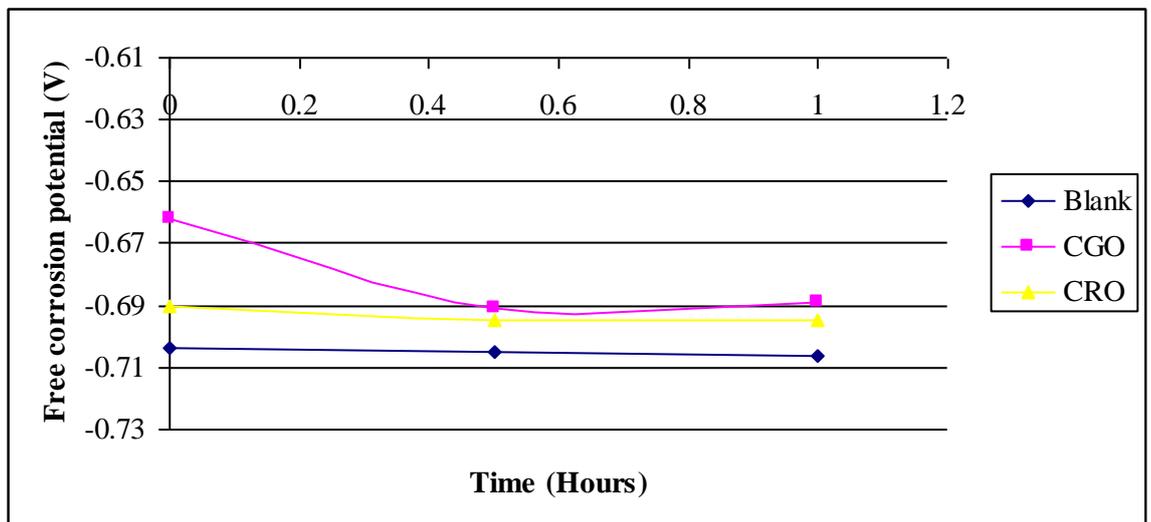
Figure 2-10 : Comparison of OCP in (V) measurement of blank solution with two inhibitors (CGO and CRO) showing increase in OCP as a reduction in the anodic reaction with the addition of the two different inhibitors [8]

The effect of electrolyte condition and changes can easily and quickly be understood with the use of potential-time measurement technique. Take for instant the use of inhibitor can make the potential to move to a more positive value with time showing that the inhibitor or MEG protects the anode by reducing the anodic reaction. For a case where the potential does not move to a positive direction, this implies that the corrosion reaction is cathodically controlled and will best be suited with inhibitors that work by reducing the cathodic reaction. However where the potential value

30

move slightly to the positive direction, may mean that the reaction is controlled both by the cathodic and anodic reaction [8]. It should be noted that the use of potential-time measurement may not be dependable for an inhibitor system in all conditions. This should be considered carefully when using the potential shift to noble state to identify the type of reaction that occur in the presence of an inhibitor [17].

The use of potential-time measurement should always be complemented with other measuring techniques as it is at best semi-quantitative. Other techniques presented later are definitively and can quantitatively be used to determine corrosion rate.

2.3.2. Linear Polarization Resistance – (DC method)

The Linear Polarization Resistance (LPR) method is a direct current (DC) measurement technique. It is one of the quickest and non-destructive methods for determination of the corrosion rate of a metal [11, 19]. It provides quick response that small changes on corrosion rate will easily be noticed in a pace of 5-15 minutes.

The LPR method was developed by Stern and Geary [4, 11, 20]. The work of Stern and Geary made some assumptions which include that the corrosion is activation controlled by the anodic and cathodic reaction of the corrosion process. In this method the metal is polarized using a direct current usually with a maximum potential range of -20mV to 20mV from the OCP value. The current flow when this voltage is applied is measured and from it the polarization resistance (R_p) can then be calculated. The graph of the potential is plotted against that of current and the slope of the linear part is taken and this gives a value of the R_p. Figure 2-11 shows the graphical calculation of the polarization resistance.
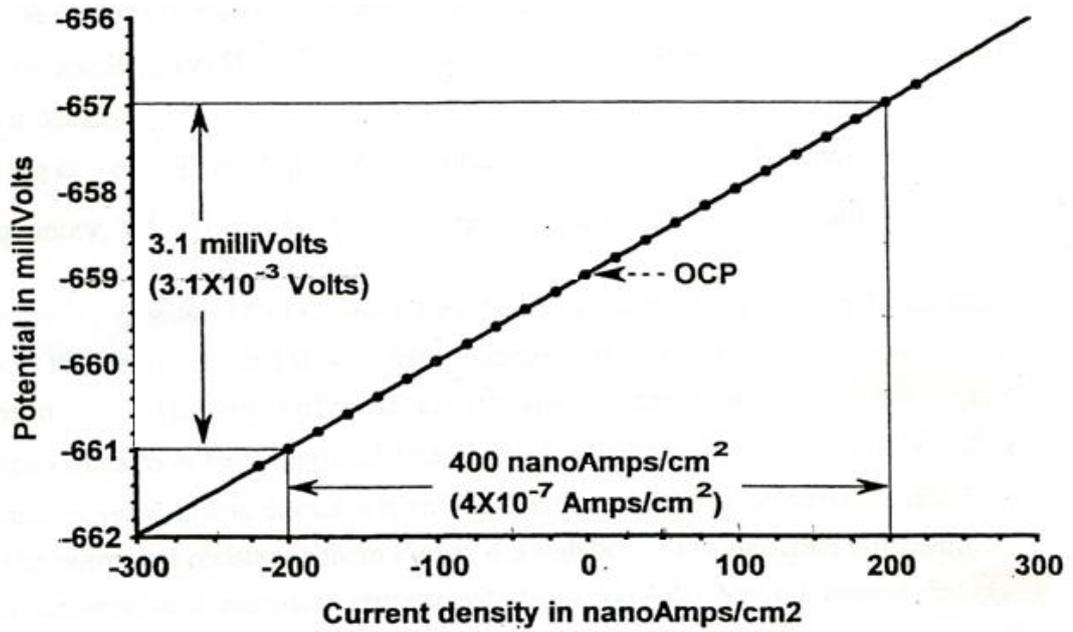
Figure 2-11: Graphical calculation of the polarization resistance (R_p) [11]

The equation for the for the linear polarization resistance (R_p) is given as

$$R_p = \frac{\Delta E}{\Delta i}$$
<div style="text-align: right">2-25</div>

Where Δi is the measured current density with respect to the applied voltage

ΔE is the difference between the applied voltage and the open circuit potential (OCP)

Using the equation derived by Stern and Geary known as the Stern-Geary equation

$$i_{corr} = \frac{\Delta i}{2.303 \Delta E} \left(\frac{\beta_a \beta_c}{\beta_a + \beta_c}\right)$$
<div style="text-align: right">2-26</div>

Where β_a is the anodic reaction Tafel constant in volts/decade and

β_c is the cathodic reaction Tafel constant in volts /decade.

$\left(\frac{\beta_a \beta_c}{\beta_a + \beta_c}\right)$ can be taken as a single constant B and $\frac{\Delta i}{\Delta E} = \frac{1}{R_p}$ making the equation become

$$i_{corr} = {}^{1}\!/_{2.303R_p}\;(B)$$

<div align="right">2-27</div>

From the above equation the i_{corr} can then be used to calculate the corrosion rate if the density, chemical equivalent is known. The chemical equivalent of the corroding metal can be defined as the ratio of the molar mass to the number of electrons (n) participating in the half-life reaction.

The equation for calculating corrosion rate in millimeter per year is given as

$$mmpy = \frac{(\Lambda)(\varepsilon)i_{corr}}{(\rho)}$$

<div align="right">2-28</div>

Where Λ is constant made of a combination of several term and is 3.27 x 10^{-1} for iron for corrosion rate in mmpy [11].

ε is the chemical equivalent of the corroding metal

ρ is the density of the reacting metal.

The LPR uses the lowest potential spectrum among any other DC method. The sample is only mildly polarized compared to other method and so it can be considered as non-destructive.

The disadvantage of linear polarization is that it does not give a good idea of how a metal material will respond to pitting corrosion and/or some other processes such as passivation and re-passivation process [19]. More still linear polarization can only be applied successfully to conductive solution. A situation where the solution in contact with the metal is not conductive, the linear polarization will give an erroneous value due to the overestimation of the resistance. Here the resistance of the non-conductive solution (R_s) will be added to the main resistance of the metal R_{ct}. This gives a lower value of the corrosion current and as such a lower corrosion rate. In reducing this problem of solution resistance, a current intercept measurement can be applied during a linear polarization measurement test with a potentiostat [11]. Alternatively the solution resistance can be determined using an AC impedance measurement and then compensated for on the LPR measurements results. This can be done using Microsoft excel as shown in appendix A. The solution resistance (R_s)

from the AC measurement is subtracted from the polarization resistance (R_p) on the excel sheet.

2.3.3. Tafel slope – (DC method)

The use of linear polarization technique in deriving corrosion rate is very useful and well applied by corrosion engineers and scientists in long term monitoring of corrosion rate. But it should however be pointed out that in most cases the results from linear polarization measurement can be an estimate rather than an exact result of the corrosion rate when the exact Tafel slope constants are unknown. To know the exact corrosion rate, the Tafel plot can be used to overcome this problem. Tafel slope makes use of a larger potential spectrum. The spectrum can be from 200mV or 250mV from OCP in both cathodic and anodic zone [11]. The measured currents are plotted on a logarithmic scale along the X-axis while the varied potentials are plotted on Y-axis.

Tafel plot can be described as activated controlled. In activated control process, the corrosion rate is determined by how fast the metal can release and gives its electron to the electrochemical actives species in the electrolyte. The activation control has a characteristics property of having both the anodic and cathodic branch increasing with potential. Diffusion controlled process is that which is controlled by the diffusion of the electrochemical active species (EAS) to the metal surface. The diffusion controlled process is characterized by the cathodic branch/ current density having a limit at a point in time while the potential is increasing. If this occurs, the graph is no longer considered a Tafel plot. The slope is then considered for regions where the limiting current effect due to diffusion does not exist. This occurs mostly below 50mV from the OCP on both the anodic and cathodic branch as illustrated in Figure 2-12. It should be pointed out that stirring of the electrolyte /solution has been found to reduce the limiting current value and this helps the EAS to migrate easily to the metal surface. Typical activated controlled Tafel plot is shown in Figure 2-12.
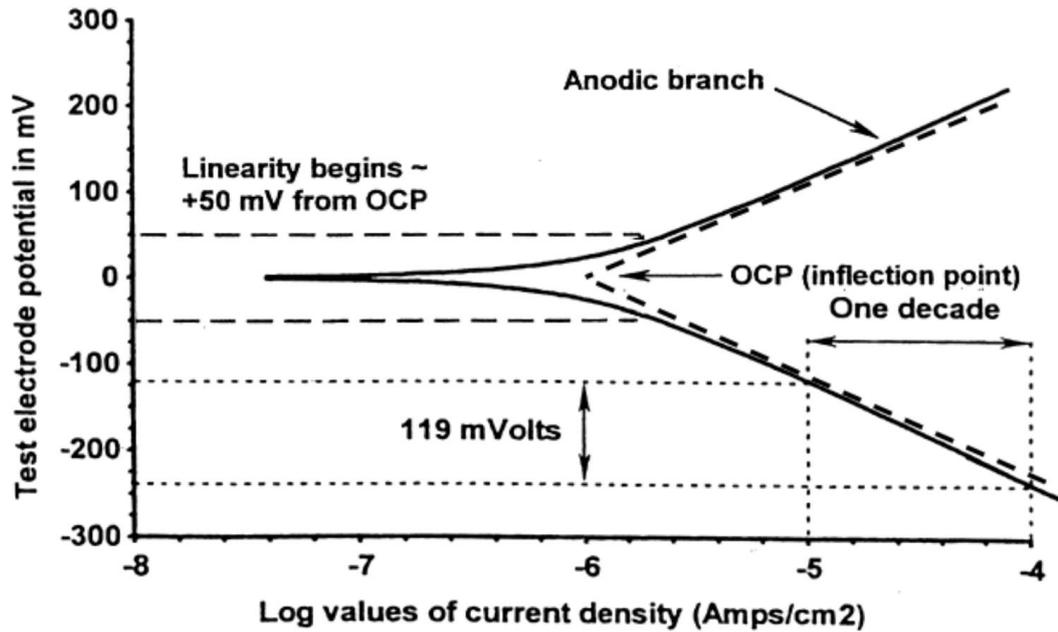
Figure 2-12 : Graphical representation of the Tafel slope showing how to determine the Tafel slope [11].

The Tafel plot can easily be used to calculate the corrosion rate using a Tafel extrapolated method. This is usually done by extrapolating the cathodic and anodic branch of the Tafel plot towards the OCP value. The point of interception the two arms will directly be read off as the corrosion current i_{corr}. This can then be used to determine the corrosion rate from the equation 2-28 previously described.

Tafel plot still have the disadvantage of being used for electrolyte with high conductivity. In a situation where the solution/electrolyte resistance is high, the Tafel slope will give a very low corrosion rate as compared with the actual corrosion rate. To avoid this, high resistance solution should be compensated using method like current interception during measurement.

2.3.1. Electrochemical Impedance Spectroscopy - (AC Method)

Electrochemical Impedance Spectroscopy (EIS) is an electrochemical corrosion measuring technique that uses the alternating current (AC) to determine the corrosion rate and also corrosion mechanism. The EIS is powerful in the sense that it can give insight into the process of corrosion and corrosion control method that

cannot be acquired easily by other DC method. Such corrosion control method like the use of inhibitor and coating to protect the surface of the metal [19].

When EIS technique is applied the metal electrode response to the use of alternating voltage with changing frequency. This response is then interpreted on the basis of circuits that resemble or mimic the response by the metal electrode. The range of polarizing voltage uses for EIS is a low but fluctuates from peak value for the anodic to the peak value for the cathodic. The impedance which determines the amplitude of the current for a given voltage represent the total resistance of metal for an applied voltage and current and is the proportionality factor for both the AC voltage and current.

2.3.1.1. AC impedance and phase behaviour

As described previously the EDL of a corroding metal behaves like an electric circuit with capacitors and resistors. In AC, there exist resistor that resist the flow of electricity, capacitance due to charge build up or discharge by the AC and inductors which try to resist the change in the flow current. The resistor in the AC is known as impedance. In an AC mode, the capacitor can take time to reach its full charge or/and inductor time to reach its full relaxation. This time lapse produces a shift in the current and voltage of the AC. The resistor does not have this time behavior like the capacitor. The difference between the voltage and the current at zero amplitude gives a phase. The magnitude of the phase angle is different for each polarizing voltage frequency. The time constant (τ) is the time taken for the relaxation to occur. In the graph of Figure 2-13, the phase angle is shown as the difference between the voltage and current at zero amplitude of the voltage. It is normally plotted as a positive value in EIS though it is negative. The vector form of the impedance is shown in Figure 2-14.
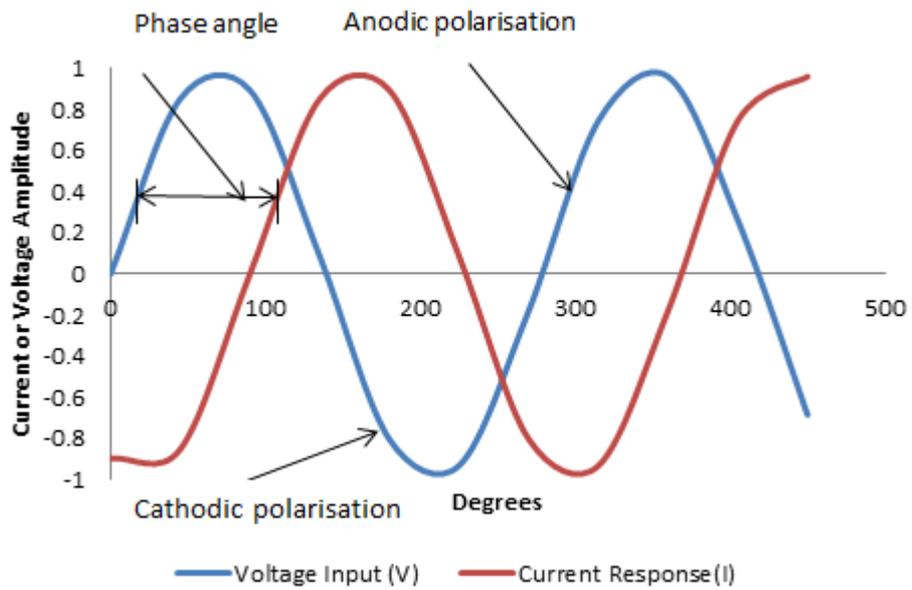
Figure 2-13 : The phase angle in and AC voltage–current circuit with a capacitor.

Since the current and voltage of the AC is a vector quantity, the impedance is also a vector quantity that has both magnitude and direction. The vector component of the impedance as shown in Figure 2-14 describes the value of the resultant impedance (Z) from the real impedance (Z') and imaginary impedance (Z'').
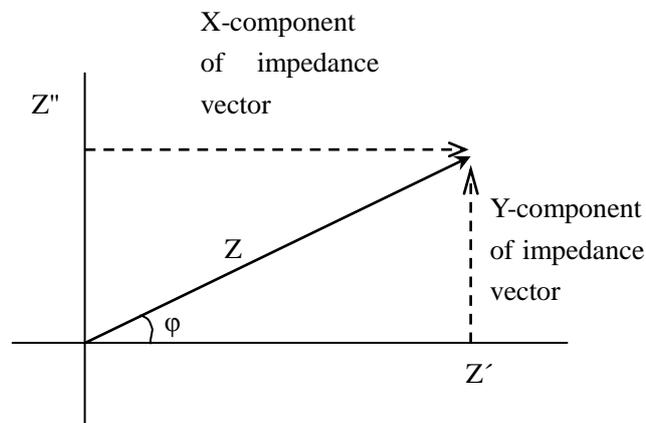
Figure 2-14 : The vector component of the impedance of an AC showing the real (Z') and imaginary (Z'') part with the total impedance (Z) [8, 11]

Typical EIS involves applying a polarizing voltage of ±5mV or ±10mV amplitude from OCP with a frequency range from 100 kilohertz to 5 millihertz or less. The EIS

data can be plotted in different format. The three major format/graph used in representing data from EIS are

   i.   Nyquist or complex plane plots

  ii.   Bode phase plot and

 iii.   Bode magnitude plot [11, 19].

2.3.1.2.   Nyquist or complex plane plot

The Nyquist or complex plane plot is derived from a plot of the real impedance against the imaginary impedance. It is always in a semi-circle form from high frequency domain to low frequency domain. A complex plane plot can have a single time constant which has one semi-circle or more time constant with more semi-circles. A time constant is equal to the product of capacitance and its corresponding parallel resistance. An example of a single complex plane plot is shown in Figure 2-15
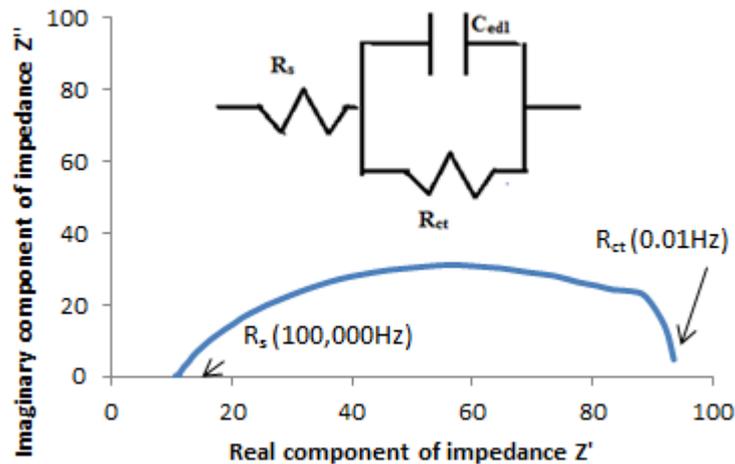
Figure 2-15 : Nyquist plot with a single time constant and EC describing the plot.

The high frequency part gives the value of the R_s which is the solution resistance. The R_{ct} which is the polarization resistance is given as the diameter of the semi-circle. The capacitance C_{edl} of the double layer is derived at the maximum frequency (f_{max}) of the imaginary impedance Z'' and the R_{ct}.

$$C_{edl} = \frac{1}{2\pi f_{max}R_{ct}} \qquad\qquad 2\text{-}29$$

For a very large corrosion resistance (R_{ct}) , the Nyquist plot may looks more like a straight line than a normal semi-circle [11, 17]. However some Nyquist plot can have two or more time constant in it. This is usually seen for situation where there is a coating or inhibitor film on the surface of the metal. The coating has its own coating capacitor with a parallel coating resistor along with the usual C_{edl} and corrosion resistor. An example of a two time coating constant is shown in the Figure 2-16.
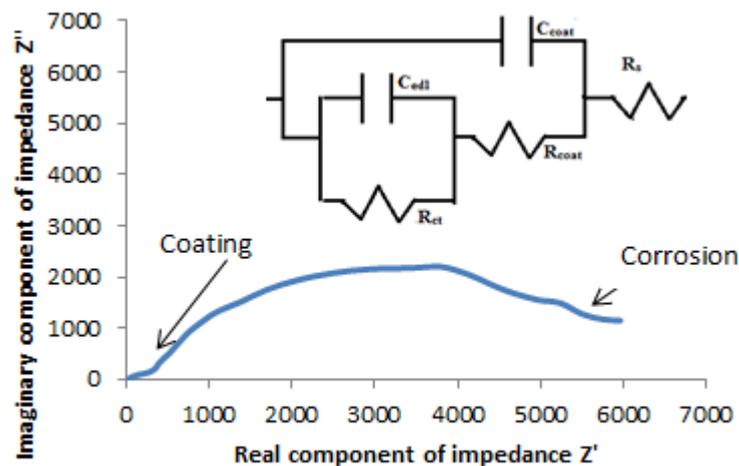
Figure 2-16 : Illustration of a corroding steel with a coating time constant at high frequency and corrosion time constant at lower frequency.

2.3.1.3.   The Bode magnitude plot

The Bode magnitude is another way of illustrating an AC impedance measurement. It is plotted by using the log values of the total impedance for each frequency on the Y-axis against the log value of the frequencies on the X-axis. The plot slope is negative when the capacitors are part of the circuit while is zero when it is only through the resistor(s). The ratio of the R_{ct} to R_s will give the magnitude of the slope and it tends towards -1 when R_{ct} is much higher than R_s.
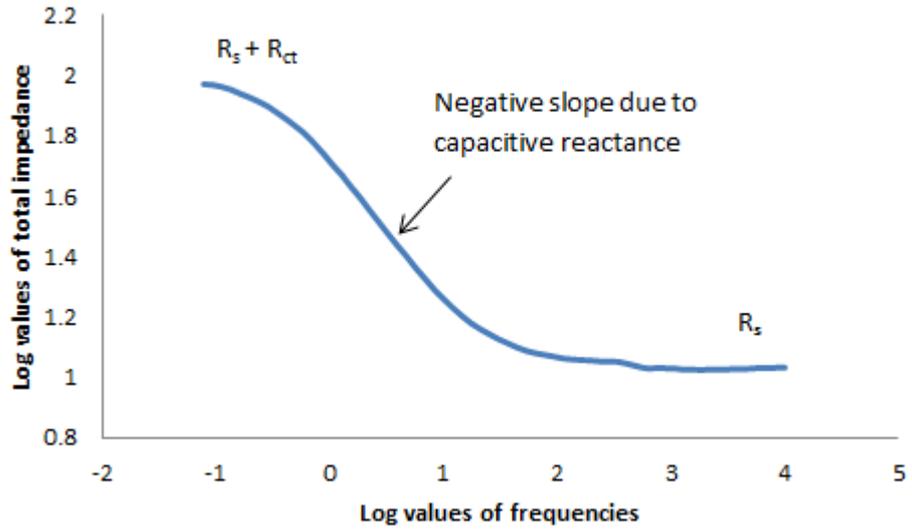
Figure 2-17 : A single time constant Bode magnitude plot for a corroding metal.

The example in the Figure 2-17 above describes the Bode magnitude plot for a single time constants corroding metal. It also describes the corresponding value of the R_1, R_2, and point for the capacitive reactance.

2.3.1.4. The Bode phase plot

Figure 2-18 shows the Bode phase plot with the capacitive reactance at the point of inflection.
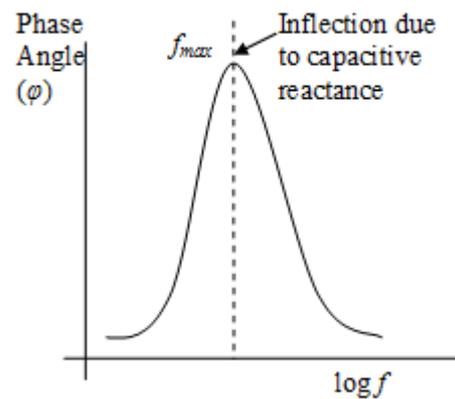
Figure 2-18 : Schematic diagram of a Bode phase plot [8].

The Bode phase plot is derived from plotting the magnitude of the phase angle for each frequency on the Y-axis against the log of difference frequencies on the X-axis. The Bode phase plot have the capacity of showing in a glance the distinctive position of any time constant that exist for the system.

2.3.1.5. Time constant sources

There are other sources of time constant which can exist within an AC impedance system apart from the usual coating and EDL time constants described above. It has been shown that different crystal orientation can corrode at different rates[15] . The inhomogeneous surfaces of metal and defect of the metal surfaces can generate multiple time constants which have the same capacitive reactance. This is normally seen as a distortion on the semicircle of a Nyquist plot rather than a distinctive time come like a coating constant.

Restricting the movement of the electrochemical active species (EAS) can also produces a time constant which is different from the corroding time constant[11].This is normally seen where diffusion of the EAS to the metal surface exist. Pitting corrosion also causes scattering of the EIS data at lower frequency area.

To distinctly observe a time constant of a corroding system, the magnitude of the constant should be separated by at least one order of magnitude. It should also be noted that some time constant that are produce for a corroding system are not actual time constant. This type of constant can be produce by the equipment when the solution resistance is very high[11]. Here the equipment will tend to follow a less resistive part to take measurement. This type of time constant is often described as a parasitic time constant.

Chapter 3. LITERATURE REVIEW

3.1. CO_2 corrosion of carbon Steel

Different researchers have studied the CO_2 corrosion of carbon and low alloy steel used in the oil and gas pipelines. Published results with regards to CO_2 corrosion has shown some incomplete understanding CO_2 mechanism [8, 21]. This is so because CO_2 corrosion is very complex and has a lot of factors that can affect it. In this part of the review the hydration of CO_2 in water/ salt solution to form corrosive acid is presented followed by corrosion reactions in CO_2.

3.1.1. Hydration and dissociation of CO_2

Sun et al. [22] proposed that the solubility of CO_2 in water and seawater is affected by the temperature and partial pressure of CO_2 and also by the acid-base relationship that exist in the solution. Temperature plays a large role in the solubility of CO_2 in water and most solution. From room temperature, higher temperature reduces the solubility of CO_2 in water or sea water. High partial pressure of CO_2 may increase the solubility in a solution [23].

CO_2 is very soluble in water and salt solution. The solubility of CO_2 is much higher than oxygen and has been estimated to be $90cm^3$ of CO_2 per 100ml of water. CO_2 gas dissolves in water as follows

$$CO_{2(g)} + H_2O_{(l)} \rightleftharpoons CO_{2(dissolve)}$$
3-1
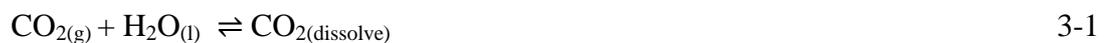
From Henry 's law, (i.e. which states that at constant temperature, the amount of a given gas that dissolves in a finite volume of a liquid is proportional to the partial pressure of that gas that is in equilibrium with the liquid surface) [24]. The relationship between the dissolved gas and partial pressure of the gas can be established. In the case of non-ideality in solution phase the activity coefficient(γ) may be introduce to account for this situation. For very high pressure and non-ideality in gas phase, the K_H may be taken to pressures dependent.

$$(\gamma)CO_{2(dissolve)} = P_{CO_2(g)}(K_H)$$ 3-2

Where $P_{CO_2\ (g)}$ is the partial pressure of the CO_2 gas in atm,

$CO_{2(dissolve)}$ is the concentration of the dissolved carbon dioxide in mol/L.

K_H is the Henry's constant.

The CO_2 partial pressure (P_{CO_2}) dissolution constant can be calculated as follows

$$K_d = \frac{P_{CO_2}(g)}{CO_2(dissolve)}$$ 3-3

The value is given as 29.41 L.atm/mol at 25°C.

The hydration reaction of the dissolve carbon dioxide ($CO_{2(dissolve)}$) is given as

$$CO_{2(dissolve)} + H_2O \rightleftharpoons H_2CO_3$$ 3-4

The hydration of $CO_{2(dissolve)}$ will give rise to carbonic acid [25].

For corrosion to occur in CO_2 environments there must be a supply of hydrogen ions from the acid and this is formed by the dissociation of carbonic acid form. The dissociation of the carbonic acid involves just a slight percentage of the carbonic acid. It has been estimated to be 0.1% of the carbonic acid molecules that dissociates at S.T.P. (standard temperature and pressure) [24, 26]. The formation of H^+, HCO_3^- or H_2CO_3 has been a point of debate on the controlling factor in CO_2 cathodic reaction. This is discussed later. The dissociation equation is shown as

$$H_2CO_3 \rightleftharpoons HCO_3^- + H^+$$ 3-5

The first dissociation constant of the carbonic acid is given as [24]

$$K_{d1} = \frac{(HCO_3^-)(H^+)}{(H_2CO_3)} = 1.72 \times 10^{-4}$$ 3-6

Where K_{d1} is the first dissociation constant.

It has been taken in most case that a lot of the CO_2 does not form the carbonic acid. If then the dissociation constant is calculated assuming the non-hydrated CO_2 is involved in the reaction as carbonic acid. Then [24]

$$K_{d1} = \frac{(HCO_3^-)(H^+)}{(H_2CO_3)} \equiv \frac{(HCO_3^-)(H^+)}{(H_2CO_3)(1+\frac{CO_2}{H_2CO_3})} = 4.42 \times 10^{-7} \qquad \text{3-7}$$

The second dissociation constant of the carbonic acid can be calculated since the bicarbonate formed from the first dissociation can proceed further to produce more hydrogen ions. This is shown in the equation below [24]

$$HCO_3^- \rightleftharpoons H^+ + CO_3^{2-} \qquad \text{3-8}$$

$$K_{d2} = \frac{(CO_3^-)(H^+)}{(HCO_3^-)} = 4.70 \times 10^{-11} \text{ (mol/L)} \qquad \text{3-9}$$

3.1.2. Anodic reaction of CO_2 corrosion

In CO_2 corrosion of carbon steel, the oxidation and dissolution of iron is the main anodic reaction that occurs. There are many reactions that occur in a CO_2 corrosion of carbon steel and this depend mainly on the environment of the carbon steel [21, 27-29]. The possible anodic reactions for carbon steel are described as

$$Fe \rightleftharpoons Fe^{2+} + 2e^- \qquad \text{3-10}$$

The process of oxidation of the iron has been elaborated by Bockris et al [29-31], as follows:

$$Fe + H_2O \rightleftharpoons FeOH_{(ad)} + H^+ + e \qquad \text{3-11}$$

The iron reacts with water and is oxidized to iron hydroxide which adheres to the surface of the metal iron. The iron is further oxidized into the Fe^{2+} which is considered as the rate determining step for the entire anodic reaction. This reaction is described as

$$FeOH_{(ad)} \rightleftharpoons FeOH^+ + e \qquad\qquad 3\text{-}12$$

$$FeOH^+ + H^+ \rightarrow Fe^{2+} + H_20 \qquad\qquad 3\text{-}13$$
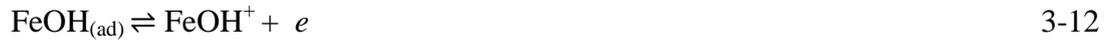
The study of carbon steel CO_2 corrosion anodic half-reactions has been done by a lot of researchers [32-35]. Many researchers and literatures including that of de Waard and Milliams[36] supported the work of Bockris et al. [29] on iron dissolution in strong acid. Bockris et al. [30] showed that the reaction order with respect with to OH^- is 1 with Tafel slope of 40mV/decade at 298K. This implies that the reaction mechanism is greatly influenced by the OH^-. From his studies it shows that the pH dependence of reaction decreases very fast with increasing pH >4.

Hurlen et al. [37] in their studies concluded that CO_2 is a stimulant too in the iron dissolution in the intermediate pre-passive form but does not really affect the iron dissolution in aqueous salt solution. The also reported a first order reaction with respect to OH^- but a Tafel slope of 30mV/decade for temperature of 298°K. This means that OH^- is still the major influence to the dissolution of iron.

Gray et al. [38, 39] on the other hand studied the effect of pH and temperature on the carbon steel corrosion mechanism in aqueous CO_2 and reported anodic Tafel constant that increases from 50mV/decade to 120mV/decade in pH range of 2-10. Their report gave an exchange current (i_o) independent of the pH unlike the Tafel slope constant that increases with pH. It was found from their report that the Tafel constant for the anodic reaction of iron was proportional to temperature (T) and exchange current (i_o) was inversely proportional to temperature up to the value of 60°C which was subsequently decreased probably because of the carbonate formed that protects the surface of iron from corroding.

Nesic et al. [40] in a later research concluded that dissolution of iron in CO_2 is affected by the present of CO_2. This they did by looking at the Tafel slope derived

from different CO_2 partial pressure tests and at different pH values. They discovered variations in the values of the Tafel slope. The found the order of reaction was higher than 1 for pH lower than 4 and the Tafel slope varying from 20mV/decade to 35mV/decade. For pH values between 4 and 5, the Tafel slope does increase from 30mV/decade to 60mV/decade. This obviously was taken to be a transition from the higher order of reaction to a single order of reaction and even lower. However for pH above 5 they found Tafel slope ranging from 80mV/decade to 120mV/decade. The influence of pH above 5 was negligible. This explains why corrosion kinetics of iron in CO_2 is much higher than corrosion of iron in strong acid. The formation of CO_2 and H_2CO_3 are both pH independent and CO_2 concentration is always higher than the carbonic acid formed. It is assumed that iron forms adsorbed chemical ligands (i.e. Fe_L = Fe-CO_2) which helps to catalyzed the oxidation process of iron in CO_2. The following steps are used to explain the oxidation process of the iron in CO_2 environment for pH >5

$$Fe + CO_2 \rightleftharpoons Fe_L \text{ (i.e. } \textit{Chemical ligands}) \tag{3-14}$$

$$Fe_L + H_2O \rightleftharpoons Fe_LOH_{ad} + H^+ + e \tag{3-15}$$

$$Fe_LOH_{ad} \rightarrow Fe_LOH^+_{ad} + e \qquad \text{(i.e. } \textit{rate determining step}) \tag{3-16}$$

$$Fe_LOH^+_{ad} + H_2O \rightleftharpoons Fe_L(OH)_{2ad} + H^+ \tag{3-17}$$

$$Fe_L(OH)_{2ad} \rightleftharpoons Fe_L(OH)_{2sol} \tag{3-18}$$

$$Fe_L(OH)_{2sol} + 2\,H^+ \rightleftharpoons Fe^{2+} + CO_2 + 2H_2O \tag{3-19}$$

It has been postulated that for lower pH value below 4, the reaction for adherence of $Fe_LOH^+_{ad}$ to the metal surface (i.e. Equation 3-16) will seize being the rate determining stage. The rate determining step will then become the de-adsorption stage where (i.e. Equation 3-18). A summary of the anodic reaction of iron is described by Kermani and Morshed [35].

3.1.3. Cathodic reactions in CO_2 corrosion

The cathodic reaction of carbon steel in CO_2 environment has been studied since the discovery of CO_2 corrosion but the mechanism is still not fully understood with absolute certainty. Controversy on the cathodic reaction lies mostly on whether the H_2CO_3 formed by CO_2 is reduced directly or dissociation H_2CO_3 is of the final step in the reaction. The CO_2 presence in the aqueous solution increases the corrosion rate of iron by increasing the amount of hydrogen evolves in the cathodic region. For strong acid that are fully dissociated, the evolution of hydrogen at the cathodic region depends on the rate at which hydrogen ions are diffuses from the bulk solution to the cathodic region. This limits the amount of hydrogen evolve at pH >4 and thus makes the corrosion of iron on strong acid not to proceed rapidly as expected. For CO_2 the presence of H_2CO_3 causes more of hydrogen to be evolving making the present of CO_2 to increase the corrosion rate of iron.

Three major mechanisms for the cathodic process that has been propose by researchers to govern the rate of cathodic reaction in CO_2 environment. de Waard and Milliams [41] proposed that the mechanism that governs the cathodic process is that of the direct reduction of the carbonic acid.

$$H_2CO_{3ad} + e \rightarrow H_{ad} + HCO^-_3 \ (\textit{rate determine step}) \hspace{2cm} 3\text{-}20$$

$$2H_{ad} \rightarrow H_2 \ \text{(The faster step)} \hspace{3cm} 3\text{-}21$$

The reaction also involves the hydrogen ions from the bulk solution reacting further with the bicarbonate acid form to reform the carbonic acid in solution.

$$HCO_3^- + H^+_{(bulk)} \rightarrow H_2CO_3 \hspace{4cm} 3\text{-}22$$

$$2H^+ + e \rightarrow H. \hspace{5cm} 3\text{-}23$$

This is the overall reaction proposed by de Waard and Williams [36] and has since been taken into account in the prediction CO_2 of carbon steel. The prediction however did not fulfilled the observations made by Schmitt and Rothmann [42-44] in flow reactions and also observations made by Ogundele and White [45].

Schmitt and Rothmann [42, 44] were the first to establish the effect of flow using rotating disc electrode. It was seen that the limiting current density (i_{lim}) is also a function of flow and thus diffusion can influence the whole process and not just the chemical reaction. The diffusion of the electrochemical active species of H^+ and H_2CO_3 affects the cathodic reaction.

$$i_{lim} = i_{lim,diff} + i_{lim,R} \qquad \text{3-24}$$

Where i_{lim} is the limiting current density for the entire reaction in CO_2

$i_{lim,diff}$ is the limiting current density effect of diffusion in CO_2

$i_{lim,R}$ is the limiting current density effect of the chemical reaction in CO_2.

The effect of flow for Schmitt and Rothmann [44] was observed for laminar flow and was only valid for that type of flow (i.e. rotating disk electrode). This also put a restriction to the validity of the results for turbulent flow region. The effect of turbulent flow was later extended by Mendoza-Flores and Turgoose [46] using the observations of smith and Rothman. John Postlethwaite and David Wang [47] also did some work in the corrosion of carbon steel on turbulent flow.

Ogundele and White [45] on the other hand made some observation on corrosion of steel in de-aerated CO_2 environment. They found out that the possible reaction that governs the cathodic process is direct reduction of the bicarbonate and further reduction of water molecule directly.

$$HCO_3^- + e \rightarrow H_{ad} + CO_3^- \qquad \text{3-25}$$

$$2H_2O + 2e \rightarrow H_2 + OH^- \qquad \text{3-26}$$

This observation of Ogundele and White [45] has been validated for pH $>4.9<5.3$ which is a less acidic situation.

Nesic et al. [48] also made some observations with the rotating cylinder and concluded that the reduction of the carbonic acid adsorbed on the surface of the metal is the predominant reaction that controls the cathodic process.

The effect of CO_2 corrosion products formed during the corrosion process were not given much consideration in most of the above cathodic reaction .Videm and Dugstad [33, 49, 50] in their studies found out that the formation of corrosion film product on the surface of the metal plays a lot of role in the subsequent corrosion kinetics and mechanism. Ikeda et al. [51, 52] on the other hand proposed that if protective films are formed on the surface of the metal, the rate-controlling factor will change from cathodic hydrogen evolution to mass transfer control. This is arguable since the protective layer will not allow the cathodic reaction to take place as rapid as it would have without a film on the surface. If this becomes true, the prediction base on the de Waard et al. [36, 53] proposal will not be effective. More so if the corrosion product formed are non-uniform, this will contribute to pitting and localized corrosion on the surface of the metal [49, 54-58]

The studies by several authors has concluded that the major corrosion product formed in CO_2 saturated environment is iron carbonate ($FeCO_3$) [59]. The formation of iron carbonate is likely due to the reaction Fe^{2+} with bicarbonate as proposes by Ogundele and white [45] or by the direct reaction of the Fe^{2+} with the carbonates ions CO_3^{2-}. The formation of iron carbonate is not rapid but it is easily formed when the saturation point of iron carbonate is attained. At this point the solubility of the iron carbonate in the solution has been exceeded. Heuer et al. [59] has shown that the formation of iron carbonate on the metal surface can reach up to 80µm. The formation of this coarse film is dependent on a lot of environmental factors. These environmental factors can be temperature, solution chemistry, fluid velocity, CO_2 partial pressure, pipe geometry, fluid phase and solution pH. Other factor that might influence the formation of the film will be steel microstructure and alloy composition. The effect of this environmental factor will be discussed in the next section.

Other corrosion products can also be formed depending on the environment. John et al. [60] reported that stable corrosion product (i.e. $FeCO_3$, Fe_2O_3, or Fe_3O_4) may form depending on the environment and this will reduce the rate of corrosion of the

iron when the corrosion product adsorbs on the steel surface. In their development of the CO_2 corrosion analysis tool (i.e. Sweetcor), the highlighted the conditions in which the three products are likely to form as

- $FeCO_3$ are formed for low temperature and high CO_2 partial pressures
- Fe_3O_4 are formed for high temperature and low CO_2
- Fe_2O_3 are formed for low temperature and low CO_2 partial pressure.

In some studies by Xia et al. [61], it was discovered that $Fe(HCO_3)_2$ was formed alongside the iron carbonate. This was seen for pH 5-8 and 21hours. For the remaining hours after 184 hours the $Fe(HCO_3)_2$ was not detected rather only $FeCO_3$ was available. The $Fe(HCO_3)_2$ are form as meta-stable phase from the redox reaction as follows

$$Fe \rightarrow Fe^{2+} + 2e \qquad\qquad 3\text{-}27$$

$$H_2CO_{3ad} + e \rightarrow H + HCO_3^- \qquad\qquad 3\text{-}28$$

$$Fe^{2+} + HCO_3^- \rightarrow Fe(HCO_3)_2 \qquad\qquad 3\text{-}29$$
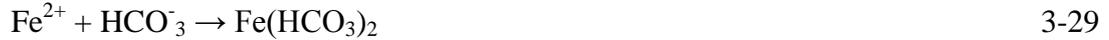
In a later period the meta-stable $Fe(HCO_3)_2$ will then be converted fully to iron carbonate by reduction process.

$$Fe(HCO_3)_2 + 2e \rightarrow FeCO_3 \qquad\qquad 3\text{-}30$$

The formation of iron carbonate can be formed for static sweet environment (i.e. CO_2 environment) within 2hrs. Sweet environment is a corrosive environment that involves only CO_2 gas as the corrosive agent with no H_2S gas involve. This formed iron carbonate film however is not uniform and compact. A more compact layer is formed with time. In some cases it will take 8 days to form a cubic crystalline iron carbonate film as studied by Ogundele and white[45]. The same type of observations were made by Farelas et al. [62] with two different type of carbon steel.

Iron carbonate ($FeCO_3$) precipitation requires super-saturation with Fe^{2+} [33]. In a study by Crolet et al. [63-65], they were able to establish that iron carbonate can also

precipitate on the Fe_3C. This is so because the cathodic reaction can also produce HCO_3^- and Fe^{2+} on the Fe_3C. The Fe_3C easily form on the surface of the metal and increase the rate of corrosion of the metal by increasing the cathodic process. The formation of Fe_3C can as well form even at velocities that are high. Videm [49] also reported that the Fe_3C can help the $FeCO_3$ to attached to the surface of the metal thereby serving as a support for $FeCO_3$. This in general helps in the reduction of the corrosion rate of the metal. They further explained that iron content in the solution will help in the formation of a protective $FeCO_3$ which will continue to be protective as long as the iron concentration does not fall. If there is a shortage of iron in the solution, there is a likelihood of the Fe_3C being exposed on the metal surface due to the re-dissolution of the $FeCO_3$. This will cause the metal surface not to be protected any more. Acidification of the solution and metal surface will in turn reduces and prevent the formation of $FeCO_3$ on the surface of the metal. At this point, even the super-saturation of the iron itself will not even cause the formation of the protective film on the surface.

3.1.4. Corrosion models for CO_2

Corrosion models for CO_2 have been developed to accommodate most of the environmental factors that can affect the CO_2 corrosion of oil and gas production. A lot of different mathematical model are now available and are in used by engineers to analyze and predict CO_2 corrosion. Typical representation of the models has all been review by Nyborg et al. [34] comparing them with data from different rigs and field. The correlation and flaws of the different models were presented in that paper base on the field data. Kermani and Morshed [35] also did a comparison studies of the models available and pointed out the effect of environmental, physical and chemical composition to the CO_2 corrosion models.

Corrosion models for CO_2 corrosion can be classified into 3 major categories namely

- Mechanistic models
- Semi-empirical models
- Empirical models

3.1.4.1. Mechanistic model

This is the model that describes the principles underlying the mechanism of the corrosion with high theoretical base. It does not use data from the oil and gas field operation as its base. This models can easily be compared with a well define experimental data as long as there is set boundary. It is mostly developed from laboratory works in university and organization with little input from the actual field data. The constants in these models are always having real literature meaning though a few can be obtained by comparing them with existing data. This is because it is based on the theory and principals of corrosion. The constant and variable in this type of model can easily be adjusted to fit in changes and variation for different conditions and situation.

The first of this type of model was propose by de Waard-Milliams [36] and was widely accepted for most of the CO_2 predictions for carbon steel. They base their model on the direct reduction of H_2CO_3 for the cathodic reaction. They used this in their equation which relates the corrosion rate with temperature along their predictive tool (Nomogram) [36, 53]. This model has now evolved to a semi-empirical model since 1991 where additional correction factors were added to improve the model.

Nesic et al. [32] in their own presented another electrochemical model for CO_2 corrosion prediction. They used constants from literature and from their various rotating cylinder glass experiment. Their values and outputs compare favourably with Gray et al. [38] and also gives good result with independent pipe flow experiment. it also compare well with Dugstad empirical model and de Waard et al modified models (semi-empirical model) [66, 67].

The electrochemical models described above by Nesic et al. [32] uses the formula below to derive the cathodic current (i_c). The formula uses the parallel resistance combination method to get total cathodic current (i_c). Parallel resistance model assumes that the voltage across a set of resistors in a circuit is equal. To get a single resistor or current that represent the combine resistor or current in the circuit, the inverse of the resistor or current are then summed up. The total cathodic current i_c is given as

$$\frac{1}{i_c} = \frac{1}{i_{ct}} + \frac{1}{i_{lim}}$$ 3-31

Where i_{ct} is the charge controlled process and is derived as

$$i_{ct} = i_o \cdot 10^{-\eta/b_c}$$ 3-32

Where i_o is the exchange current density,

      b_c is the cathodic Tafel slope constant,

      η is the over-potential as previously describe.

And the i_{lim} is the limiting current control and for H$^+$ the limiting current for mass transfer of the hydrogen ion to the surface of the metal cathodic region is given as

$$I^d_{\lim(H^+)} = K_m F \cdot [H^+]_b$$ 3-33

Where K_m is the mass transfer coefficient and F is the Faraday constant, while (H$^+$)$_b$ is the bulk concentration of the species of hydrogen ion.

And the limiting current control for carbonic acid as a result of the hydration of the CO_2 occurring slowly is given as

$$I^d_{\lim(H_2CO_3)} = F \cdot (CO_2)_b (D_{H_2CO_3} K_{hyd} K^f_{hyd})^{0.5}$$ 3-34

George et al. [68] extended the above proposal to take into account the effect of acetic acid for the mass transfer limit.

$$I^d_{\lim(H^+)} = K_m F \cdot [HAc]_b$$ 3-35

Where $[HAc]_b$ is the bulk concentration of acetic acid and

      K_m here is the transfer coefficient of the HAc in m/s

Nesic et al. [21, 32] proposed that when H_2O is involved there is no limiting current like that of Hydrogen ions and carbonic acid. The Tafel slope for the anodic process involving iron (Fe) was taken close to the corrosion potential. The anodic current was given as

$$i_a = i_{o(Fe)} . 10^{\eta/b_a} \qquad\qquad\qquad 3\text{-}36$$

The corrosion current and potential are then determined by equality of the total cathodic current to the anodic current (i.e. $\sum i_c = i_a$) . The corrosion rate can then be easily calculated from the anodic current when it is equal to the total cathodic current.

The problem with the above type of electrochemical model is the ignorance of the chemical and transport process which can give a detail contribution to effects such as protective scale that can be formed during corrosion process. A mechanistic model based on transport process and electrochemical process was developed to cover the neglected transport and chemical process. A simple overview of this process is described

The main equation which describes the transport effect is written below [69]

$$\frac{\partial(sc_j)}{\partial t} = \frac{\partial}{\partial x}\left(\varepsilon^{1.5} D_j^{eff} \frac{\partial c_j}{\partial x}\right) + \varepsilon R_j \qquad\qquad\qquad 3\text{-}37$$

Accumulator   Net flux   Source or sink due to chemical reaction

Turgoose et al. [46] was among the first to propose a more realistic approach with the use of transport model. Their model was improved by Pots [70, 71] who made sure that the electrochemical process was not oversimplified while trying to implement the transport model as seen in the case of Turgoose et al. [46] The model is based on the fact that some species like hydrogen ion is reduced at the metal surface while species like iron (ii) are produced at the metal surface. This inevitably

54

means that some species will diffuse in while others will diffuse out due to the concentration gradient that exists on the surface.

Due to the changes that are involved in the transport process, analysing it will need boundary condition. The boundary conditions may be set for at the steel surface and the other for the bulk solution [69]. The transient nature of the transport equation also makes it necessary to define the boundary conditions such as at the beginning of the corrosion process when there is no film on the metal surface. Solving the transport at any time enables the corrosion rate to be determined.

In a further work by Philip L.Fosbø et al. [3], they argue on the ideal nature of using diffusion of the EAS in the corrosion of carbon steel. This they show were prone to errors as the practical fluid are non-ideal in nature. They introduce an activity coefficient for the diffusion process since the electrolyte in corrosion is non-ideal.

A selection of some mechanistic models are shown in Table 3-1

3.1.4.2. Semi-empirical models

The semi-empirical models were mostly developed primary from the original mechanist model of de Waard [53]. de Waard and Milliams [53] modified their previous mechanistic model to take into account the new wave of experimental details which emerge. They recalibrated the existing constant to take into considerations these effects. They also improved the models by adding correction factors to take into account the missing or additional effect of some variables. Dugstad [33, 50, 66, 72] experimental works was one of the major work used in the improvement of the de Waard models. Figure 3-1 shows a typical nomogram used by de Waard and Milliams [53, 67] to predict corrosion.

The equation that relates the corrosion rate, partial pressure of CO_2 and the temperature along the nomogram is given as

$$logV_{nomo} = 7.96 - \frac{2320}{T+273} - 5.55 \times 10^{-3}T + 0.67logp_{CO_2} \qquad \text{3-38}$$

Where $logV_{nomo}$ is the corrosion rate and T and p_{CO_2} having their previous definition.

Table 3-1 : Mechanistic models of CO_2 corrosion of carbon steel (Here + means model include this, - means model does not include, ± means model only available to consortium members and (*) information not available or cannot be obtained.[3]

Developers	Published	Publicly Available	Model Name	Software	Surface model	Porous Scale	Diffusion	Bulk
Turgoose et al	1990	-	(M1)	-	RDE	-	Fick	S
Nesic	1993	-	(M2)	-	DCVB	-	Fick	C
Crolet et al	1993-98	-	(M3)	-	*	+	Fick	S
Pots	1995	-	(M4)	+	VB	-	NP	C
Dayalan et al	1995-98	±	Tulsa/ SPPS:CO_2(M5)	+	VB	-	CC	C
Sundaram et al and High et al Kvarekvai	1996-00	-	Dream(M6)	-	VB	+	NP	AC
Zhang et al	1997	-	(M7)	+	DCVB	-	Fick	C
Rajappa et al	1997	-	(M8)	-	VB	-	CC	AC
Wang and Postlethwaite	1998	-	M9)	-	*	+	CC	AC
	1998-01	-	(M10)	-	VB	-	Fick	C
Anderko et al	1999	+	Corrosion Analyze (M11)	+	VB	+	CC	AC
Nesic et al	2001-03	-	KSC (M12)	+	VB	+	MP	C
Wang et al	2002	-	(M13)	-	VB	-	CC	C
Nesic et al	2002	±	MULTICORP(M14)	+	VB	+	Fick	C
Heppner et al	2003	-	(M15)	-	VB	-	NP	AC
Nesic et al	2004-05	±	WWCORP (M16)	+	VB	+	Fick	C
Song et al	2004-05	-	(M17)	*	VB	-	Fick	C
Nesic et al	2008	+	FREECORP(M18)	+	*	*	*	*
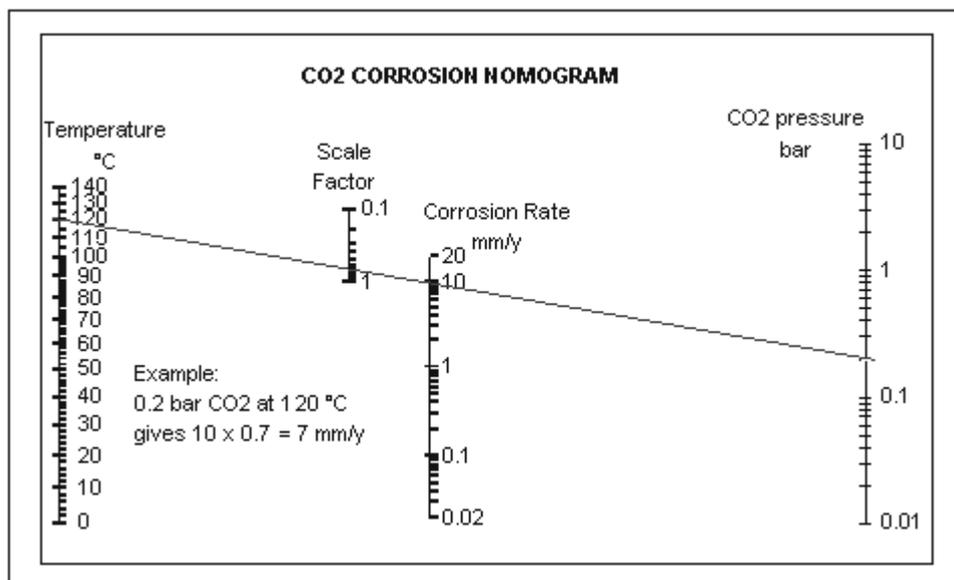
Figure 3-1 : de Waard and Milliams CO_2 corrosion nomogram for predicting [53]

The values of the temperature in their equation were derived from the temperature relation in Arrhenius type of equation that relates control by charge transfer. The 0.67 in front of the pCO_2 was determined by the assumption that pH is a function of only the available H^+ from the carbonic acid.

This equation of de Waard may give a good corrosion rate for most condition but still has flaws on its own. Some of the flaws are that in actual situation the pH is not just control by the H^+ ion present but by other electrochemical active species (EAS) that may be present in the solution. The controlling factor of the corrosion in some cases may be mass transfer and not charge transfer as assumed by their equation. Typical example of a shift from charge transfer to mass transfer was seen for works by Farelas et al. [62] were the corrosion rate was high as expected at 80°C but reduced drastically when iron carbonate films were formed. Also the assumption that Bockris et al. [30] proposition for the corrosion reaction which the used for temperature effect does not hold in all situation as presented earlier in the previous section.

Corrections have been applied to this equation to make compatible with current issues that arise due to environmental condition of the corrosion reaction. Dugstad et al. [66] have done some experiment and have applied their result to improve the equation. But this tends to make the equation more semi-empirical than mechanism.

Researchers have made a lot of effort to achieve a better electrochemical model that involves the mechanism of CO_2 of steel. Gray et al. [39] model involves a number of mechanisms of CO_2 corrosion which the derived through their glass cell experiment. The encompasses a complete range of parameter such as pH 2-11, and temperature 25°C to 125°C which look non practical and such make the model look too simple in some area. Key factors which were omitted in the de Waard and William which is the formation of protective film was also neglected.

The original works of de Waard were improved using a correction factor for protective films. The correction factor was base of Ikeda et al work [52]. Here a multi-dimensional regression analysis on high temperature CO_2 corrosion of steel experiments by Ikeda et al was used. Though this was a good approach the problem lies that the initial results were based on the activated controlled corrosion rather than on both diffusion and activation controlled process as previously described by Nesic et al. The correction factor was also added to take into account the effect of pH on corrosion rate.

The effect of velocity was added by using the electrical circuit model addition. The equation is showed below

$$\frac{1}{V_{cor}} = \frac{1}{V_r} + \frac{1}{V_m}$$
<div align="right">3-39</div>

Where the first terms give the rate of electrochemical process and the second gives the mass transfer effect.

Water wetting factor was used to account for the effect of hydrocarbon oil on the corrosion rate [73]. Wicks and Frasers [74] using their experiment results proposed that oil- wetting effect can occur for value less than 30% of the water cuts only. This has been proven otherwise since data from oil field has suggested that corrosion occur at cut off of 2% and corrosion effect was less noticeable for cut off of 50%. The reason may be the differences in the type of hydrocarbon oil and also the effect of pipe geometry and other factors not considered. All this can affect the minimum water cut off requirement.

The model of de Waard later improved in 2001 and 2003. The effect of water cut off was modified by considering the point in which the emulsion breaks. They took into consideration the interfacial tensions that exist for the steel, oil and water system. This really agreed well with the field data that was compared with it. The only problem is that it becomes empirical and such cannot be easily extrapolated to take into account different environment condition.

Other semi-empirical models do exist and a summary of some of them are given in Table 3-2.

Table 3-2 : Semi-Empirical models of CO_2 corrosion of carbon steel. (Here + means model include this, - means model does not include, ± means model only available to consortium members and (*) information not available or cannot be obtained[3]

Developers	Published	Publicly Available	Model Name	Software
De Waard and Milliams	1975	+	Shell 75(S1)	-
Crolet and Bonis	1985-91	-	CORMED (S2)	*
Simons et al	1987	+	Shell 87 (S3)	-
Dugstad and Videm	1989	+	(S4)	-
Fang et al	1989-04	+	(USL) or (ULL) (S5)	+
De Waard et al	1991	+	Shell 91 (S6)	-
Efird and Jepson	1993-97	+	(S7)	-
De Waard and Lotz	1993	+	Shell 93 (S8)	-
Dugstad et al	1994	-	IFE (S9)	*
De Waard et al	1995	+	Shell 95 (S10)	-
Markin	1996	+	(S11)	-
Gulnatun	1996-00	-	LIPUCOR (S12)	+
Srinivasan et al	1996-03	+	PREDICT (S13)	+
Mishra et al	1997	-	(S14)	-
Halvorsen et al	1998-05	+	NORSOK m-506 (S15)	+
Gartland et al	1998-99	+	CorPos (S16)	+
Sridhar et al	1999	-	(S17)	*
Nordsveen et al	1999-00	-	OLGAS-de	+
Hedges and Mc Veigh	1999	-	Waard (S18)	+
Kapusta et al	2001-06	-	Cassandra (S19) HYDROCOR (S20)	+
De Waard et al	2001-03	-	(S21)	-
Vitse et al	2002	-	(S22)	*
Smith and de Waard	2005	+	EFE (S23)	+
Teevens and Sand	2005-08	+	(24)	+

3.1.4.3. Empirical models

One of the most popular empirical model is that developed by Dugstad et al. [34, 75]. Here the used a series of correction factor and equation to develop the model. The used a temperature–dependent equation which they added to it the effect pH, velocity, partial pressure of CO_2 (pCO_2) and steel alloying in the case of Cr content. The equation assumes a maximum at high temperature. This model is the basic for the popular NORSOK model which is commonly used for corrosion prediction and analysis. The NORSOK model is taken as a standard by the Norwegian oil industry [34].

Other empirical models existed such as that developed by Adams et al. [76] using a linear multiple regressions that included a lot of variables. The problem is that corrosion is so complex to be predicted using a linear approach.

Nesic et al. [32] proposed a nonlinear approach unlike the Adams linear approach. This was based on neural network and not on linear multiple regressions. This eliminates the problem encountered with the use of Adams et al. [76] model while giving a good result. The disadvantage being that as an empirical model, it cannot be easily modified or extrapolated to fit outside the available criterion.

The difference between the empirical model and the semi-empirical model is that the empirical model is not based on corrosion theories but only on field/laboratory data, mathematical equations and empirical correlations. This poses a limit to extrapolating the model to areas where the initial range of data does not cover. While the semi-empirical models are based on both corrosion theories and laboratory/field data inputs which also uses mathematical equations and empirical correlations. This makes it friendlier in extrapolating using correction factors.

Table 3-3 : Empirical model of CO_2 corrosion of carbon steel. (Here + means model include this, - means model does not include, ± means model only available to consortium members and (*) information not available or cannot be obtained, DB means data base driven, NN means Neural Network model, Diagram means Model by nomogram approach [3]

Developers	Published	Publicly Available	Model Name	Software	Surface model
Townshend et al	1972	+	(E1)	-	Diagram
Gatzke and	1983-90	+	COPRA (E2)	-	Non linear
Hausler	1987	+	USL (E3)	-	Non linear
Bodegom et al	1992	+	(E4)	-	Statistical
Morrison	1993-94	+	USL Model F(E5)	-	Non linear
Adams et al					
Walter et al	1994	+	(E6)	-	Linear
Lule and Schutt	1998	+	(E7)	-	Non linear
John et al	1998	+	SweetCor (E8)	-	Non linear
Cottis et al	1999	-	(E9)	-	NN
Nesic et al	1999-06	-	(E10)	+	NN
Sridhar et al	2001	+	(E11)	-	Non linear
Sinha and	2002	*	(E12)	+	NN
Pandey	2007	-	CBR-TS (E13)	+	DB
Khajotia et al					

3.1.5. Factors that affect CO_2 corrosion prediction

The prediction of CO_2 corrosions is crucial because wrong prediction can give erroneous result in real life situation. Good prediction will have to involve taking into consideration most parameter that can affect the result in a practical situation. The major factors that affect CO_2 Prediction in the oil and gas industries are namely: Solution chemistry, In-situ pH value, pCO_2, Protective films, Temperature, Flow velocity /flow type, Steel type and Microstructure, Glycol, effect of Partial pressure H_2S, effect of partial pressure of HAc. All these factors are interdependent with each other and can affect the corrosion processes. The above factors will be discussed briefly

- **Solution Chemistry:** The effect of the solution chemistry is very important. The amount of chemical species that are in the solution will affect the corrosion reaction. In some case the solution chemistry might contain few species like CO_2, H_2CO_3, HCO_3^+, Fe^{2+} and H^+ for CO_2 corrosion in

61

condensed water form during natural gas transportation. While in some cases there will be a lot of chemical species which then makes the solution chemistry complex [21]. This is seen in the case of crude oil transportation with formation water, where the species can transfer to the water phase. The possible chemical species that can occur in a sweet environment are dissolve carbon dioxide, Hydrogen ion , Carbonic acid, Bicarbonate ion, Carbonate ion, Sodium ion, Chlorine ion, Magnesium ion, Calcium ion, Potassium ion, Barium ion, Hydroxide ion, Iron ion, Strontium ion , Acetate ion, Sulphate ion, Bisulphate ion, Acetic ion and Chloride [21].

- **In-situ pH Value:** The pH value of the solution affects the CO_2 corrosion of steel. The value of the pH to a great extent controls the cathodic rate determining step [39]. It also affects the formation of protective film on the surface of the metal. An increase in pH from 4 to 5 will only decrease the solubility of iron ions (Fe^{2+}) by 5 times but For pH 6 and above, the solubility of iron ion (Fe^{2+}) will drastically reduce about 100 times therefore encouraging precipitation of the iron carbonate [35, 77]. This in effect will make iron carbonate film to be deposited on the metal surface forming a barrier to chemical species that can cause corrosion. For pH < 5 the solubility of iron ion (Fe^{2+}) is high and there is a less chance of having protective iron carbonate forming on the surface of the steel.

- **Partial pressure of CO_2:** The partial pressure of carbon dioxide is of immerse important. High partial pressure of CO_2 will led to more CO_2 dissolving in the solution to form the carbonic acid. The carbonic acid will encourage and increase the rate of the cathodic reaction. This is in a free film corrosion point of view will ultimately led to an increase in corrosion rate [21].

  Conversely in a film forming corrosion reaction, the increase in the partial pressure of CO2 will lead to the formation of more iron carbonate. This will in turn increase the chance of more iron carbonate film forming on the surface of the metal.

- **Protective film:** The formation of protective film is very important since it reduces the rate of corrosion of the metal. When uniform iron carbonate films are formed at the surface of the metal, they tend to form a barrier for

the chemical species from the solution to reach the cathodic site of the metal surface. This in turn reduces the cathodic process and makes the general corrosion rate to reduce [22, 33, 78, 79].

There are different types of films which may form on the surface of a CO2 corroded carbon steel namely transparent films, iron carbide (Fe_3C) films, iron carbonate ($FeCO_3$) and iron carbonate plus iron carbide ($Fe_3C + FeCO_3$) films. The property of the film formed and in some case the thickness determines how protective the films may be to corrosion attack [35].

Transparent film is formed at lower temperature and is less than 1μm thick. This contains mostly iron and oxygen and is usually unprotective. Iron carbide (cementite) are formed when the corrosion of the ferrite part of the carbon steel leaves behind a formation of iron carbide on the surface in a non -buffered solution. This film is not a protective film and in some case can increase corrosion rate due to galvanic reaction. A description of the protective and non-protective film is describe in Figure 3-2
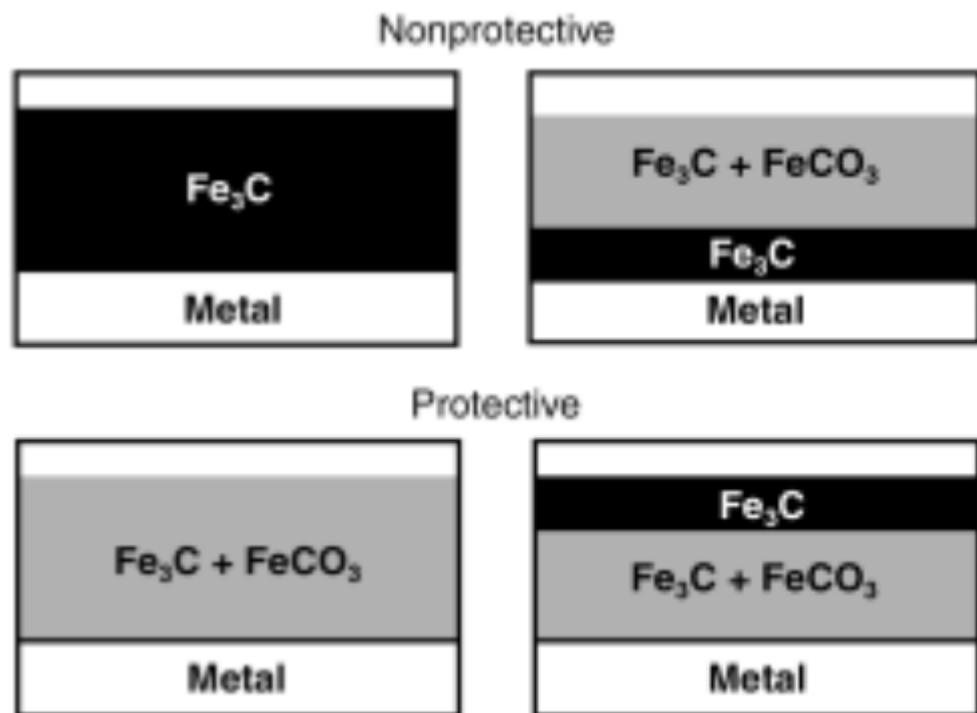
Figure 3-2 : Different morphologies observed for protective and non-protective corrosion layers [65]

Protective film of iron carbonate is formed when a favorable condition leads to high super-saturation of $FeCO_3$. This films forms in two processes of nucleation and particle growth which often determine the morphology of the film. The formation of $FeCO_3$ film directly on the surface of carbon steel often gives a protective film. Here the $FeCO_3$ forms directly on the surface and integrate with the Fe_3C to form a protective layer. Another type of protective film may be form with a combination of $Fe_3C + FeCO_3$ where the $FeCO_3$ is formed directly on the surface and is seal by the Fe_3C on top [65]. Where the Fe_3C forms first with a subsequent layer of $FeCO_3$ the films are non-protective [80].

a   b
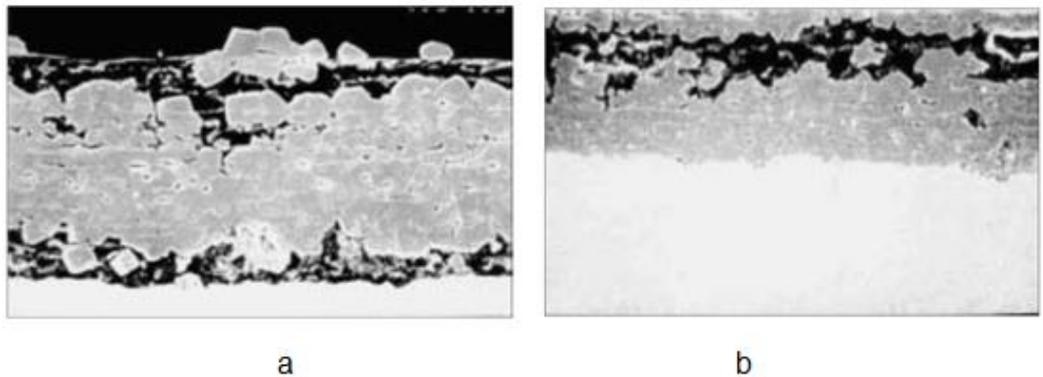
Figure 3-3 : Typical film formation on the surface of the steel a) siderite partial sealing the surface with an already formed iron carbide forming a non-protective layer [80] b) iron carbide layer sealed by siderite forming protective layer [33, 65]

When unprotective non uniform films are formed, the metal surface will not be protected fully and in some case localized corrosion will formed. This is so because the exposed part of the metal from the film will form the anodic side to the film which will act as the cathode and lead to localized corrosion [28, 65].

- **Temperature:** From Arrhenius equation

$$K = Aexp^{\Delta E_a^\circ/RT} \qquad\qquad 3\text{-}40$$

Where k is the rate coefficient, A is a constant, ΔE_a° is the change in the standard activation energy, R is the universal gas constant, and T is the absolute temperature in Kelvin.

It is expected that an increase in temperature will increase the electrochemical and chemical reaction of metal. The temperature of the environment at which the corrosion reaction occurs will affect the rate of corrosion. It assumes that an increase in the temperature will increase the reaction rate and even the mass transportation and hence the corrosion rate of steel. The increased corrosion rate is normally seen in situation where the pH is low and there is no formation of protective film. This is not always the case due to the formation of protective iron carbonate film. At high temperature the solubility of iron carbonate reduces and this will lead to the formation of protective iron carbonate film or other films on the surface of the metal [22]. This in turn will reduce the corrosion rate of the metal. The corrosion rate tends to reach maximum at temperature between 60°C to 80°C.

- **Flow velocity and multiphase flow type:** The flow and flow velocity of the corroding system affects the corrosion process in two ways [21]. For the process which do not produce protective films on the metal e.g. in condensed water situation where the pH is low with no film being form. In this case the flows increase the mass transfer of the reactive species to and from the metal surface. This in turn will increase the corrosion rate of the system.

  On the other hand for film forming surface and the use of inhibitor the flow velocity does not really affect the rate of mass transfer of the species to the metal surface. In the film forming or inhibitor system the flow interrupt with formation of the film on the metal surface [81, 82]. High flow velocity will tend to remove the film formed on the surface.

  Multiphase flow system which is usually applied in the oil and gas industry is common and this makes the transportation of oil and gas to have two or three phase flow conditions. The flow pattern commonly involve is slug, annular and stratified flow. The different flow pattern will brings about different wetting mechanism on the metal surface. This in general can affect the corrosion process and rate. More so, where no protective films are

65

formed, multi-phase flow system will bring about changes in mass transfer rate (especially for slug flow pattern). Pots et al. [71] has done some studies on the mass transfer in multi-phase system and propose a flow pattern model. While Jepson et al. [83] suggested that Froude number is necessary to characterize the effect of multi-phase flow (especially slug flow pattern) for corrosion in sweet environment. Nesic et al. [32] on the other propose an integrated model for multiphase system that can be used to predict flow pattern, predict water entrainment/wetting and also calculated the associated hydrodynamic properties necessary for corrosion.

- **Steel type / microstructure:** The type of steel and microstructure can affect the corrosion rate. The variation in the steel microstructure can contribute to the corrosion of the steel. A steel structure with a lot of FeC compared to the ferrite will have micro galvanic reaction occurring. This is because the FeC will act as the cathode while the ferrite will act as the anode. This will lead to the dissolution of the ferrite material into the solution that will lead to localized corrosion,

  The driving force for corrosion is from the potential different between the heterogeneous areas of the metal. Heterogeneous within the microstructure are mostly caused by defects in the crystal structure, phase difference and metallic inclusion. This can also go a long way increasing the corrosion rate. A study by Al Hassan et al. [84] has shown that the microstructure and chemical composition of a steel contributes a lot in determine the corrosion rate and process.

  The inclusion of 0.5wt% to 3wt% of chromium can be beneficial in preventing sweet corrosion. The chromium forms a protective chromium oxide film on the surface which helps to reduce corrosion of the carbon steel [33, 85]. More so the composition of the steel microstructure can affect the adsorption of inhibitors and formation of protective films. The increase in the Chromium content leads to the formation of protective film but can as well not favour the inhibitor adsorption and performance. This effect of microstructure is complex and will need more research.

  Dugstad and Dronon [86] have shown that the type of steel affects the precipitation of iron carbonate on the surface using pH stabilization

technique. They showed that St.35 carbon steel encouraged the formation and precipitation of protective iron carbonate at 20°C which reduces the corrosion rate compared to X65 and 0.5Cr carbon steel which had no protective iron carbonate within the same period. Figure 3-4 shows the effect of the three steel types on the precipitation of protective iron carbonate film.

St.35, X500   X-65, X200   0.5Cr, X550
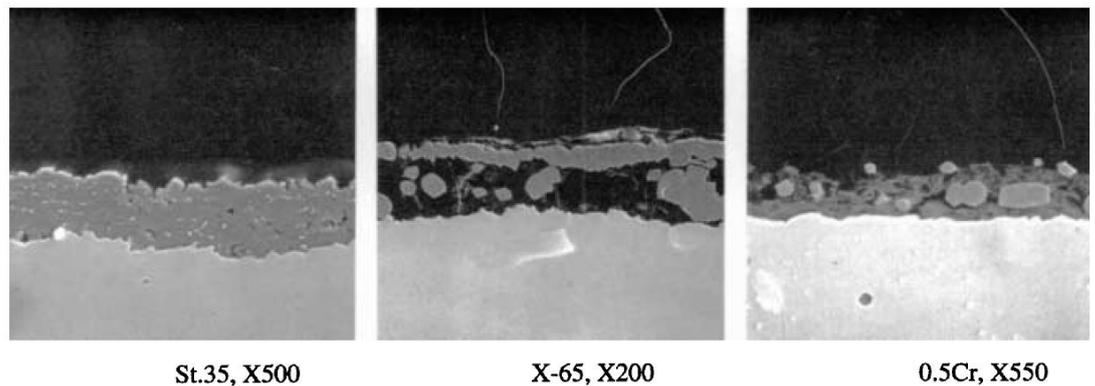
Figure 3-4 : Cross section of the corrosion films form on fresh ground specimens of steel under flowing conditions (3 m/s), 50% DEG solution,1% NaCl at pH 6.5, 0.6MPa CO_2, showing the effect of different type of steel [86].

- **Effect of H_2S:** The comprehensive knowledge of the effect of H_2S is not known yet. H_2S effect on CO_2 can have both negative and positive effect. A small trace of H_2S can be beneficial to the corrosion of the steel by forming protective film on the surface of the metal. On the hand, increase in the partial pressure of H_2S can lead to an increase in the corrosion rate. In some case the film form by H_2S is non-protective and can cause more harm. The non-protective film can set up a micro-galvanic cell which will lead to localized corrosion on the surface of the metal. More studies are needed to fully understand the effect of H_2S of carbon steel corrosion.

Effect of Glycol: Glycol is one of the chemical used in the prevention of hydrates in the oil and gas pipeline. The use of glycol can be beneficial to corrosion prevention. The effect of glycol can be seen in the reduction of water activities by making less water available for corrosion reaction [87]. The effect depends a lot on the quantity of glycol present in the solution. In

most case where glycol serves as a hydrate inhibitor and corrosion inhibitor, a minimum of 50% mass concentration of glycol is needed. In most gas pipeline glycol as high as 80%-90% mass concentration is injected into the pipeline system. The effect of glycol is seen in the de Waard's equation [87]. It shows that glycol reduces the corrosion rate to certain level. Table 3-4 gives the correction factor for difference mass % of water or MEG mass %.

$$Log\, f = 1.6(log(w\%)-2) \hspace{3cm} 3\text{-}41$$

$$Vw\% = f\, Vw\% = 100 \hspace{3.5cm} 3\text{-}42$$

Where f is the multiplier effect that gives the corrosion rate in w% mixture when multiply with the corrosion rate in a glycol free solution with same temperature, pH & partial pressure of CO_2. And w% is the mass % of water in the glycol solution. V is the corrosion rate [53, 87].

Table 3-4 : The correction factor for difference mass % of water or MEG mass %.

W% (mass % of water)	M%(mass % of MEG)	F(correction factor)
10	90	0.03
20	80	0.08
30	70	0.15
40	60	0.23
50	50	0.33
60	40	0.44
70	30	0.57
80	20	0.70
90	10	0.84
100	0	1

- **Effect of Acetic acid (HAc):** HAc is an organic acid which is weak but stronger than carbonic acid. Hedges and Mc Veigh [88, 89] gave a report that reaction at the cathode is increase with the presence of HAc. Sun et al. [90] also presented a study which shows that HAc effect is on the cathodic reaction. George et al. [91] reported that un-dissociated HAc is much harmful and contribute a lot to the corrosion rate. They also show that the effect of HAc is particularly harmful at high temperature and low pH. Theoretically iron acetate is expected to precipitate on the surface of the metal, but this does not happen in practices mostly because of the high solubility of iron acetate. The presence of HAc has been seen to affect the formation of iron carbonate on the metal surface. Recent study shows that the prevention of the iron carbonate forming is likely due to a reduction in the pH of the solution that undermined the formation of iron carbonate [92-94].

3.2. MonoEthylene Glycol (MEG) in the oil industry

The search of oil and gas is moving to offshore and deeper reservoirs to produce more products. This extreme environment encourages/facilitates hydrate formation, scaling and corrosion of oil and gas facilities/structures and hence requires the adequate measures. In order to prevent the above, series of measures are applied such as the use of corrosion inhibitors, scale inhibitors, hydrates inhibitors or combination of one or two of the measures. In this study MEG which is used as a hydrate inhibitor in the oil and gas industry is considered.

3.2.1. An overview of MEG properties and applications

MEG is one of the chemicals used as a hydrate inhibitor owing to some of its properties [95, 96]. The specific properties that make MEG a good hydrate inhibitor will be discussed later.

The properties includes [97]:

Chemical formula = $OH-CH_2-CH_2-OH$

Melting temperature = -13.0°C

Boiling temperature $= 197.6°C$

Molar mass $= 62.07 \text{gmol}^{-1}$

Density at $20°C = 1.1135 \text{g/cm}$

Solubility in H_2O = highly soluble.

Vapour Density $= 2.14$
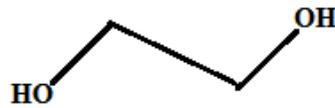
Figure 3-5 : Chemical structure of MEG showing two hydroxyl groups at both ends.

In the oil and gas industry, multiphase transportation through carbon steel pipelines is commonly apply to reduce cost especially from offshore oil source [95]. This has led to transportation of corrosive fluids and wet gases through pipeline. The water from the natural gas is not entirely removed due to the cost, safety and difficulties of doing it at the production site. Besides, water exists from gas condensation due to the temperature drops along the line.

Experiment and field observations have shown that hydrates can begin to form from temperatures below $20°C$ depending on the pressure of the gas mostly from 30 bar and above [98-100]. The hydrates themselves are stable at a much lower temperature that can be higher than the freezing temperature of water (i.e. $0°C$). This hydrates are formed from water and low hydrocarbons (C_1 to C_4) or/and CO_2, H2S [101-104]. There are three types of hydrates that can easily be formed of which two types are common in the oil and gas industries. The first of the common ones involves water molecules with methane or ethane and the second one involves the first type with addition of propane and iso-butane. This hydrate can form plugs which stop the flow of fluid and are difficult to remove [105]. To avoid this and shutdown of the flow line, the use hydrate inhibitors are employed. Methanol, MEG and DiEthylene Glycol (DEG) has been applied for a long time in the oil and gas industry to prevent hydrate formation [106]. Figure 3-6 shows a typical hydrate that was formed on a subsea pipeline

Figure 3-6 : A typical subsea pipeline plug by hydrate formation [105]

Other type of inhibitors like Low Dose Hydrate Inhibitors LDHI that requires lower dosage is also considered [101, 102, 107]. Health and safety reason has led to the less use of methanol because of its toxic nature. Methanol also cause more salt precipitation than MEG which can lead to scaling, for this reason MEG is generally preferred to Methanol [2]. MEG is a thermodynamic hydrate inhibitor. It does so because of its solubility/miscibility with water at all ratios and its synergist reduction effect on the freezing point of MEG/Water mixture. The freezing temperature of MEG is less than that of water (i.e. -13°C for MEG compared to 0°C for water) and when mixed with water the freezing temperature is even lowered. This is why MEG is used as anti-freeze not just in the oil industries but at other industry like the automobile industry. MEG reduces the formation and stability of hydrate by occupying the lattice space in water and reducing the freezing temperature. Since it is highly miscible with water, it displaces other hydrate forming hydrocarbon and molecules like CO_2 and H_2S. Application of MEG is also favourable because it can easily be recycled by regenerating at the process plant during production [77, 108]. This is done by the use of boilers and storage tank at the process plant usually on shore to heat up the water/MEG mixture and then it is stored and re-pumped into the

system. MEG, though toxic does not evaporate easily so can be worked with less or no harm to the body unless ingested [2].

MEG is normally introduced at the upper end (inlet) of the multiphase natural gas pipeline at high temperature of 80°C to 90°C. The concentration of MEG at this point is very high and can be in the region of 80% to 90% mass concentration referred to as Lean MEG [3]. It is called lean MEG because the amount of water it contains at this high concentration of 80% and 90% MEG is very small compared to the MEG. The temperature gradient along the pipeline leads to condensation of water which can cause corrosion and hydrate formation.

Table 3-5 shows the synergistic effect of MEG as antifreeze in water.

Table 3-5 : Synergistic effect of MEG as antifreeze in water. MEG freezing point vs concentration in water [96, 109]

Mass Percent MEG (%)	Freezing Point (deg °F)	Freezing Point (deg °C)
0	32	0
10	25	-4
20	20	-7
30	5	-15
40	-10	-23
50	-30	-34
60	-55	-48
70	-60	-51
80	-50	-45
90	-20	-29
100	10	-12

Normally the additional condensation also reduces the concentration of MEG to about 50% MEG mass at the lower end (outlet). Though hydrates are unlikely to

form at the upper end (inlet) due to the high temperature, it is necessary to consider corrosion effect at the upper end (inlet) since the production source and temperature of MEG are usually high at that point. High corrosion rate may be obtained at this point due to the high temperature.

3.2.2. Effect of MEG on Corrosion of Carbon Steel

MEG has an effect on the corrosion of carbon steel. Generally, carbon steel corrosion (uniform corrosion) is reduced by MEG at ambient temperature and pressure [77, 87, 110-112]. The effect of MEG in combination of other materials and condition can be classified below.

- Concentration: The concentration of MEG/water affects the corrosion of carbon steel. High concentration of MEG up to 50% and more (i.e.50% - 90%) has an effective inhibiting effect on corrosion of carbon steel. The higher the mass% the more the uniform corrosion will be reduced [53, 87].

- Temperature: Temperature conditions with MEG affect the corrosion of carbon steel. The lower the temperature the more corrosion is reduced. The effectiveness of MEG in reducing corrosion as temperature changes needs to be studied since most of the test were carried at lower temperature below 40°C or in the presence of pH stabilizers for higher temperatures [53, 87, 113].

- Pressure (CO_2): The partial pressure of CO_2 at ambient condition affects the corrosion of mild steel. At CO_2 partial pressure of 0.1bar to 1bar, the corrosion rate of carbon steel is reduced in the presence of MEG. At high partial pressure of CO_2 the corrosion rate may not reduce [110].

- Pressure (H_2S): partial pressure of H_2S between 0.1bar-0.2bar with MEG and partial pressure of CO_2 0.1bar-1.0bar will reduce the corrosion rate and may also induce pitting/localized corrosion at a long period of time. Higher partial pressure of H2S and CO2 with MEG will cause more pitting/localized corrosion [108, 110, 114].

- pH stabilizers: The use of pH stabilizer in the presence of partial pressure of CO_2 (0.1-1bar) reduces the corrosion rate of carbon steel. pH stabilizers like MonoEthanolAmine (MEA) and NaOH has been found useful in this aspect [106]. But for higher partial pressure of H_2S and partial pressure of CO_2 the

mild steel is prone to localized corrosion and in some case the reduction in the uniform corrosion experience before might not be any relevant again [77, 108, 110, 114, 115].

- Iron and iron carbonate: MEG generally reduces the solubility of iron carbonates and increases its precipitation. Watterud et al. [116] were able to determine the effect of MEG on the solubility of iron carbonate. The went further to estimate the possible growth rate for iron carbonate in the present of MEG and concluded that increase in temperature increase the growth rate of iron carbonate. Their values are presented in Figure 3-7 and Figure 3-8. At high pH, the iron carbonate is precipitated and forms as protective cover for the mild steel [77, 117, 118]. The formation of protective iron carbonate at very low temperature of 20°C may not occur unless the pH of the solution is increase up to 7.4 [86, 106].
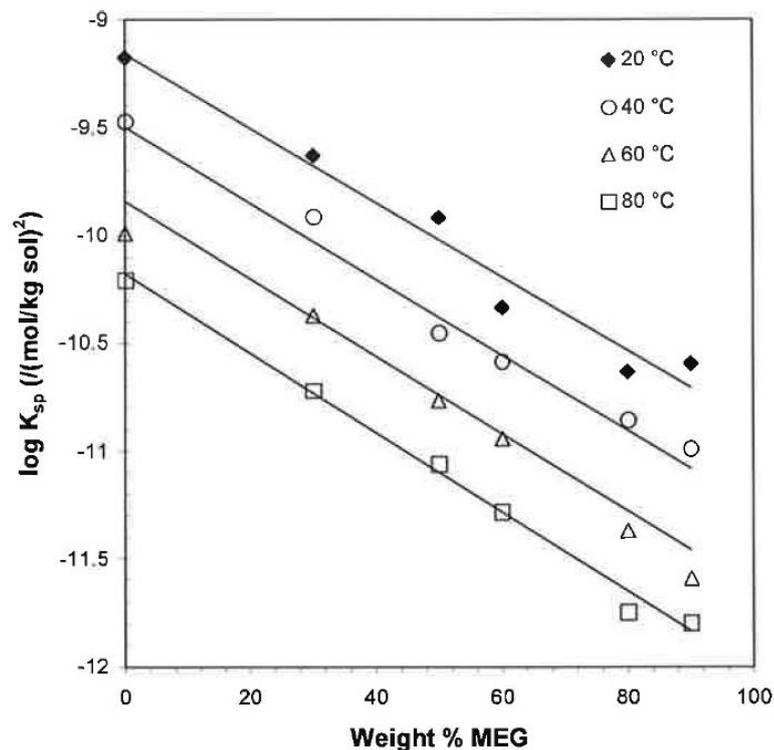
Figure 3-7 : The solubility product (K_{sp}) of iron carbonate in the presence of different MEG concentration and at different temperature [116]
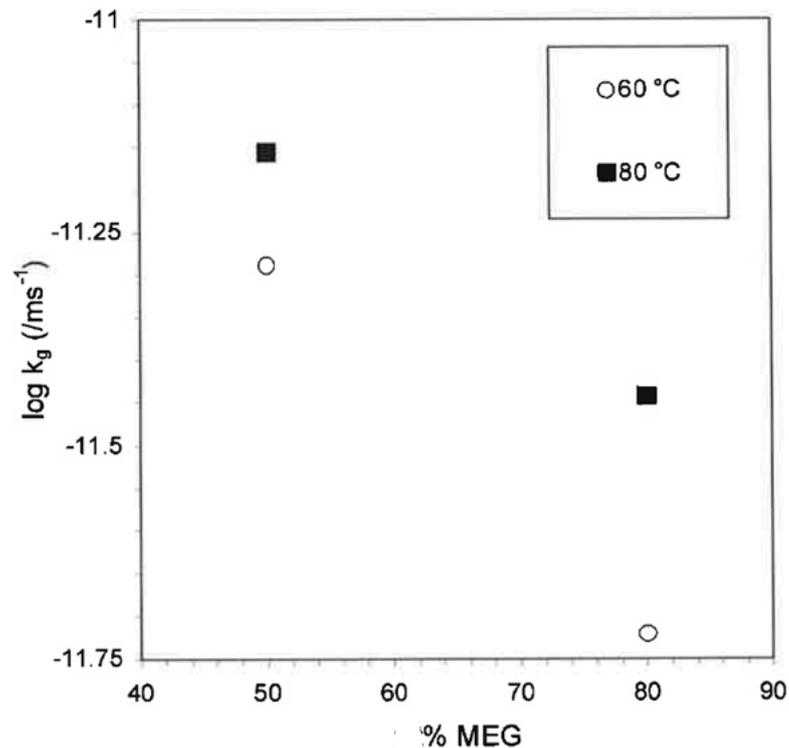
Figure 3-8 : Calculated growth rate for MEG-water mixtures [116]

- pH value: Low pH has a drastic effect on the carbon steel. A higher pH with MEG reduces uniform corrosion in mild steel. It has been observed that measured pH in the presence of MEG is about 0.2 higher than in the presence of only water/brine electrolyte. This shows that MEG increases the pH of the solvent and electrolyte slightly [115, 119].

- Flow velocity: The flow velocity with MEG in some case can affect the corrosion of mild steel. Studies show that stagnant flow in the presence of high partial pressure of H_2S and CO_2 can actually induce localized corrosion (pitting). Though more studies is needed to prove this [110].

- Inhibitors: Depending on the type of organic inhibitor though, most uniform corrosion of mild steel are reduce in the presence of inhibitor and MEG. In high sour condition the MEG may reduce the effect of some inhibitors. More studies are required in the area of MEG with organic inhibitors [87, 110].

MEG also has some effect on corrosion of mild steel by changing the water chemistry of solution. Lower brine concentration in the presence of MEG reduces corrosion. The viscosity of the solvent are generally increased by MEG

[87]. Experiments have also shown that the CO_2 diffusivity is reduced in the presence of MEG. The solubility of CO_2 and H_2S is slightly increased and this is shown in the slight increase in the Henry's constant when MEG is presence. Other salts solubility is reduced by MEG. Though there is a slight increase in the solubility of CO_2 and H_2S, its effect is annulled by the reduction of the first dissociation constant of the formed carbonic and sulphide acid. This effect reduces the amount of H^+ available for the cathodic reaction and hence reduces the corrosion rate of the carbon steel in the presence of MEG. Figures 3-9 shows Henry's constants for CO_2 and H_2S in MEG and DEG at different concentration.
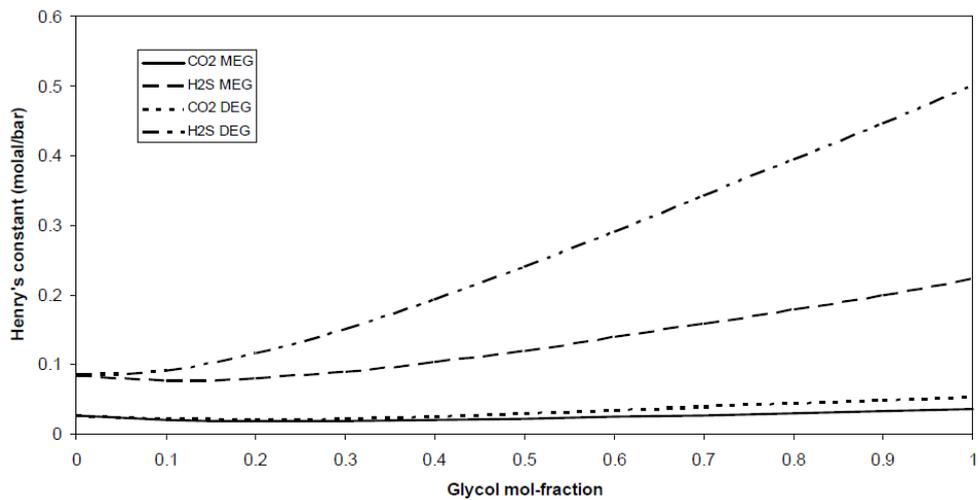
Figure 3-9 : Henry's constant for CO_2 and H_2S vs MEG and (DiEthylene Glycol) DEG concentration in a solvent at 25^oC and ionic strength =1 [19]

Figure 3-10 shows the first dissociation constant for CO_2 and H_2S in different concentration of MEG while Figure 3-11 shows CO_2 diffusivity in MEG and the solution viscosity of MEG and DEG at different concentration.
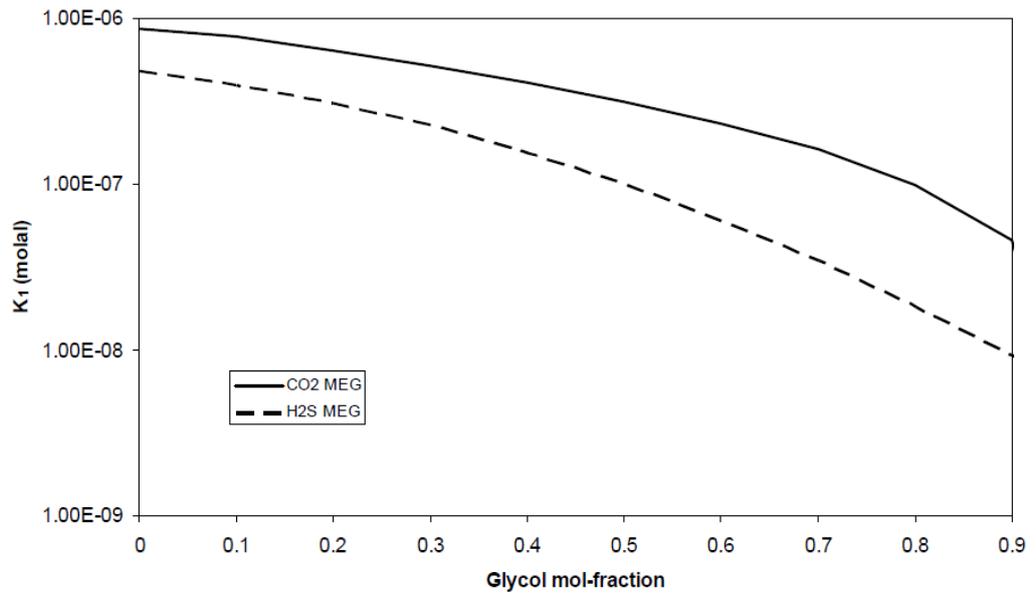
Figure 3-10 : First dissociation constant (K_1) for CO_2 and H_2S Vs MEG mol fraction at 25°C and ionic strength =1 [19]
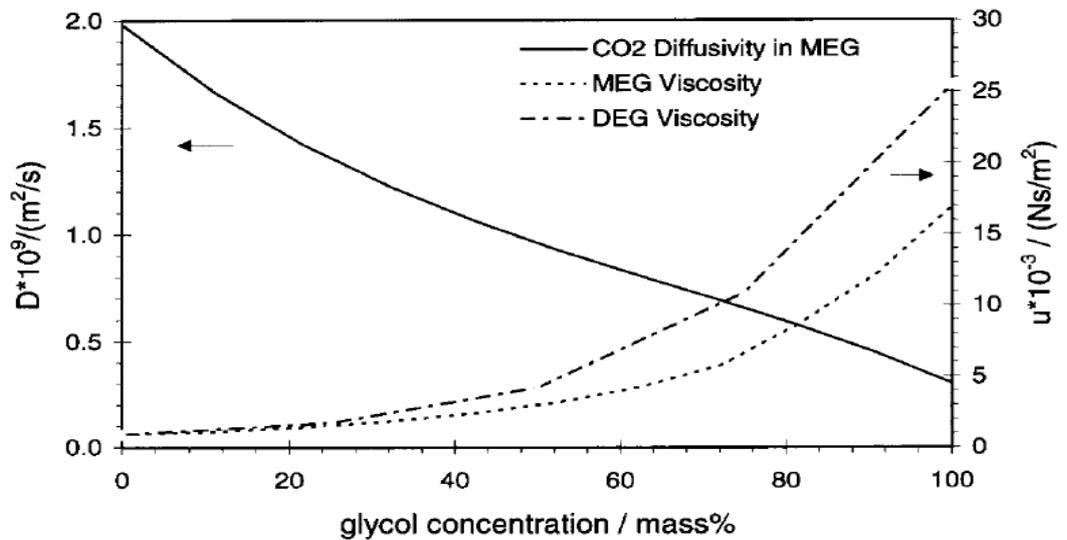
Figure 3-11 : CO_2 diffusivity (left) and solution viscosity (right) vs MEG concentration and DEG concentration at 25°C [52]

The reduction in the CO_2 diffusivity and the increase in the viscosity of MEG with increase in MEG concentration play a role in reducing the corrosion rate of carbon steel in MEG solution. More so, the reduction in the first dissociation constant (K_1) for CO_2 in MEG solution also reduces corrosion by reducing the amount of H^+.

3.2.2.1.   Corrosion reactions for CO_2 corrosion in MEG

The corrosion reactions in the presence of MEG are similar to the corrosion reactions in the presence of a simple brine solution. The corrosion reaction for CO_2 corrosion in MEG can be described as follows

$$Fe = Fe^{2+} + 2e^- \qquad\qquad\qquad\qquad\qquad\qquad\qquad 3\text{-}43$$

$$Fe^{2+} + CO_3^{2-} = FeCO_3 \qquad\quad (anodic) \qquad\qquad\qquad 3\text{-}44$$

$$CO_2 + H_2O = H_2CO_3 \ (K_H) \qquad\qquad\qquad\qquad\qquad\quad 3\text{-}45$$

$$H_2CO_3 = H^+ + HCO_3^- (K_1) \qquad\qquad\qquad\qquad\qquad 3\text{-}46$$

$$2H_2CO_3 + 2e^- = H_2 + 2HCO_3^- \ (cathodic) \qquad\qquad\quad 3\text{-}47$$
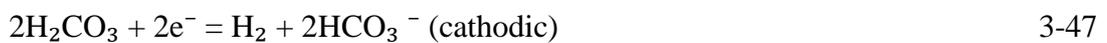
The reaction in the presence of CO_2 leads to the formation of iron carbonate at the anode and the liberation of hydrogen at the cathode.

3.2.3. Improving the corrosion of carbon steel in the presence of MEG

The corrosion rate in the presence of MEG may be more than 1mm/y and in some case up to 2mm/y. This corrosion rate in the presence of MEG alone is mostly unacceptable in the oil and gas industry as the maximum allowable corrosion tolerance of 0.1mm/y are often allowed for oil and gas pipeline [120]. There is need to improve the corrosion

The use of pH stabilization in improving the corrosion rate of multiphase natural gas carbon steel pipeline in the presence of MEG has been successful under some conditions. PH stabilization is a method that uses addition of organic or inorganic base to increase the pH of the multiphase gas pipeline with MEG to pH of 6.5 to 7.5 and encourage the formation of protective iron carbonate film on the carbon steel surface [77, 108, 110, 115, 121-123]. Possible organic base which has been used for pH stabilization method are mercaptobezothiazole salt (MBTNa) and Methlydiethanolamine (MDEA). Inorganic base of NaOH and $NaHCO_3$ can also be used to raise the pH of the gas pipeline to the desirable high pH. Troll gas pipeline project in the Norwegian oil and gas sector has used the $NaHCO_3$ as pH stabilization base [77]. In most sweet environment the use of the pH stabilization has been

successful in reducing corrosion but still may develop problems under certain condition. High sour environment (i.e. H_2S and CO_2 environment) may not find effective solution from pH stabilization method as this has led to localised attack on the surface of carbon steel [110, 114].

The used of pH stabilizers is mostly seen on the formation of bisulfide and bicarbonate with the compounds [111]. This increases the pH and thereby encourages the formation of protective iron carbonate and iron sulphide films. These protective films are attached on the surface of the carbon steel and serve as a diffusion barrier thereby reduces the general corrosion.

The equation below describes the formation of bisulphide and bicarbonate on addition of pH stabilizers (NaOH, MEA and MDEA). The NaOH reacts with CO_2 or H_2S to form bicarbonate or bisulphide as follows

$$CO_2 + H_2O + NaOH \rightarrow H^+NaOH + HCO_3^- \qquad\qquad 3\text{-}48$$

$$H_2S + NaOH \rightarrow H^+NaOH + HS^- \qquad\qquad 3\text{-}49$$
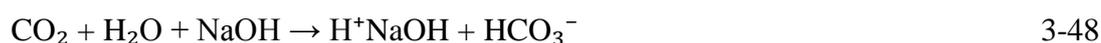
For the use of MEA or MDEA the reaction also give bicarbonate or bisulphide for CO_2 or H_2S respectively.

$$CO_2 + H_2O + MDEA \rightarrow H^+MDEA + HCO_3^- \qquad\qquad 3\text{-}50$$

$$H_2S + MDEA \rightarrow H^+MDEA + HS^- \qquad\qquad 3\text{-}51$$
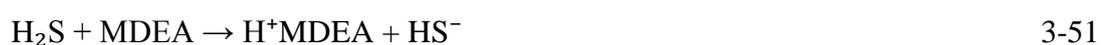
This reaction encourages the formation of protective film of iron carbonate and iron sulphide at low temperature and partial pressure of 1bar CO_2 and less than 0.2bar H_2S [114, 115, 124].

The pH increases reduce the corrosion rate but the chance of the formation of uncontrollable iron carbonate scale and other mineral scale in cases where high formation water are presence may occur. This may also lead to reduces flow pressure in the presence of iron mineral scaling [77, 118]. Likewise the condensation of the water along the pipeline which cause more corrosion will lead to the reduction of the high MEG concentrated solution refer to as lean MEG to lower MEG

concentrated solution refer to as rich MEG at the lower end (outlet) of the pipeline. This rich MEG usually contains dissolve corrosion products and iron concentration close to saturation. This dissolve corrosion product mainly iron saturated with respect to carbonate may precipitate at the high temperature reboiler section of MEG loop system to causes problems [118]. If the dissolve corrosion products on the hand find their way back into the MEG injection point, this will cause additional mineral scaling that will reduce the flow assurance in the pipeline.

A typical MEG recycling system is shown in Figure 3-12. It shows the basic units requires for a successful MEG application. In some situation reclaimer are used on the separation facility to remove the excess corrosion product before reclaiming back the MEG at the reboiler section. Formation of scaling may become detrimental in some situation with the use of pH stabilization that often reduces the solubility of most corrosion product. It may then become necessary to employ additional or alternative method to reduce corrosion problem and other corrosion related problem encountered by using pH stabilization method [113, 117, 123].
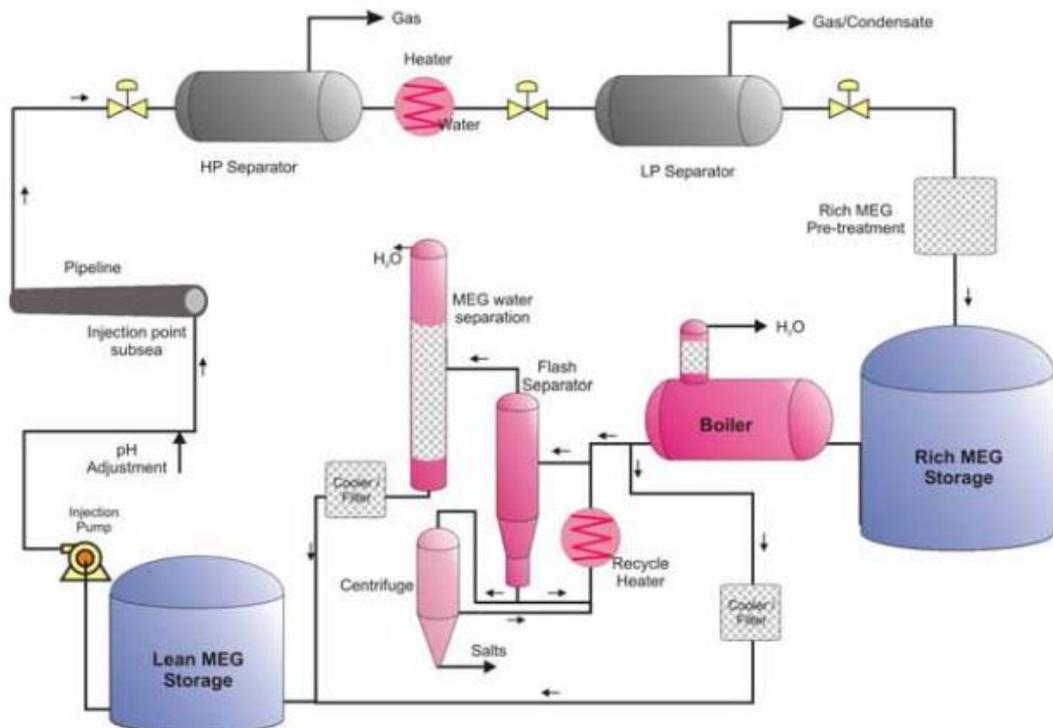
Figure 3-12 : Typical MEG loop system [118]

The use of organic corrosion inhibitors can help to reduce the corrosion rate of the carbon steel pipeline with and without pH stabilization [87, 117, 123]. The use of corrosion inhibitors should be tested against the conditions where it is to be applied. Such conditions as in the presence of MEG and at different temperature need then to be considered if effective improvement in the corrosion rate of carbon steel pipe are to be obtained. One research has given an idea that the presence of MEG has reduced the effectiveness of a certain corrosion inhibitor [101]. This may become significant in cases where the reduction is more. It may also be that corrosion efficiency of inhibitor is affected insignificantly but the formation of localised corrosion may then occur in the presence of the MEG. This questions need to be examined and answered inorder to effectively use a corrosion inhibitor in improving the corrosion rate of carbon steel in the presence of MEG.

3.3. Corrosion inhibitors

3.3.1. Type of inhibitors

Corrosion inhibitors can be defined as any chemical substances or chemical compound that can be added in minute quantity or concentration (typically part per million) to a corroding environment with sole purpose of decreasing the corrosion rate effectively [4]. Other definition has it that inhibitors are chemical substances /combination of substances when added in the adequate state and concentration in the environment, prevent corrosion of the metal without significantly changing the concentration of any other corrosive agent [17, 61]. Inhibitors can conveniently be classified into three types namely [4, 125]

1. Passivators,
2. Vapour inhibitors and
3. Organic inhibitors

In this study more focus will be directed to the organic inhibitors which are mostly applied in the oil and industry. But first the other type of inhibitors is described below together with organic inhibitors.

Passivators: The well-known passivators are inorganic substances that have an oxidising power. They passivators in most cases increase the potential of the metal to a more stable state. The increase to a more stable state can be in the range of tenths of volts. Common examples of passivators are chromates, molybdates, and nitrates. The mechanism of inhibition by passivators on metals is in their ability to act as depolarizers on the surface of the metal. The initiate high current density which normally exceeds the critical current density $i_{critical}$ for the passivation on the anodic sites [4].

Some other substances which reduce the corrosion rate but do not increase the potential of the metal to a more noble state more than a few milli or centivolts are not classified as passivator. Passivators have oxidising power and they are also readily reduced in the process. Substances which has only oxidising power and itself not easily reduces are not acceptable passivators e.g. ClO_4^-.

More so, the concentration of the passivator must reach a minimum critical level in order to effectively protect the metal by passivation. A concentration below the critical level will make the passivator act as an active site for corrosion rate to increase at local site e.g. pit site [4].

The major problem in applying the Passivators is the new law impose by a lot of state on the environment and health. Passivator of chromium (vi) has been found to form cancer on the human body. This has led to the reduction in the application of this type of passivator in some areas.

Vapour inhibitors: The vapour inhibitors are generally inhibitors with low but appreciable vapour pressure which can be release gradually inorder to prevent corrosion of some sensitive part [126]. It can easily be applied and are used for the prevention of corrosion at places like the critical machine parts. It can have a disadvantage of dis colouring some of the plastics part near the machine part. The mechanism of vapour has been assumed to be of film forming type on the metal surface. The film forms a protective cover for water and oxygen which act corrosion agent.

Dicyclohexylammonium nitrile, cyclohexylamine and ethanolamine carbonate are examples of vapour inhibitors. The worked by slowly releasing their vapour onto the

metal part which needed to be protected. The release product saturates the air around it and makes it non corrosive.

Organic inhibitors: Organic inhibitors are film forming substance which adsorbed on the surface of the metal. This type of corrosion inhibitors is mostly applied in the oil and gas industry to prevent the internal corrosion of carbon steel pipeline [127]. The film form on the surface of the metal which is mostly monolayer in thickness prevents the dissolution of the metal in the solution and also the hydrogen ions discharge. Some of the organic inhibitors acts on the cathodic process and in general reduce the corrosion rate while some organic inhibitors act on the anodic process and effectively reduces the corrosion process. There are also some inhibitors which act on both the anodic and cathodic process to reduce the corrosion rate [128-130]. Commercial inhibitors for the oil and gas industries are always complex mixture of different inhibitors and other additives. Some of the organic structure constituents of commercially available inhibitors are shown in Figure 3-13

In general most organic inhibitors does not drastically increase the free corrosion potential of the metal by more than 0.1V [131, 132]. Organic inhibitors are made of two parts the non-polar part (hydrophobic part) and the polar part (hydrophilic part). The polar part is used to attach to the surface of the metal by adsorption process. Examples of the polar part include amine and OH group. In some situation the hydrophobic part of the adsorbed inhibitor will add together with the other free hydrophobic part in the solution to form micelles. This helps to improve the efficiency of the inhibitor too. The corrosion efficiency of the corrosion inhibitors depends a lot on many factors such as the chemisorption effect, adsorption of the organic molecule on the metal surface and the size, shape, orientation and electric charge on the inhibitor molecule [132, 133].

Some inhibitors function more efficiently at high temperature while some can function better at low temperature. This is sometimes assumed to be an increase in the adsorption rate at high temperature or stabilization of the film on the surface of the metal at the said temperature [4] .

Light aromatic naphtha	
Amine derivative	NH_2 ... $)_n$
Phosphates	
Quaternary ammonium chloride	H_3C, N^+, R, CH_3, Cl^-
Methanol	R OH
Ethoxylated imidazoline	N, N, O, OH, R, n
Sulphur compound	**R-S**
Polycarboxylic acid	R C OH (O)
Heavy aromatic naphtha	COOH
2-Butoxyethanol	O OH
Morpholine	H N ... O
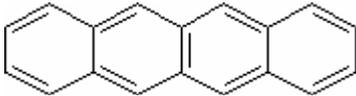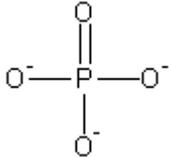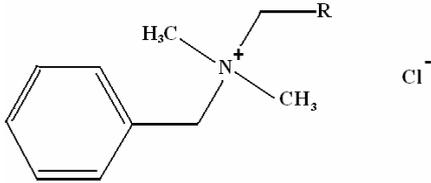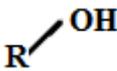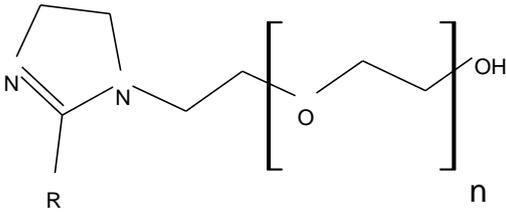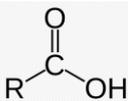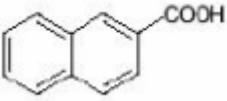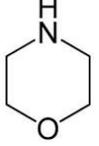
Figure 3-13 : Organic structure of some commercially available inhibitors

Some organic inhibitors for steel are formaldehyde, quinolinethiodide, *o-* and *p-*tolylthiourea, proply sulphide, diamyly amine, oleic imidalzoline, imidalzoline group, phosphate ester, ethoxylated amines, quaternary amines, amine/amide salts, propyl sulphide, formaldehyde and *p*-thiocresol, pyridines and propionate [134-136].

Most organic corrosion inhibitor adsorbs to the metallic surface by displacing the water molecules on the surface [137]. For uniform corrosion of metallic surface, the surface coverage by the adsorbed organic inhibitor is given as the difference between active corroding site and passive sites covered by the inhibitor. In general the surface coverage in the presence of a corrosion inhibitor can be expressed as [138]

$$\theta = \left[\frac{i_{corr}(blank) - i_{corr}(inhibited)}{i_{corr}(blank)} \right] \qquad 3\text{-}52$$

Where, θ is the surface coverage, $i_{corr}(blank)$ is the corrosion rate of the blank and $i_{corr}(inhibited)$ is the corrosion rate in the presence of inhibitor.

The use of adsorption isotherms in the study of adsorption of organic corrosion inhibitor on the metal surface can help to determine the mechanism of the organic corrosion inhibitor. Adsorption isotherms for organic corrosion inhibitors include Langmuir isotherm, Temkin isotherm, Frumkin isotherm, and Freundlich isotherm. [4, 137, 139-142].

Langmuir described the relationship between the amounts of adsorption on the surface of the metal with concentration of the inhibitor adsorbate. Langmuir developed a mathematical relation between the concentration of the adsorbed species and the surface coverage. The equation for the relationship in corrosion terms can be written to include surface coverage (θ) as [137, 138]

$$K_{ad}C = \frac{\theta}{1-\theta} \qquad 3\text{-}53$$

Where K_{ad} is the adsorption equilibrium constant, C is the analytical concentration of the inhibitor, and f is the molecular interaction constant.

A plot of Log $\frac{\theta}{1-\theta}$ against Log C will give a straight line graph if the adsorption of the inhibitor obeys the Langmuir isotherm [132, 141].

The Temkin isotherm is described by the equation [137]

$$K_{ad}C = e^{f\theta} \qquad\qquad 3\text{-}54$$

A plot of θ against lnC is used to test for fitting of an inhibitor to Temkins adsorption isotherm.

The Freundlich isotherm equation is given by [132]

$$q = -q_m L_n\theta + q_m L_n(n_o q_m) \qquad\qquad 3\text{-}55$$

A plot of θ against log q is used to test for fitting of an inhibitor to Freundlich adsorption isotherm. For corrosion purpose the equation is re-written as[137, 138]

$$K_{ad}C\frac{1}{n} = \theta \qquad\qquad 3\text{-}56$$

The Frumkin isotherm can be represented as [137, 138]

$$K_{ad}C = \frac{\theta}{1-\theta}e^{-f\theta} \qquad\qquad 3\text{-}57$$

Adsorption isotherm fits can be very important since it will help to derive the thermodynamics properties of the inhibitor during adsorption. Durnie et al. [137, 142] were able to use the Temkin adsorption isotherm to derive the thermodynamics properties of some commercial organic corrosion inhibitors. They were able to derive the changes in enthalpy of adsorption (ΔH_{ad}) and other thermodynamic properties that helped to classify the inhibitors adsorption to the metal reasonably. Other authors [139-141] were also able to use different adsorption isotherms to

derive the mechanism and thermodynamics properties of some organic corrosion inhibitors.

The physical or electrostatic adsorption (i.e. physisorption) process involves the inhibitor electrostatic force acting on the metal surface to adhere to the metal. The ions or dipoles of the inhibitors are attracted to the charge on the surface of the metal. The surface charge on the metal surface is defined by its open circuit potential with respect to its potential of zero charge PZC. The PZC is equal to zero because the net charge on the surface is zero. When the potential is negative, the electrode is negatively charge while a positive charge on the electrode means that the potential is positive to the PZC. This force is generally weak and has a layer of water molecule separating it from direct contact with the metal [17]. The formation of electrostatic form of adsorption is very fast because the activation energy (E_a) for the process is low. Physisorption adsorption process will occur with little dependence on temperature increase unlike the chemisorption process that depends heavily on temperature increase. When the enthalpy of adsorption (ΔH_{ad}) is determined to be negative, this often indicate exothermic reaction that is common for physisorption mechanism [142].

For a more effective inhibition by organic corrosion inhibitors, a more reliable and stronger force is required between the metal and the inhibitor. The chemisorption process is more reliable and effective mode of adsorption [142, 143]. The process requires high activation energy and as such does not occur easily and fast like the electrostatic adsorption. In chemisorption process there is an actual interaction between the inhibitor molecules and the surface of the electrode or metal. Some literature has it that there is an actual coordinated bond type where electron are transfer to the metal by inhibitor while some few like Bockris [29, 31] does not agreed that there exist a chemical bond between the metal and inhibitor. More recent studies by De Marco R., et al. [138] has shown that persistence of most inhibitors are due to chemisorption.

The chemisorption is temperature dependent and can occur more in higher temperature than lower temperature. This is because the activation energy is very high. In most case, the chemisorption process is specific to a particular metal and might not occur for other metal [127]. The nature of the inhibitor affects the

formation of chemisorption. The presence of unshared lone pair of electron on the donor atom of the inhibitor also facilitates the transfer of electron. It has been shown that the availability of π electrons also facilitates the formation of chemisorption. Hackerman et al. [144] also showed how the existence of unshared pair electron of its nitrogen in the test with polymethyleneimines on the corrosion of iron in a hydrochloric acid solution improved the efficiency of the chemical. Wang et al. [145] work with imidazoline derivatives also showed that the existence of C-N-C bond is due to the existence of the π electrons that helps to form a p-π type of bond.

The organic inhibitors used for the prevention of corrosion always have a reactive functional group which makes the chemisorption. The strength of the bond depends mostly on the polarizability of the functional group and also on the electron density. The efficiency of the organic inhibitors are based on the functional group accordingly as [4, 132].

$$Se> S > N> O.$$
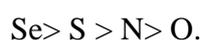
The sequence is based on the polarizability and electronegativity of the elements. The only problem for S (sulphide) is that it might also introduce other problem to the metal through hydrogen that causes hydrogen embrittlement and hydrogen induce cracking [4].

Molecular structure also plays a part in the adsorption on the metal surface. It has been found that the corrosion inhibition of the cyclic amines is more effective than that of their counterpart aliphatic amines. This is due to more electrons available for the electron transfer since the cyclic amine structure has more lone pair electron available for the chemisorption. Aramaki and Hackerman [146] presented their work on the effect of molecular size on inhibition of dimethylpolymethylene ammonium chloride which showed that high molecular weight of the same chemical improves the effectiveness of the inhibitor. Other process that can influence the adsorption process is the introduction of electron donating substituents on aromatic amines and nitriles which helps to increase the efficiency. Molecular weight area and configuration also affects the adsorption of inhibitors. Mostly an increase in the molecular chain and molecular weight increase the adsorption on the metal except for case where steric effect can reduces the inhibition as seen in the inhibition of iron in sulphuric acid where the t-butyl derivatives gave a poor result. Other case

where van der Waals forces are involve within the adsorption process can also increase the efficiency of the inhibition[4].

3.3.2. Stability and behaviour of organic inhibitors

The stability of organic inhibitor can be very important in determining the efficiency of the inhibitor. In an acidic solution, the addition of an inhibitor can give rise to another product if the inhibitor is unstable. In some situation, the new product from the unstable inhibitor will then either improve the inhibition efficiency or may reduce it [4]. The inhibition which occurs due to the initial addition of the inhibitor is known as the primary inhibition while that which occurs because of the reaction from the unstable inhibitor is known as the secondary inhibition. The nature of the product from the unstable inhibitor will determine the efficiency of the inhibitor. In the use of thiourea for inhibition of iron, bisulfide is usually produces from the unstable reaction and this will give rise to more corrosion since the bisulfide is an active agent in sour corrosion process. A beneficial effect of unstable reaction of the inhibitor is seen in the use of dibenzoyl sulfoxide which gives a more stable and efficient sulfide inhibitor as the secondary product [4]. Other effect is seen in the polymerization effect as seen with acetylene compounds. The polymer film form helps in preventing corrosion on the metal surface.

In acid environment, the inhibitor can either work through the reduction of metal activity, changing of the electric double layer, acting as a barrier to the electrochemical active species or by joining as a partial electrode reaction. The inhibitor might not cover the whole metal surface but can be seen at active anodic site where it reduces the anodic reaction [17]. In some case the inhibitor when absorbed on the surface of the metal can change the reaction mechanism and increase the anodic Tafel slope .On the other hand the corrosion inhibitor can increase the over potential of hydrogen ion discharge at the cathodic site thereby reducing the corrosion rate.

3.3.3. Corrosion inhibitors in oil and gas industry

Control of long carbon steel pipeline corrosion in the oil and gas industry is very necessary due to the aggressive and corrosive nature of the oil and gas production environment. The use of organic corrosion inhibitors is common in the industry to

prevent and reduce corrosion rate to the minimal because of the ease and flexibility of their application [82].

Some oil and gas pipeline are protected from corrosion using complex organic inhibitor which may be harmful to the environment and the operators. Recent developments and legislation requires many oil and gas operators to use green inhibitors. Non–green inhibitors are toxic, non-biodegradable and non-bioaccumulation [147-149]. These conditions pose a lot of problem to life and the environment if there is improper disposal of the non-green inhibitors. Waste and leakage of these chemicals may cause devastating problems to the environment. With more restriction on non-green inhibitor use, there is also an additional task to produce green inhibitors which will be effective at this high temperature. Green inhibitors are mostly non-toxic, bioaccumulation and biodegradable but the use is limited when it comes to high temperature application. In the UK, guidelines from Paris commission (PARCOM) are followed to protect the North Sea marine environment. Other countries like Norway (OSPARCOM), and the USA also have their own guidelines [6].A typical acceptance criteria for the north sea is described in Table 3-6.

Table 3-6 : Acceptance criteria for inhibitors for North Sea application. where EC_{50} is the effective concentration of chemical required to adversely affect 50% of the species and LC_{50} is the concentration of chemical required to kill 50% of the species and Log(Po/w) is the log of the octanol/water partition coefficient [6]

Toxicity	EC_{50} and $LC_{50} > 10mg/L$ to North Sea species
Biodegradability	Greater than 60% in 28 days
Bioaccumulation	Log(Po/w) is less than 3

Most organic corrosion inhibitor in the oil and gas industry can undergo either anodic or cathodic or mixed reaction in order to protect the steel surface [150]. Riggs L.O. [132] described this type of inhibitors and gave a list of possible organic inhibitor compounds. For oil and gas industry application, addition formulating agents/additives are added to the organic inhibitor to make it work effectively. Such

additives like surfactants, solvents, hydrate inhibitor and demulsifier may be added to the main organic inhibitor to improve its efficiency [151, 152]. These organic corrosion inhibitors are mostly film forming inhibitors. They work by forming a thin film on the surface of the carbon steel which helps to form a barrier between the metal and the corrosion species. Most of the organic corrosion inhibitors are design to have structures like those of surfactant molecule. They organic inhibitors are made of two parts, the hydrophilic (polar end) and the hydrophobic (non-polar end)[153]. The polar end of the inhibitor is always attached to the surface of the carbon steel forming a bond between them. The other end which is the hydrophobic end tends to be attracted to the oil and this helps to form an oil barrier on the surface. This condition makes an inhibitor to form a good and effective film against corrosion. A description of the process of organic corrosion inhibitor and its adsorption to the surface of the carbon steel is shown in Figure 3-14

Inhibitor film formed at cathodic site of the metal surface

Inhibitor film formed at anodic site of the metal surface
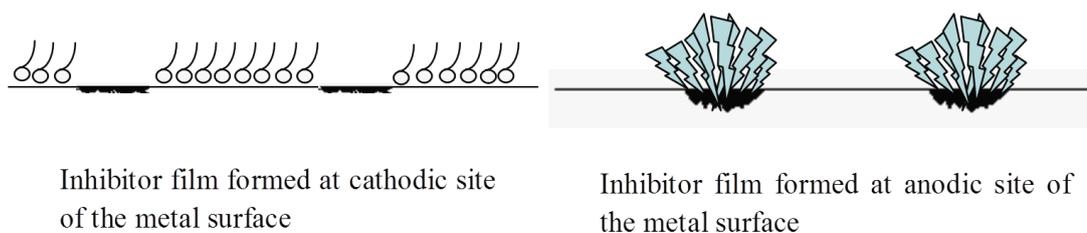
Figure 3-14 : Corrosion inhibitor preventing attack by formation attaching to the metal cathodic or anodic site to form a barrier on the metal surface[8]

There are many views on the mechanism of organic corrosion used in the oil and gas industry. A simple view describes the inhibition process as a tailored process of precipitation of the inhibitor on to the carbon steel surface from the water and hydrocarbons environment. The process normally led to the adsorption of the inhibitor onto the surface charge of the metal in it aqueous environment. The process of adsorption is said to be fast and reversible and normally lead to the reduction of the concentration of the inhibitor.

Mansfield et al. [154] suggested that there is a strong interaction between the inhibitor and the metal corroding surface. This makes the thin film formed by the

inhibitor to persist on the surface of the metal and become more resistance to electron and ions flow.

On the other hand Akbar [155] in his work observed that some organic inhibitor may not be able to form protective film in the presence of iron carbonate scale at some stated condition. Though it was observed that these inhibitors may be able to protect the carbon steel in the presence of iron carbonate in a jet impingement test condition.

However Wong et al. [156-158] studied the effect of iron ions and iron carbonate on the functions of some inhibitors. They were able to show that some inhibitors like the quaternary ammonium chloride performed very well in the presence of iron carbonate while imidazoline and phosphate ester type of inhibitor may prevent the formation of iron carbonate scale and do not have any synergy effect with the iron carbonate scale.

3.3.4. Application of corrosion inhibitors in oil and gas industry

The application of corrosion in oil and gas industry is also necessary bearing in mind the different type of inhibitors, cost and environmental conditions that exist within the system. Three type of application method are normally employed in the application of inhibitor in oil and gas system. They three are batch application method, Squeeze application method and Continuous application method [6]. Table 3-7 shows the application method for different types of corrosion inhibitors.

The method to be used is determined by the type of inhibitor used. Persistence and high performance may be the major reason for the use of a choice method.

Batch application method are often used for organic corrosion inhibitor that are very persistence and can withstand being detached from the surface of the steel for a very long period [128]. This means that the corrosion inhibitor will be able to protect the surface of the steel from corrosion until another batch of inhibitor is introduced.

The squeeze application method is similar to the batch method. It involves the squeezing of the inhibitor in a carrier fluid into the formation. Normally the well is shut down for at least 24 hours to enable the inhibitor flow into the formation. During operation the inhibitor will gradually come out from the formation water along with the oil. This process can be perform between 2 week and 6 months period

[6]. In Continuous application method, the inhibitor is continuously applied at a measured concentration to maintain the integrity of the pipeline.

Table 3-7 : Types of corrosion inhibitors for various applications [6]

Application	Mode of Inhibitor Application	Typical type of Corrosion Inhibitor
Oil wells	Continuous inhibition (capillary injection)	Oil soluble-water dispersible Water soluble-oil dispersible(if water content is high)
	Continuous (through annular space)	Oil soluble Water soluble-oil dispersible(if water content is high)
	Squeeze	Oil dispersible-water dispersible
	Batch	Oil soluble-water dispersible
Oil wells(lifted by gas)	Continuous injection (capillary injection)	Oil soluble-water dispersible
Gas wells and gas condensate wells	Batch Continuous	Oil soluble-water dispersible Oil soluble-water dispersible; Water soluble-oil dispersible
Gas pipeline	Batch	Oil soluble
Oil pipeline	Batch	Oil soluble
Multiphase	Continuous	Water soluble-oil dispersible
Refinery	Continuous	

In practices most corrosion inhibition programme involve the use of batch method in large amount of inhibitor concentration with a short period of time. This will allow the inhibitor film to adsorb effectively of the metal surface. After the said period, the use of medium concentration of inhibitor is applied continuously to ensure the

integrity of the film on the metal surface. Further continuous application of the inhibitor will then be apply to maintain the integrity of the inhibitor film on the metal surface [6].

3.4. Summary of literature review

In this literature review chapter, several aspects of CO_2 corrosion were reviewed. The first section dealt with

- Carbon dioxide and how it contributes to the corrosion of carbon steel in oil and gas industry. It also reviews the anodic and cathodic reactions of CO_2 corrosion of carbon steel. The rate determining factor for the CO_2 corrosion was also discussed.

- Further review was also made on the CO_2 corrosion models which include the mechanistic model, semi-empirical models and the empirical model. . De Waard semi-empirical model using nomogram was also reviewed. Some of the models were discussed and possible advantages and disadvantages in applying any of the model was highlighted

- Factors that affect CO_2 corrosion were reported. These factors include solution chemistry, effect of pH, effect of temperature, effect of corrosion product of iron carbonate and others. pH of 6 and above was revealed to reduce the solubility of iron carbonate and encourages precipitation of iron carbonate. It was reported that the formation of protective iron carbonate occurs at high pH and high temperature and helps to reduce corrosion rate.

The second section reviewed the following

- The properties of MEG and how this influences the use of MEG as a hydrate inhibitor. The application of MEG as a hydrate inhibitor in a MEG-containing system was also reported.

- The effect of MEG on corrosion of carbon steel was also reviewed. There was hardly a comprehensive study of the effect of MEG without addition of pH stabilization at high temperature. Nonetheless the effect of MEG on

corrosion of carbon steel based on de Waard model was review and this showed that the correction factor was based on low temperature test at 40°C.

- The complete mechanism of MEG in reducing corrosion is not fully understood. However it was revealed that higher concentrations of MEG have more positive effect on reducing corrosion.

- pH stabilization in MEG-containing systems reduces corrosion rate of carbon steel. However formation of undesirable scale like calcium carbonates may make it unsuitable for the prevention of corrosion.

- Organic corrosion inhibitors can be applied to a MEG-containing system as an alternative to pH stabilization as long as there is no negative interaction with the oil field chemicals. This area needs to be further researched.

The final section of this chapter 3 dealt with the review on inhibitors as follows

- There are different types of inhibitors of which organic corrosion inhibitors are one type applied in the oil and gas industry. The organic corrosion inhibitors are film forming inhibitors and usually adsorbed on the surface of the metal through physical or chemical process.

- Determination of the adsorption properties of organic corrosion inhibitors can be used to determine the mechanism of adsorption of most corrosion inhibitor.

- The interaction of organic corrosion inhibitors with iron carbonate was also discussed with some inhibitors having a complementary effect with iron carbonate scale while others have little or negative effect on iron carbonate scale.

- Lastly the application of corrosion inhibitors in the oil and gas industry was reviewed. Three application methods were revealed and suitable inhibitors for each method was also highlighted.

Chapter 4. EXPERIMENTAL SET-UP

The tests for all the experiments carried in this study can be grouped into the following major groupings namely

- Corrosion tests in the presence of MEG only
- Corrosion tests in the presence of inhibitor alone
- Corrosion tests in the presence of MEG and inhibitor
- Pre-corrosion tests of the carbon steel in the excess of Fe^{2+} from iron (ii) chloride tetra-hydrate (supersaturated conditions)
- Corrosion tests for pre-corroded samples in the presence of MEG
- Corrosion tests for pre-corroded samples in the presence of MEG and inhibitor
- Post and pre-surface analysis procedures using SEM, EDX, FTIR and Profilometer

Two types of electrochemical techniques that were applied in the corrosion test for the samples are

1. **DC measurements;** include potentiostatic measurements and potentiodynamic measurement of linear polarization resistance (LPR) method and Tafel plot method.
2. **AC measurement;** include EIS test and plots.

The electrochemical tests were conducted using a reference electrode (RE) made of Ag/AgCl Electrode (+0.197V vs SHE) while the counter electrode was made of platinum with cylindrical surface. Both the reference electrode and the counter electrode were combined together as one. A typical set up for the test conducted in this work is shown in Figure 4-1

Figure 4-1 : A typical set up for the test conducted in this work in CO_2 environment

4.1. Test material

4.1.1. Test samples

The test samples were made of X65 carbon steel typically used in the natural gas pipeline. The samples were cut to 1cm by 1cm by 0.4cm. The samples were the embedded into a plastic resin with a conducting coated wire attached to one side of the covered surface. The general composition of the X65 carbon steel used for the entire test is given in the Table 4.1

The test surface measuring 1cm^2 was left bare and serve as the corrosion test surface. The samples were ground with 240, 600 and 800 SiC grit paper and finally finished with a 1200 grit SiC paper. The samples were cleaned with acetone to remove any dirt on the surface and later rinsed with distilled water. The samples were dried with pressurized air to eliminate any trace of water that can lead to the

corrosion of the surface before the test in the vessel. The samples were always prepared just before using them for the test. In some situation the samples were polished and kept in a desiccator until the test time. In this case the samples were also re-polished again using the final finishing grade of paper (i.e.1200 grit paper). This is to make sure that all corrosion on the surface occur due to the test in the test solution and not from outside the test.

Table 4-1 : Chemical Composition of carbon steel X65 in percentage. The balance is made up of Fe.

C	0.12
Si	0.19
P	0.01
Cr	0.12
Mn	1.35
Mo	0.17
Ni	0.06
S	0.0014
Cu	0.05
Sn	0.05
Al	0.05
B	0.0005
Nb	0.033
Ti	0.0003
V	0.059
O	0.0006

4.1.2. Post-test sample preparation

In this study, most of the experiments performed using the test sample was later prepared for surface analysis. Some of them required special preparation. For the general samples used for surfaces analysis, the samples were rinse with distilled water, dry and kept in a desiccator. For SEM test, most of the samples were removed from the plastic resin and part of it was coated with graphite unto the SEM sample holder. This is to allow for more conductivity of the sample and also to allow many of the samples to fit into the SEM at once. In some special requirement where the plastic is left with sample, the surface of the sample was coated with carbon in special coating machine.

Samples from the pre-corrosion test which were used for the profilometer were all prepared by cleaning the surface with Clarke solution. This was done to get the actual carbon steel surface. Most of the samples were also remove from the plastic resin before testing them on the profilometer.

4.1.3. Tested chemicals

In this study Monoethylene glycol (MEG) of 99% purity or more was used for all the experiments involving MEG.

Two types of organic corrosion inhibitors were employed in this study. The inhibitors are commercially available complex mixture. One of the inhibitor used is a non-green inhibitor while the other inhibitor used was a newly formulated green inhibitor. The green inhibitor is based on aminoxy-ethyl-ester with addition of other additives which are generally available in most corrosion inhibitor. The non-green inhibitor is based on benzyl alkyl pyridinyl quaternary ammonium chloride. The non-green inhibitor also contains additives to improve their performance. The non-green inhibitor is denoted as inhibitor 1 while the green inhibitor is denoted as inhibitor 2 throughout this study.

4.2. Composition of test solution

4.2.1. Blank solution

The blank solution was made up of 10g of NaCl solution in 1 litre of distilled water (i.e. 1% NaCl). This is to simulate a simple condensate solution from a gas condensate system with no formation water in it. In most condensate system, the amount of NaCl content may be less than 1% NaCl [77]. The blank solutions used were freshly prepared from distilled water and AR grade of NaCl.

In the experiment with blank solution, the entire test was carried out at atmospheric pressure. Before the test was started, the blank solution was bubble with CO_2 for a minimum of 6 hours to remove all the oxygen in the blank solution with other gaseous impurities such as nitrogen. At the start of the experiment, the solution was attached to a supply of CO_2 from a gas cylinder. This was used to purge CO_2 through to the blank solution at a slow rate during the experiment to keep the test vessel saturated with CO_2. After saturation of the blank solution with CO_2, the pH of the solution was 3.9-4.0 for low temperature of 20°C and pH of 4.1-4.2 for high temperature of 80°C. The low pH is due to the high solubility of CO_2 in the blank solution with only NaCl. The blank solution was mostly used for control test inorder to understand the effect of other test chemicals.

4.2.2. MEG solution

The test solution for the experiment with MEG was prepared using part of the blank solution and the required amount of MEG for any given concentration. The required amount of MEG solution was mixed with blank solution which had previously been saturated with CO_2. For the 1 litre test vessel, 0.5 litres of MEG was mixed with 0.5 litres of blank solution to make 50% MEG solution. The resultant solution was then purged again for 2 hours to remove any trace of oxygen. For the 80% MEG, 0.8 litres of MEG was mixed with 0.2 litres of blank solution. The resultant solution was again purged for 2 hours to remove the oxygen in the solution. The pH at the start of the test for 50% MEG solution was 4.2 at 20°C while for higher temperature of 80°C the pH was 4.4. For the 80% MEG solution the pH for the solution at the start of the test was 4.3 at 20°C while for higher temperature of 80°C it was 4.6.

The solution for other concentration of the MEG solution was also prepared with the blank solution according to the required percentage. For 40% MEG solution in 1 litre, 0.4 litre of MEG was mixed with 0.6 litre of blank solution. For the 30% MEG solution in 1 litre, 0.3 litre of MEG was mixed with 0.7 litre of blank solution. For the 20% MEG solution in 1 litre, 0.2 litre of MEG was mixed with 0.8 litre of blank solution and so on. The solutions were all purged continuously with CO_2 before and during the test to remove the oxygen and saturated the solution with CO_2.

4.2.3. Inhibitor solution

The inhibitors used here are commercial inhibitors as described earlier in the tested chemical section. The amount of inhibitor used was measured out using the micro-pipette with high accuracy of 0.1μm and then introduce in to the solution immediately the carbon steel sample was inserted in the solution. Different amount of the inhibitor were used ranging from 10ppm, 50pppm and 100ppm. The required amount depends on the type of test carried out. For the solution with blank and inhibitor only, the inhibitor was introduced immediately after the carbon steel was inserted inside the solution without pre-corrosion.

4.2.4. Pre-corrosion solution

The formation of iron carbonate on the surface of the carbon steel was performed using pre-corrosion solution. The pre-corrosion solution was made up of blank solution as described previously. The solution was then adjusted for pre-corrosion by introducing iron in the form of iron (ii) chloride tetra hydrate ($FeCl_2.4H_2O$). 0.8 grams of $FeCl_2.4H_2O$ was used for 0.9 litre of blank solution. This gave approximately 250ppm of iron in the solution. The solution pH was also adjusted to required pH of 6.8-7 by introducing 3 grams of sodium bicarbonate ($NaHCO_3$). This solution make up the pre-corroded solution which was used for the formation of protective iron carbonate scale on the surface of the carbon steel. MultiScale (7.1) was used to predict possible precipitation of $FeCO_3$ base on the super-saturation ratio calculations.

4.3. Test procedure for the electrochemical test

The test procedure for the electrochemical test performed in this study is described below. Most of the test has the same procedure with few variations in the electrochemical technique used or the test solution. All electrochemical test conducted here were repeated at least three times and the mean of the results were taken. Error bars were used to show the difference of other results from the mean result.

4.3.1. Test procedure for MEG

These tests were conducted in a litre glass culture vessel with lid made of acetal plastic. The vessel was equipped with CO_2 inlet supply and the lid had a position for the electrodes, pH meter and temperature probe. The vessel was placed on a heating device and stirred consistently at a speed of 250 rpm using a magnetic stirrer. The experiment involves the use of multichannel electrochemical equipment capable of performing both DC corrosion test and AC impedance test was used for the corrosion measurement. This multichannel electrochemical equipment allows for three experiments to be performed at the same. This made it easier to do repetitive test on each experiment conducted .The test utilized a combined reference electrode and counter electrode which was made of Ag/AgCl as the reference electrode and cylindrical platinum as the counter electrode. The CO_2 cylinder was connected to the test vessel for a continuous supply of CO_2 to saturate the vessel and keep the whole vessel at atmospheric pressure. A pressure gauge and valve was attached to the CO_2 supply system and used to monitor and control the pressure during the test. The entire pressure of the vessel was regulated at atmospheric pressure.

At the start of the test, the carbon steel sample of $1cm^2$ was inserted into the test vessel containing the test solution (i.e. MEG solution) for the MEG test alone. For the 50% MEG test, the samples were inserted in a 50% MEG solution while for the 80% MEG solution, the samples were inserted in an 80% MEG solution. For all other concentration of MEG, the carbon steel sample was inserted in the right solution for the test. The pH of the solution was taken and the open circuit potential (OCP) recorded too. The corrosion rate was measured using the Linear Polarization Resistance (LPR) technique. A slow scan rate of 0.167mV/s was used to scan from -

0.02V to OCP and then to 0.02V for the linear polarization to give adequate time for measurement to slow changes during scanning. In order to measure the corrosion resistance and solution resistance, the AC impedance was also used. The AC impedance used frequencies ranging from 10 kHz to 0.1 Hz with RMS amplitude of 10 mV. At the end of each test, the AC impedance value was used to derive the solution resistance which is used to compensate for the resistance from the linear polarisation method. This was performed in order to get the actual resistance since the MEG solution has low conductivity and will give erroneous high value for the resistance and hence a lower corrosion rate to the actual corrosion rate. After the test, the samples were removed carefully and stored in a desiccator for further surface analysis. A typical equivalent circuit (EC) for fitting the AC impedance measurement data is represented in Figure 4.2
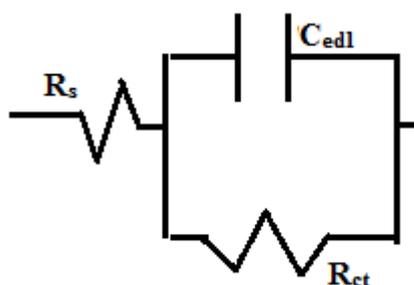
Figure 4-2: Equivalent Circuit (EC) Used in Representing the AC impedance measurement data for blank, 50% MEG, and 80%MEG.

The C_{edl} is the capacitance due to the double layer, R_s is the solution resistance, and R_{ct} is the resistance due to charge transfer.

Using the equation

$$R_s + R_{ct} = R_p \qquad\qquad\qquad 4\text{-}1$$

Where, R_p is the polarization resistance measured by the linear polarization techniques, the actual resistance due to charge transfer (i.e. corrosion of the carbon

steel) can then be derived and used in the calculation of the corrosion rate from the LPR result.

Table 4-2 shows the summary of test condition for the MEG test.

Table 4-2 : Summary of the experimental conditions of the electrochemical test performed in the presence of MEG

Experiment	MEG (%)	Temp(˚C)	pH	Flow	Time (hrs)
MEG Test	50	20	4.2	Consistent Stirring	4
MEG Test	50	80	4.4	Consistent stirring	4
MEG Test	80	20	4.3	Consistent Stirring	4
MEG Test	80	80	4.6	Consistent Stirring	4

4.3.2. Test procedure for organic corrosion inhibitors

These tests were conducted in 1 litre glass culture vessel with lid made of acetal plastic as was used for the MEG test. The vessel was also equipped with CO_2 inlet supply and the lid had a position for the electrodes, pH meter and temperature probe. The vessel was placed on a heating device and stirred consistently at a speed of 250 rpm using a magnetic stirrer. The test involves the use of multichannel potentiostat capable of performing both DC electrochemical measurements and AC impedance measurement. This multichannel potentiostat allows for three experiments to be performed at the same time. This made it easier to do repetitive test on each experiment conducted.

 At the start of the test, the carbon steel sample of $1cm^2$ was inserted into the test vessel containing the test solution usually the blank solution. The required concentration of inhibitor was measured using a micro pipette. The measured quantity of inhibitor was then inserted into the blank solution with the carbon steel

sample through an opening on the lid. The pH of the solution was taken and the open circuit potential (OCP) recorded too. The corrosion rate was measured using the Linear Polarization Resistance (LPR) technique. A slow scan rate of 0.167mV/s was also used to scan from -0.02V to OCP and then to 0.02V for the linear polarization to give adequate time for measurement to slow changes during scanning. In order to measure the corrosion resistance and solution resistance, the AC impedance was also used. The AC impedance used frequencies ranging from 10 kHz to 0.01 Hz with RMS amplitude of 10 mV. The AC impedance was also used to determine the resistance due to the formation of film on the surface of the carbon steel by the inhibitor. At the end of some of the test, the Tafel constant were derived for the two different concentrations of both inhibitors used. This was done by scanning from 0 to -0.25V to get the cathodic slope while a scan of 0 to 0.25V was used to get the anodic slope separately. After the test, the samples were removed carefully and stored in a desiccator for surface analysis. A typical equivalent circuit (EC) of the measurement by the AC impedance measurement for the inhibitor is represented in Figure 4-3. Summary of the experimental conditions of the electrochemical test performed in the presence of corrosion inhibitors are shown in Table 4-3

Table 4-3: Summary of the experimental conditions of the electrochemical test performed in the presence of corrosion inhibitors

Experiment	NaCl (%)	Temp (˚C)	pH	Flow	Time (hrs)
Inhibitor 1 test (10,50 & 100ppm)	1	20	4.0	Consistent stirring	4
Inhibitor 1 test (10,50 & 100ppm)	1	80	4.2	Consistent Stirring	4
Inhibitor 2 test (10,50 & 100ppm)	1	20	4.0	Consistent stirring	4
Inhibitor 2 test (10,50&100ppm)	1	80	4.2	Consistent Stirring	4
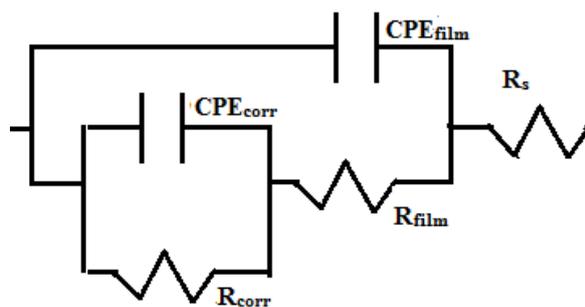
Figure 4-3 : Equivalent circuit (EC) used in representing the AC impedance measurement. Here the CPE_{film} and CPE_{corr} represents Constant phase element due to the inhibitor film and corrosion, R_s, R_{film} and R_{corr} represents solution resistance, resistance due to film and corrosion resistance respectively.

4.3.3. Test procedure for MEG and organic corrosion inhibitor

These tests were also conducted in a litre glass culture vessel with lid made of acetal plastic. The vessel was equipped with CO_2 inlet supply and the lid had a position for the electrodes, pH meter and temperature probe. The vessel was placed on a heating device and stirred consistently at a speed of 250 rpm using a magnetic stirrer.

At the start of the test, the carbon steel sample of $1cm^2$ was inserted into the test vessel containing the test solution of MEG. The required concentration of inhibitor was measured using a micro pipette. The measured concentration of inhibitor was then inserted immediately into the MEG solution with the carbon steel sample. The pH of the solution was taken and the open circuit potential (OCP) recorded too. The corrosion rate was measured using the Linear Polarization Resistance (LPR) technique. A slow scan rate of 0.167mV/s was used to scan from -0.02V to OCP and then to 0.02V for the linear polarization to give adequate time for measurement to slow changes during scanning. In order to measure the corrosion resistance and solution resistance, the AC impedance was also used. The AC impedance used frequencies ranging from 10 kHz to 0.01 Hz with RMS amplitude of 10 mV. The AC impedance was also used to determine the resistance due to the formation of film on the surface of the carbon steel by the inhibitor for some selected test. After the test, the samples were removed carefully and stored in a desiccator for surface analysis. Table 4-4 gives a summary of the test conditions.

Table 4-4 : Summary of the experimental conditions of the electrochemical test performed in the presence of MEG and organic corrosion inhibitors

Experiment	MEG (%)	Temp (˚C)	pH	Flow	Time (hrs)
MEG & inhibitor 1 test (10,50&100 ppm)	50	20	4.2	Consistent Stirring	4
MEG & inhibitor 1 test(10,50&100 ppm)	80	80	4.4	Consistent stirring	4
MEG & inhibitor 2 test (10, 50 and 100 ppm)	50	80	4.3	Consistent Stirring	4
MEG & inhibitor 2 test (10,50 and 100 ppm)	80	80	4.6	Consistent stirring	4

4.3.4. Test procedure for pre-corrosion test

These tests were conducted in a litre glass culture vessel with lid made of acetal plastic as previously described. The solution was de-aerated as usual and heated required temperature of 80°C.

At the start of the test, the carbon steel sample of $1cm^2$ was inserted into the test vessel containing 0.9 litre of the blank solution in the 1 litre test vessel. 3 grams of $NaHCO_3$ was added to the blank solution to raise the pH to near neutral point. 0.8 grams of $FeCl_2.4H_2O$ was added to the solution to increase the amount of iron ions in the solution to 250ppm. The pH of the solution was taken and the open circuit potential (OCP) recorded too. The corrosion rate was measured using the Linear Polarization Resistance (LPR) technique. A slow scan rate of 0.167mV/s was used to scan from -0.02V to OCP and then to 0.02V for the linear polarization to give adequate time for measurement to slow changes during scanning. The test was performed for short time of 4 hours and longer time of 24hrs to determine the rate of growth of the iron carbonate. After the test, the samples were removed carefully and cleaned first with ethanol to avoid oxygen reacting with the tested samples surface.

They were then stored in a desiccator for surface analysis. Table 4-5 gives a summary of the test conditions.

Table 4-5 : Summary of the experimental conditions of the electrochemical test performed for pre-corrosion of the carbon steel

Experiment	NaCl (%)	Temp (˚C)	pH	Flow	Time (hrs)
Pre-corrosion Test	1	80	6.8- 7	Consistent stirring	4, 24

4.3.5. Test procedure for pre-corrosion test and MEG

These tests were conducted in a litre glass culture vessel with lid made of acetal plastic as previously described. The solution was continuously purged with CO_2.

At the start of the test, 4hrs or 24hrs pre-corroded carbon steel was transferred to the vessel containing the required concentration of MEG solution. This pre-corroded sample served as the test sample in the MEG solution. The pH of the MEG solution was never raised as during the pre-corrosion and there was no addition of iron from $FeCl_2.4H_2O$. This allows the test to be done at the prevailing low pH. The pH of the solution was taken and the open circuit potential (OCP) recorded too. The corrosion rate was measured using the Linear Polarization Resistance (LPR) technique as previously described. At the end of some test, the AC impedance measurement was performed and the solution resistance was derived and used to compensate for the resistance from the linear polarisation method. This was performed inorder to get the actual resistance since the MEG solution has low conductivity and will give erroneous high value for the resistance and hence a lower corrosion rate compare to the actual corrosion rate. After the test, the samples were removed carefully and stored in a desiccator for surface analysis.

Table 4-6 gives a summary of the test conditions.

4.3.6. Test procedure for pre-corrosion test, MEG and organic corrosion inhibitor

The test procedure for pre-corrosion test, MEG and organic corrosion inhibitor was similar to test procedure for pre-corrosion test and MEG.

Table 4-6 : Summary of the experimental conditions of the electrochemical test performed on pre-corroded samples in the presence of MEG only

Experiment	MEG (%)	Temp (˚C)	pH	Flow	Time (hrs)
4hrs Pre-corrosion & MEG Test	50	20	4.2	Consistent Stirring	4
4hrs Pre-corrosion & MEG Test	50	80	4.4	Consistent Stirring	4
4hrs Pre-corrosion & MEG Test	80	20	4.3	Consistent Stirring	4
4hrs Pre-corrosion & MEG Test	80	80	4.6	Consistent Stirring	4
24hrs Pre-corrosion & MEG Test	50	80	4.4	Consistent stirring	4
24hrs Pre-corrosion & MEG Test	80	80	4.6	Consistent Stirring	4

The difference is the addition of the inhibitors and MEG at the same time after 4hrs or 24hrs pre-corroded carbon steel samples was added. The required concentration of the inhibitor were introduce using micro pipette in a solution containing the

require concentration of MEG and the pre-corroded carbon steel sample. Electrochemical test were performed on the samples for 4 hours period as described for the test of pre-corrosion and MEG only. At the end of the test, the sample was removed carefully and stored in a desiccator for surface analysis.

Table 4-7 gives a summary of the test conditions.

Table 4-7 : Summary of the experimental conditions of the electrochemical test performed on pre-corrode sample in the presence of MEG and organic corrosion inhibitors

Experiment	MEG (%)	Temp (˚C)	pH	Flow	Time (hrs)
4hrs & 24hrs Pre-corrosion MEG & inhibitor 1 test	50	20,80	4.2,4.4	Consistent Stirring	4
4hrs & 24hrs Pre-corrosion MEG & inhibitor 1 test	80	20,80	4.3,4.6	Consistent Stirring	4
4hrs & 24hrs Pre-corrosion MEG & inhibitor 2 test	50	20,80	4.2,4.4	Consistent stirring	4
4hrs & 24hrs Pre-corrosion MEG & inhibitor 2 Test	80	20,80	4.6,4.6	Consistent Stirring	4

4.4. Surface analysis

The samples from the electrochemical test can be analyses using different surface analysis. In this study the Scanning electron microscopy/Electron diffractive X-ray

analysis (SEM/EDX), Fourier transform Infrared (FTIR) and Interferometer techniques were used in the post-analysis of the tested samples. The post-analysis test on the electrochemical tested samples are crucial in the whole research since it will give an in-depth understanding of the electrochemical damage done on the sample both in the presences and non-presence of MEG, inhibitors and pre-corrosion. Damages like the general corrosion and localised corrosion in the form of pitting. It will also give an understanding of the type of and amount of scale formed on the surface of the electrochemically tested samples.

4.4.1. Scanning Electron Microscopy/ Energy Dispersive X-ray Analysis (SEM/EDX)

The SEM was used to analysis the electrochemically tested sample to have a good picture of the damage on the samples. They samples were analysis at different magnification to identify any general or localise corrosion on the surface. Iron carbonate scale formations were also observed for using the SEM. The SEM was also used to derive the thickness of the iron carbonate scale formed on the surface of the electrochemically pre-corroded sample.

EDX was used for some sample to identify the elemental composition of the sample surface. This was especially important for the pre-corroded tested sample as it helps to identify the type of scale formed on the surface where necessary.

In preparing the samples for the SEM and EDX analysis, the samples are normally coated with carbon on the non-conductive part (i.e. epoxy resin) to make it electrically conductive. In the determination of the thickness of the film/scale formed on the surface of a pre-corroded tested sample, graphite carbon coating was specially coated on the cross-sectional area of the sample to make it conductive. The SEM prepared samples are inserted into the Carl Zeiss EVO MA15 with a high resolution secondary electron and primary electron used for imaging of the sample. The area where the samples are kept was pumped to remove any trace of air or nitrogen gas. Then the surface was scan with an electron beam which is then reflected back onto a cathode tube to show surface image of the sample area. For EDX, back scattered electron (BSE) was used to identify the atomic number of the element present in the scanned surface area. This test is mostly qualitative and may need further test such as the FTIR to identify the actual element presence. A high

level of carbon and low level iron on the sample surface may be an indication of the formation of scales containing iron carbonate. Figure 4-4 and Figure 4-5 shows the SEM and carbon coating machine used for the studies.

Figure 4-4 : The Carl Zeiss EVO MA15 used for SEM and EDX surface analysis.

Figure 4-5 : The Emscope graphite carbon coating machine used for carbon coating of some of the SEM sample.

4.4.2. Fourier Transform Infrared Spectrometry (FTIR)

FTIR was used on the surfaces of the electrochemically tested sample to determine the type of bonding that exist on the surface. This bonding is normally formed when there is a formation of scale or film on the surface by an inhibitor or other film forming compound/reaction. The adsorption of inhibitor on the surface of the electrochemically tested sample can be identified using the FTIR method. This will give an idea of the possible inhibitor mechanism for most of the inhibitor.

The FTIR uses a liquid nitrogen gas to cool the detector system. It has an optical system, spectrometer and a stage controller. The spectrometer in this case uses a Helium Neon laser to produce wave radiation at 633nano meter wavelength. Using the optical system, a wide range of data ranging from (500 to 4000 cm^{-1}) can be collected. Each range of wavelength normally corresponds to a particular type of bonding or ion on the surface of the tested sample. The (CO_3^{2-}), wave number range on the FTIR corresponds to 880-800 cm^{-1} [134]. The FTIR used for this test is shown in Figure 4-6.

The ATR which also uses infra-red beam for identification of the bonding or ions presences on a sample or solution were used for some part of the test. This gave a satisfactory result for most of the liquid sample e.g. MEG and inhibitors.

Figure 4-6 : The Perkin Elmer Spectrum 100 FTIR machine used for FTIR surface analysis of electrochemically tested sample.

4.4.3. Interferometry

The interferometer was used to analysis the formation of localised corrosion, pit and variations on the surfaces of the sample. The Wyko and Bruker profilometer was used for most of the profiling test on the sample. It uses beam of light in imaging and profiling the surface of the sample. The sample was placed on the stage and the required objective lens is place on top of the surface with a light focused on the surface of the sample. The focus of light is done using a fringe system which allows for optimal focus and level to be attained on the surface sample. The interferometer was capable of producing high level 3D image. The profilometer can give a 3D image of the electrochemically tested sample and quantify valleys and peaks.

Analysis of the images from the profilometer will give various results including maximum pit depth and classification of general and localised corrosion when a threshold is used. The volume of the sample removed by the electrochemical can be obtained using the profilometer analysis software. Further analysis and result may be obtained using the profilometer. Figure 4-7 shows one of the profilometer machine used for this study.
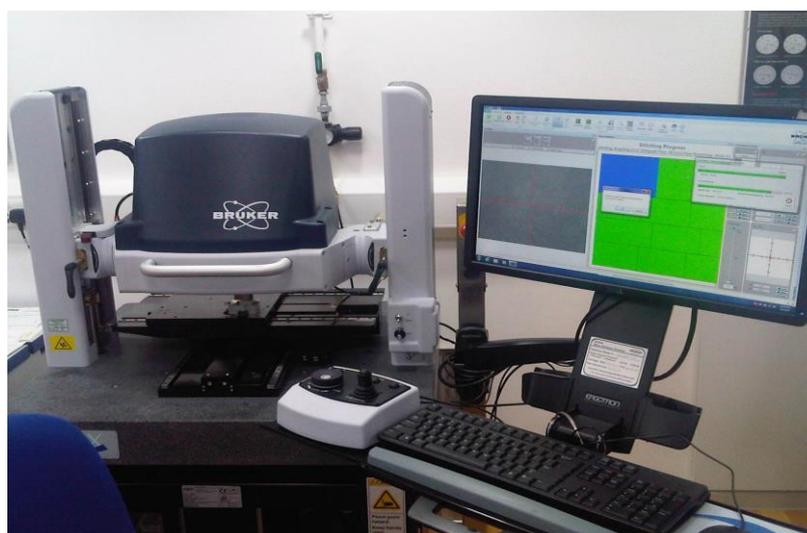
Figure 4-7 : The Bruker Profilometer machine used for interferometer surface analysis.

4.5.Summary of experimental set-up

This chapter described all the experimental methodology and set up applied in the studies. The different type of test performed with the carbon steel X65 test material was described. The chemical materials used and operation conditions and procedures were all described. It also described the different surface analysis which was performed on the tested sample to further support the electrochemical test result.

Chapter 5. CORROSION ASSESSMENT IN THE PRESENCE OF MONOETHYLENE GLYCOL

5.1. Introduction

MonoEthylene Glycol (MEG) is used in multiphase gas pipeline transportation as a thermodynamic hydrate inhibitor [2, 77, 99, 100, 113, 159]. The corrosion rates and mechanisms occurring at the injection point of the MEG and along the pipeline in a MEG loop system are of interest for corrosion management. The effect of MEG on the corrosion of carbon steel at various temperatures is considered here. The low temperature test is relevant for corrosion along the pipeline as the temperature of the pipeline decreases with time while the high temperature test will be relevant at the injection point of MEG. The concentration of the MEG was varied from 50% MEG to 80% MEG to give an insight of the effect of concentration on the corrosion of the carbon steel. As described by Dugstad et al. [77] the 50% MEG is the rich glycol while the lean glycol is the 80% MEG. The lean glycol is normally injected at the inlet of the pipe at high temperature of about 80°C while the rich glycol is received mostly along the pipeline and at the outlet at lower temperature around 20°C.

Open Circuit Potential (OCP) and Linear Polarisation Resistance (LPR) measurements were employed to determine how effectively MEG inhibits corrosion of carbon steel. AC impedance measurements were used to determine the impedance and the resistance due to low conductivity of MEG solution. Blank tests were conducted to compare with results of tests in the presence of MEG. The inhibition mechanism in the presence of MEG was also investigated by using post–test surface analysis as described in chapter 4.

5.2. Open Circuit Potential (OCP) measurement

The OCP can be used to describe the way in which a corroding system behaves as described in chapter 2. In a test, the OCP of the blank solution at a set temperature indicates point of pseudo-equilibrium when the net anodic and cathodic current in the system is zero. This measured value indicates how the surface of the metal

naturally corrodes in the solution in which it is immersed. In this test the OCP of the blank solution without MEG and the solution and with MEG was observed at different immersion times during the test. The OCP values at 20°C are shown in Figure 5-1. The OCP value for the blank solution at 20°C was around -673mV for the 4 hour period tested. A change in the value of the OCP was seen immediately for 50% MEG solution test and 80% MEG solution tests. The value of the OCP for the 50% MEG is -640mV compared to -673mV for the blank solution. At 80% MEG there was further ennoblement of the OCP to values around -590mV.
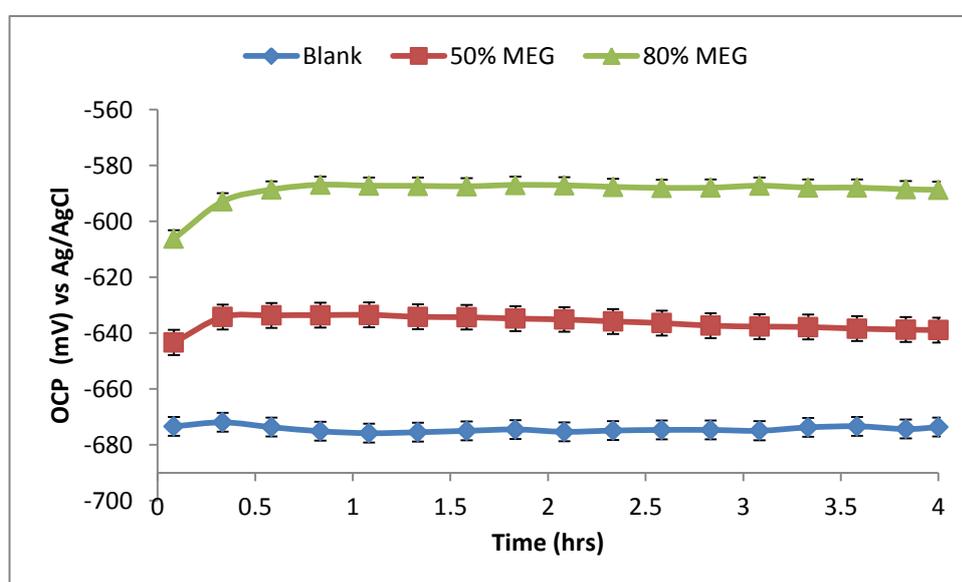
Figure 5-1: OCP values against time for blank, 50% MEG, and 80% MEG at 20°C.

As the concentration of MEG increases, the coverage of the active anodic sites increases. This is seen in the more noble value of the OCP when 80% MEG solution is used. The reduction in the anodic sites leads to reduction in the anodic corrosion reaction. The reduction in anodic corrosion reaction leads to an ennoblement in the OCP.

The results of the OCP at high temperature were also in line with those at low temperature but with a slight reduction in the value of OCP with MEG. Figure 5-2 shows the OCP value for the blank test and with different concentrations of MEG at 80°C. At 80°C the blank solution did not have a considerable change in OCP as

compared to the value at 20°C. The OCP value for the blank solution at 20°C was on average -673mV for the 4 hour period tested. For the 50% MEG solution the OCP was -649mV for the tested period of 4 hours. This is a slight reduction in the average value of the OCP at 20°C (i.e. -639mV). This reduction in the OCP value in the presence of MEG was seen also for the 80% MEG which average -623mV at 80°C as compared to the -590mV at 20°C. This may mean a reduction in the corrosion inhibition efficiency of MEG at high temperature of 80°C as compared to the low temperature of 20°C. Further results will give an insight of what may cause the different OCP at high temperature compared to lower temperature.
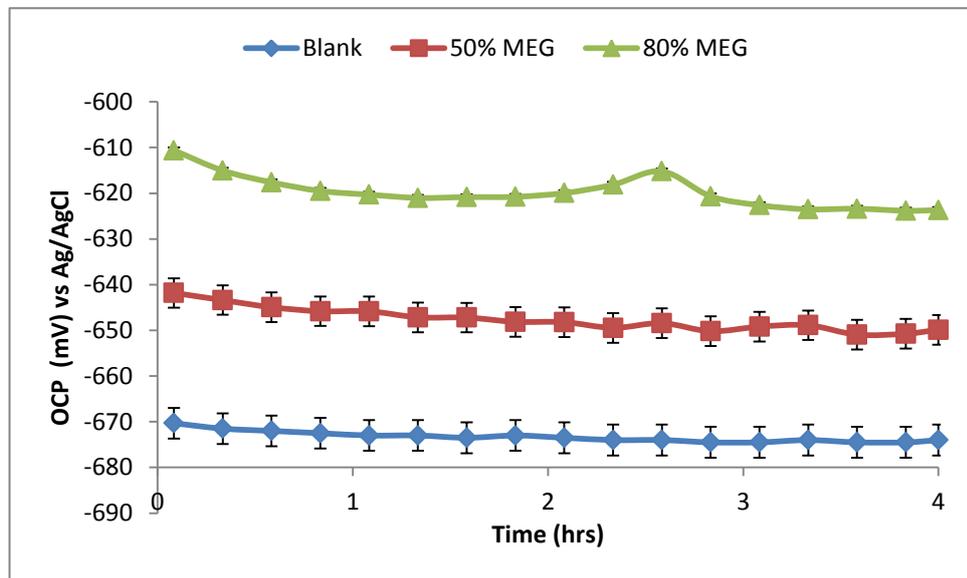
Figure 5-2 : OCP values against Time for blank, 50%MEG, and 80%MEG at 80°C.

5.3. AC Impedance

The use of the AC Impedance method has some advantages over DC measurement techniques. In the use of AC impedance the corrosion resistance of the carbon steel can be derived together with the solution resistance. The solution resistance gives the resistance due to a non-conductive or less conductive electrolyte/solution. MEG increases the solution resistance of the blank solution by making it less polar [87]. The Nyquist plot for solutions with very high solution resistance shows an unusual time constant which is attributed to the solution resistance. This normally manifests

at the very beginning of the measurement for high frequency range of 1 kHz to 100 kHz. Calculations which compensate for the solution resistance will then give the actual resistance to corrosion. AC impedance measurements have been used here to derive this solution resistance for tests conducted in the presence of MEG. This will make the calculated corrosion rate accurate when MEG solution resistance is compensated for in corrosion rate calculation.

The AC impedance method can also be used to determine other characteristics of the corrosion reaction such as the formation and behaviour of any films on the surface of the carbon steel. In this result the behaviour of the carbon steel in the presence and absence of MEG was monitored. The results for AC impedance for 4 hour period at 20°C for frequencies from 10 kHz to 0.1 kHz are shown in Figure 5-3.
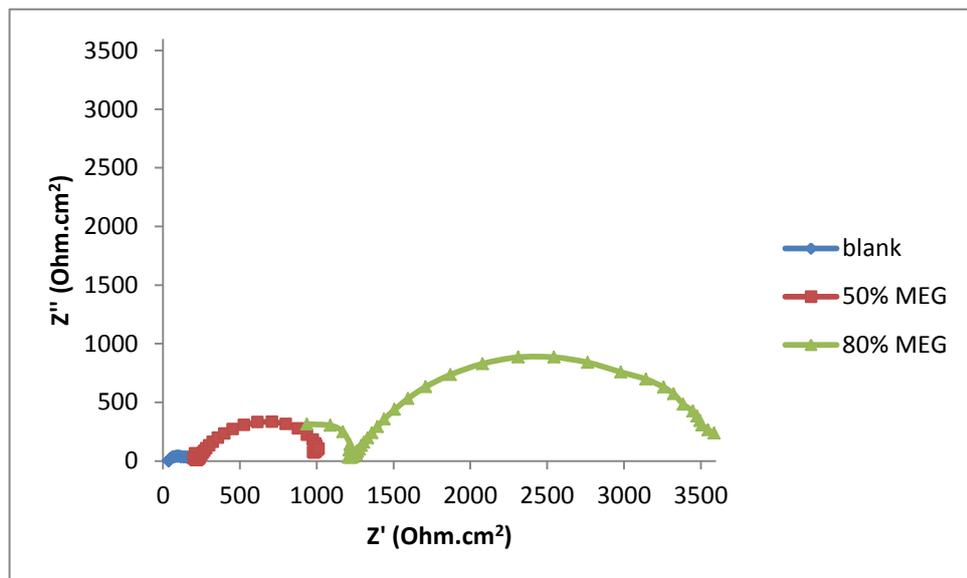
Figure 5-3 : Comparison of the AC impedance measurement (Nyquist plot) for test with blank solution, 50% MEG and 80% MEG at 20°C.

The result for the blank solution does not exhibit any of this usual time constant due to high solution resistance. Actually the blank solution resistance is so small that it can be neglected. The blank solution has a very small impedance value when compared with the test with MEG solution. This is an indication of very low resistance of the carbon steel in the blank solution. The results observation showed that the solution resistance of MEG increases with increase in MEG concentration.

119

The 50% MEG shows high solution resistance while the 80% MEG show even a higher solution resistance as expected. The blank solution impedance value is so small compared to the 50% MEG and 80% MEG and is neglected in the calculation of the actual corrosion rate for the test in blank solution. A comparison plot of the solution resistance (R_s) with MEG and blank solution is shown later.

The 80% MEG has the highest impedance value. This is an indication that the corrosion resistance of the carbon steel at 80% MEG is higher than that at 50% MEG and also the blank solution. To determine the solution resistance and the corrosion resistance, an equivalent circuit (EC) is used. The equivalent circuit (EC) used in representing the corrosion reaction in the presence and absence of the MEG solution is represented in Figure 5-4, where C_{edl} is the capacitance due to the electric double layer, R_s is the solution resistance of the electrolyte and R_{ct} is the resistance to charge transfer by the corroding surface.

From the EC modelling and calculations, the average solution resistance for the 50% MEG is 250 Ohms.cm^2 while that of the 80% MEG shows even a higher average value of 1200 Ohms.cm^2. In all test conducted here using LPR method, the solution resistance was accounted for and used to compensate the polarisation resistance results.
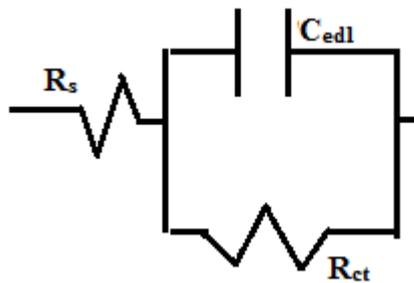
Figure 5-4: Equivalent Circuit (EC) used in representing the AC impedance measurement for blank, 50% MEG and 80% MEG.

At high temperature of 80°C, the results of the Nyquist plot for the AC impedance test shows a smaller impedance value compared to that of the MEG solution at 20°C. The highest impedance values were seen for the 80% MEG solution as expected. It should be noted that there is a total drop in the value of the impedance

which indicates an increase in corrosion rate at this high temperature. This is true for high temperature corrosion where there is no formation of protective iron carbonate scale [39, 160]. Figure 5-5 shows the comparison of the Nyquist plot for the AC impedance measurement for the blank, 50% MEG and 80% MEG test.
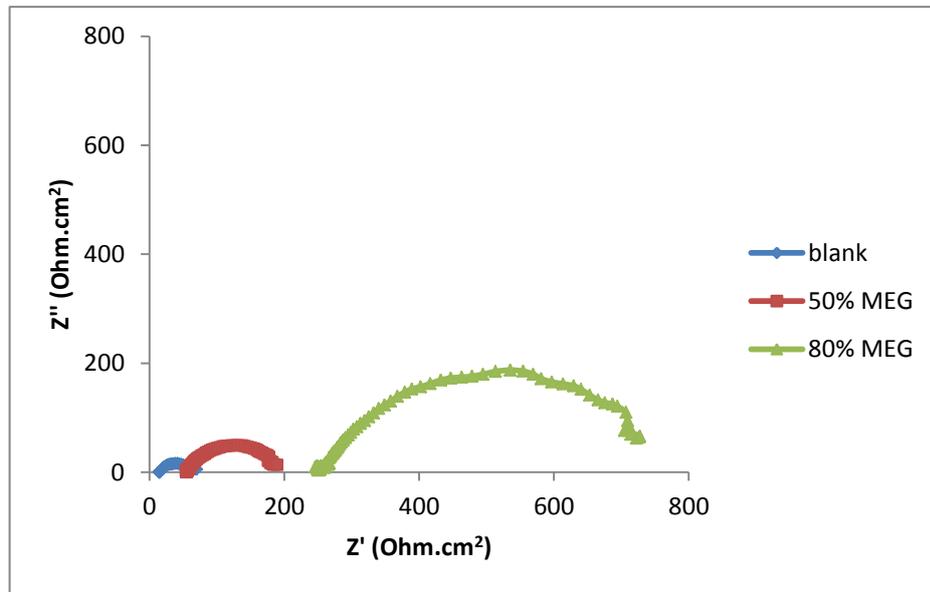
Figure 5-5 : Comparison of the AC impedance measurement (Nyquist plot) for test with blank solution, 50% MEG and 80% MEG at 80°C.

The solution resistance for tests with MEG at this high temperature also reduced. The solution resistance at 80°C for 80% MEG was reduced to 250 Ohms.cm^2 from 1200 Ohms.cm^2 at 20°C while that at 80°C for 50% MEG reduced to 50 Ohms.cm^2 from 250 Ohms.cm^2 at 20°C. The blank solution resistance is also negligible at this temperature compared to that of the MEG solutions. The reduction in the solution resistance value at high temperature of 80°C indicates that the conductivity of the solution increased with temperature. This is expected as increase in the temperature of electrolyte increases the mobility of the ions in the solution which affects the conductivity positively [161, 162]. This will be compared with the results from the conductivity test in the next section.

Figure 5-6 shows a comparison of the corrosion charge transfer resistance (R_{ct}) of the blank, 50% MEG and 80% MEG at both 20°C and 80°C while Figure 5-7 shows

a comparison of the solution resistance of the blank, 50% MEG and 80% MEG at both 20°C and 80°C.
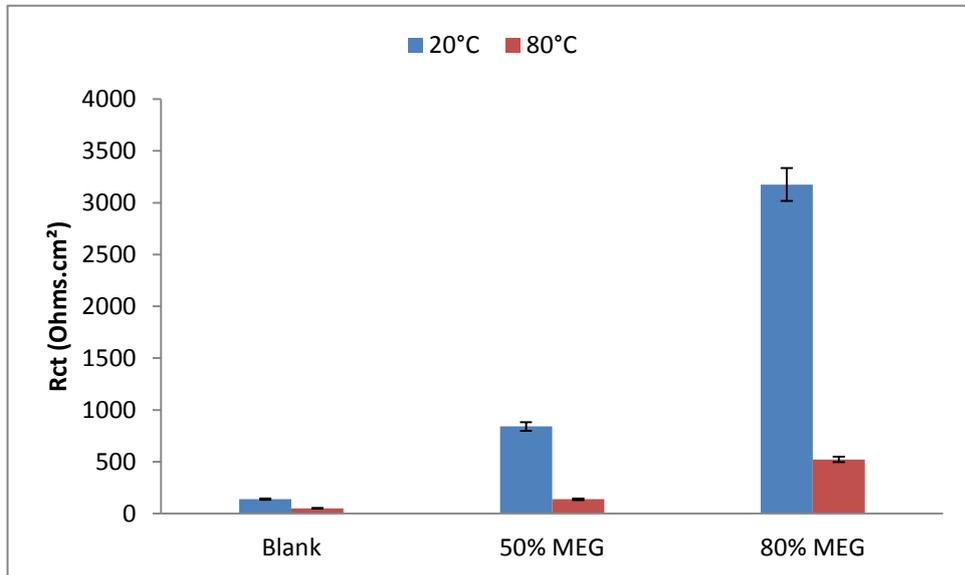
Figure 5-6 : Comparison of the corrosion charge transfer resistance R_{ct} of test for blank, 50% MEG and 80% MEG at 20°C and 80°C (AC impedance measurement).
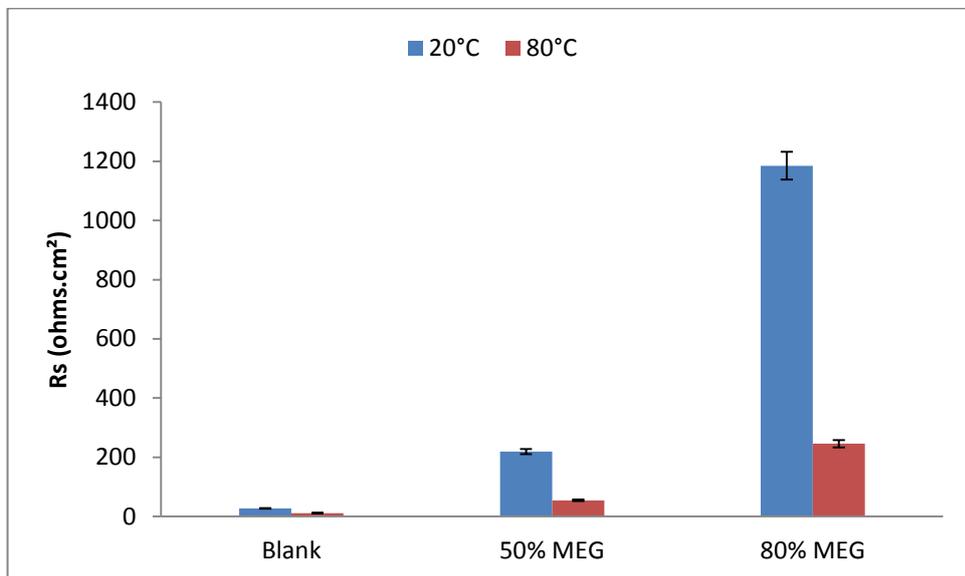
Figure 5-7 : Comparison of the solution resistance R_s of test for blank, 50% MEG and 80% MEG at 20°C and 80°C (AC impedance measurement).

5.3.1. Solution conductivity:

In other to verify the authenticity of the solution resistance values from this result, a conductivity test was performed for the solution. The solution conductivity of the test solution gives an insight into the conduction of electrons in the electrolyte solution. The conductivity of the solution can be said to be the inverse of the resistivity. The solution conductivity is affected by the amount of total dissolved inorganic solids in the solution.

In corrosion measurement the test solution needs to be conductive to enable the accurate measurement of the polarization resistance. A measure of the conductivity is required to understand the solution resistance of an electrolyte. The measurements were made with MEG solution of different concentration using Meterold conductivity machine. The solutions were stir in a closed beaker and heated to the required temperature before measurements were taken. Here the results of the solution resistance were measured for 1% NaCl, 50% MEG solution and 80% MEG solution. Figure 5-8 shows that conductivity of the 1% NaCl is the highest and up to 16,000 μScm^{-1} while that of the 50% MEG is as low as 2,350 μScm^{-1} at 20°C. The 80% MEG has the lowest value with conductivity value of 410 μScm^{-1} at 20°C. The result is in agreement with the AC impedance result for the 50% MEG and 80% MEG solution which shows that solution resistance is highest for the 80% MEG and high for 50% MEG as compared to value of the 1% NaCl that was negligible. These values shows that a test of corrosion rate of carbon steel in a solution of MEG using LPR technique will not give a reliable result if not compensated.

The value of the conductivity is affected by temperature [163, 164]. The graph of Figure 5-8 shows an increase in the conductivity of the solutions as the temperature increases. The increase is very rapid for the 1% NaCl. The value for the 1% NaCl was increased from 16,000 μScm^{-1} to around 39,700 μScm^{-1}. There was also an increase for both MEG solution. At high temperature of 80°C the value of the 50% MEG and 80% MEG are 8,300 μScm^{-1} and 1,726 μScm^{-1} respectively. This increase indicates a reduction in the solution resistance of the MEG solution. This is so because the solution resistance is inversely proportional to the conductivity. As temperature increase the solution resistance for MEG solution reduce.
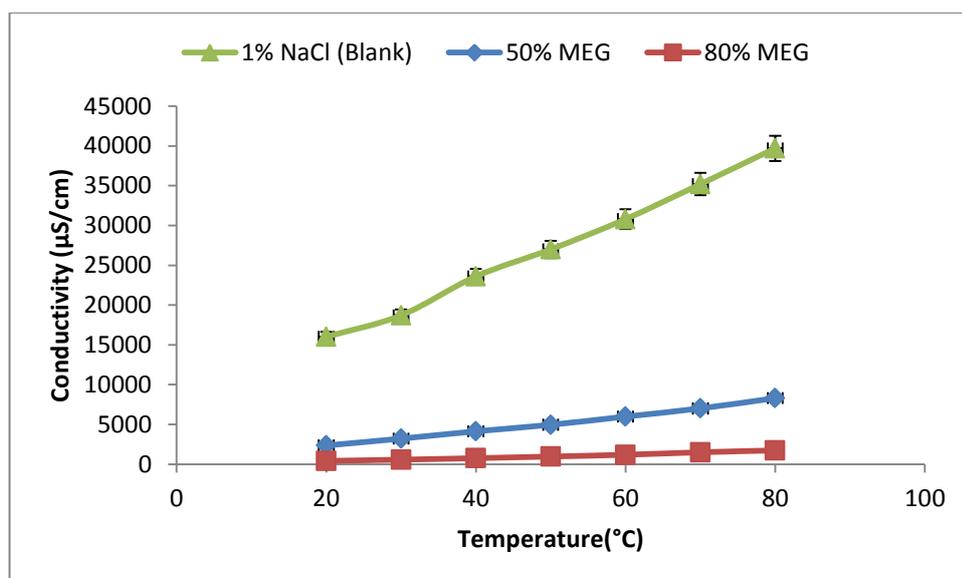
Figure 5-8 : Conductivity measurements for 1% NaCl (blank), 50% MEG and 80% MEG at different temperature.

5.4. Linear Polarization Resistance (LPR) measurement

OCP measurement is a quick and easy way to observe the corrosion reaction trends of carbon steel. This method can give limited and semi-quantitative information on the corrosion reaction of the carbon steel. In order to get more information, the linear polarization measurement of the carbon steel was taken for blank solution and also in the presence of MEG. The R_p values of the blank solution were used directly to calculate the corrosion rate because the solution resistance was negligible. For the R_p value of solution with MEG (i.e. 50% MEG and 80% MEG), the solution resistance was high and so was not neglected. The solution resistance values were calculated using the AC impedance method as described in the previous section. These values of solution resistance were compensated for each reading before using them to calculate the corrosion rate.

The corrosion rate from LPR was calculated using the Stern-Geary equation presented previously and using a *(B)* value of 26. The *(B)* was used as it is the value generated from the potentiostat software and commonly used in the industry.

The results of linear polarization test for the blank solution with no MEG shows a final corrosion rate of 2.25mm/y for the period of 4 hours. This level of corrosion

124

rate is still high for the low temperature of 20°C. The use of 50% MEG reduces the corrosion rate to a final corrosion rate of 0.44mm/y. The result of 80% MEG shows a further reduction in the final corrosion rate to be 0.14mm/y.
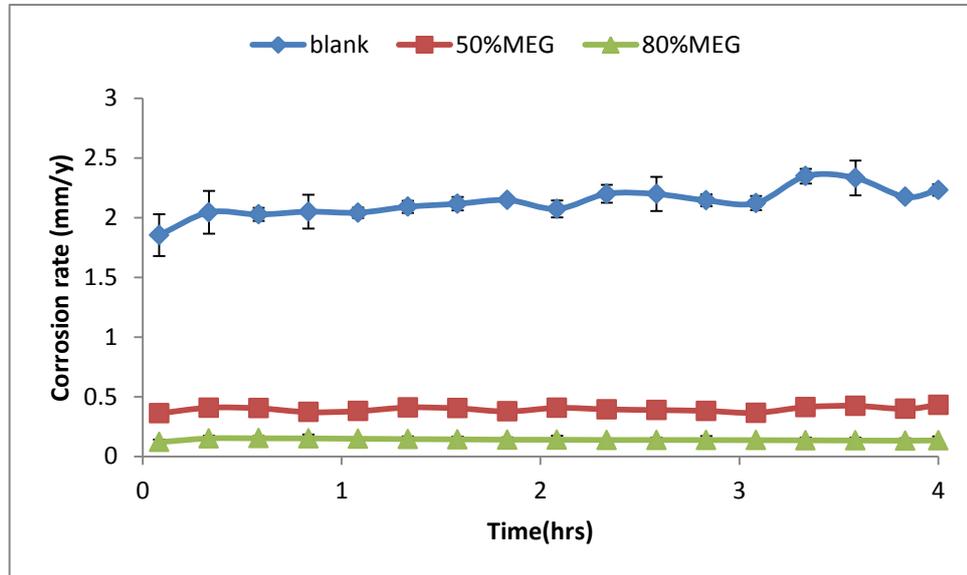
Figure 5-9 : Comparison of the corrosion rate for blank, 50% MEG and 80% MEG at 20°C (compensated LPR measurement).

The result for the 80°C shows high values of corrosion rate for the blank tests. The average final corrosion rate is 5.6mm/y at the end of the 4 hour test for Tafel constant (B) of 26. This is expected as the corrosion species (i.e. H^+, H_2CO_3, HCO_3^-) are very active at high temperature which increases the corrosion reaction. This is true as long as there is no formation of protective corrosion product on the surface of the metal [3, 165]. The bulk solution pH was in the region of 4.0 and was not favourable for a protective iron carbonate film to form [70, 115]. In the presence of 50% MEG, the corrosion rate was also high but much less than the blank solution. The value of the average final corrosion rate is 2.34mm/y. This is quite high as compared to the corrosion rate achieved at the end of the 20°C test. 80% MEG reduces the corrosion rate further to an average final corrosion rate of 0.48mm/y. The corrosion rate is not as low as the corrosion rate 20°C. This is also expected as the corrosion rate of carbon steel increases with high temperature unless there is a formation of protective iron carbonate scale at that temperature [53, 67, 166].
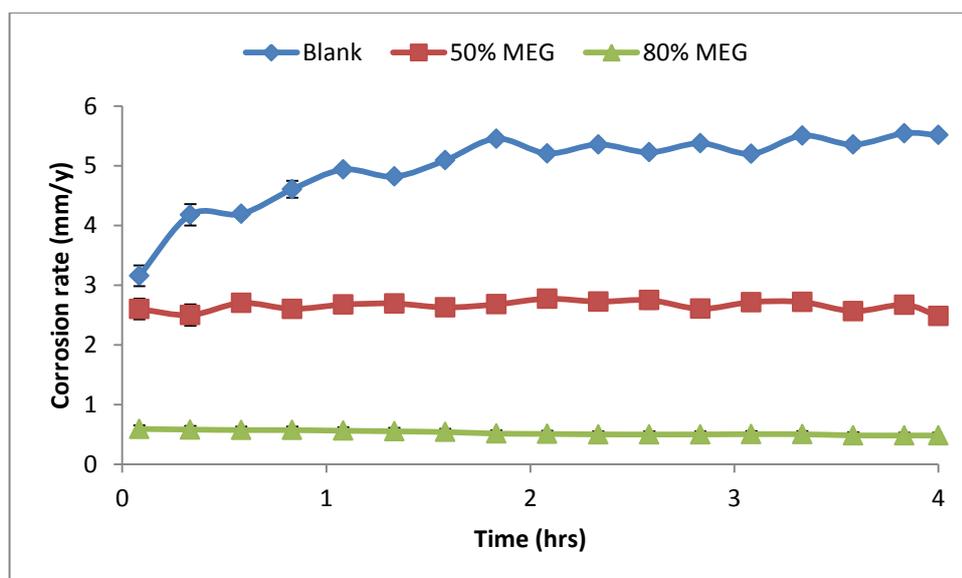
Figure 5-10: Comparison of the corrosion rate for blank, 50% MEG and 80% MEG at 80°C (compensated LPR measurement).

5.5. Surface analysis

Electrochemical tests give the quantitative corrosion rate but give no information on the corrosion mechanisms. As an example the localised corrosion or type of degradation that may have occurred needs to be assessed by post-test microscopy. The results of the surface analysis are described in this section.

5.5.1. Scanning Electron Microscopy (SEM)

The samples which were used for electrochemical tests were kept in a desiccator after each experiment. SEM images of the samples were then taken to identify possible types of damage on the surface. The results for the SEM of the carbon steel sample at 20°C after the electrochemical test are shown in Figure 5-11 (a, b, and c). From the results of the SEM analysis of the blank samples at 20°C it was seen that the surface of the sample had both general corrosion and localised corrosion. The corrosion has removed the ferrite leaving behind the iron carbide (Fe_3C). The SEM image on the surface of the sample with 50% MEG solution show less general corrosion as compared to that of the blank sample. This is mainly due to the protection of the sample in the presence of the MEG. This is in line with the lower corrosion rate from the LPR results which showed that the general corrosion rate for 50% MEG test was lower compared to the blank test. The SEM image of the surface

126

of the sample with 80% MEG also showed even surface indicating low general corrosion.
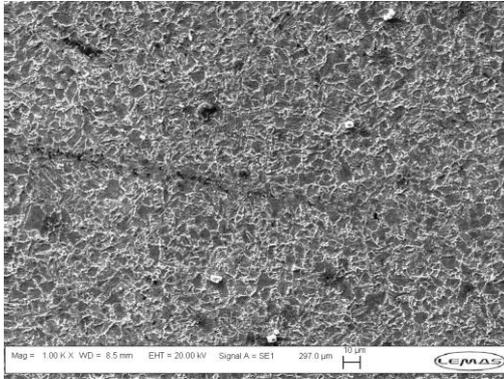
<p style="text-align:center">(a)</p>
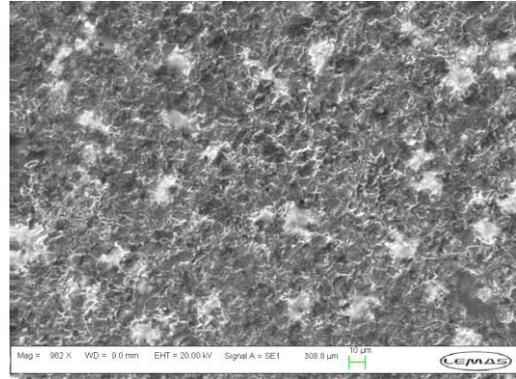
<p style="text-align:center">(d)</p>

<p style="text-align:center">(b)</p>
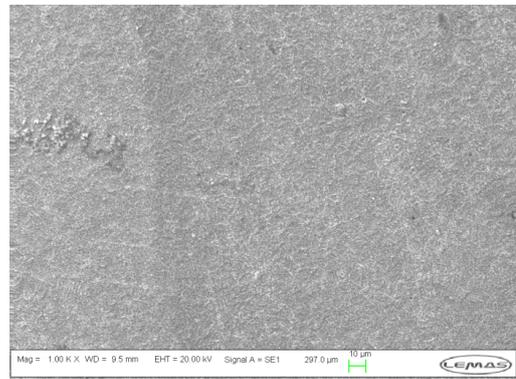
<p style="text-align:center">(e)</p>
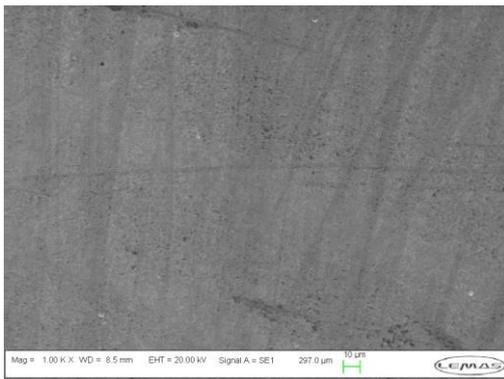
<p style="text-align:center">(c)</p>
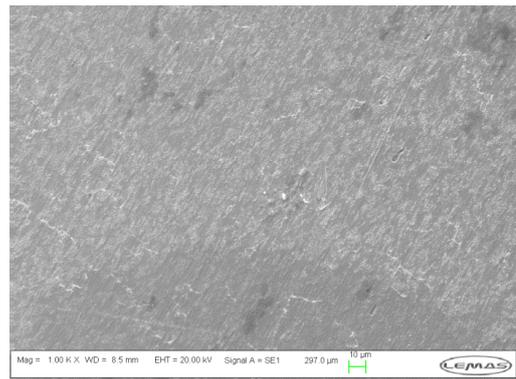
<p style="text-align:center">(f)</p>

Figure 5-11 : SEM images of X-65 carbon steel after 4 hours test for (a) blank (b) 50% MEG (c) 80% MEG at 20°C and (d) blank (e) 50% MEG (f) 80% MEG at 80°C.

The results of the SEM analysis of the carbon steel sample at 80°C after the electrochemical tests are also shown in Figure 5-11 (d, e, and f). From the result of the SEM of the blank solution at 80°C it was seen that the surface of the sample had both high general corrosion and localised corrosion on the surface of the sample. The ferrite had also being removed by the high corrosion rate leaving behind the iron carbide (Fe_3C). The high general corrosion is in line with the high corrosion rate from the LPR results of the blank sample. The SEM however showed the mixture of general and localised corrosion on the surface of the blank sample. The SEM image on the surface of the sample with 50% MEG and 80% MEG solution showed general corrosion and localised corrosion which were less compared to the blank sample. On the other hand, the SEM image for samples tested in both MEG at 20°C showed less general corrosion that that at 80°C. This was evident in the smooth surface of the SEM images at 20°C compared to the rough surface for SEM images at 80°C.

A summary of the average final corrosion of blank, 50% MEG and 80% MEG is shown in Table 5-1. The Table also shows the damage mechanism due to corrosion as observed from the SEM image.

Table 5-1 : Summary of the average final corrosion rate and damage mechanism for blank, 50% MEG, and 80% MEG. Here G represents general corrosion, G+L represents general and localised corrosion.

	Blank		50% MEG		80%MEG	
Temperature	20°C	80°C	20°C	80°C	20°C	80°C
Corrosion rate (mm/y)	2.25	5.60	0.44	2.34	0.14	0.50
Type of corrosion damage	High G+L	High G+L	G	G+L	G	G+L

5.5.1. Fourier Transform Infrared Spectroscopy (FTIR)

FTIR analysis was performed on the surface of the samples in experiments with MEG. The MEG solution was first scanned to get the FTIR spectrum of a typical

MEG. This spectrum was compared to the FTIR spectrum of the electrochemically tested MEG sample. Results showed that the spectrum of the electrochemically tested samples for both 50% MEG and 80% MEG were different from that of a typical MEG. Figure 5-12 shows the FTIR spectrum for MEG only and 50% MEG experiment samples at 80 °C. The tested samples from the 50% MEG did not show the C-O stretch between 1100 and 1200 cm^{-1} wavenumber and the peculiar O-H stretch of MEG was not visible at 3230 and 3550 cm^{-1} wavenumber. The two O-H and C-O stretches were both present for the typical MEG spectrum. This result indicates that MEG may not reduce corrosion by forming a strong interactive film (chemisorbed) on the surface. To verify the idea that MEG does not form a tenacious film on the surface of the carbon steel, further tests were performed in the next section to determine the type of mechanism for the reduction of corrosion by MEG.
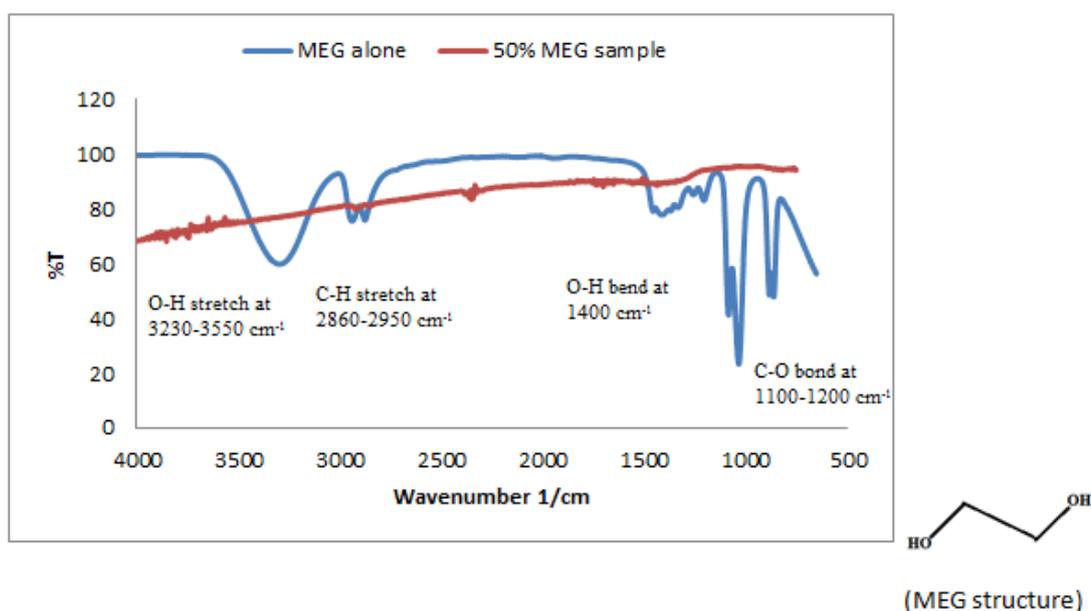
Figure 5-12 : FTIR spectrum for MEG only and 50% MEG experiment samples done at 80 °C.

5.5.2. Interferometry

The results from the profilometer are summarized together in Table 5-2. These were used to determine the damage and type of corrosion attack on the electrochemically

tested sample surfaces. The samples were tested as they were received after the electrochemical test with no additional surface clean up. In order to determine the type of corrosion on the surface of the sample, a threshold was assigned to the depth measurement. 1 µm depth was taken as the threshold to identify localised corrosion. Measurements below 1 µm depth were taken to be general corrosion while measurements above 1 µm depth were taken to be shallow pit. Any measurement above 10 µm depth was classified to be a deep pit. A schematic diagram describing the process of benchmarking on the tested sample to identify the type of corrosion that occurred is shown in Figure 5-13. The low value for the benchmark was taken due to the short period of test as the expected localized corrosion for the time taken for the experiment in this condition will be very low [167]. Interferometry test results showed that the maximum pit depths for MEG-only experiments at 20°C were less than 1 µm for the 4 hour duration test. At 80 °C, most of the samples with MEG had both shallow pitting and general corrosion. The maximum pit depths were for the blank samples which were expected with the consideration of the linear polarisation results. The pits for the blank samples were however wider in shape. This is due to several localised corrosion coming together to form one pit.
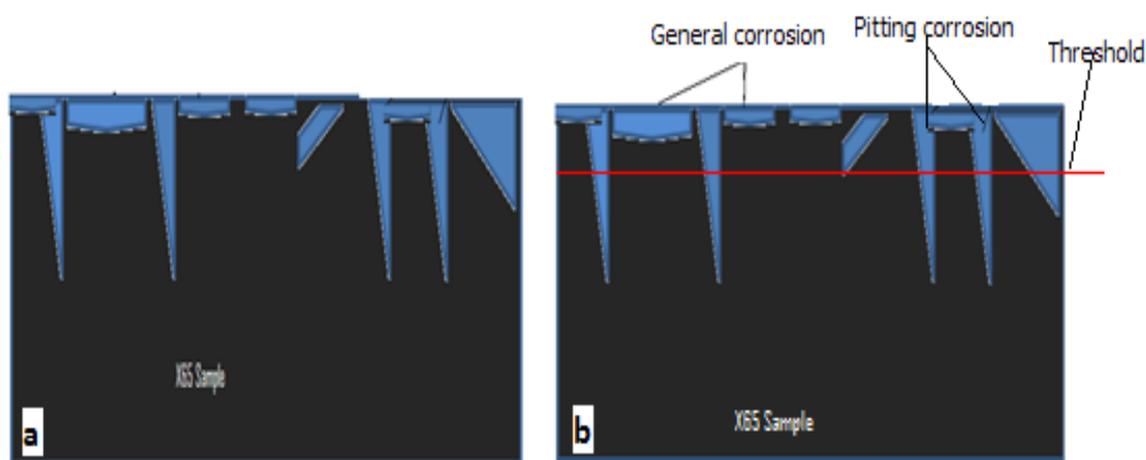
Figure 5-13 : Schematic representation of a sample after test (a)showing general and localised corrosion and (b) showing threshold cut off for pit classification.

Table 5-2 : Summary of the results from the profilometry tests.

Test	Average Corrosion rate (mm/y)	Temperature of test (°C)	Type of corrosion	Maximum pit depth (μm)	Total volume loss/mm^2 by corrosion (μm^3)
Blank	2.25	20	G +P	> 1	
50% MEG	0.44	20	G	< 1	$2.14*10^5$
80% MEG	0.14	20	G	< 1	$4.92*10^4$
Blank	5.6	80	G+P	> 1	
50% MEG	2.34	80	G+P	> 1	$3.52*10^5$
80% MEG	0.50	80	G+P	> 1	$2.48*10^5$

5.6. Determination of the adsorption property and enthalpy of adsorption of MEG

To determine further the mechanisms involved in the inhibition of carbon steel corrosion in the presence of MEG, the adsorption properties of MEG and the enthalpy of adsorption were predicted. The value of the enthalpy of adsorption gives the type of adsorption by MEG on the surface of the carbon steel.

5.6.1. Corrosion rate for different concentrations of MEG

The experiment for the different concentrations of MEG was performed to determine the corrosion rate and surface coverage (θ) on the carbon steel for 50% (i.e. $\theta_{0.5}$) . Tests were carried out at four different temperatures namely 20°C, 30°C, 50°C and 70°C. Initial results from the tests conducted for 50% MEG and 80%

MEG shows that the inhibitor surface coverage (θ) was more than 0.5 and so the concentration needed for MEG to achieve inhibitor surface coverage (θ) of 0.5 were below 50% MEG. This was also in agreement with the correction factor for de Waard previously presented in chapter 3 which gave 0.5 surface coverage (θ) to be below 50% MEG concentration [53]. For example, the surface coverage for 50% MEG on blank corrosion rate of 2.25mm/y at 20°C using de Waard correction factor will give (θ) to be 0.67. The starting point for the corrosion rate was then chosen to be 40% MEG as an estimate. Using equation 3-52 previously presented, the result for the 40% MEG shows that the surface coverage (θ) was more than 0.5 (i.e. $\theta >$ 0.5).

$$\theta = \frac{2.5817 - 0.6779}{2.5817} = 0.7374 \qquad\qquad 5\text{-}1$$

Efficiency is the surface coverage (θ) multiplied by 100

Figure 5-14 through Figure 5-17 shows the results for tests at different temperatures and concentrations of MEG. All the LPR results were compensated for solution resistance. It is worth noting that the solution resistance for the solution reduces with temperature and increases with the mass content of the MEG in the solution.
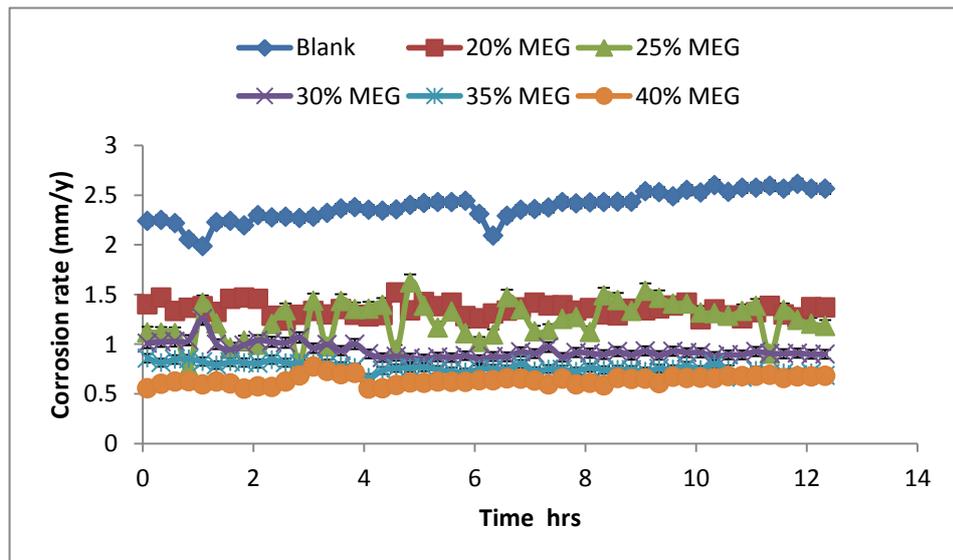
Figure 5-14 : Comparison of the corrosion rate for blank and different concentrations of MEG at 20°C (compensated LPR measurement)
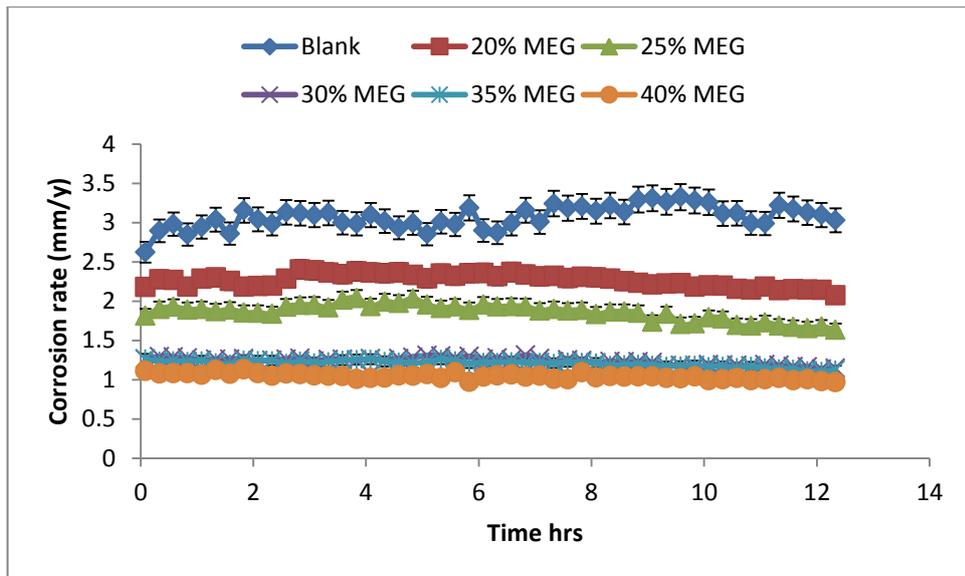
Figure 5-15 : Comparison of the corrosion rate for blank and different concentrations of MEG at 30°C (compensated LPR measurement)
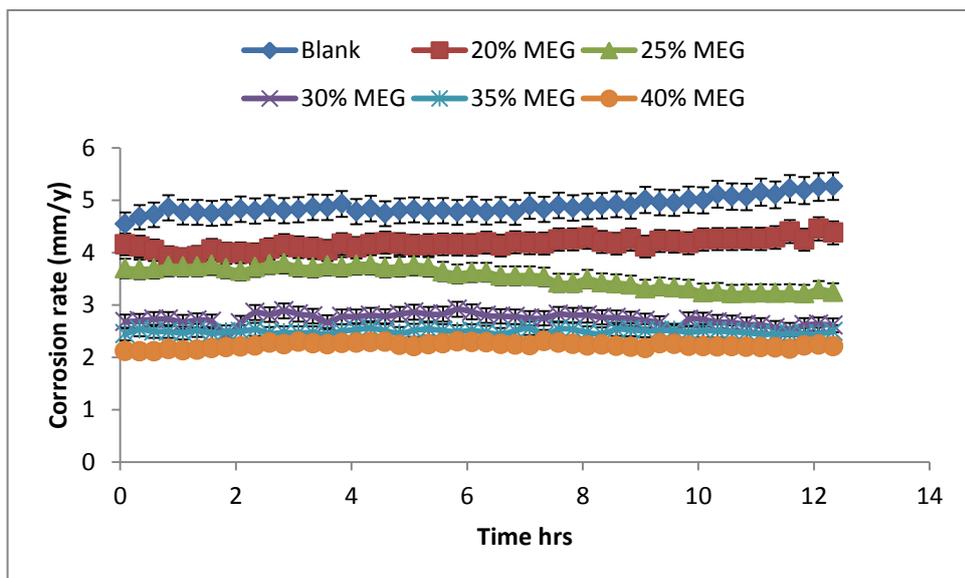
Figure 5-16 : Comparison of the corrosion rate for blank and different concentrations of MEG at 50°C (compensated LPR measurement)
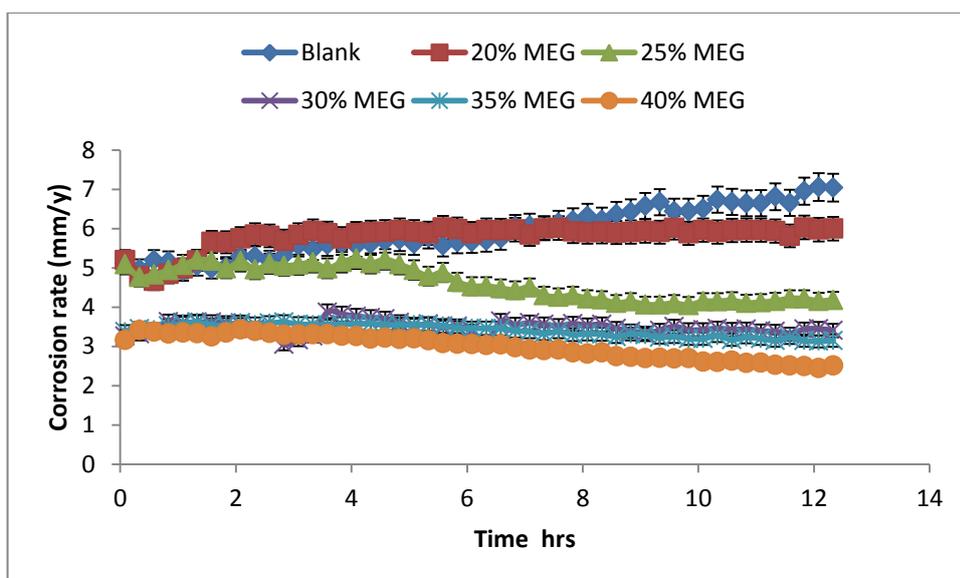
Figure 5-17 : Comparison of the corrosion rate for blank and different concentrations of MEG at 70°C (compensated LPR measurement)

The corrosion rate for the different concentrations of MEG showed similar trends as the temperature is increased. The increase temperature increases the corrosion rate of the carbon steel in the presence of MEG. Table 5-3 shows the summary of the surface coverage (θ) for carbon steel in different MEG concentration and different temperature.

Table 5-3 : Summary of the surface coverage (θ) for carbon steel in different MEG concentration and different temperature.

Concentration of MEG in percentage (%)	Concentration of MEG (mol/L)	Surface coverage (θ)			
		20°C	30°C	50°C	70°C
20	3.59	0.48	0.23	0.23	0.14
25	4.49	0.59	0.40	0.43	0.40
30	5.38	0.70	0.58	0.54	0.51
35	6.28	0.76	0.60	0.57	0.55
40	7.18	0.77	0.75	0.61	0.64

The results from the different concentrations were fitted into two adsorption isotherm equations for liquids (i.e. Langmuir isotherm and Temkin isotherm). Initial results show that high temperature results did not fit well for the Langmuir isotherm plots. Temkin isotherm plots were then considered for the fitting of the results. Equation 5-2 was derived from equation 3-54 previously presented in chapter 3. To construct the Temkin adsorption isotherm plots, the surface coverage θ was plotted against ln C for the different concentrations.

$$\theta = \left(1/f\right) ln K_{ad} + (1/f) ln C \qquad \text{5-2}$$

Where K_{ad} is the adsorption equilibrium constant, C is the analytical concentration of the MEG and f is the molecular interaction constant.

The slope of the graph gives the inverse of the molecular interaction while the intercept gives the product of the molecular interaction and the adsorption equilibrium constant [137, 142].

The surface coverage (θ) was derived from the average final corrosion rate results for 20°C, 30°C, 50°C and 70°C. The plot of the graph for temperature of 20°C is shown in Figure 5-18. This gives a reasonable straight line graph that fits to Temkins adsorption equation. The R^2 value was 95% for the line fitting.

The plot of the graph θ vs. *ln* C for the different concentrations of MEG was also performed for the 30°C temperature. The graph gave a good fit on the Temkin adsorption equation with R^2 value equal to 97%. The same result is achieved for the two other temperatures of 50°C and 70°C with the higher temperature having less R^2 value than the previous lower temperature. The results are shown in Figures 5-19 through Figure 5-21.
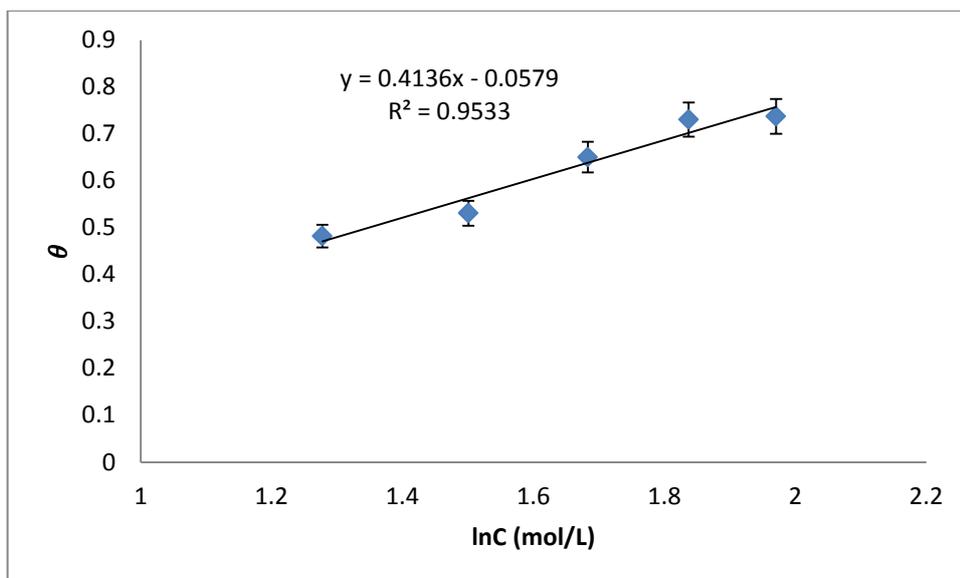
Figure 5-18 : Temkin adsorption isotherm plots at 20°C for different concentration of MEG.
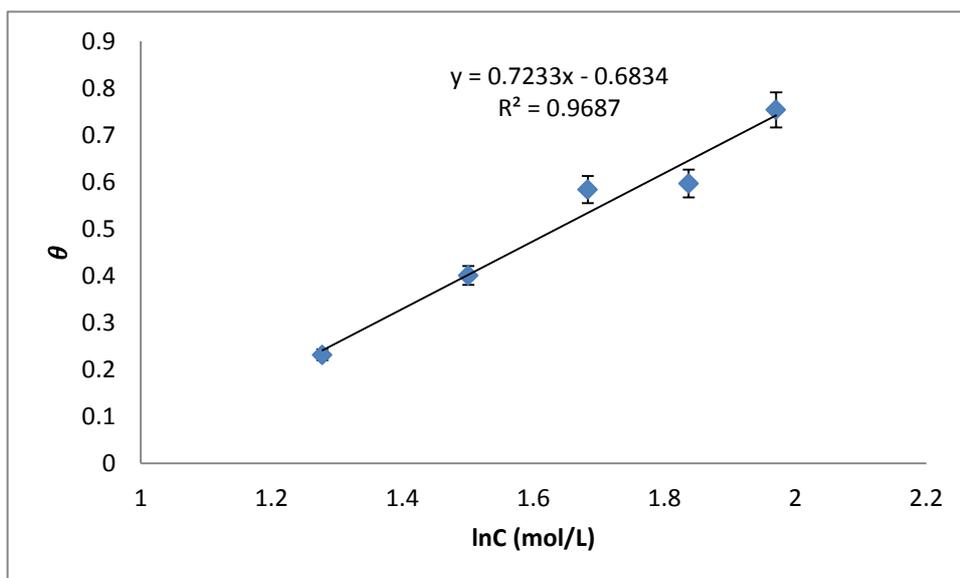
Figure 5-19 : Temkin adsorption isotherm plots at 30°C for different concentration of MEG
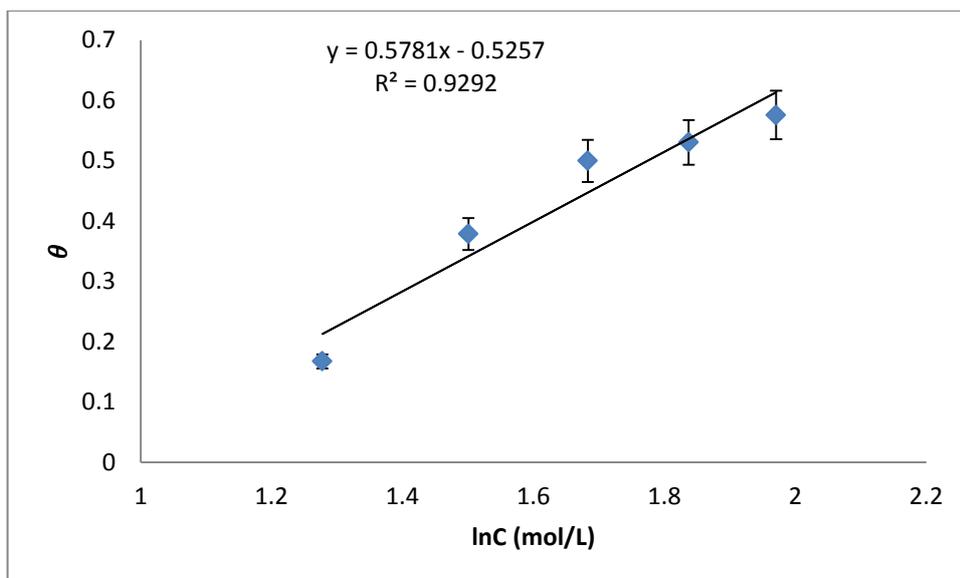
Figure 5-20 : Temkin adsorption isotherm plots at 50°C for different concentration of MEG
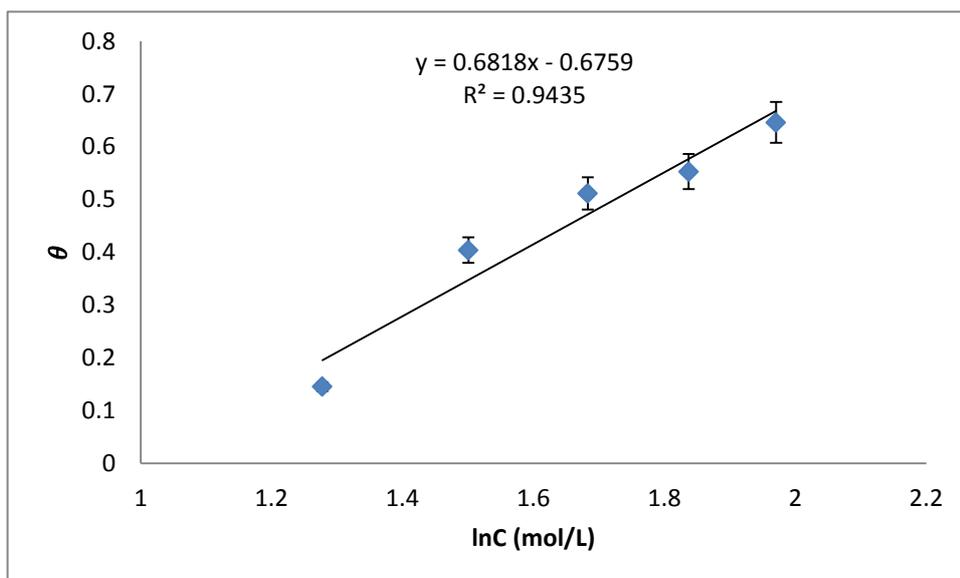
Figure 5-21 : Temkin adsorption isotherm plots at 70°C for different concentration of MEG

The Van't hoff plot for MEG, where the surface coverage (θ) = 0.5 for each temperature of 20, 30, 50 and 70 is derived. The Van't hoff type of equation is described in equation 5-3. The natural log of concentration in mol/L is plotted against the inverse of the temperature in Kelvin scale based on equation 5-3 [168].

$$InC_{\theta 0.5} = \Delta H^{\circ}_{ad}/_{RT} + Constant \qquad\qquad 5\text{-}3$$

Where R is the universal gas constant ($8.314 Jmol^{-1}K^{-1}$) and $InC_{\theta 0.5}$ is equivalent to the concentration of inhibitor required for $\theta = 0.5$ and ΔH_{ad}° is the isosteric enthalpy of adsorption.

The slope of the Van't hoff plot will give the value of $\Delta H_{ad}^{\circ}/$ R. The value of the enthalpy of adsorption will determine the type of adsorption that exists between the metal surface and the MEG. The concentration of the inhibitor is in mol/L. From the result of the plot in Figure 5-22, the negative slope in the graph indicates that the enthalpy of adsorption is negative. The actual calculation for the enthalpy of adsorption is given as

$\Delta H_{ad}^{\circ}/ R = $ -519.96 K $\qquad\qquad\qquad\qquad\qquad\qquad\qquad$ 5-4

$\Delta H_{ad}^{\circ} = $ -4.32 kJ/mol $\qquad\qquad\qquad\qquad\qquad\qquad\qquad$ 5-5
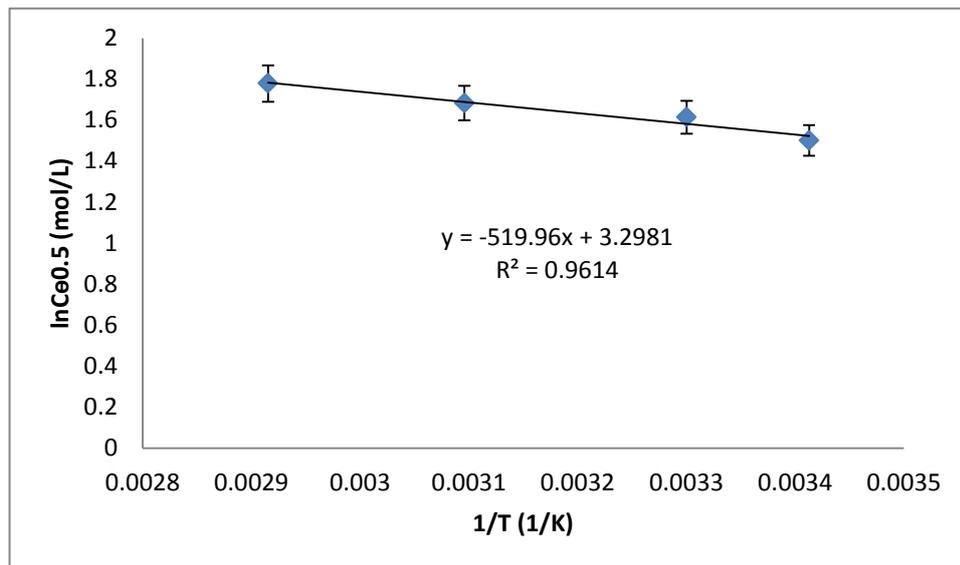
Figure 5-22 : Van't Hoff plots of $lnC_{\theta 0.5}$ against 1/T for temperature range of (20°C to 70°C)

The value of the isosteric enthalpy of adsorption $\Delta H_{ad}°$ is -4.32kJ/mol. The reaction is exothermic and shows that the mode of adsorption of MEG to surface of the carbon steel is by physisorption and not by chemisorption [139, 142, 169].

To further verify the type of adsorption, activation energy (E_a) was derived. Values above 80kJ/mol indicate chemisorption while values below 80kJ/mol infer physisorption [140]. The activation corrosion energy (E_a) can be calculated using the values of corrosion rate at different temperature. This is achieved using the Arrhenius type of equation derived from equation 3-40. This equation is given as

$$CR = Ae^{\frac{-E_a}{RT}} \qquad\qquad\qquad 5\text{-}6$$

Where CR is the corrosion rate, A is the Arrhenius pre-exponential constant E_a is the apparent activation corrosion energy and RT has their usual meaning as previously described.

A plot of $lnCR$ against the inverse of absolute temperature (1/T) will give a slope equal to E_a/R from which E_a can be derived. A typical plot of $lnCR$ against 1/T at 20% MEG and 30% MEG is shown in Figure 5-23.
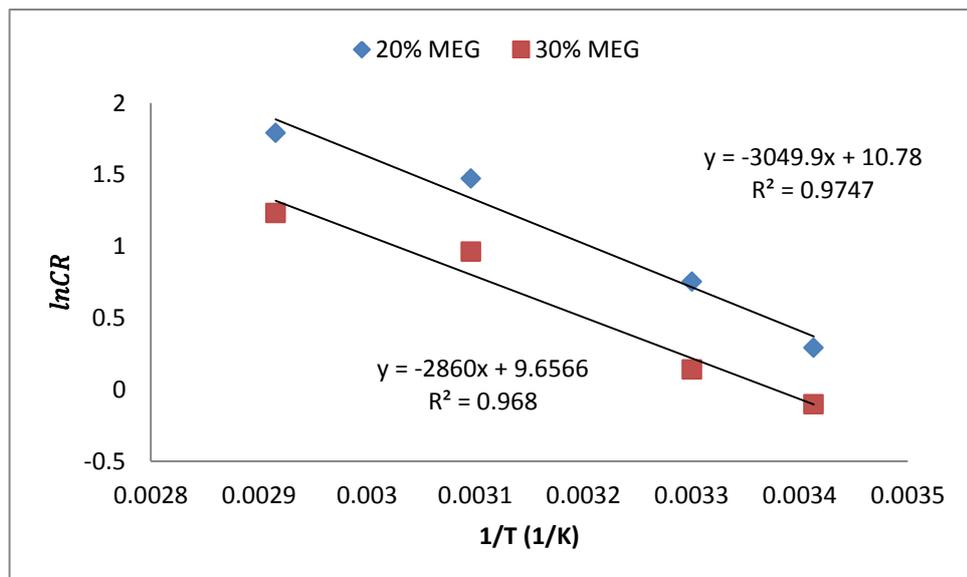
Figure 5-23 : Log of corrosion rate vs inverse of temperature (1/T) for the derivation of activation energy (E_a) based on Arrhenius type of equation.

Table 5-4 : Summary of the activation energy (E_a) for corrosion test in MEG.

Concentration of MEG in percentage (%)	Concentration of MEG (mol/L)	Activation energy (E_a) KJ/mol
20	3.59	25
25	4.49	22
30	5.38	23
35	6.28	25
40	7.18	23

The results of the apparent activation energy for the different concentrations of MEG tested were in the range of 22kJ/mol and 25kJ/mol. The activation energies were below 80kJ/mol and in line with the results from isosteric heat of adsorption that indicate that physisorption of MEG to the surface of the carbon steel was likely.

5.7. Summary of results of corrosion process in the presence MEG

This chapter described the result and discussion of the test performed on carbon steel X65 in the presence of MEG. It can be summarised as follows.

- AC and DC tests results showed that MEG was able to reduce the corrosion rate of carbon steel with the effect being higher for 80% MEG as compared to the 50% MEG. However, its effectiveness reduces at high temperature (i.e. 80°C)

- Conductivity test shows that MEG containing solution has low conductivity which supports the fact that MEG will give high solution resistance as seen in the AC impedance results.

- The study showed that the conductivity of MEG solution reduces with the concentration of MEG and the corrosion resistance of carbon steel in the solution increases with the concentration of MEG for both low and high temperature.

- LPR method can give erroneously high corrosion resistance for tests carried out with MEG solution if the solution resistance is not accounted for using techniques such as AC impedance method.

- SEM was used to characterize carbon steel samples after tests and showed lower general corrosion for MEG test compared to the blank test.

- FTIR analysis suggests that MEG does not reduce corrosion by the formation of a strong interactive film on the surface of the carbon steel.

- Adsorption properties study of MEG in the presence of carbon steel corrosion showed that MEG can fit into the Temkins adsorption isotherm. A negative isosteric enthalpy indicates exothermic adsorption reaction by MEG and indicates physisorption process of adsorption.

- The low values of the activation corrosion energy in the range of 25kJ/mol and 22kJ/mol support the fact the MEG physical interacts with the carbon steel.

Chapter 6. CORROSION PROCESSES IN THE PRESENCE OF ORGANIC CORROSION INHIBITORS

6.1.Introduction

The use of corrosion inhibitors is common in the oil and gas industry in preventing CO_2 internal corrosion on long carbon steel pipelines [148, 170, 171]. This is due to the ease of application of these corrosion inhibitors, the effectiveness and cost compared to most methods such as internal coatings for prevention. Most of these inhibitors are complex organic compounds which basically work by attaching themselves to the steel surface and forming a film that acts as a barrier to the corrosion species. They may do so through physisorption or chemisorption as previously described. The corrosion inhibitors can be applied in different conditions and in combination with other inhibitors such as hydrate inhibitors and scale inhibitors. For successful deployment of corrosion inhibitors, they must be compatible with other oilfield chemicals. This means that they must not compete against the other chemicals or induce processes such as foaming or emulsion formation.

This chapter investigates two potential commercial inhibitors which are applied in pipelines in combination with MEG as a hydrate inhibitor. The tests will be used to determine the manner in which these inhibitors work on their own. The inhibitors comprise a non-green inhibitor (i.e. benzyl alkyl pyridinyl quaternary ammonium chloride) and green inhibitor (i.e. aminoxy-ethyl-ester) as described in the experimental set up. The non-green inhibitor will be denoted as inhibitor 1 and the green inhibitor will be denoted as inhibitor 2.

6.2. Open Circuit Potential (OCP) measurement

As previously described, the OCP can be used to describe the way in which a corroding system behaves in the presence of an inhibitor. The measured OCP value indicates how the surface of the metal behaves with the solution in which it is immersed. If an inhibitor forms a protective film on the surface of the metal, the

change in the EDL will be reflected in the changes in the potential of the metal which will affect the OCP values. In most cases the change will lead to an increase in the OCP to a noble value. This gives an insight of how the inhibitor works[17].

In this test the OCP of the blank solution without inhibitor and the solution with inhibitor was observed at different points using a Ag/AgCl reference electrode. The final average OCP values for the blank test and those with inhibitor 1 at 20°C and 80°C are shown in Figure 6-1 and Figure 6-2 respectively. The final average OCP value for the blank solution at 20°C was -673mV for the tested period. A positive change in the value of the OCP was seen for the solution with inhibitor 1 at all concentration. The 100ppm inhibitor 1 concentrations had the most positive increase with 10ppm inhibitor 1 concentration having the least increase. The increase in the OCP may likely be an indication of the reduction in the corrosion activities on the surface of the metal. Wang [8] had used the OCP measurement as a semi-quantitative method to understand the behaviour of corrosion inhibitors and also determine the reduction of corrosion activity on the surface of carbon steel in the presence of those corrosion inhibitors. Similar behaviour was also observed at higher temperature of 80°C. This again indicated possible reduction in the corrosion rate of the carbon steel in the presence of the inhibitor.
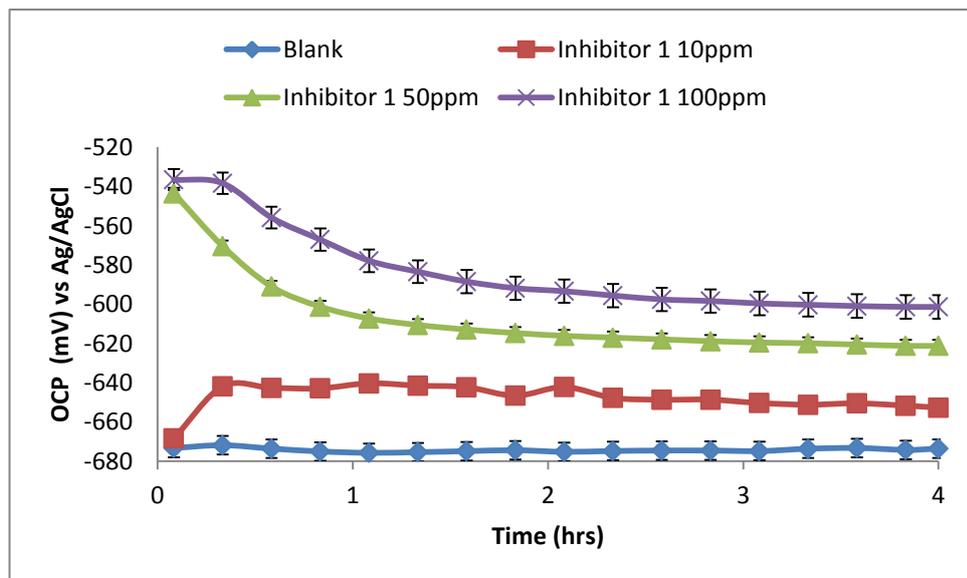
Figure 6-1 : OCP values against time for blank, 10ppm inhibitor 1, 50ppm inhibitor 1, and 100ppm inhibitor 1 at 20°C
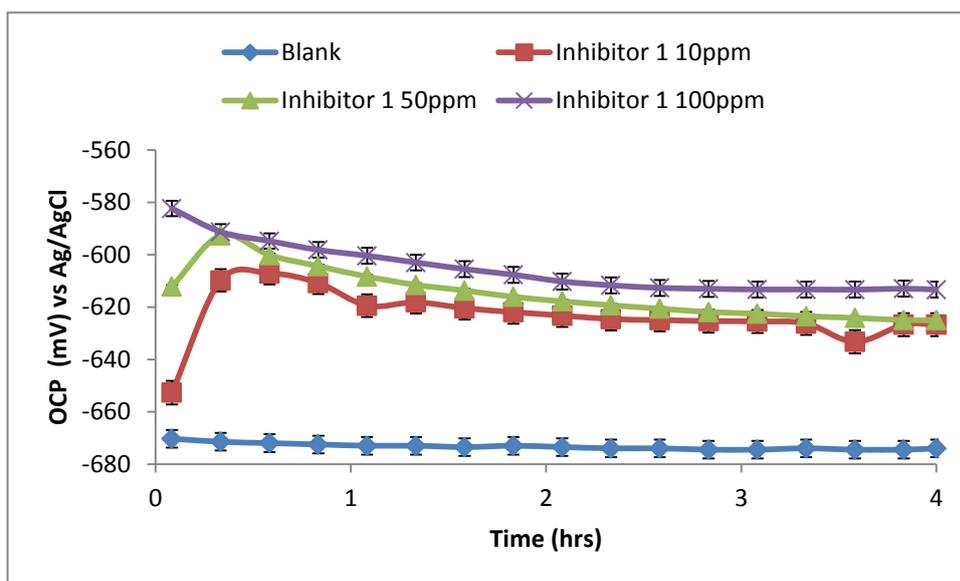
Figure 6-2 : OCP values against time for blank, 10ppm inhibitor 1, 50ppm inhibitor 1, and 100ppm inhibitor 1 at 80°C

The final average OCP values for the blank and inhibitor 2 at both 20°C and 80°C are shown in Figure 6-3 and Figure 6-4 respectively. For test carried out at 20°C all concentrations of inhibitor 2 shifted the final OCP values in the positive as compared to the final average OCP value for the blank solution. The change in OCP for inhibitor 2 did not seem very dependent on concentration. This may mean that there are no much difference in the concentration needed to reduce corrosion with 10ppm and 50ppm inhibitor 2. The 100ppm showed the most positive and noble final OCP value at this temperature.

For high temperature of 80°C, the average final OCP value also showed an increased in the positive direction as compared to the blank solution. However there was an overall reduction at this high temperature as compared to the low temperature. This was seen especially for the 10ppm and 50ppm inhibitor 2 concentration. It may mean that the reduction in the corrosion activities at this high temperature for the two concentration of inhibitor 2 is minimal.

144
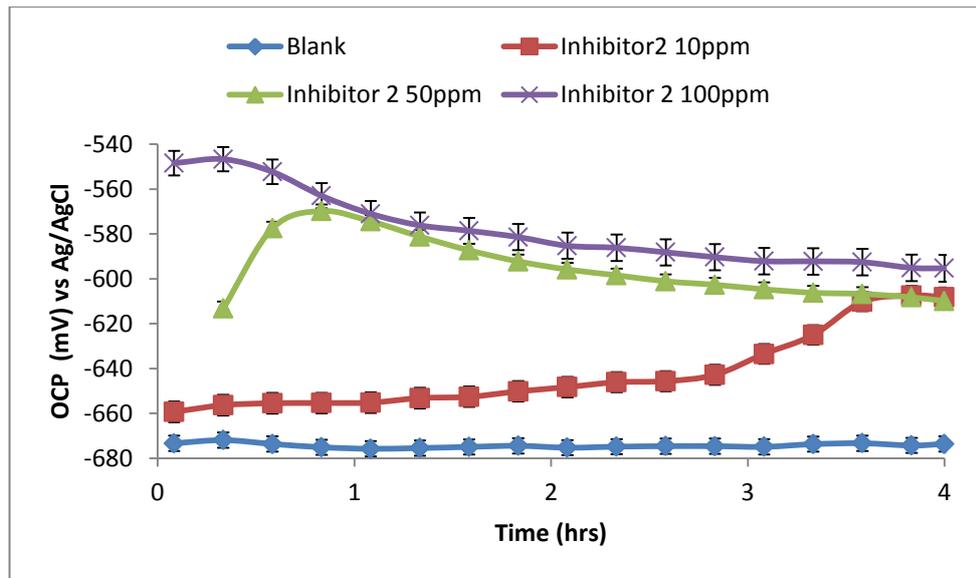
Figure 6-3 : OCP values against time for blank, 10ppm inhibitor 2, 50ppm inhibitor 2, and 100ppm inhibitor 2 at 20°C
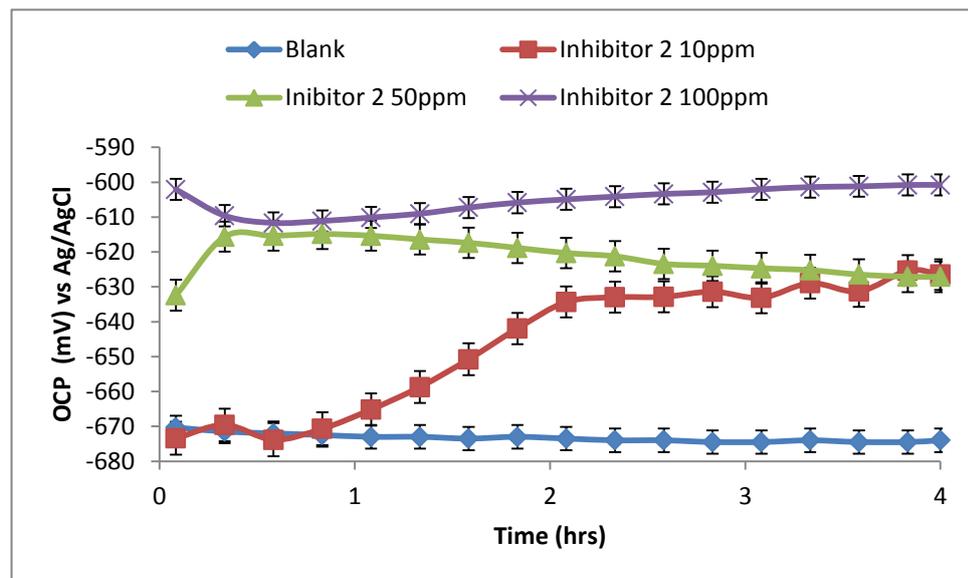
Figure 6-4 : OCP values against time for blank, 10ppm inhibitor 2, 50ppm inhibitor 2, and 100ppm inhibitor 2 at 80°C

Table 6-1 shows the ssummary of the final OCP values for blank and different concentrations of inhibitor 1 and inhibitor 2 at 20°C and 80°C. The final OCP value for all the test with both inhibitors showed an increase from the OCP value of the

blank. This is an indication that the inhibitors even at low concentration has reduction in the anodic reaction.

Table 6-1 : Summary of the final OCP values for blank, and different concentrations of inhibitor 1 and inhibitor 2 at 20°C and 80°C.

Temperature	Blank	Inhibitor 1			Inhibitor 2		
		10ppm	50ppm	100ppm	10ppm	50ppm	100ppm
20°C	-673	-653	-621	-601	-609	-610	-595
80°C	-674	-627	-625	-613	-626	-627	-601

6.3. Linear Polarization Resistance (LPR) measurement

The use of OCP measurement as described previously is always a quick and easy way to observe the corrosion reaction of carbon steel but it is not quantitative. This method can often give limited information on the corrosion reaction of the carbon steel in the presence of inhibitor. The information in some instances may not be conclusive or confirmatory [17]. In order to get more information, the linear polarization measurement of the carbon steel was taken for a blank solution and also in the presence of both inhibitors for different concentrations. In chapter 5, the R_p values of the blank solution were used directly to calculate the corrosion rate because the solution resistance was negligible. The R_p values in the presence of the inhibitors were also used for the calculation of the corrosion rate as the solution resistance was also found to be negligible as well. The solution resistance was calculated using the AC impedance method as described further in the next section. The linear polarization results are shown and described below.

Two separate potential scans from 0 to -250mV and 0 to 250mV were performed for the inhibitors to derive the anodic and cathodic slope Tafel constants. The potentiodynamic sweeps were analysed and at 80°C shows the anodic slope constant β_a was reduced from 120mV/decade to 98mV/decade, while there was little effect on the cathodic slope constant (i.e. β_c is 136 mV/decade) for inhibitor 1. This is shown

in Figure 6-5. This suggests that the inhibitor 1 is mostly an anodic inhibitor [8, 172]. It tends to reduce more of the anodic reaction from occurring on the carbon steel surface.

The potentiodynamic test in Figure 6-6 using inhibitor 2 also shows a similar reduction in the anodic constant slope of β_a to 86mV/decade and while the β_c still gave 133mV/decade. This also indicate that the inhibitor 2 also work by reducing mainly the anodic reaction. However the Tafel constant (B) of 26 as generated from the potentiostat software were used for the calculation of the corrosion rate. The difference with the use of the Tafel constant from the software was not much when compared to the actual calculated Tafel constant with the later giving a slightly lower corrosion rate. The corrosion rate from LPR was calculated using the Stern-Geary equation as previously described.

The linear polarization results for 4 hours period for the inhibitor 1 at 20°C are shown in Figure 6-7. The results gave the polarisation results for the different concentration of 10ppm, 50ppm, and 100ppm tested with the inhibitor. It is clearly seen that at this temperature, the corrosion rate of the carbon steel decreases with the addition of the inhibitor as expected. At higher inhibitor concentrations, the corrosion rate reduces further indicating that concentration of the inhibitor plays a major role in reducing the corrosion rate. From the result, it can be seen that the corrosion rate reduces further with the 100ppm having the lowest corrosion rate. The final average corrosion rates were 0.19mm/y for the 10ppm concentration, 0.13mm/y for the 50ppm concentration and 0.04mm/y for the 100ppm concentration. The reduction with concentration level indicates that the lower concentrations are not the optimum concentration. This is also in line with the observations from the OCP measurements for inhibitor 1 that shows that increase in concentration increases the OCP values to a more noble state.

For tests carried out using inhibitor 2 at 20°C, the results in Figure 6-8 show a reduction in the corrosion rate for all concentrations used. The corrosion rate for concentration of 10ppm inhibitor 2 reduces drastically and a further slight reduction in corrosion rate was seen for concentration of 50ppm. The final average corrosion rates were 0.03mm/y for the 10ppm concentration, 0.02mm/y for the 50ppm concentration and 0.02mm/y for the 100ppm concentration.

147
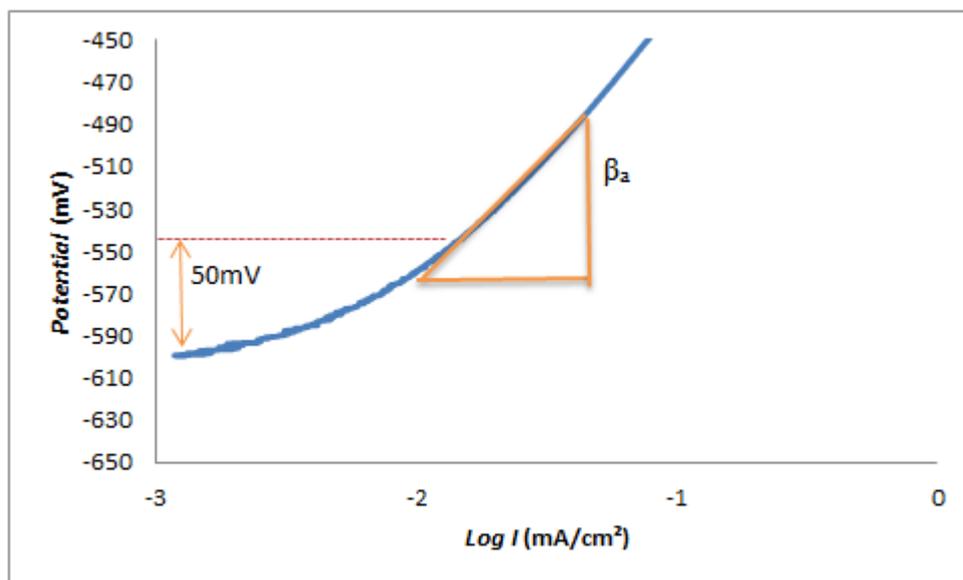
(a)
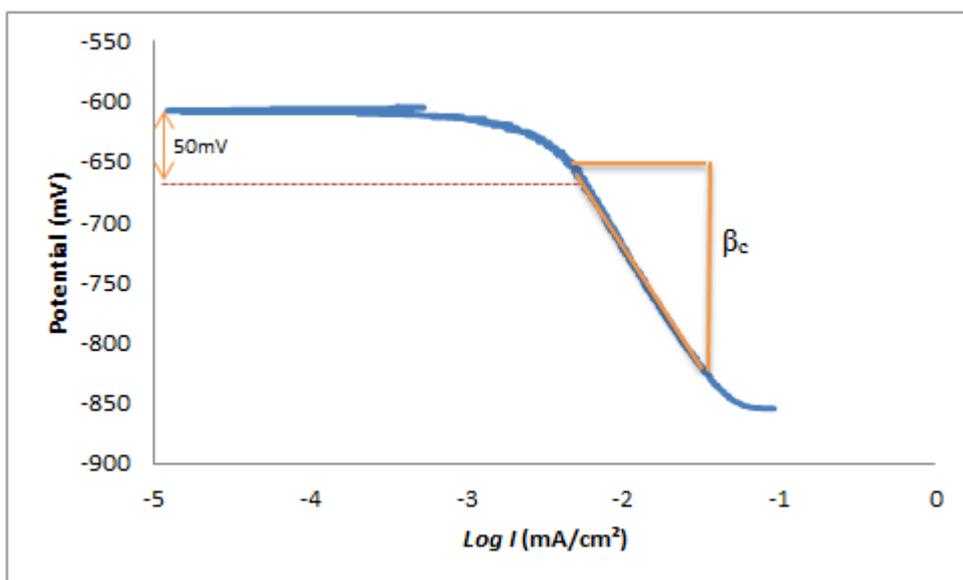
(b)

Figure 6-5 : Result for the calculation of the (a) anodic Tafel constant (b) cathodic Tafel constant for 100ppm inhibitor 1 at 80°C.
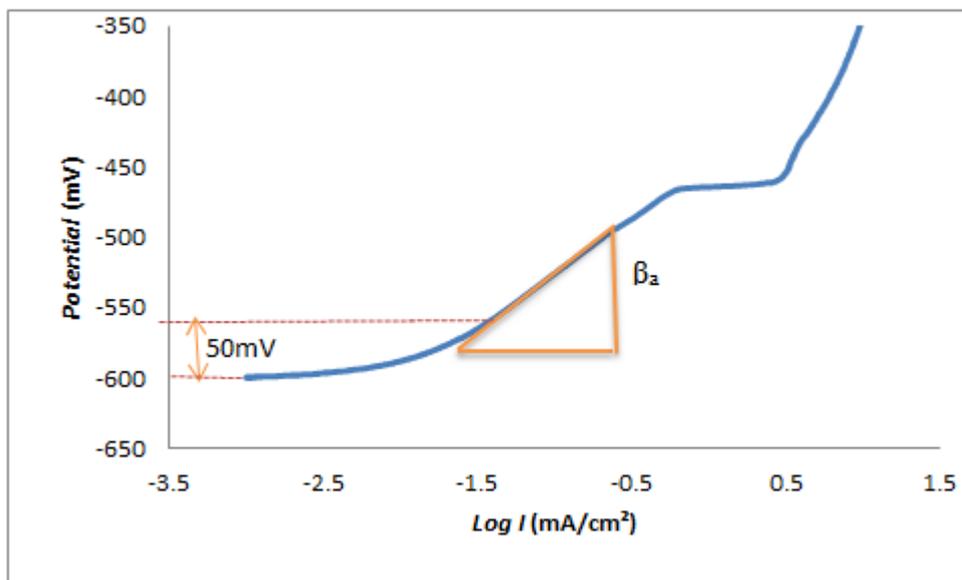
(a)
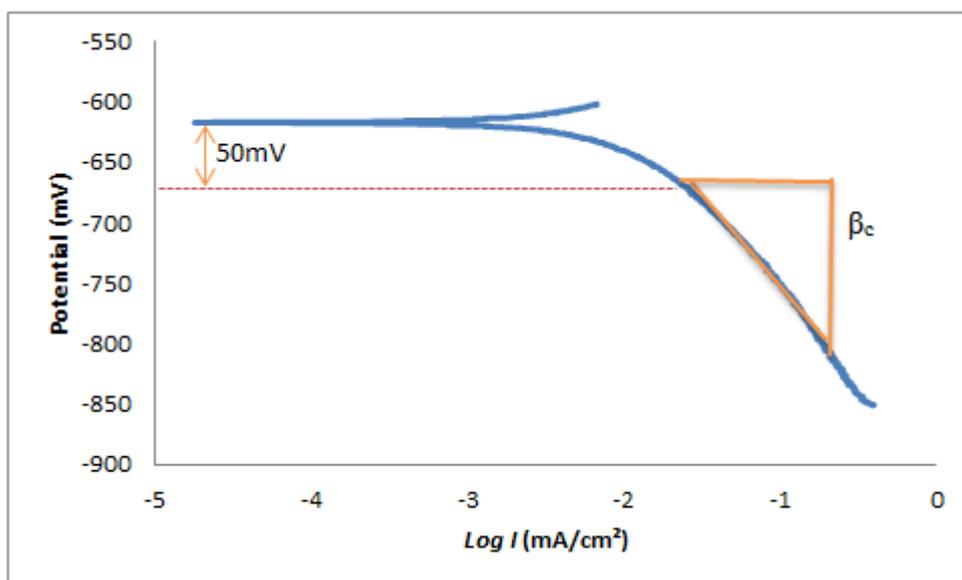
(b)

Figure 6-6 : Result for the calculation of the (a) anodic Tafel constant (b) cathodic Tafel constant for 100ppm inhibitor 2 at 80°C.
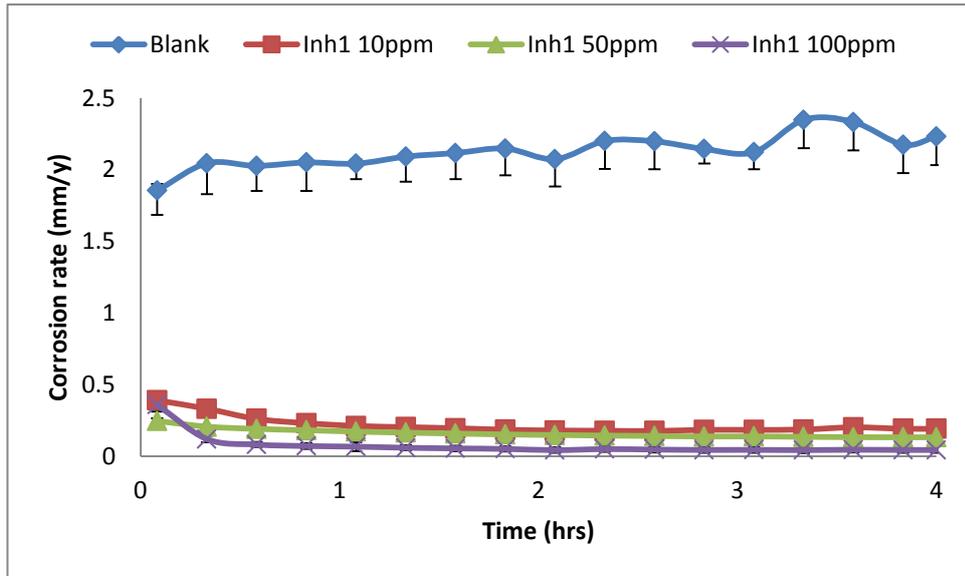
(a)
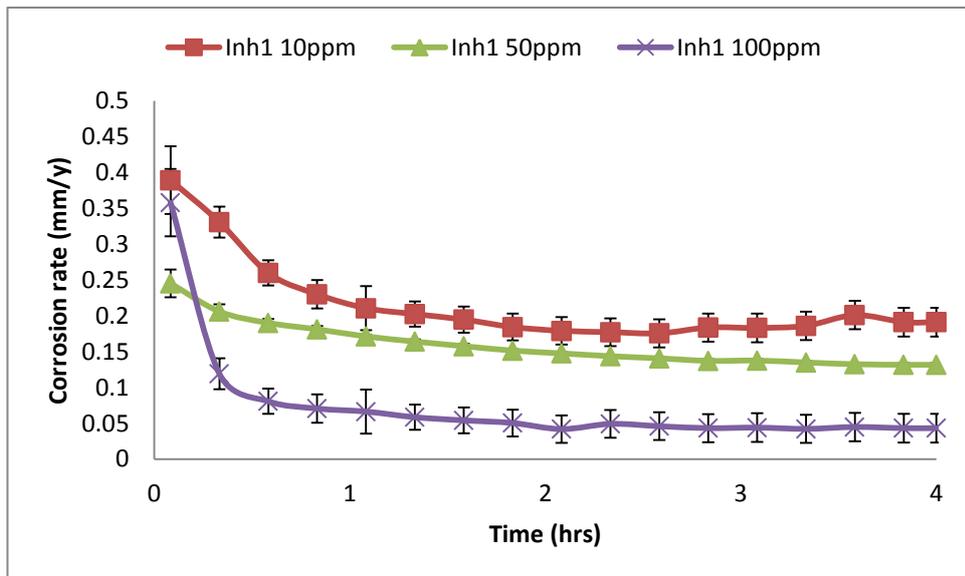
(b)

Figure 6-7 : Corrosion rate at 20°C: (a) blank and different concentrations of inhibitor 1; (b) different concentrations of inhibitor 1.
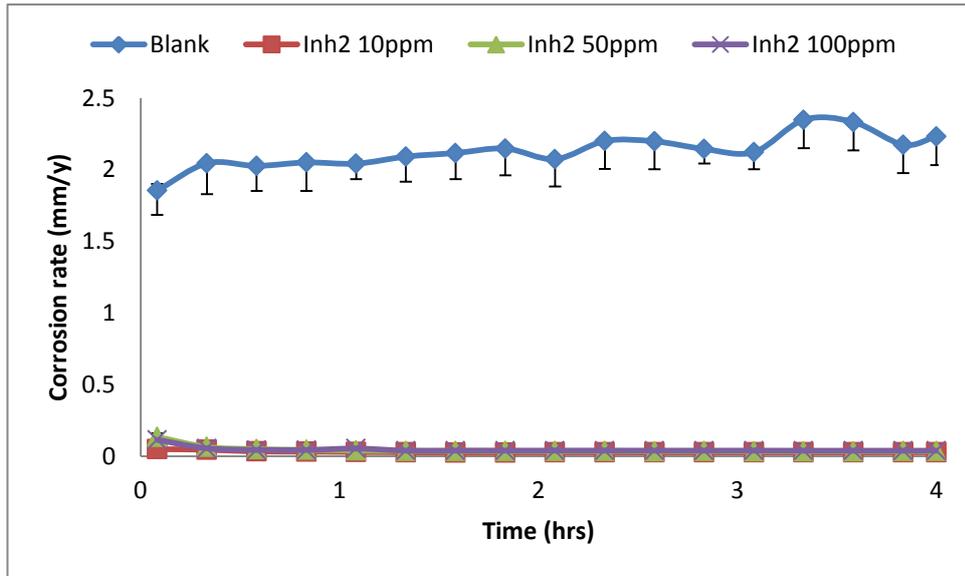
(a)
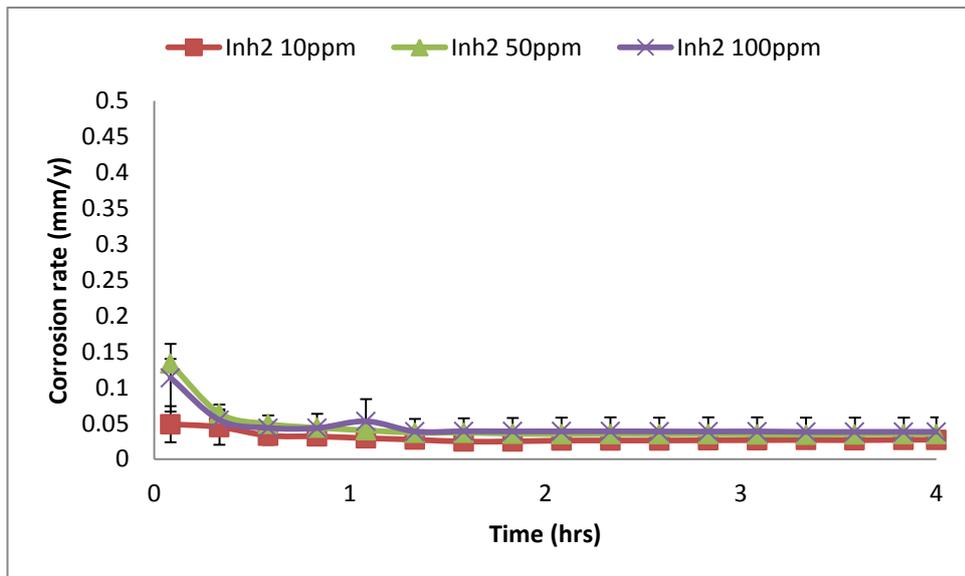
(b)

Figure 6-8 : Corrosion rate at 20°C: (a) blank and different concentrations of inhibitor 2; (b) different concentrations of inhibitor 2.

An increase in the concentration from 10ppm to 100ppm does not give a corresponding large reduction in the corrosion rate as expected. This may be that the optimum concentration for the inhibitor is below the 100ppm concentration. If this occur the efficiency of the inhibitor may even reduce at concentration above the optimum concentration [173]. This is quite different from the results of inhibitor 1

151

that shows reduction in the corrosion rate with concentration from 10ppm to 100ppm. This is in agreement with OCP measurements of inhibitor 2 which showed that an increase in the concentration of inhibitor 2 from 10ppm does not play much role in the increase of the final average OCP value.

Figure 6-9 shows a comparison of the corrosion rate for inhibitor 1 and inhibitor 2 at 20°C. It is observed that the corrosion rate in the presence of the inhibitor 2 reduces more than the corrosion rate in the presence of inhibitor 1 for the same concentration. This suggests that the inhibitor 2 is a very efficient inhibitor at low temperature of 20°C. The efficiency of the inhibitors are summarised in the Table 6-2.

Table 6-2 : Summary of the efficiency of both inhibitors at 20°C

	INHIBITOR 1			INHIBITOR 2		
Concentration	10ppm	50ppm	100ppm	10ppm	50ppm	100ppm
Efficiency (%)	91	94	98	97	98	98
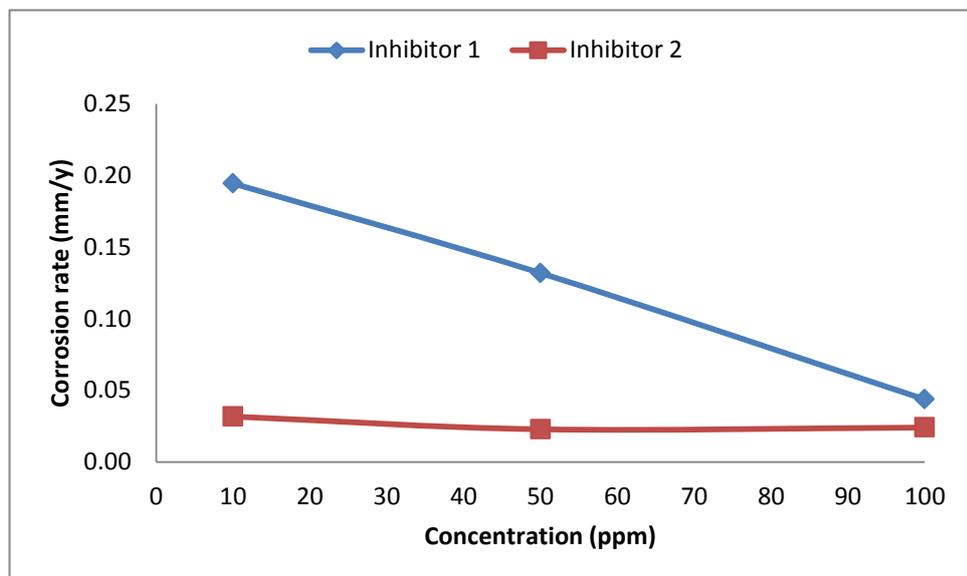
Figure 6-9 : Comparison of the final average corrosion rate of blank, inhibitor 1 and inhibitor 2 for different concentrations at 20°C (LPR Measurement)

The linear polarization results of tests carried out with inhibitor 1 at 80°C for 4 hours are shown in Figure 6-10.
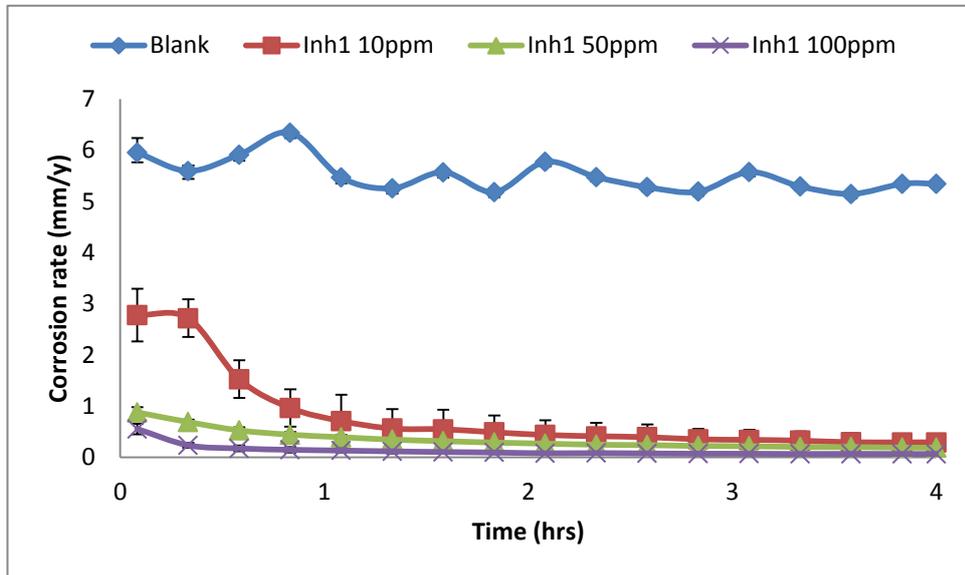
(a)
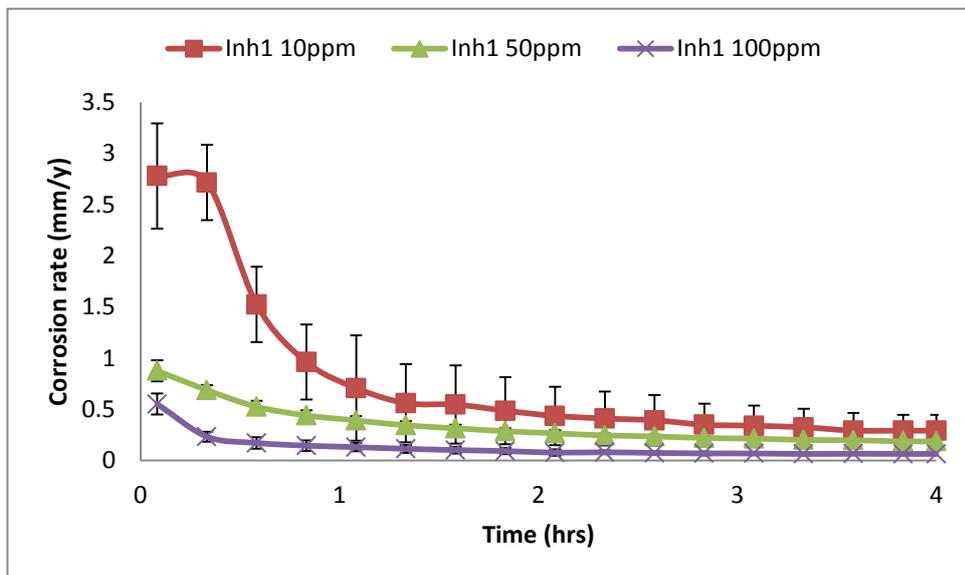
(b)

Figure 6-10 : Corrosion rate at 80°C: (a) blank and different concentrations of inhibitor 1; (b) different concentrations of inhibitor 1.

There was a reduction in the corrosion rate with higher concentration having lower corrosion rate. This is similar to the corrosion rate results derived at 20°C. Electrochemical measurement results from LPR show that the corrosion rate of the carbon steel in inhibitor 1 was higher at high temperature of 80°C except for one with 100ppm inhibitor 1. 100ppm inhibitor 1 at 80°C has a corrosion rate of 0.06mm/y after 4hrs. The surface coverage is 0.99 and the efficiency is highest at this concentration. For the test using inhibitor 2 at temperature of 80°C, the results as seen in Figure 6-11 did not show a drastic reduction in the corrosion rate at all concentration used as seen at the lower 20°C.

The corrosion rate for concentration of 10ppm inhibitor 2 was as high as 0.25mm/y and also high for concentration of 50ppm at 0.20mm/y. The final average corrosion rates were 0.16mm/y for the 100ppm concentration. It can be seen at 80°C that the corrosion rate reduces with increase in concentration level from 10ppm to 100ppm. This is quite different from the lower temperature where the optimum concentration was observed to be below 100ppm. This change is quite critical and shows that the optimum temperature for this type of inhibitor should only be given after it has been tested at the operating temperature. The poor inhibition observed at this temperature for lower concentration gives an indication that inhibitor 2 may not work effectively at high temperature as compared to lower temperature.

The efficiency of the inhibitors at high temperature of 80°C is calculated. A summary of it is presented on Table 6-3. A comparison of the final corrosion rate of blank, inhibitor 1 and inhibitor 2 for different concentrations at 80°C is also shown in Figure 6-12

A comparison of the corrosion rate of both inhibitors at this temperature of 80°C shows that the corrosion rate in the presence of the inhibitor 1 reduce more than the corrosion rate in the presence of inhibitor 2 for the same concentration except for 10ppm concentration. This may mean that the inhibitor 1 is very efficient inhibitor at 80°C. The fractional surface coverage is 0.99 and the efficiency is highest at that concentration of 100ppm for inhibitor 1. It may be that the optimum concentration for inhibitor 1 is 100ppm at 80°C. Inhibitor 1 at 100ppm was also able to reduce the corrosion rate below 0.1mm/y. All concentrations tested for inhibitor 2 did not show satisfactory reduction in the corrosion rate below 0.1mm/y at 80°C. This may be that

154

the inhibitor 2 does not function well at 80°C unlike inhibitor 1 which is very active at that temperature [174]. In other to learn more about the inhibition behaviour of the two inhibitors AC impedance test and surface analysis were performed on the sample.
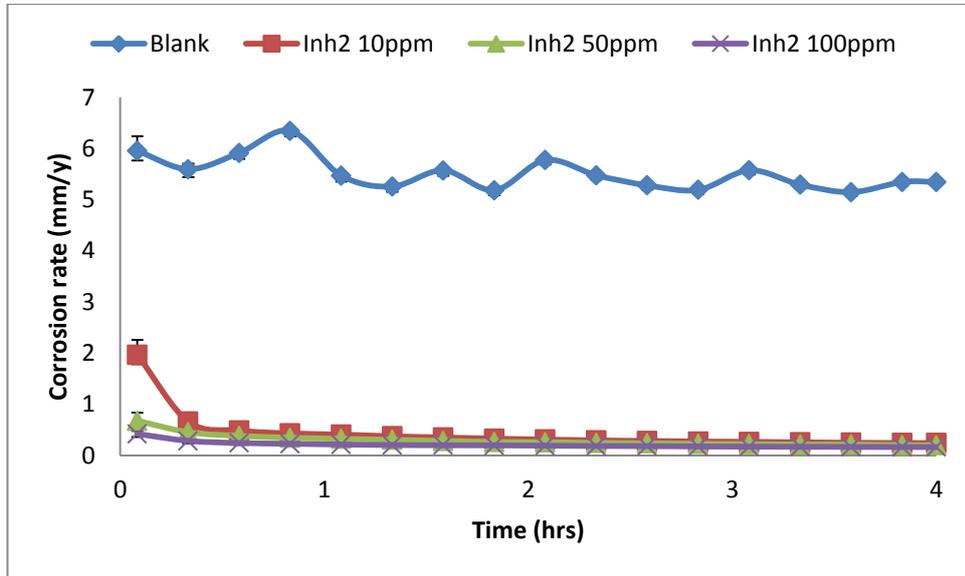
(a)
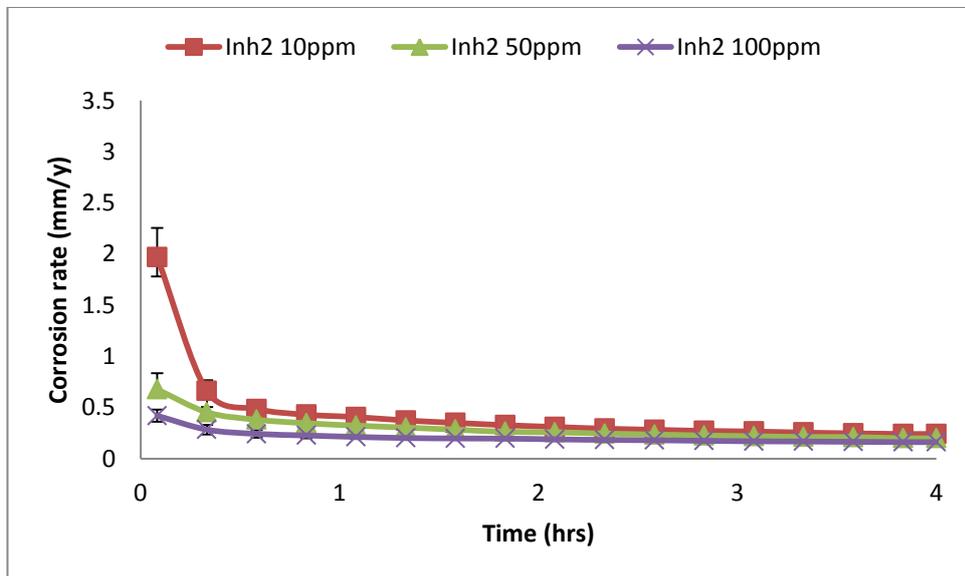
(b)

Figure 6-11: Corrosion rate at 80°C: (a) blank and different concentrations of inhibitor 2; (b) different concentrations of inhibitor 2.

Table 6-3 : Summary of the efficiency of both inhibitors at 80°C

	INHIBITOR1			INHIBITOR2		
Concentration	10ppm	50ppm	100ppm	10ppm	50ppm	100ppm
Efficiency (%)	95	97	99	95	96	97
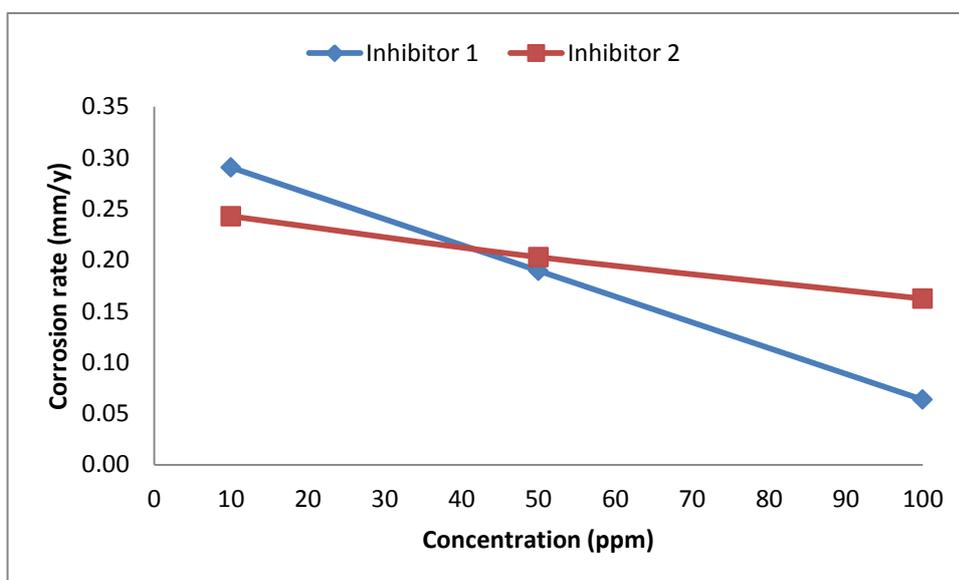
Figure 6-12 : Comparison of the final corrosion rate of inhibitor 1 and inhibitor 2 for different concentrations at 80°C (LPR Measurement)

6.4. AC Impedance

The use of linear polarisation method above has so far given corrosion results of the carbon steel in the presence of the inhibitors. It does not really provide information on the possible mechanism of corrosion inhibition by the inhibitors. AC impedance measurement was used in addition to the linear polarisation method to understand the possible inhibitor mechanism and also to compliment the results for the AC impedance. When film forming inhibitors are used, the film resistance due to the inhibitor can be derived using the AC impedance method [19, 175-179].

Figure 6-13 shows the Nyquist plot for inhibitor 1 at temperature of 20°C and 80°C.
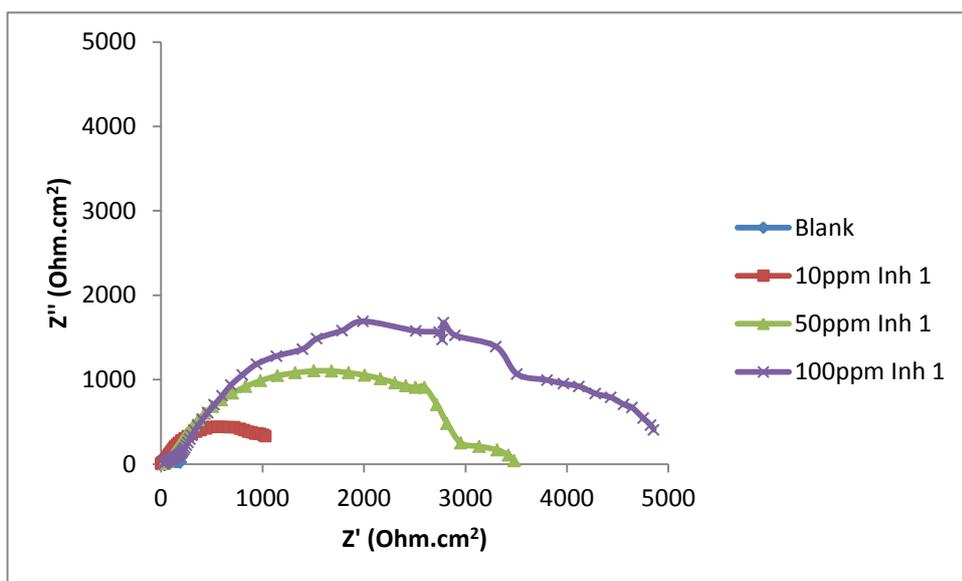
(a)
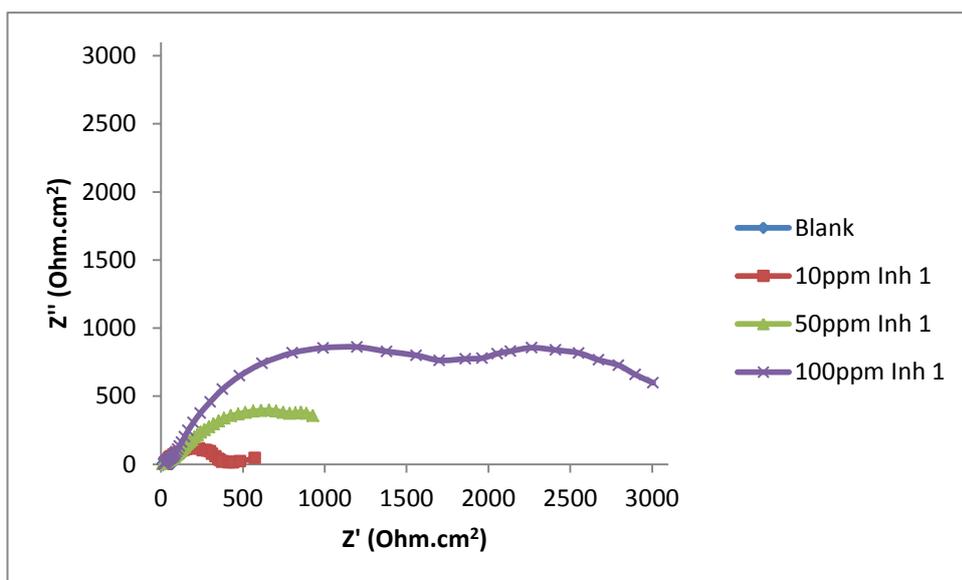
(b)

Figure 6-13 : Nyquist plot for (a) blank, 10 ppm, 50ppm and 100ppm inhibitor 1 at 20°C and (b) blank, 10ppm, 50ppm and 100ppm inhibitor 1 at 80°C

The results showed two time constants which were more prominent for 50ppm and 100ppm concentration. Two-time constants are common for a corroding system with a coating or inhibitor film on the surface of the carbon steel [180-182]. The first time constant at higher frequency represents the inhibitor organic film layer on the surface of the sample as the corrosion process is impeded [142]. This gives a resistance of corrosion process due to the inhibitor film (R_{film}). The film formed on the surface by the corrosion inhibitor at the initial 4 hours may have pores which still allows the electro-chemical active species to penetrate and meet the carbon steel surface [8]. This may still cause a corrosion of the surface. On the other hand the resistance of the corrosion by the carbon steel surface is described by the second time constant which is given as the resistance to charge transfer R_{corr}. The resistance due to charge transfer is accompanied by a capacitance due to electric double layer (EDL) CPE_{corr}. From the result of the Nyquist plot it is seen that there was an increase in the total impedance from 10ppm concentration to 100ppm concentration which may be due to the formation of thicker and persistence film on the surface of the carbon steel by the inhibitor. This is in line with the result of the LPR that shows that the concentration of 50ppm and 100ppm gave lower corrosion rate than the 10ppm concentration. The increase in total resistance of the film with inhibitor concentration, suggest that the optimum concentration lies at higher concentration of 100ppm for inhibitor 1.

In order to analyse the result of the AC impedance on the use of inhibitor 1, the electrical equivalent circuit (EC) used is illustrated in Figure 6-14. One of the EC (i.e. Figure 6-14(b)) is similar to that of a failed coating as suggested by Mansfeld [183]. The EC describes a conducting carbon steel surface covered with another layer of low conducting surface due to the formation of inhibitor film. As described by Wang [8], the nested EC is adopted to take into consideration the pores that may exist on the surface of the film which enable the electro-chemical actives species to reach the metal surface. Esih et al. [184] describes the process of corrosion in the presence of inhibitor to involve the diffusion and electrochemical kinetic. The CPE_{film} and the R_{film} are in parallel. This parallel arrangement is in series with another pair of parallel CPE_{corr} and R_{corr}.

(a)   (b)
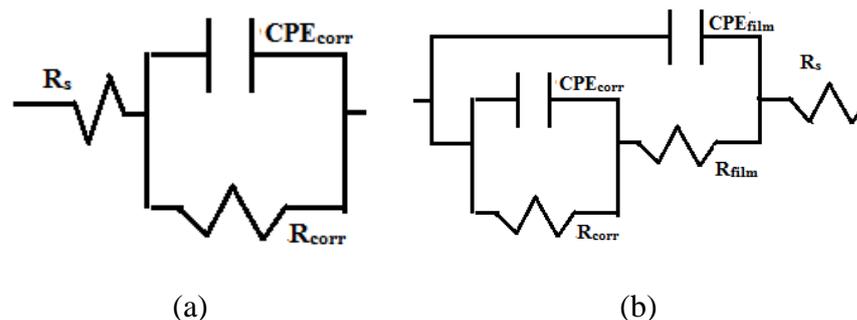
Figure 6-14 : Equivalent circuit (EC) used in representing the AC impedance measurement (a) simple circuit does not differentiate the resistance due to film formation by the inhibitor (b) circuit showing resistance due to film formation by the inhibitor.

Here the CPE_{film} and CPE_{corr} represent constant phase element due to the inhibitor film and corrosion, R_s, R_{film} and R_{corr} represent solution resistance, resistance due to film and corrosion resistance respectively. The CPE was used in place of the usual capacitor (C_{edl}) to take into consideration of the roughness and inhomogeneous of the surface of the corroding carbon steel. This makes the fitting of the experimental data with EC closer than with the use of the usual capacitor (C_{edl}). It should however be noted that some of the lower concentrations for inhibitor 1 were able to fit in a simpler EC model for Figure 6-14(a). This simpler model was not able to distinguish the contribution from the inhibitor film alone.

The result of the Nyquist plot for inhibitor 2 at 20°C and 80°C are shown in Figure 6-15. The results show high impedance value on all the concentration at 20°C. This is evidence of a protective non-porous film formation by the inhibitor. The formation of a thick film prevent the diffusion of corrosion actives species from the entire solution to the carbon steel surface and can also change the anodic and cathodic energy barriers . The Nyquist plot at 80°C however showed drastic reduction in the impedance for 10ppm and 50ppm concentration. This may suggest that the film formed on the metal surface may be more porous compared to those ones formed at lower temperature of 20°C. The reduction in the impedance for the inhibitor at these concentrations is evident of lower surface coverage and efficiency for the inhibitor at 80°C. This may suggest that the optimum concentration of inhibitor 2 changes with increase in temperature.
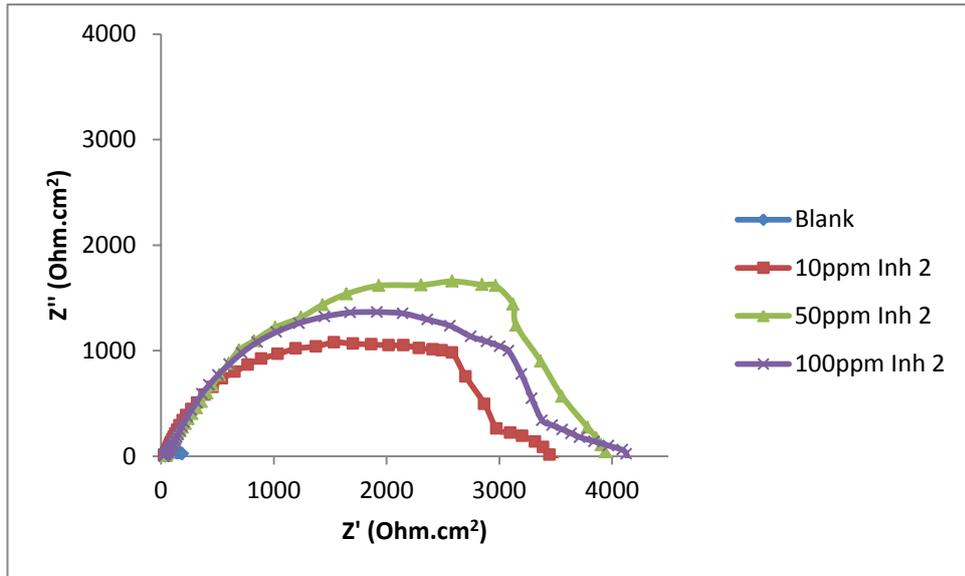
(a)
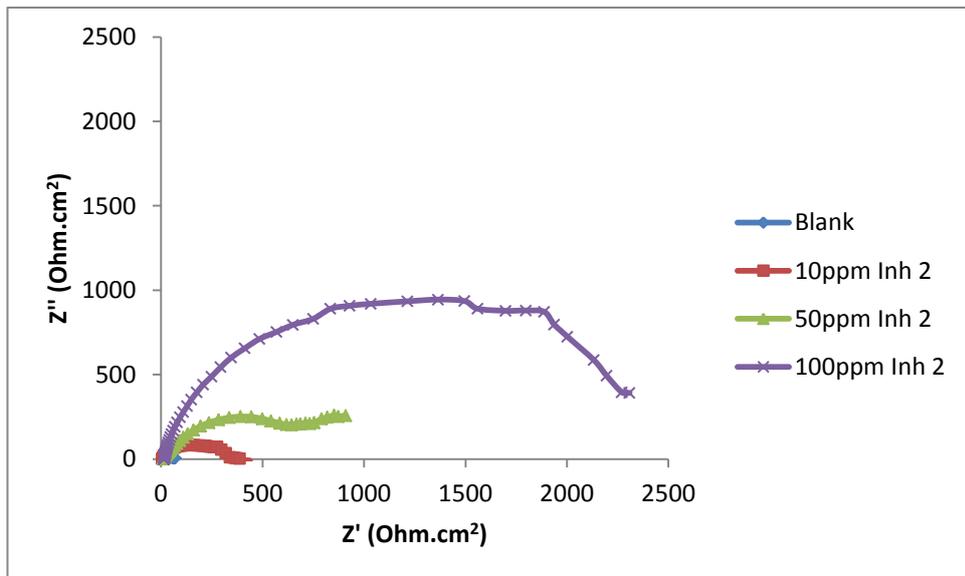
(b)

Figure 6-15 : Nyquist plot for (a) blank, 10ppm, 50ppm and 100ppm inhibitor 2 at 20°C and (b) blank, 10ppm, 50ppm and 100ppm inhibitor 2 at 80°C

In analysing the result of the AC impedance for the Nyquist plot of inhibitor 2, the electrical equivalent circuit (EC) used were similar to those used for inhibitor 1. As most of the result of inhibitor 2 and inhibitor 1 are similar, the process of corrosion in the presence of inhibitor 2   is assumed to involve the diffusion and electrochemical kinetic.

6.5. Surface analysis

Electrochemical tests as previously discussed give the corrosion rate but may not give an idea of any localised corrosion or type of degradation that may have occurred. Although AC impedance method can give an idea of where the surface of the metal becomes rough, this may not show how rough the surface is. To further understand the behaviour of the metal in the presence of the inhibitors, it is always good to have a good surface analysis on the metal after the electrochemical test. The formation of localized corrosion often occurs on metal surfaces with poorly formed films on the surface. It is therefore important to examine the surface of the carbon steel in the presence of these two film forming inhibitors. The results of the surface analysis are described in the following section.

6.5.1. Scanning Electron Microscopy (SEM)

The samples which were used for electrochemical test were kept in the desiccator after each experiment. SEM images of the samples were then taken to identify the possible type of damage on the surface. SEM images of blank samples and some of the inhibitor 1 samples after the electrochemical test are shown in Figures 6-16. The SEM image at 20°C showed that after 4 hours test with inhibitor 1 the carbon steel surfaces had only low general corrosion on the surface. The 100ppm had a very mildly corroded surface. The 10ppm inhibitor did not show signs of localised corrosion at this temperature but the surface had more general corrosion when compared to 100ppm inhibitor 1 sample surfaces. This is in agreement with LPR measurement and AC measurement that shows low corrosion rate for the carbon steel sample at 20°C with the 10ppm having a higher corrosion rate than the 50ppm inhibitor and 100ppm inhibitor.

At 80°C, SEM images of the 100ppm inhibitor 1 samples showed resistance to localised corrosion and general corrosion. General and shallow localised corrosion was seen for samples tested with 10ppm inhibitor 1. This may be due to the lack of adequate film cover on the surface of the carbon steel at this temperature. This occurs when the inhibitor is under dosed or ineffective. Overall all the images for inhibitor 1 showed lower general corrosion compared to the blank samples with high general and localised corrosion.
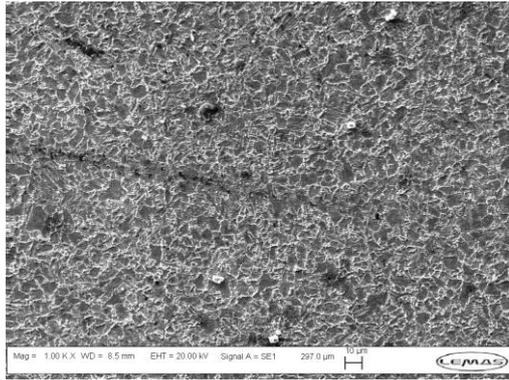
(a)
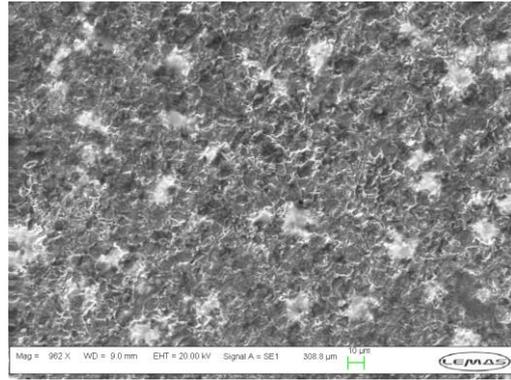
(d)
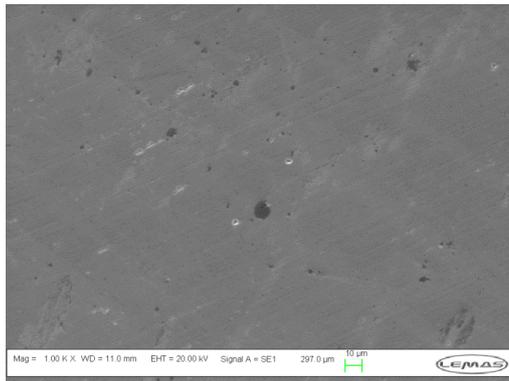
(b)
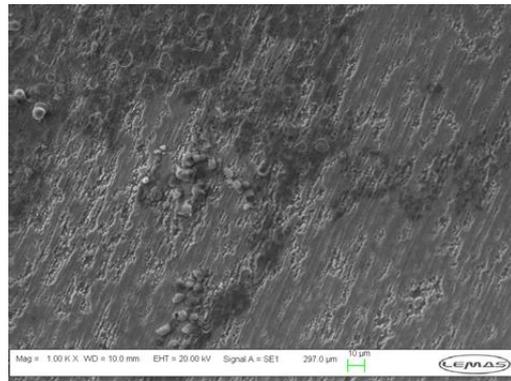
(e)
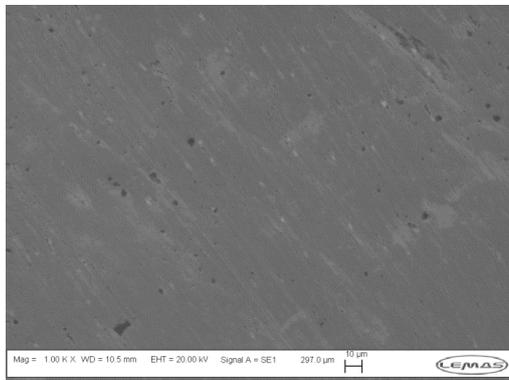
(c)
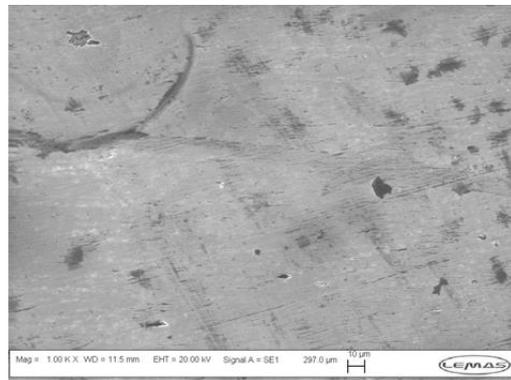
(f)

Figure 6-16 : SEM image of (a) blank, (b) 10ppm inhibitor 1, (c) 100ppm inhibitor 1 at 20°C and (d) blank (e) 10ppm inhibitor 1 (f) 100ppm inhibitor 1 at 80°C.
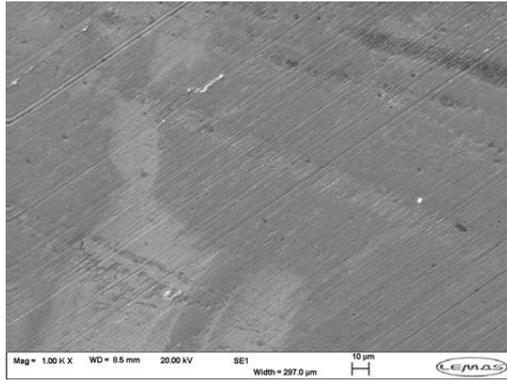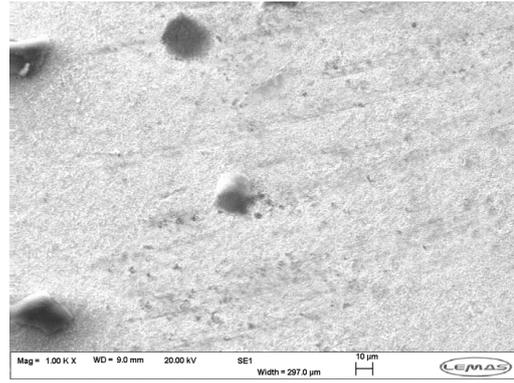
(a) (d)
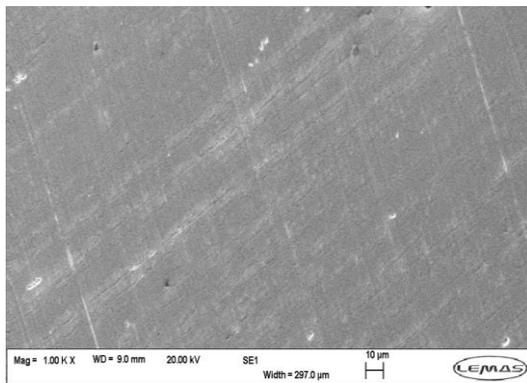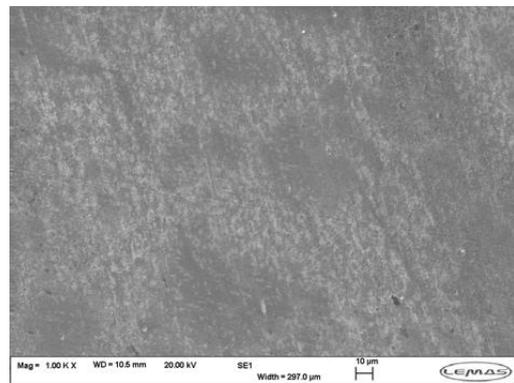
(b) (e)
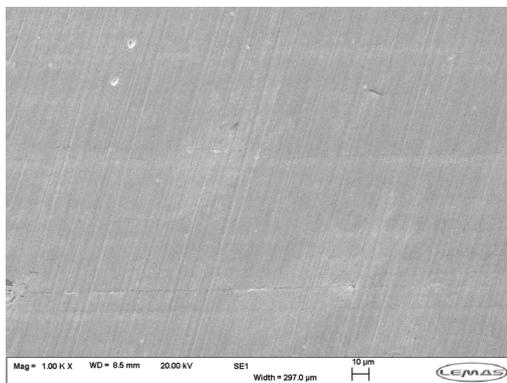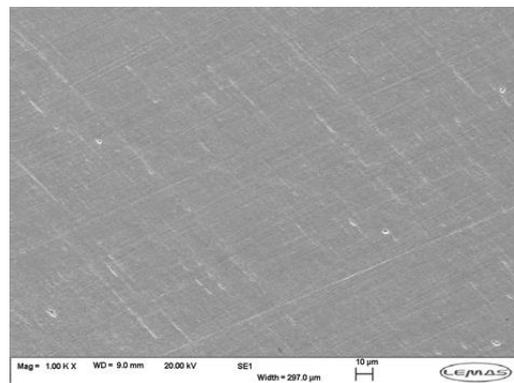
(c) (f)

Figure 6-17 : SEM image of (a) blank, (b) 10ppm inhibitor 2, (c) 100ppm inhibitor 2 at 20°C and (d) blank (e) 10ppm inhibitor 2 (f) 100ppm inhibitor 2 at 80°C.

The SEM results for the blank sample compared with some inhibitor 2 samples at 20°C and 80°C after the electrochemical test are shown in Figures 6-17. The SEM image at 20°C shows that after 4 hours test with inhibitor 2 the carbon steel surfaces

only had general corrosion. This is an indication of the formation of protective inhibitor film on the surface of the sample.

At 80°C, The SEM image showed higher general corrosion on the surface for 10ppm inhibitor. 10ppm inhibitor also showed possible localised corrosion on the surfaces of the sample. The 100ppm inhibitor 2 samples showed the least corroded surface with no signs of localised corrosion. All the inhibitor 2 samples did have lower general corrosion rate on the surface when compared to blank samples at both high and low temperature.

6.5.2. Fourier Transform Infrared Spectrometry (FTIR)

FTIR was used to characterise some of the tested samples used in the presence of inhibitor 1 and inhibitor 2. FTIR can be used to identify any chemical bond that may exist on the surface of the tested sample with the inhibitor. The results of the FTIR spectra for the inhibitors on some selected tests are shown in Figure 6-18 and Figure 6-19. The spectra obtained from the inhibitor 1 surface showed spectra which are similar to that of the FTIR spectra of only inhibitor 1 solution alone. The difference was the low count on the spectra which is expected as the samples will normally have less concentration on the tested sample as compared to the solution of inhibitor 1 alone.
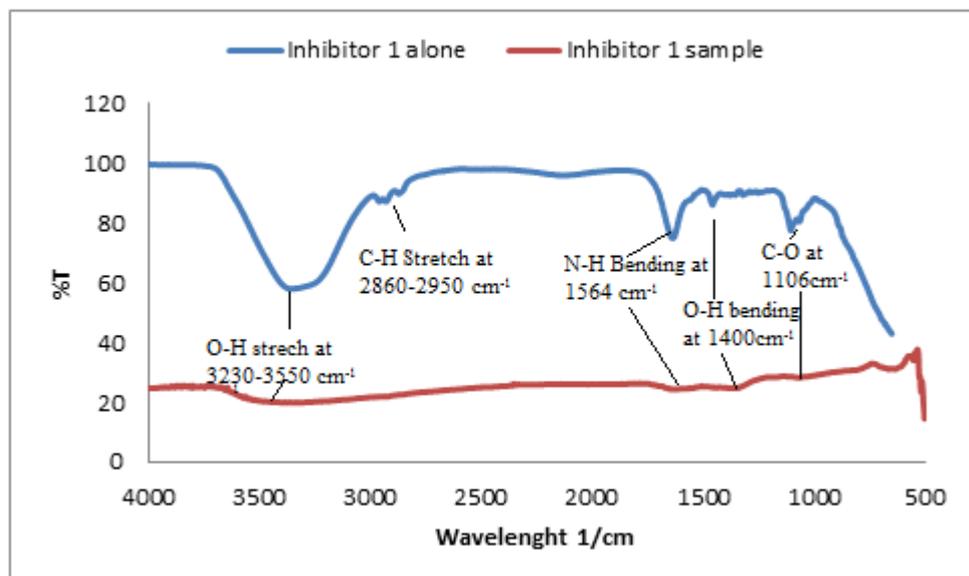
Figure 6-18 : FTIR spectra for inhibitor 1 solution alone and sample tested 50ppm Inhibitor 1 at 80°C for 4 hours period.

The spectra on inhibitor 1 solution alone showed the presence of the N-H bonding in the region of 1564 cm^{-1}. This was also visible for the tested sample in inhibitor 1. The spectra of only inhibitor 1 solution alone showed the presence of the O-H stretching in the region of 3230-3550 cm^{-1}. This was also visible for the electrochemical tested sample surface. The O-H bending and the C-O bond was also present in both the inhibitor 1 solution and the tested samples. Though C-H stretch at 2860-2950 cm^{-1} was not present for the tested sample in inhibitor 1, the spectra of the tested sample were similar in most case with the spectra of the solution for inhibitor 1 alone.

None of the tested samples in the presence of inhibitor 2 showed FTIR spectra which was able to match the FTIR spectrum for inhibitor 2 done separately. They did not show the O-H stretch between 3230 and 3550 cm^{-1} wavenumber and also the C-O stretch between 1100 and 1200 cm^{-1} wavenumber. This may mean that the film formed by inhibitor 2 is not tenaciously bonded to the surface of the carbon steel within the tested period. Further test may be required to confirm this.
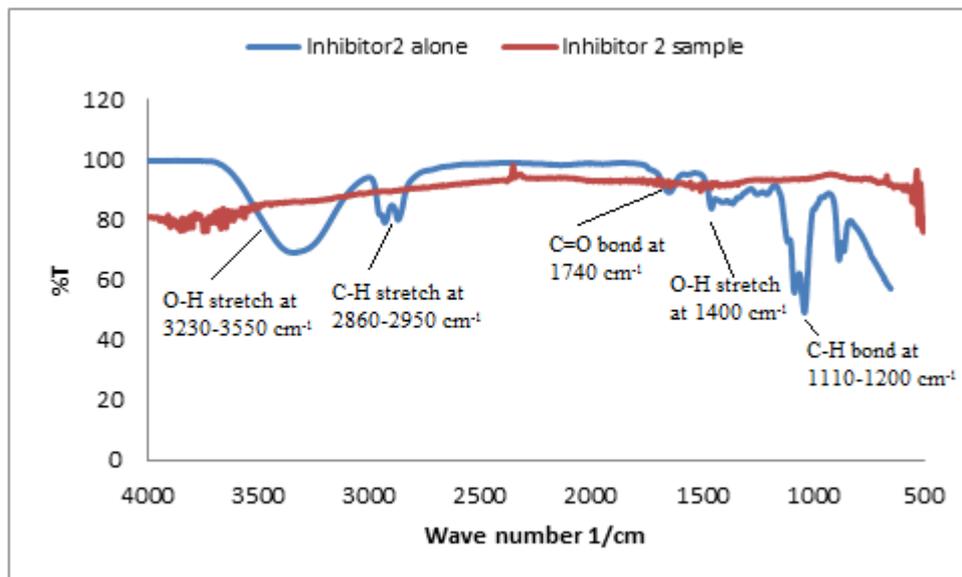
Figure 6-19 : FTIR spectra for inhibitor 2 solution alone and sample tested 50ppm Inhibitor 2 at 80°C for 4 hours period.

6.5.3. Interferometry

A Wyko light profilometer was used to assess the topography of the tested samples. It was used to determine the damage and type of corrosion attack on the electrochemically tested sample surface. In order to determine the type of corrosion on the surface of the sample, a threshold of 1 μm was assigned as the depth measurement to identify general corrosion or localised corrosion. Measurements below 1 μm depth were taken to be general corrosion while measurement above 1 μm depth was taken to be localised corrosion (shallow pits). Any measurements above 5 μm depth were taken to be deep pits. A threshold was assigned to the volume measurement to ascertain the percentage volume due to deep pits. A schematic diagram describing the process of benchmarking on the tested sample to identify the pit has been described in the previous section. Figure 6-20 shows a typical measurement result for inhibitor 2.

From the tests carried out at 20°C, it was observed that the 10 ppm inhibitor 1 sample mostly had general corrosion on the surface with some very shallow pits on the surface. The maximum depth of the shallow pit was 1.4μm.

Further volume measurement on the 10ppm inhibitor 1 sample using a threshold of 1μm showed that the depth below this pit threshold made up just $6.03 \times 10^3 \mu m^3$ of the total volume. The volume measurement on the 10ppm inhibitor 1 is shown in Figure 6-21. The number of pit on the surface was also less than the 99.76% of the total volume of the surface. This is an indication that the localised corrosion level was very small and occurred in small area. This is also in line with the observation of the images of the SEM that showed few points with shallow localised corrosion. Profilometer results for all other concentration of inhibitor 1 showed resistance to localised corrosion of pit.

At higher temperature, the localised corrosion was also observed in the measurement for the 10ppm inhibitor 1 concentration. Higher concentration of 50ppm and 100ppm inhibitor 1 did not show any pit formation on the surface. This shows that at 80°C, the inhibitor 1 with 50ppm concentration was able to protect the carbon steel surface from corrosion.
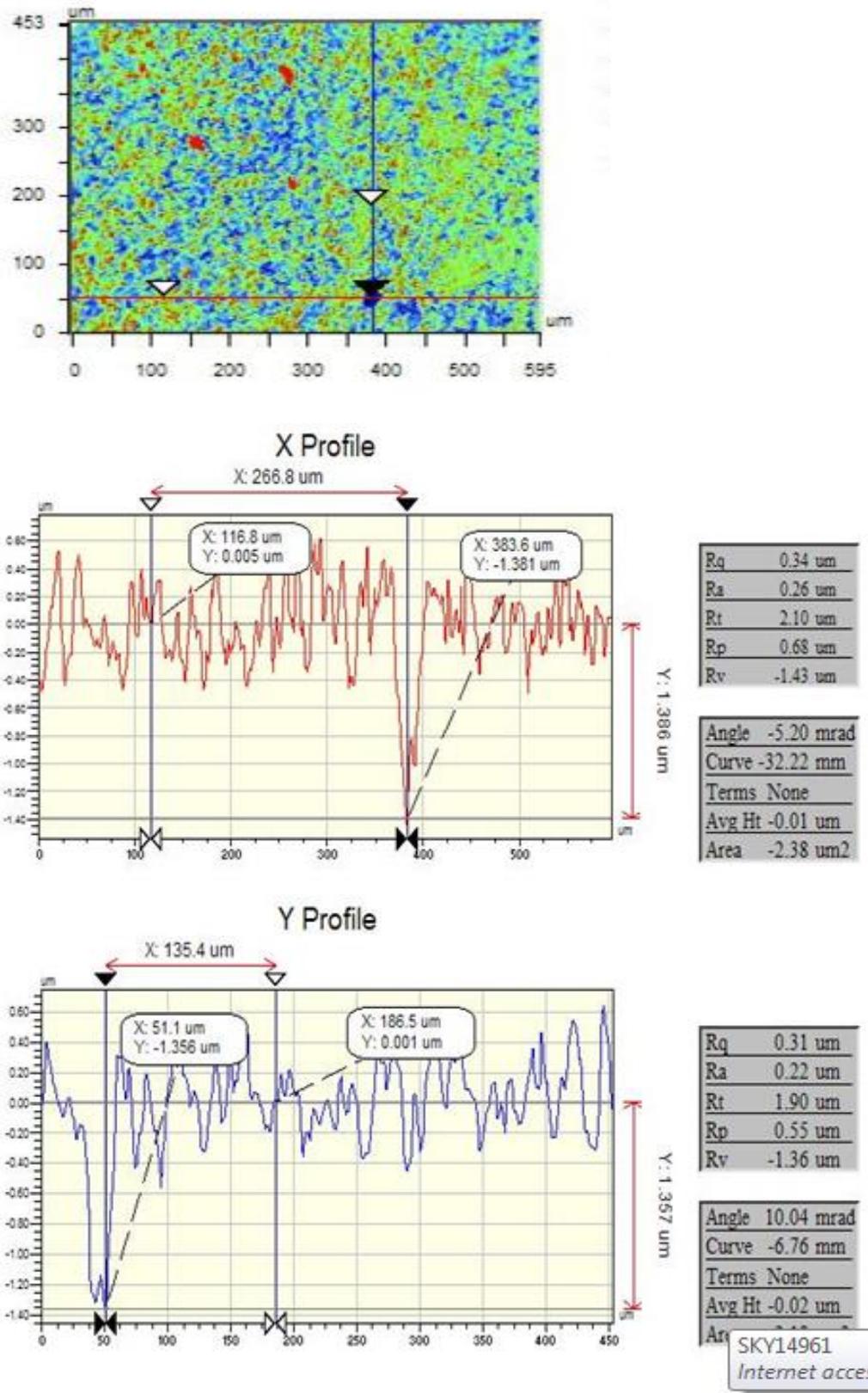
Figure 6-20 : Profilometer measurement for 10ppm Inhibitor 1 at 20°C showing the maximum depth obtained on the surface of the sample.

Volume Calculations

Volume Options	Normal
Natural Volume	209055.81 um3
Normal Volume	0.50 BCM
Negative Volume	27907.46 um3
Positive Volume	29904.46 um3
Net Missing Volume	-1997.00 um3
Total Displaced Volume	57811.93 um3
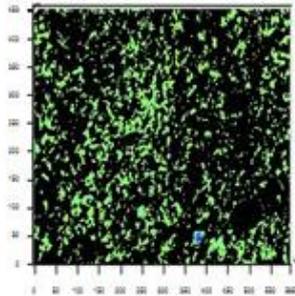
Thresh: 1.02 um 41.96% of P-V
Pts Below: 99.76% of Total
Vol: 6.30e+003 um3 3.01% of Total
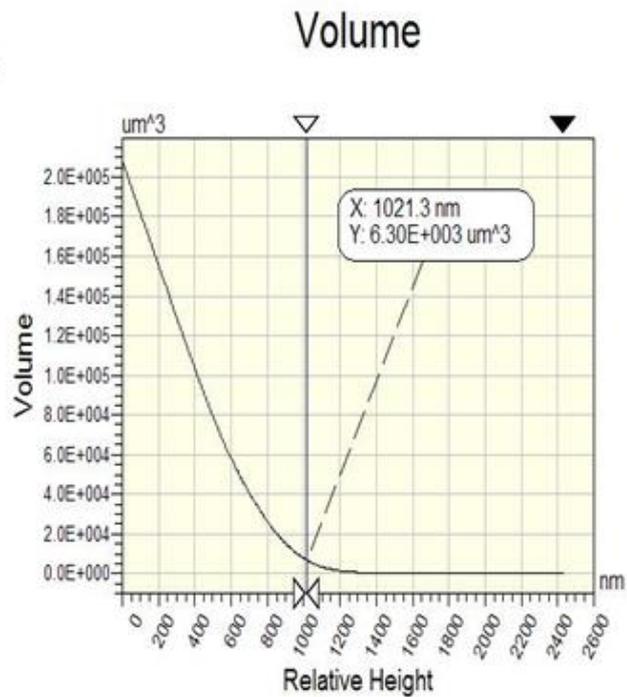
Figure 6-21 : Profilometer measurement for 10ppm inhibitor 1 at 20°C showing threshold for volume depth obtained on the surface of the sample.

This is also in line with the electrochemical test result and the SEM image that shows no localised corrosion on the surface of the tested carbon steel sample. The result indicate that the film formed by inhibitor 1 with 50ppm and higher concentration are stable, compact and less porous than that of 10 ppm.

Profilometry measurements for the 10 ppm inhibitor 2 sample on the other hand showed mostly general corrosion on the surface without any recognised pit based on the threshold measurement. This an indication that there were no formation of pits on the surface due to the coverage achieved on the surface of the carbon steel by the 10ppm inhibitor 2 concentration. The measurement of the other concentration of inhibitor 2 also gave maximum depth below the 1 μm. This result is line with the electrochemical measurement result that shows low corrosion rate and high efficiency of inhibitor 2 at 20°C. The SEM image for the inhibitor 2 for all concentration at a low temperature also agrees with the profilometer result which shows no formation of localised corrosion on the surface of the carbon steel samples.

168
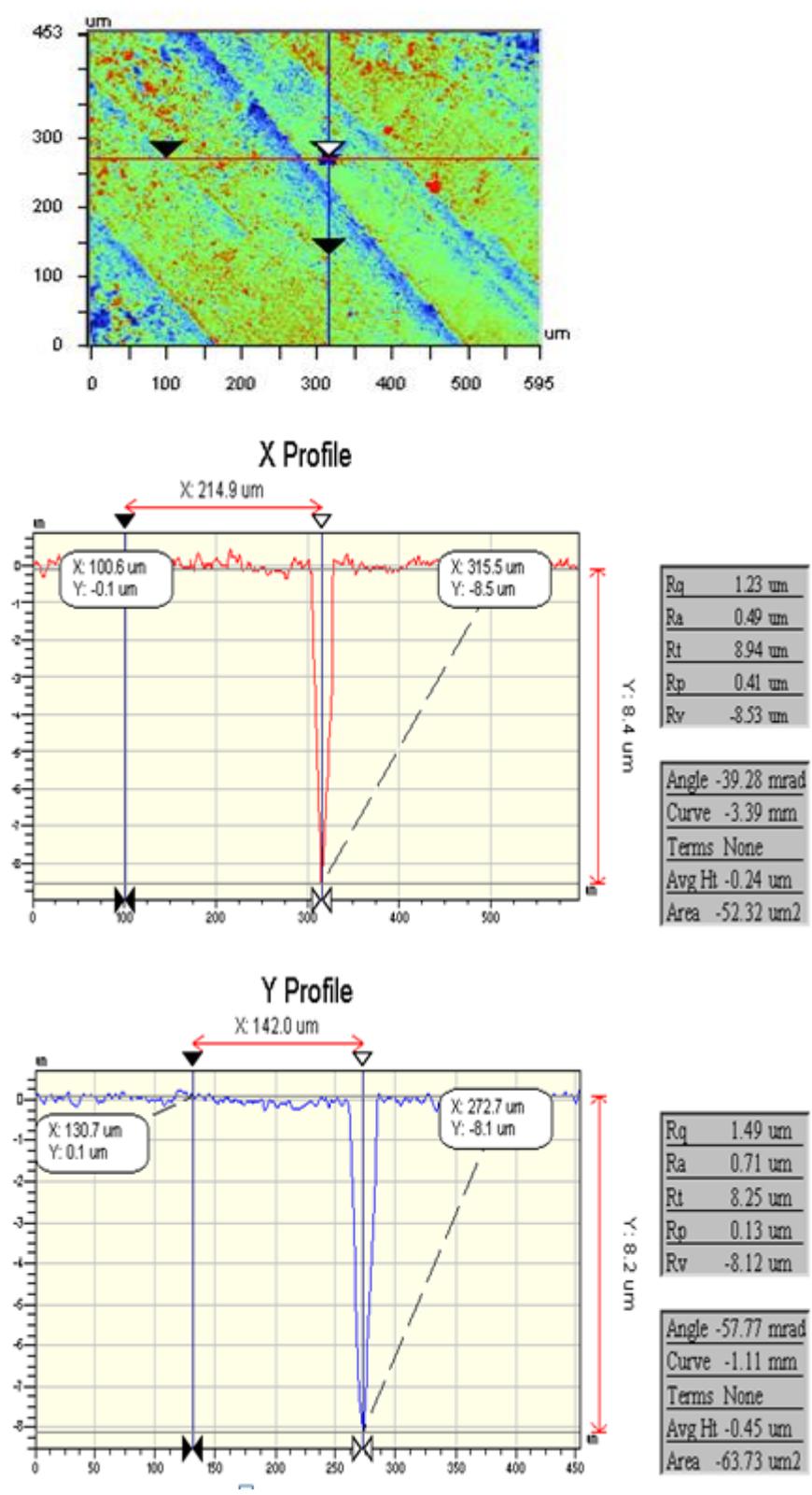
Figure 6-22 : Profilometer measurement for the 4hrs test of Inhibitor 2 10ppm at 80°C showing the maximum depth obtain on the surface of the sample.

At higher temperature, localised corrosion was also observed for measurement on the 10ppm inhibitor 2 concentrations. Higher concentration of inhibitor 2 did not show any pit formation on the surface for the 4 hours test. The maximum depth on the surface was quite high and up to 8.5 µm .This was far more than the threshold of 1 µm for surfaces considered as pit. This shows that at high temperature of 80°C, the lower concentration of 10ppm inhibitor 2 was not able to protect the carbon steel surface from corrosion. This is also in line with the SEM image that shows localised corrosion on the surface of the tested carbon steel sample. 10ppm for inhibitor 2 is no longer the minimum required concentration at high temperature. The results for the other test also showed that the other concentration of inhibitor 2 did not have localised corrosion on the surface of the inhibitor 2 as the measured depth were below the 1 µm threshold. Figure 6-22 shows the profilometer measurement for samples tested with 10ppm inhibitor 2 at 80°C for 4 hrs.

6.6. Summary of results of corrosion processes in the presence of organic corrosion inhibitors

This chapter has presented results from an assessment of the corrosion of carbon steel in the presence of the two inhibitors. It can be summarised as follows

- OCP measurements can give a semi-quantitative behavior of both inhibitors. It was observed from these measurements that the two inhibitors showed reduction in corrosion by reducing the anodic activities.
- AC and DC measurements for both inhibitor tests showed good correlation and demonstrated that the inhibitors reduce corrosion rate of carbon steel.
- The two inhibitors were able to reduce the corrosion by formation of thin film on the surface of the sample which was seen from the AC impedance results.
- Inhibitor 2 has a lower minimum concentration requirement as compared to inhibitor 1 and reduces corrosion rate more at a lower temperature.

- At 80°C inhibitor 1 at high concentration of 100ppm performs better than inhibitor 2 at the same concentration and gives a more persistent film on the surface of the steel.
- Inhibitor 2 may not be an effective corrosion inhibitor at high temperature application especially at lower concentrations.

Chapter 7. CORROSION RATES AND PROCESSES IN THE PRESENCE OF MONOETHYLENE GLYCOL AND ORGANIC CORROSION INHIBITORS

7.1. Introduction

The integrity of oil and gas pipelines is very important. There is a need to manage hydrate formation and corrosion on carbon steel pipeline or keep to minimal acceptable rate. In preventing hydrate formation, a thermodynamic hydrate inhibitor MEG is often used [115, 122, 185]. This can also help to prevent corrosion of the carbon steel. The reduction in corrosion rate is not always to the required minimum levels and hence the corrosion rate needs to be reduced further. One way of reducing the corrosion rate is by application of suitable organic corrosion inhibitors. Organic corrosion inhibitors usually adsorb to the surface of the carbon steel to form a protective film. The organic corrosion inhibitor needs to be compatible with the function of the hydrate inhibitor MEG. In order to verify this, the two organic corrosion inhibitors (i.e. inhibitor 1 and inhibitor 2) tested in the previous section were used in the presence of MEG.

7.2. Linear Polarization Resistance (LPR) measurement

LPR measurements were taken for the carbon steel in the presence of a solution of MEG and inhibitor. The LPR tests were conducted on 50% MEG solution with three different concentrations of inhibitor 1 and inhibitor 2 at 20°C and 80°C respectively. The same tests were also performed using 80% MEG solution with three different concentrations of inhibitor 1 and inhibitor 2 at 20°C and 80°C. The solution resistance due to the presence of MEG was calculated using the AC impedance method which will be described later. Polarisation resistance from the LPR measurements were compensated for solution resistance on each reading before using them to calculate the corrosion rate.

The results from Figure 7-1 and Figure 7-2 show the corrosion rate of carbon steel in the presence of solution of 50% MEG with inhibitor 1 and 80% MEG with inhibitor 1 at 20°C respectively. Figure 7-3 and Figure 7-4 show the corrosion rate for the carbon steel in the presence of solution of 50% MEG with inhibitor 2 and 80% MEG with inhibitor 2 at 20°C. From the result, there was a drastic reduction in the corrosion rate with the combination of all concentrations of inhibitor 2 with both 50% MEG and 80% MEG. On the other hand the drastic reduction in the corrosion rate was not seen for the combination of 10ppm inhibitor 1 with 50% MEG. This was even prominent when 80% MEG solution was used in combination with 10ppm inhibitor 1. The reduction in corrosion rate was less than the reduction in the corrosion rate in the presence of MEG alone (i.e. 0ppm inhibitor 1).

The results with higher concentration of inhibitor 1 showed reduction in the corrosion rate which was observed more for the 100ppm inhibitor 1 with MEG. Overall the corrosion rate of inhibitor 2 in combination with MEG was lower than that of inhibitor 1.
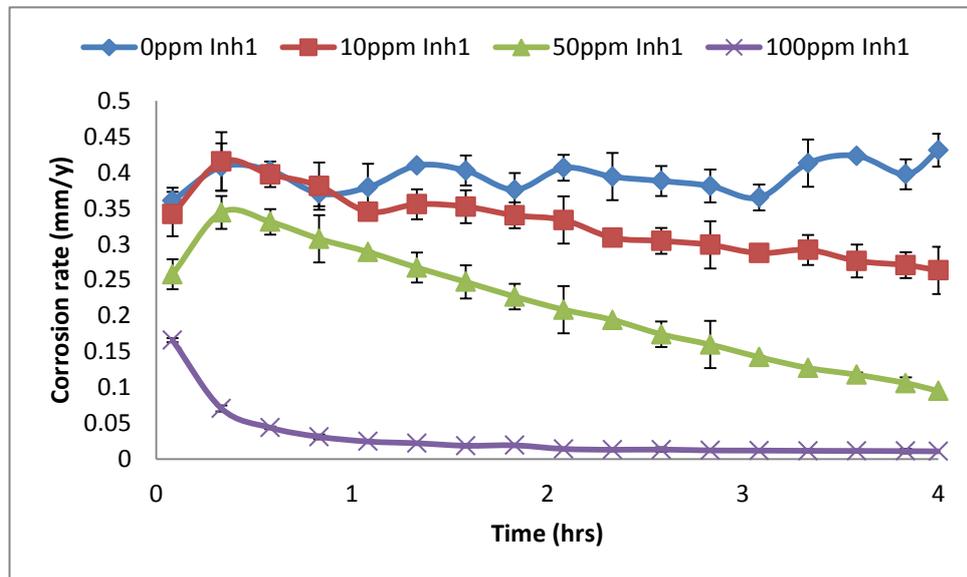
Figure 7-1 : Comparison of the corrosion rate for carbon steel in different concentrations of inhibitor 1 with 50% MEG at 20°C
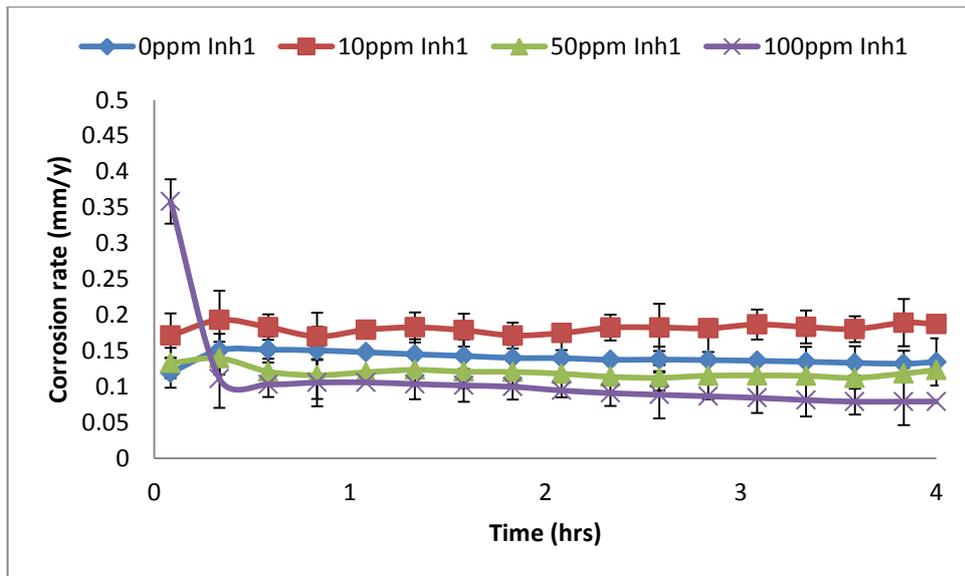
Figure 7-2 : Comparison of the corrosion rate for carbon steel in different concentrations of inhibitor 1 with 80% MEG at 20°C
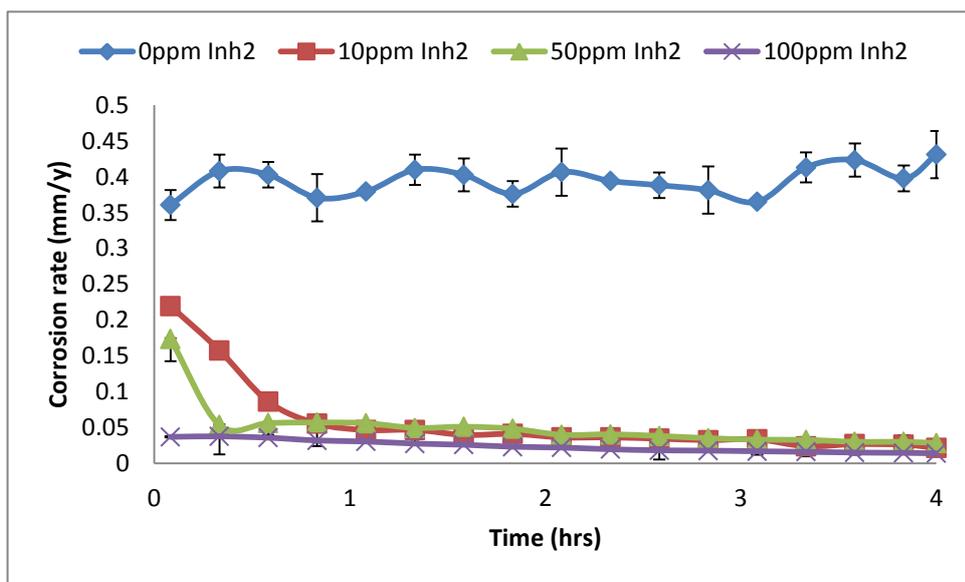
Figure 7-3 : Comparison of the corrosion rate for carbon steel in different concentrations of inhibitor 2 with 50% MEG at 20°C

The results from Figure 7-5 and Figure 7-6 show the corrosion rate of carbon steel in the 50% MEG solution with inhibitor 1 and 80% MEG solution with inhibitor 1 at 80°C while Figure 7-7 and Figure 7-8 shows the corrosion rate of carbon steel in 50% MEG solution with inhibitor 2 and 80% MEG solution with inhibitor 2 at 80°C.
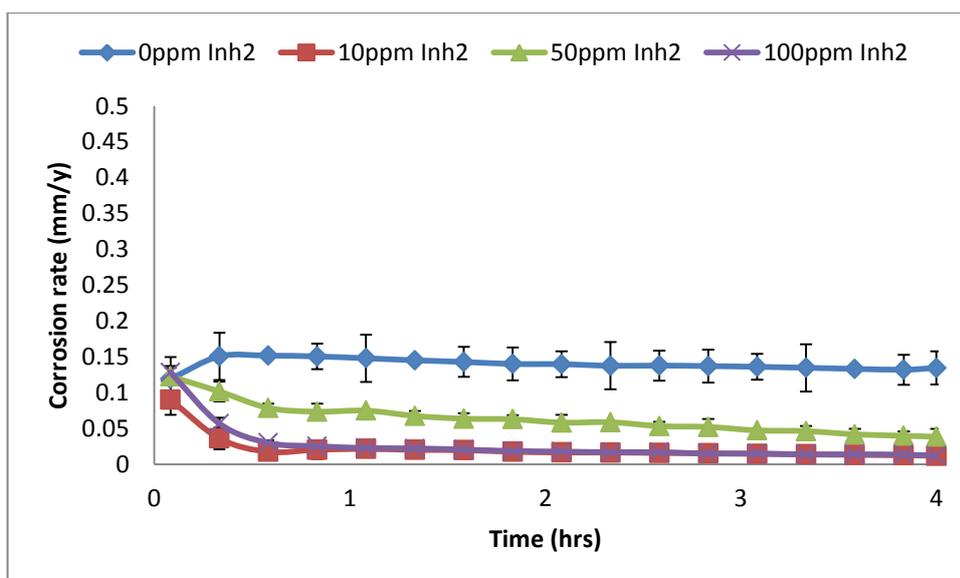
Figure 7-4 : Comparison of the corrosion rate for carbon steel in different concentrations of inhibitor 2 with 80% MEG at 20°C

The results of the LPR tests at 80°C for a combination of 50% MEG and inhibitor 1 showed that the corrosion rate did not reduce as expected. The 10ppm inhibitor 1 concentration had the least effect on the corrosion rate. The higher concentration of 50ppm and 80pppm though reduce the corrosion rate but still did not reach the maximum acceptable corrosion rate of 0.1mm/y. Similar results were also achieved with a combination of 80% MEG and inhibitor 1. The combination did not achieve any reduction in corrosion rate below the maximum acceptable rate of 0.1mm/y. This also showed a negative effect of combining MEG with inhibitor 1

On the other hand, the 50 ppm and 100 ppm of inhibitor 2 in combination with 50% MEG or 80% MEG was able to reduce the corrosion rate below the maximum required limit of 0.1mm/y. The 10 ppm inhibitor 2 in combination with 50% MEG or 80% MEG was not able to reduce the corrosion rate below the maximum required rate. This may mean that at higher temperature additional quantities of inhibitor 2 may be required to reduce the corrosion rate of the carbon steel in the presence of MEG to the required limit.
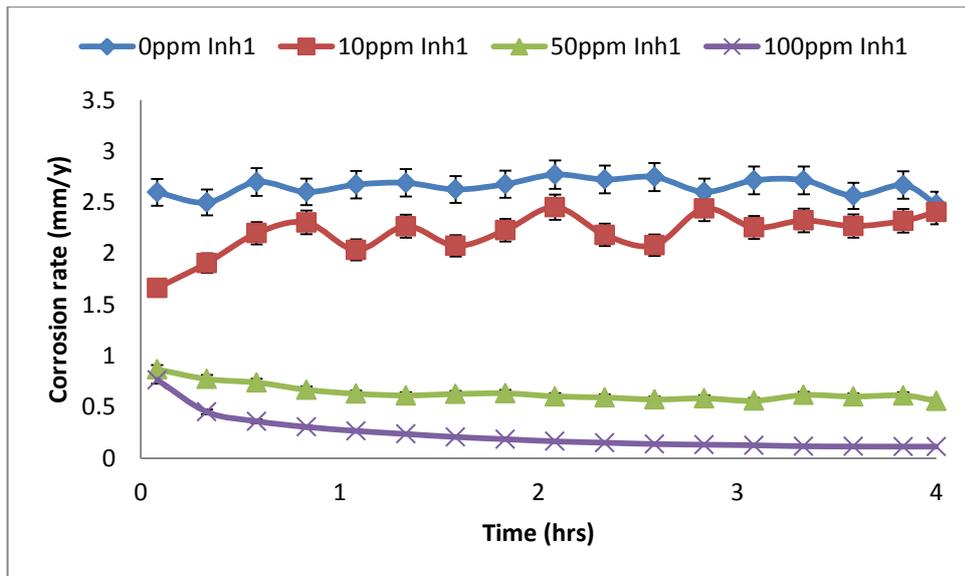
Figure 7-5 : Comparison of the corrosion rate for carbon steel in different concentrations of inhibitor 1 with 50% MEG at 80°C
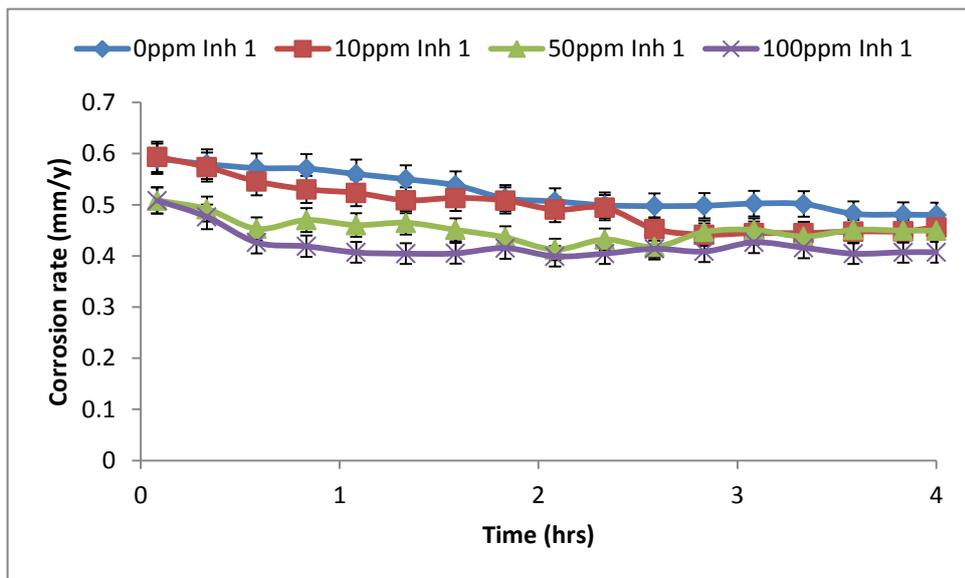
Figure 7-6 : Comparison of the corrosion rate for carbon steel in different concentrations of inhibitor 1 with 80% MEG at 80°C

A summary of the corrosion rates in mm/y for the blank (i.e.0ppm inhibitor 1), inhibitor 1 in blank solution only, MEG only, and inhibitor 1 in MEG solution for the carbon steel at 20°C and 80°C is presented in Table 7-1. While Table 7-2 shows the summary of the corrosion rates for the blank (i.e.0ppm inhibitor 1), MEG only,

inhibitor 2 in blank solution only, and inhibitor 2 in MEG solution for the carbon steel at 20°C and 80°C. The results shows red, yellow and green for corrosion rate $\geq$ 0.2mm/y, > 0.2mm/y $\geq$ 0.1mm/y, and < 0.1mm/y respectively.
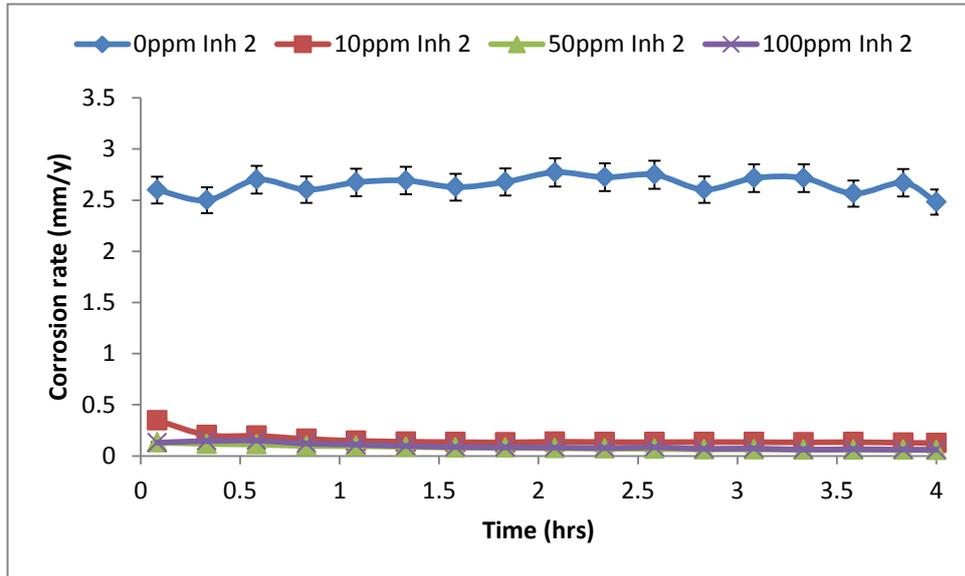
Figure 7-7 : Comparison of the corrosion rate for carbon steel in different concentrations of inhibitor 2 with 50% MEG at 80°C
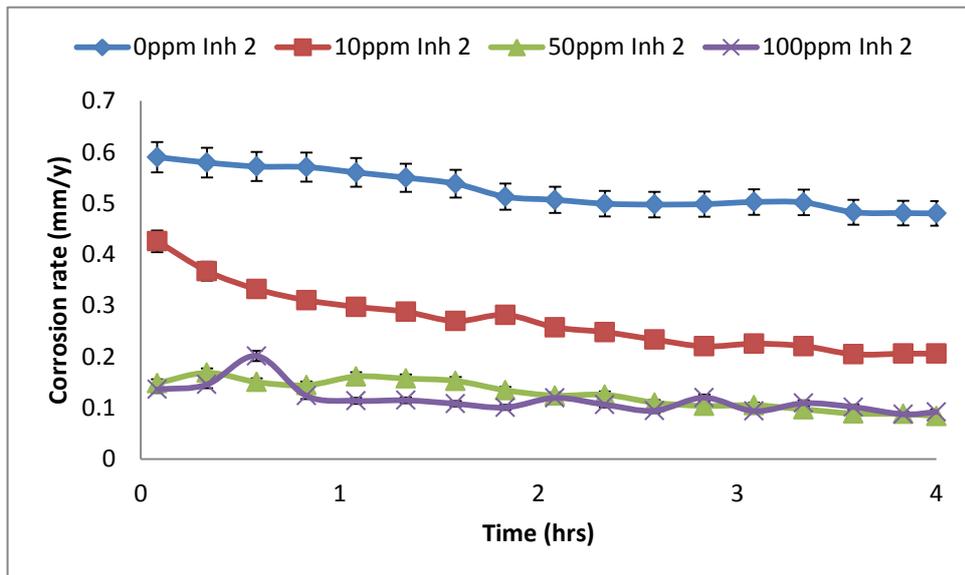
Figure 7-8 : Comparison of the corrosion rate for carbon steel in different concentrations of inhibitor 2 with 80% MEG at 80°C

Table 7-1 : Summary of the corrosion rate mm/y for different concentrations inhibitor 1 in blank solution and inhibitor 1 in MEG solution.

Inhibitor 1 concentration (ppm)	Temperature (°C)	Inhibitor 1 in blank only	Inhibitor 1 in 50% MEG	Inhibitor 1 in 80% MEG
0	20	2.25	0.44	0.14
10	20	0.19	0.27	0.19
50	20	0.13	0.10	0.12
100	20	0.04	0.02	0.08
0	80	5.6	2.34	0.50
10	80	0.29	2.20	0.45
50	80	0.19	0.60	0.48
100	80	0.06	0.11	0.40

Table 7-2 : Summary of the corrosion rate mm/y for different concentrations inhibitor 2 in blank solution and inhibitor 2 in MEG solution.

Inhibitor 2 concentration (ppm)	Temperature (°C)	Inhibitor 2 in blank only	Inhibitor 2 in 50% MEG	Inhibitor 2 in 80% MEG
0	20	2.25	0.44	0.14
10	20	0.03	0.02	0.01
50	20	0.02	0.02	0.04
100	20	0.02	0.01	0.01
0	80	5.6	2.34	0.50
10	80	0.24	0.13	0.20
50	80	0.20	0.06	0.09
100	80	0.16	0.06	0.09

7.3. AC Impedance

AC Impedance method was used to complement the results of the LPR. The AC impedance method gives the solution resistance due to the presence of MEG. The AC Impedance method also gives information that can help in the identification of possible mechanisms involved in the reduction of corrosion rate with the combination of the inhibitors and MEG.

Figure 7-9 shows the Nyquist plot for 50% MEG with inhibitor 1 at 20°C. From the results for 50% MEG with inhibitor 1, it is observed that there was an unusual time constant at the beginning of the plot which is attributed to the solution resistance of MEG. This occurs for all concentration of the inhibitor. The results show that 10ppm inhibitor 1 gave the least value for the impedance which was closer to the 0ppm inhibitor 1 (i.e. 50% MEG only) value. This indicates that the addition of 10ppm inhibitor 1 is not an effective concentration at this condition. The impedance for the 50% MEG and 80% MEG was high but did not increase as expected. This indicated that there was no synergistic effect between 50% MEG and inhibitor 1.

Figure 7-10 shows the Nyquist plot for 80% MEG with inhibitor 1 at 20°C. From the results for 80% MEG and inhibitor 1, the unusual time constant at the beginning was also observed which also indicated the presence of high solution resistance. This was higher than that for 50% MEG as expected. The results also showed that the use of 10ppm inhibitor 1 had lower impedance than when no inhibitor was used (i.e. 80% MEG). This shows a reduction in the efficiency of the inhibitor 1 at this concentration. This is in line with LPR results where the corrosion rate for a combination of 10ppm inhibitor with 80% MEG was higher than that of 80% MEG alone.

Figure 7-11 shows the Nyquist plot for 50% MEG with inhibitor 1 at 20°C. The results of 50% MEG and inhibitor 2, also showed the effect of solution resistance as the unusual time constant at the beginning. There was an increase in the total impedance for all the concentration. This is an indication of positive effect on inhibitor 2 in the presence of 50% MEG. A similar result was also observed for test for 80% MEG and inhibitor 2 which is shown in Figure 7-12. This again indicates positive effect on inhibitor 2 in the presence of 80% MEG. This is in agreement with

results of the LPR that shows very low corrosion rate for all the inhibitor 2 concentration with 50% MEG or 80% MEG concentration.
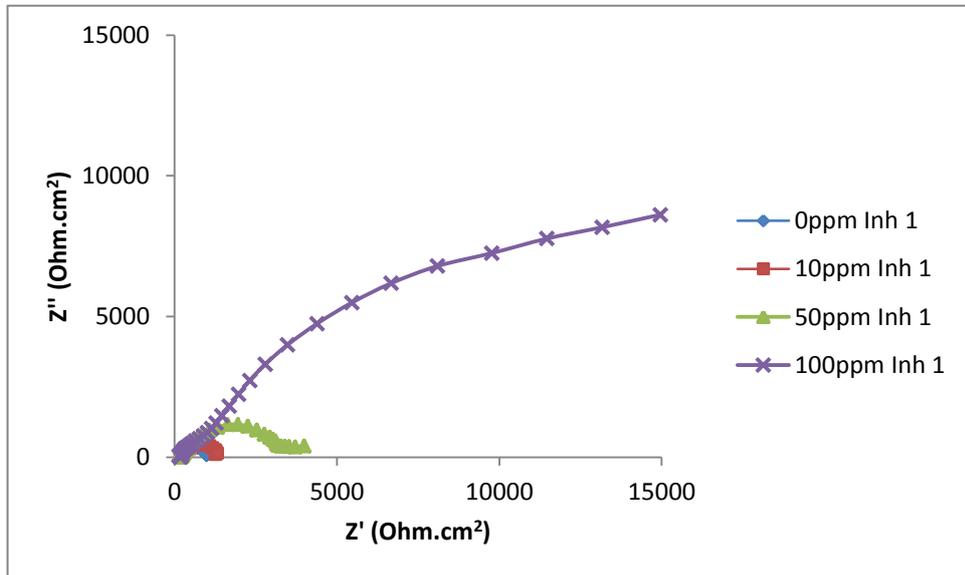
Figure 7-9 : Nyquist plot for 0ppm inhibitor 1 (i.e. 50% MEG) and inhibitor 1 (10ppm, 50ppm and 100ppm) with 50% MEG at 20°C.
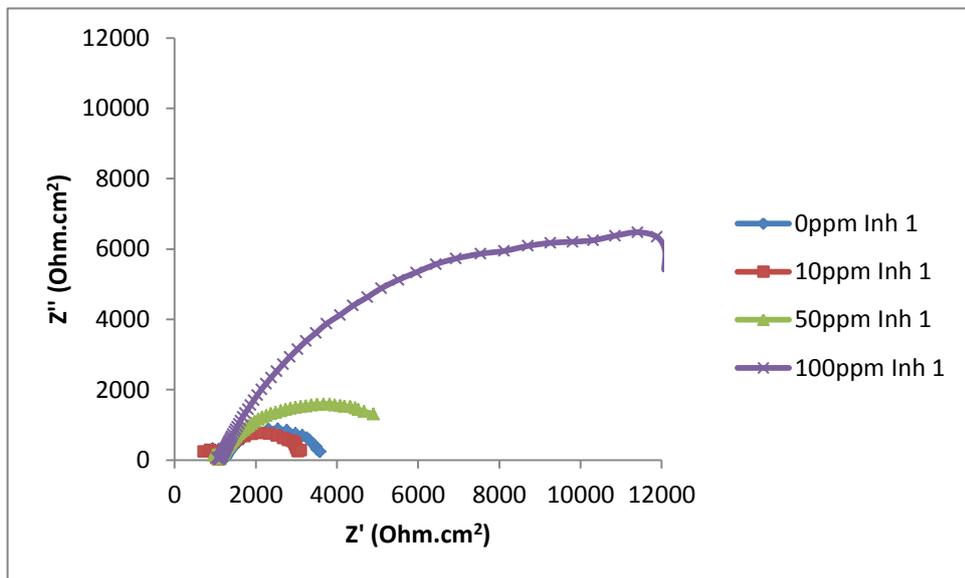
Figure 7-10 : Nyquist plot for (a) 0ppm inhibitor 1 (i.e. 80% MEG) and inhibitor 1 (10ppm, 50ppm and 100ppm) with 80% MEG at 20°C.
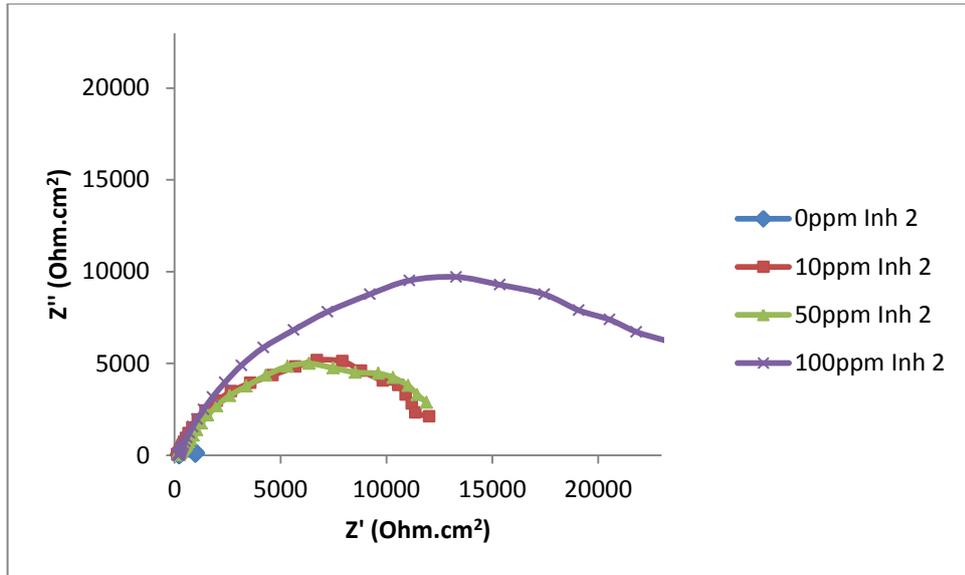
Figure 7-11 : Nyquist plot for 0ppm inhibitor 2 (i.e. 50% MEG) and inhibitor 2 (10ppm, 50ppm and 100ppm) with 50% MEG at 20°C.
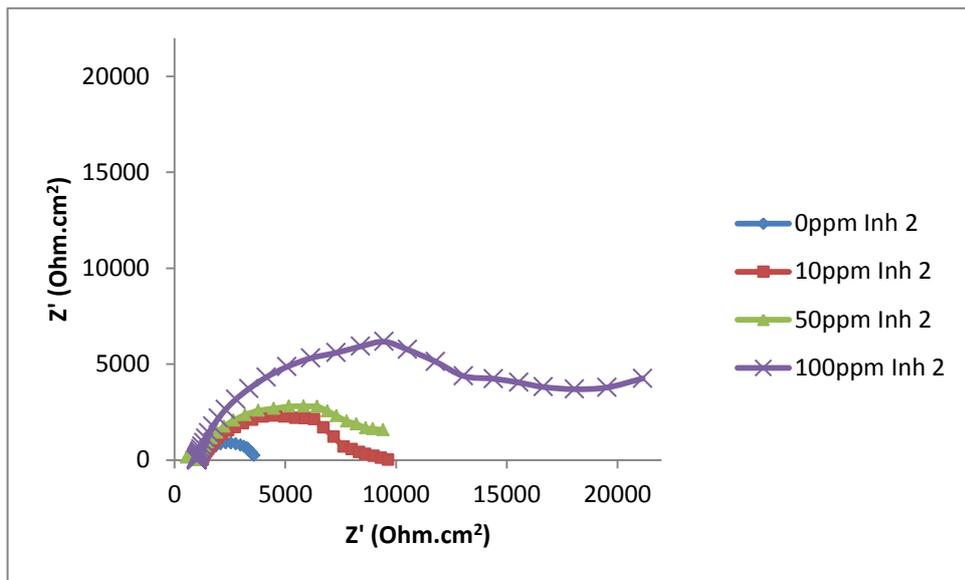
Figure 7-12 : Nyquist plot for 0ppm inhibitor 2 (i.e. 80% MEG) and inhibitor 2 (10ppm, 50ppm and 100ppm) with 80% MEG at 20°C.

To analyse the result of the AC impedance for the combination of MEG with the inhibitor, the electrical equivalent circuit (EC) used is illustrated in Figure 7-13. Figure 7-13(b) describes a conducting carbon steel surface covered with another layer of low conducting surface due to the formation of an inhibitor film. The EC were similar to those used for the inhibitors in the previous section. It assumes that

181

there is a formation of a film on the surface by the inhibitor in the presence of MEG. This inhibitor film generates a capacitor and a resistance in addition to the capacitor and resistance due to charge transfer. The capacitors were both replace with the CPE_{film} and CPE_{corr} to accommodate the inhomogeneous and roughness of the corroding surface. This makes the fitting of the experimental data with EC closer than with the use of the usual capacitor (C_{edl}). Where the inhibitor film was not prominent the simpler EC illustrated in Figure 7-13(a) was employed in fitting the experimental results. The EC analysis was used to derive the solution resistance in the presence of MEG and the inhibitor. The solution resistance was used to compensate for all the results of the LPR previously presented.

(a)   (b)
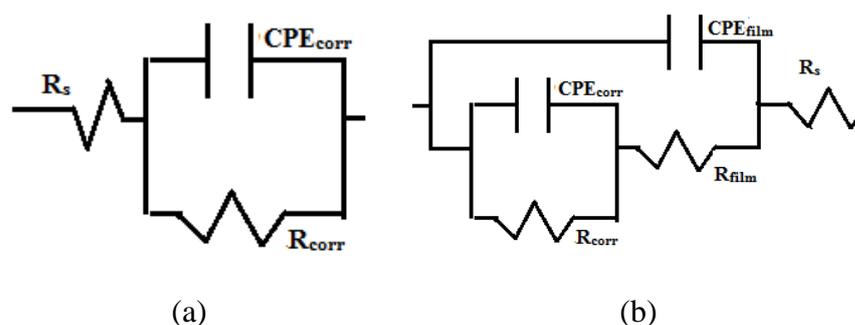
Figure 7-13 : Equivalent circuit (EC) used in representing the AC impedance measurement (a) simple circuit (b) circuit showing resistance due to film formation by the inhibitor in the presence of MEG.

At 80°C, the Nyquist plots for the combination of 50% MEG with inhibitor 1 and 80% MEG with inhibitor 1 are shown in Figure 7-14 and Figure 7-15 respectively. From the Nyquist plot it was observed that the impedance were generally low for all concentrations of inhibitor 1 in 50% MEG solution. This indicates that even at a higher temperature the presence of MEG reduces the efficiency of inhibitor 1. In the presence of 80% MEG the impedance for the whole concentration of inhibitor 1 increased a little. However, the impedances were much lower than expected especially for higher concentration of 50ppm and 100ppm which normally gives high impedance at 80°C with MEG as seen in chapter 6. The reduction in impedance

indicates high corrosion rate which was in line with the results from the LPR where the corrosion rate for the inhibitor 1 in both 50% MEG and 80% MEG was high.
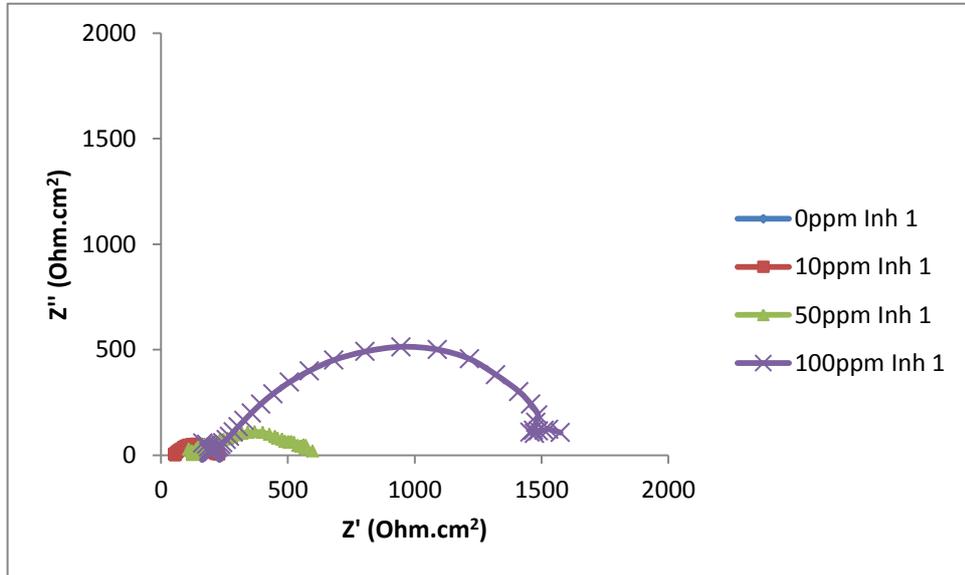
Figure 7-14 : Nyquist plot for 0ppm inhibitor 1 (i.e. 50% MEG) and inhibitor 1 (10ppm, 50ppm and 100ppm) with 50% MEG at 80°C.
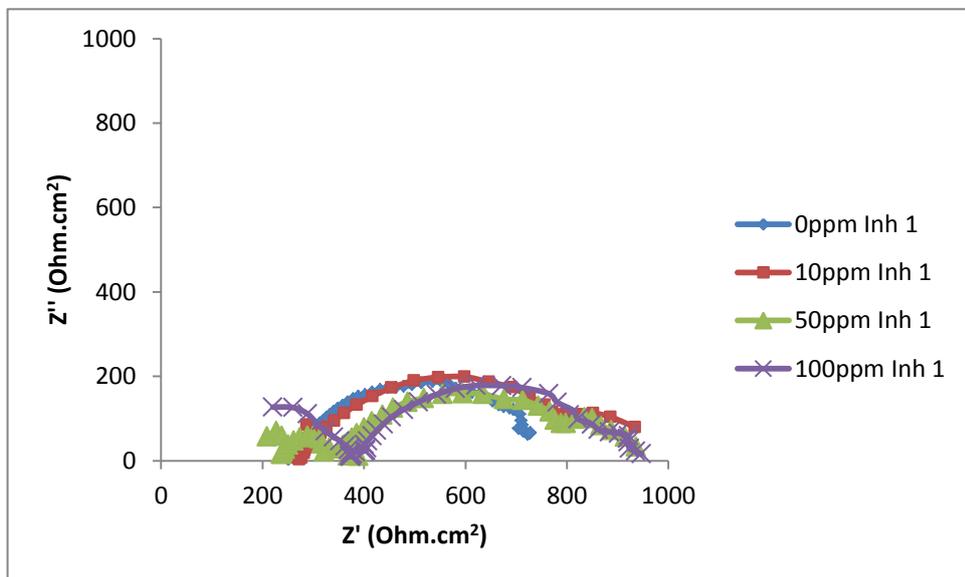
Figure 7-15 : Nyquist plot for 0ppm inhibitor 1 (i.e. 80% MEG) and inhibitor 1 (10ppm, 50ppm and 100ppm) with 80% MEG at 80°C

Figure 7-16 and Figure 7-17 shows the Nyquist plot for 50% MEG with inhibitor 2 and 80% MEG with inhibitor 2 at 80°C respectively. The result showed an increase in the impedance value for all concentration of inhibitor 2. This was in agreement with the result of the LPR previously presented.
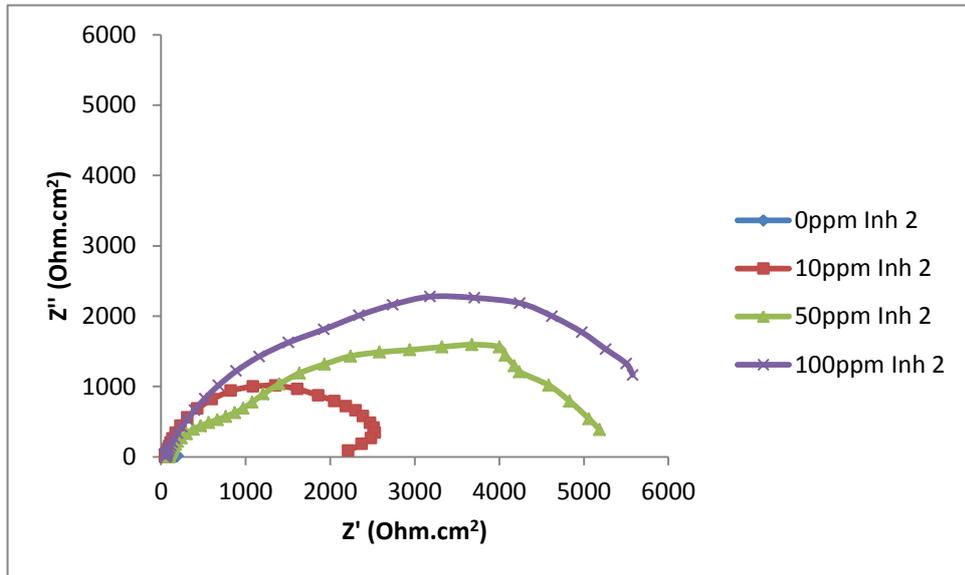
Figure 7-16 : Nyquist plot for 0ppm inhibitor 2 (i.e. 50% MEG) and inhibitor 2 (10ppm, 50ppm and 100ppm) with 50% MEG at 80°C
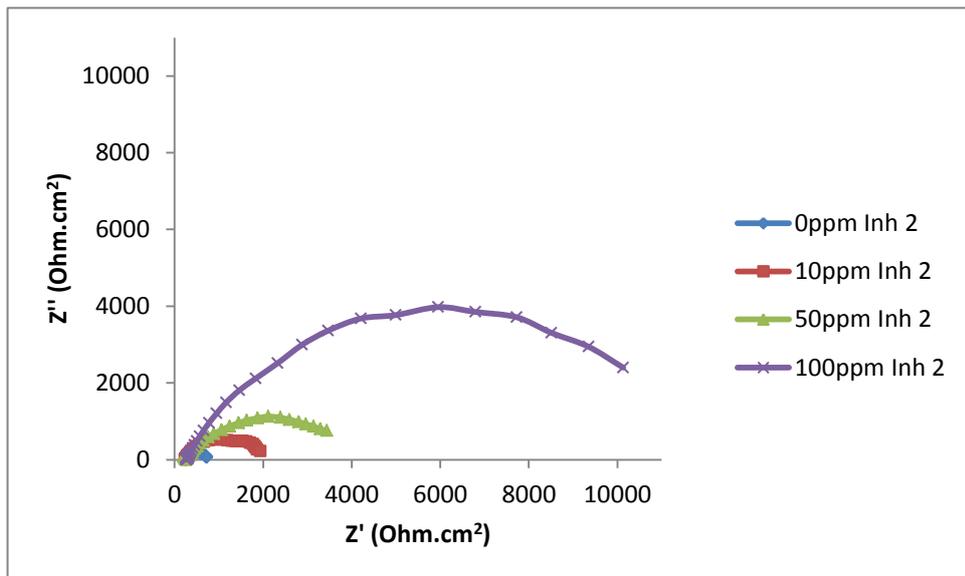
Figure 7-17 : Nyquist plot for 0ppm inhibitor 2 (i.e. 80% MEG) and inhibitor 2 (10ppm, 50ppm and 100ppm) with 80% MEG at 80°C

This increase in impedance indicates that the corrosion rate in the presence of MEG and inhibitor reduces even at high temperatures. However the impedance value for the 10ppm inhibitor 2 and MEG was the least among the other concentrations. This also indicates the increase in the minimal concentration of inhibitor 2 needed to reduces the corrosion rate as the temperature increases. The minimal inhibitor concentration (MIC) increased from 10ppm inhibitor 2 concentration to 50ppm inhibitor 2 concentration at 80°C. The EC in Figure 7-13 used for the corrosion result at 20°C was also used to analyses the result at 80°C. Solution resistance derived from the analysis were used to compensate for the LPR results for 80°C previously presented.

7.4. Surface analysis

Post-test analyses of the samples from the test with the combination of MEG with inhibitors were performed using SEM and interferometry. This will help identify the type of corrosion that occurs on the surface of the tested samples.

7.4.1. Scanning Electron Microscopy (SEM) and Energy Dispersive X-ray Analysis (EDX)

The SEM image was used to analyse the surface of the sample and determine the possible types of corrosion that occurred on the surface of the sample. Some of the results of the SEM image are shown in Figure 7-18. Observation of the image showed general corrosion and clusters of shallow pits/localised corrosion on the surface of samples tested with a combination of 80% MEG with 10ppm inhibitor 1 at 20°C. This indicates the antagonistic effect of a combination of both the 10 ppm and high concentration of MEG (i.e. 80% MEG solution). The SEM image for samples with a combination of inhibitor 2 and MEG solutions did not show any sign of localised corrosion at the surface but rather signs of low general corrosion. This is expected as the LPR results gave a low general corrosion in most of the inhibitor 2 with MEG test. This indicates a synergistic effect with MEG and inhibitor 2.
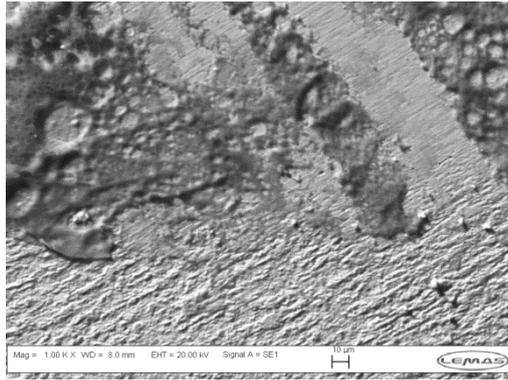
(a)
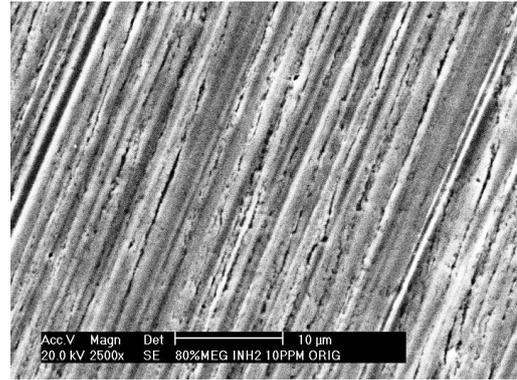
(c)
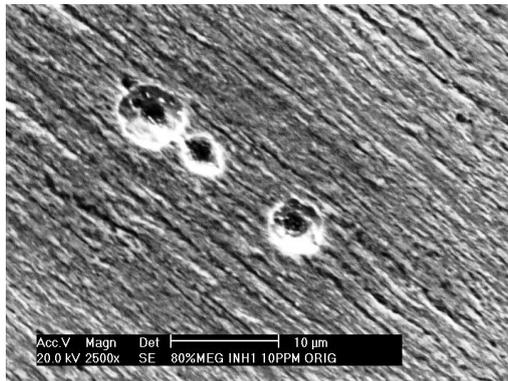
(b)
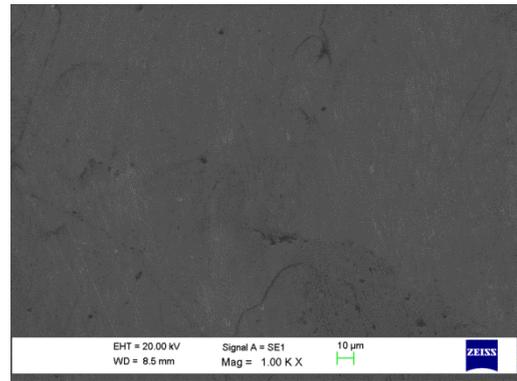
(d)

Figure 7-18 : SEM image at 20°C (a) 10ppm inhibitor 1 with 50% MEG (b) 10ppm inhibitor 1 with 80% MEG (c) 10ppm inhibitor 2 with 80% MEG (d) 100ppm inhibitor 2 with 80% MEG.

SEM images were also taken for the samples tested at 80°C. The results for some of the SEM images are shown in Figure 7-19. The SEM images showed that lower concentration of 10ppm for both inhibitors with MEG have high level of general corrosion. However the SEM images for 10ppm inhibitor 1 with 50% MEG had the highest level of general corrosion. This was evident in the LPR measurement which shows that the combination of 10ppm inhibitor 1 and 50% MEG gave the highest corrosion rate.

The 100ppm inhibitor 2 with 50% MEG showed the least level of corrosion among the SEM images at 80°C.
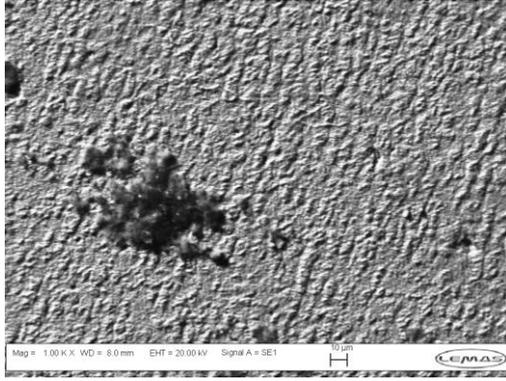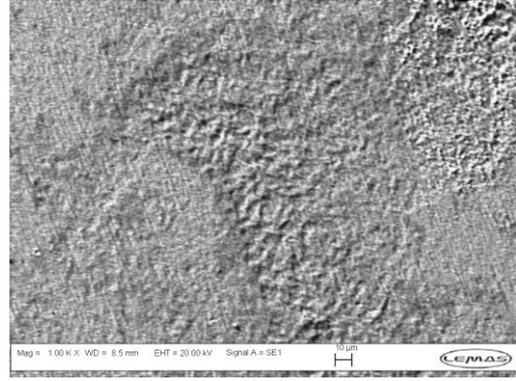
(a)   (d)
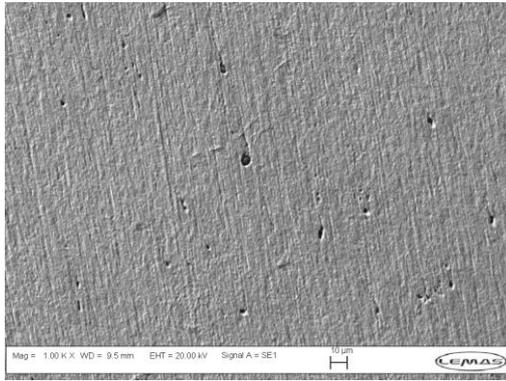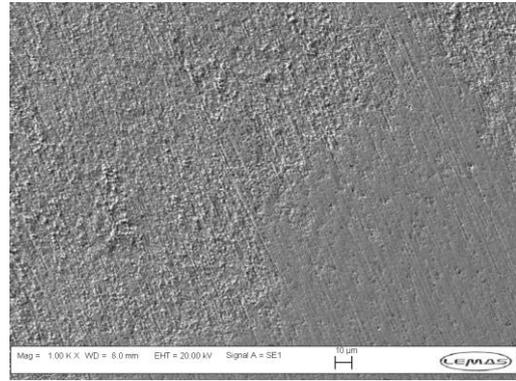
(b)   (e)
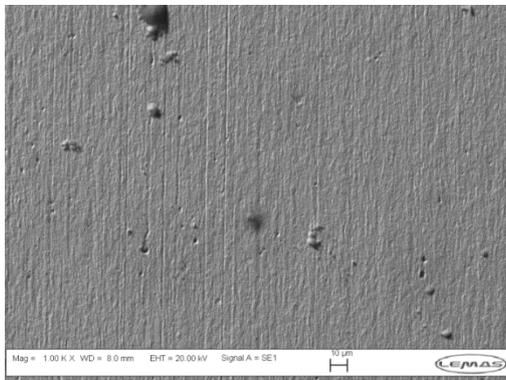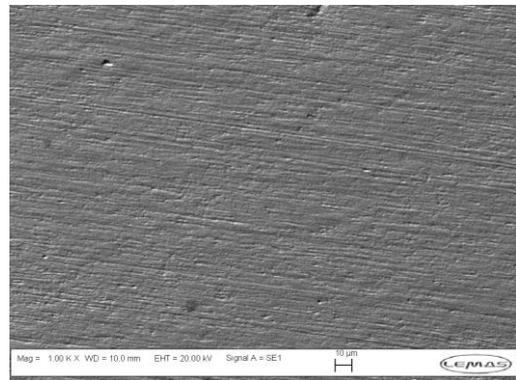
(c)   (f)

Figure 7-19 : SEM image at 80°C (a) 10ppm inhibitor 1 with 50% MEG (b) 10ppm inhibitor 1 with 80% MEG (c) 100ppm inhibitor 1 with 50% MEG (d) 10ppm inhibitor 2 with 50% MEG (e) 10ppm inhibitor 2 with 80% MEG (f) 100ppm inhibitor 2 with 50% MEG.

7.4.2. Interferometry

Wyko light profilometer was also employed to analyses the surface of the samples from the test performed in the presence of MEG with the inhibitors. The result of inhibitor 1 in the presence of 80% MEG is described in Figure 7-20.
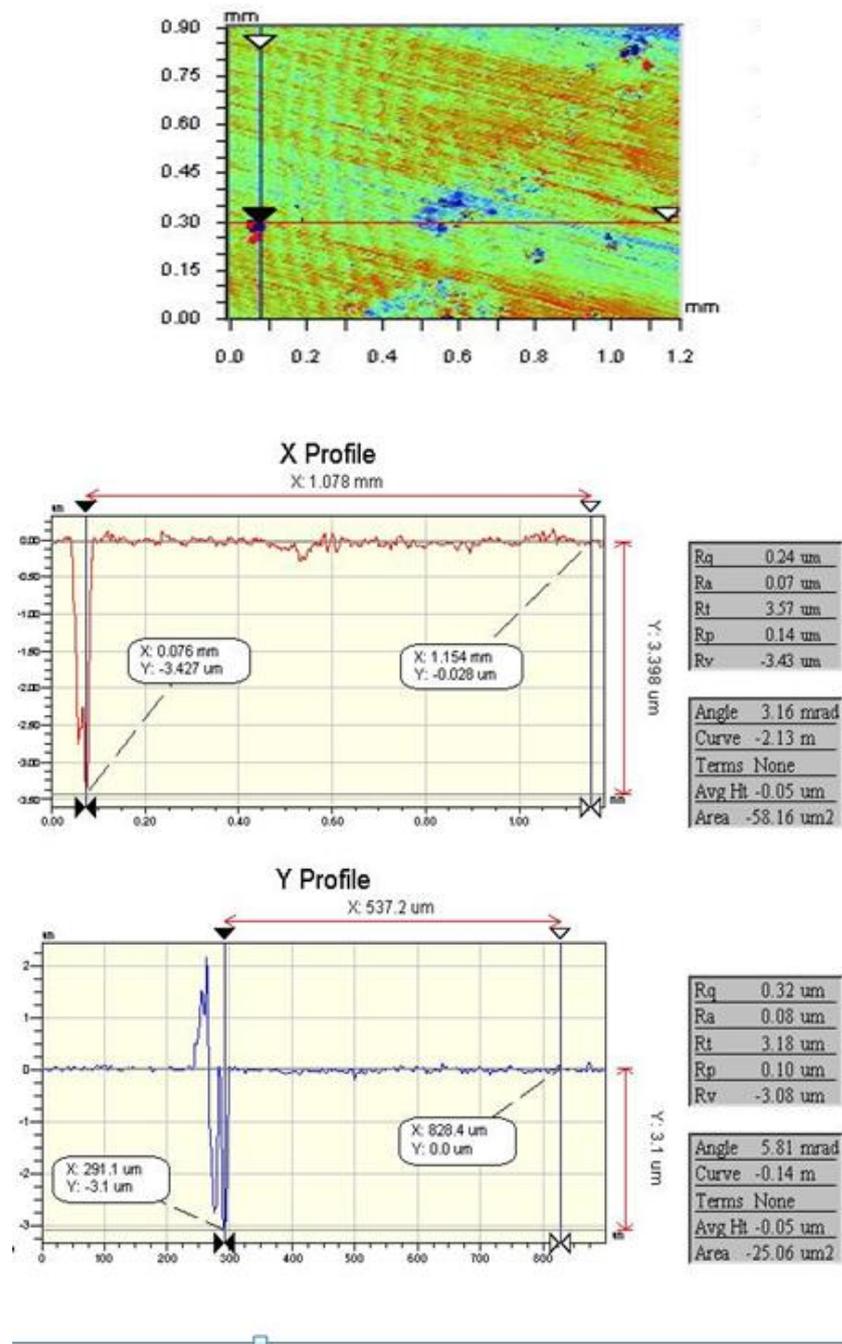
Figure 7-20 : Typical pit measurement for a combination of 80% MEG with 10ppm inhibitor 1 at 20 °C showing pit depth of 3.4μm.

A threshold was assigned to the depth measurement to determine the type of corrosion on the surface of the carbon steel sample. This was used to determine the type of corrosion that occurred on the surface of the sample. The threshold taken was 1 μm as used for the test in the previous chapters. From the results it is seen that the combination of 80% MEG with 10ppm inhibitor at 20°C gave a maximum depth of 3.5μm. This indicates that shallow pits are formed within the 4 hour test period on the sample. This pit depth was more than that observed for the same test with samples from 10ppm inhibitor 1 in the previous section.

7.4.3. Summary of results of corrosion processes in the presence of MEG and organic corrosion inhibitors

This chapter described the results of the corrosion of carbon steel in the presence of MEG with the two inhibitors used. It can be summarised as follows

- The use of corrosion inhibitor further reduces the corrosion rate of carbon steel in the presence of MEG at low temperatures.
- A higher concentration of MEG and a lower concentration of inhibitor 1 10 ppm (i.e. under dosing) can cause localized attack on steel surface.
- Inhibitor 1 showed an antagonistic effect with MEG for most of the test.
- Inhibitor 2 showed better efficiency and compatibility with MEG at 20°C and 80°C and is acceptable for all concentrations tested at 20 °C temperature.
- The use of corrosion inhibitor with MEG may reduce or increase the efficiency of the inhibitor depending on the type of inhibitor and the experimental/testing conditions.

Chapter 8. CORROSION PROCESS IN THE PRESENCE OF IRON CARBONATE SCALE (PRE-CORROSION)

8.1. Introduction

The corrosion process of carbon steel can lead to formation of corrosion products on the surface of the steel. Formation of corrosion products can be beneficial to the reduction of corrosion rate if a protective film is formed [65, 67, 70, 186]. Iron carbonate is the major corrosion product formed in the CO_2 corrosion of carbon steel. This product when properly formed and deposited on the surface can lead to the reduction of corrosion of carbon steel. In real life situations carbon steel pipelines will normally be pre-corroded before application of an inhibitor or injection of MEG as a hydrate inhibitor. In this chapter, pre-corrosion to form iron carbonate which is protective was explored in certain conditions. These pre-corroded carbon steel samples were then used to determine the effect of the presence of MEG and inhibitors in the corrosion of carbon steel in the next chapter.

8.2. Open Circuit Potential (OCP) measurement

As presented in the previous sections, the OCP is one of the quickest semi-quantitative methods to determine what is happening on the surface of corroding carbon steel during corrosion. The results presented here are for corrosion tests of solutions with super-saturated iron carbonate. Super-saturation was achieved by using 250ppm of Fe in the form of $FeCl_2.4H_2O$ and increasing the pH value within 6.8-7 using $NaHCO_3$ as described in chapter 4. Using the MultiScale software, the saturation ratio SR for iron carbonate was calculated to be 4,685 which gave a high scaling tendency.

The result of the OCP monitoring and corrosion resistance for the blank and pre-corrosion test is shown in Figure 8-1. The OCP for the pre-corrosion test shows a negative change as compared to the OCP value of blank solution. This may mean

that the anodic reaction increases in the solution saturated with iron ions (Fe^{2+}) as more iron ions (Fe^{2+}) are formed in the solution. The anodic reaction needs to be accompanied by the cathodic reaction for the corrosion rate of the carbon steel to increase as the corrosion reaction is a redox reaction that produces (Fe^{2+}) and H^+. The increase in the pH of the blank solution from 4 to 6.8 or more for the pre-corrosion test reduces the potential of H^+ and makes the cathodic reaction to reduce. This in effect will reduce the corrosion rate of the steel since the anodic reaction forming Fe^{2+} will require H^+ to complete the corrosion reaction. The high level of Fe^{2+} was produced from the reaction of $FeCl_2.4H_2O$. It then means that the increase in the Fe^{2+} will not lead to additional corrosion of the steel as expected. The result in fact shows that the polarisation resistance (R_p) of the pre-corrosion samples was higher than that of the blank test alone. This shows that the corrosion rate may be reducing due to the cathodic reduction of the corrosion reaction.
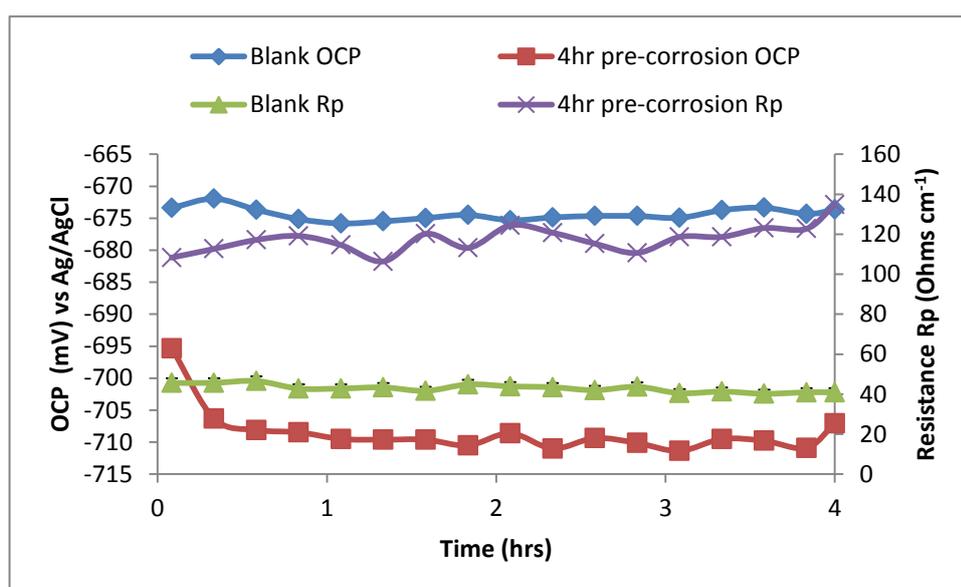
Figure 8-1 : OCP and R_p measurement for the corrosion of carbon steel in the presence of Iron carbonate for 4 hours at 80°C.

An additional test was performed for a longer period of time. The result of the OCP test for a 24 hour period is shown in Figure 8-2. Interestingly the OCP measurement decreases as usual for most part of the test until 10 hour point when the OCP gradually starts rising with time. The increase in OCP occurs slowly and steadily

throughout the remaining part of the experiment. This increase may be a response to additional increase in the resistance of the steel with time. The result of the OCP with time and the resistance with time for both blank and solution with Fe^{2+} is shown in Figure 8-2. This demonstrates the effect on the OCP as further increase in the polarisation resistance was observed due to barriers formed against the corrosion species.
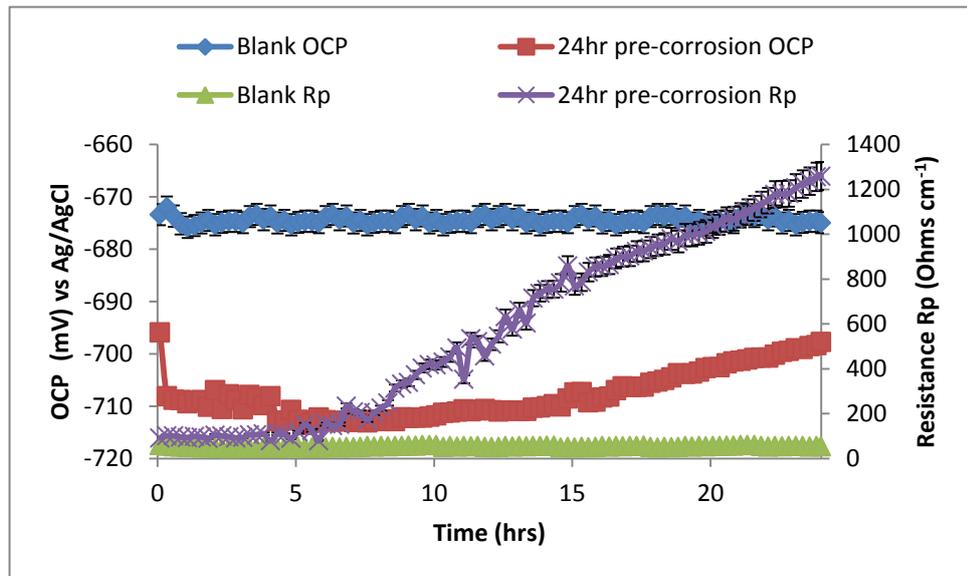
Figure 8-2 : OCP measurement for the corrosion of carbon steel in the presence of Iron carbonate for 24hrs period at 80°C.

8.3. Linear Polarization Resistance (LPR) measurement

In order to understand the corrosion resistance of the carbon steel as the iron carbonate scales are formed, there is a need to do a LPR test on the sample.

The LPR result is shown in Figure 8-3. The blank showed high corrosion rate with time. The blank solution shows the same corrosion rate or an increase in corrosion rate with time. This is an indication that the corrosion for the carbon steel in blank solution occur continuously without any protection. The lack of formation of protective iron carbonate film on surface of the steel in the blank solution may be due to the low pH of 4 used for the blank test. It has been shown that deposition of protective iron carbonate occurs at high pH value above 5 [78, 187, 188].

For the pre-corrosion test, the LPR showed a reduction in corrosion rate with time. This is an indication that corrosion product, probably iron carbonate films, are being formed on the surface of the carbon steel. This in effect causes a reduction of the corrosion rate from the initial start and further along as the test progresses with time. The result of the 4 hour test for the blank and pre-corrosion is shown in Figure 8-3. The result showed a reduction in corrosion rate with time. However the corrosion rate was still not below 1mm/y. This may be an indication that the corrosion product that forms on the surface is still porous. The chemical reaction forming this protective film on the surface may need a longer time. A further test was then performed for a 24 hour period to study the effect of time.
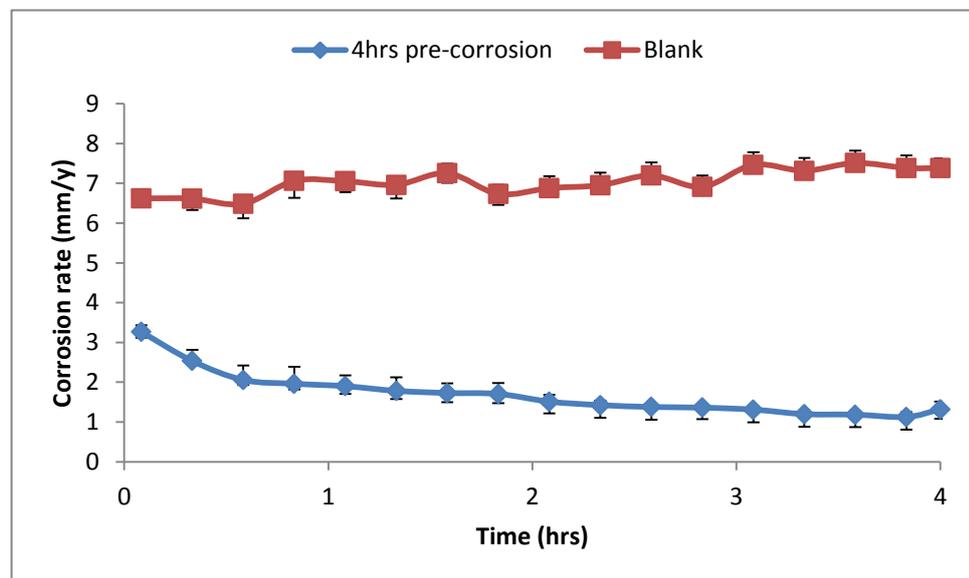
Figure 8-3 : Corrosion rate measurement for blank and pre-corroded sample at 80°C.

Results of the corrosion test for the 24 hours period showed further reduction in the corrosion as the test progressed. This is an indication that the deposition of iron carbonate on the surface of the carbon steel progress with time. A more protective barrier that reduces the corrosion species reaching the surfaces of the carbon steel is formed. This process reduces the anodic reaction as corrosion chemical species can't reach the surface of the carbon steel. This is evident in the OCP trend which previously decreased for the 4 hour pre-corrosion test and later started increasing slowly after 10 hour time in the 24 hour test. This is an indication that the reduction

in corrosion rate is no longer due to the reduction in the cathodic reaction alone but also a reduction in the anodic reaction.
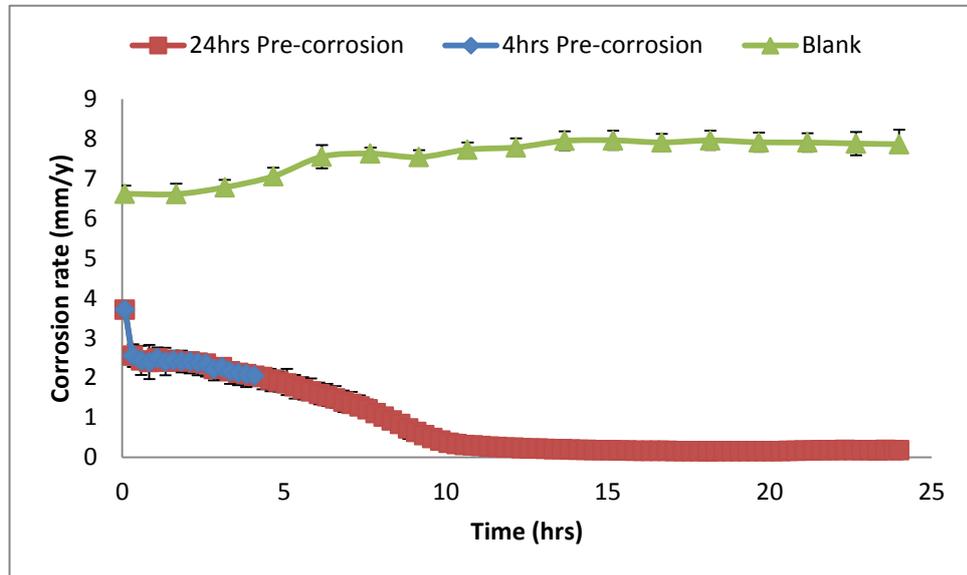
Figure 8-4 : Comparison of the corrosion rate for blank and pre-corrosion for 4 hour period and 24 hour period showing lower corrosion rate with pre-corrosion time.

8.4. Surface analysis

8.4.1. Scanning Electron Microscopy/ Energy Dispersive X-ray Spectroscopy (SEM/EDX)

Carbon steel samples used for the different test were prepared and kept in a desiccator for further test. The test result includes SEM and EDX. The SEM was used to visually determine the formation of general corrosion, localised corrosion and deposition of corrosion product on the surface. Further test were done on selected sample to determine the surface constituent using EDX techniques. The results for the 4 hours test are shown in Figure 8-5. As expected the carbon steel sample from the blank solution shows massive degradation due to corrosion on the surface. The corrosion was mostly large general corrosion and localised corrosion on the metal surface. This is due to lack of protection on the surface of the carbon steel surface as corrosion occurs. It shows that there is no protective corrosion product

forming on the surface. The lack of protection on the metal surface may be due to lack of super saturation of the corrosion product of iron carbonate. Studies by Nesic et al. [40, 65, 78, 187] shows that for iron carbonate to deposit on the surface the pH of the solution needs to be high . This may not occur within the time of the experiment as shown. The SEM image is in line with the LPR measurement which indicates high corrosion rate which may be increasing slightly with time.
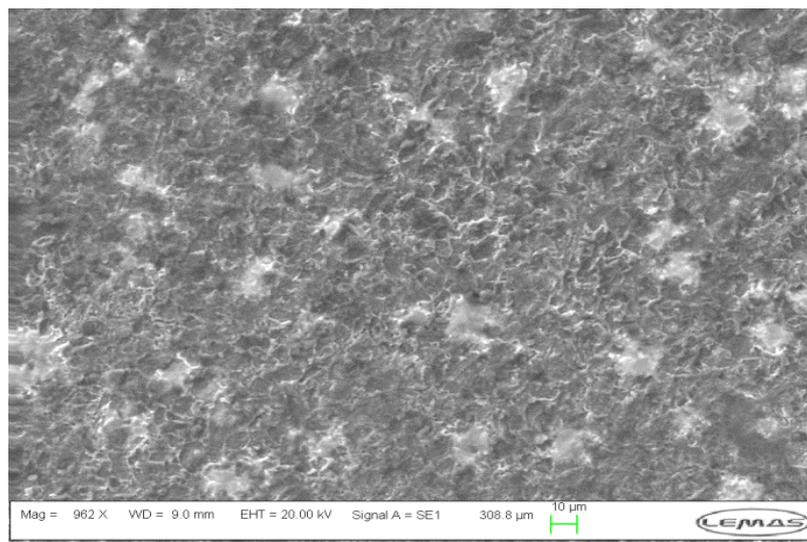
Figure 8-5: SEM image of samples from blank solution after 4hrs period.

The result of pre-corrosion in the presence of $FeCl_2.4H_2O$ for 4 hours is shown in Figure 8-6. The pre-corrosion SEM image shows the formation of spherical rounded crystals which are believe to be mainly iron carbonate as the experiments was conducted in CO_2 saturated environment. The crystals were large in size and had many gaps in between them. This crystal may serve as a selective barrier to the corrosion species. This is the reason why the corrosion rate of the 4hrs pre-corrosion of the carbon steel reduces from approximately 6mm/y on blank solution to approximately 2mm/y for the pre-corrosion. The formation of crystallised iron carbonate has been shown to give protection to the corroding carbon steel [33, 34, 78, 189]. The crystal formation on the surface reduces the anodic reaction on the surface by reducing the amount of corrosion species reacting on the bare ferrite. The reduction in corrosion rate was not very much and maybe due to the gap between the

crystals of the corrosion product. The thickness of the film may also be an issue. A very thick film will likely form a bigger barrier to corrosion chemical species.
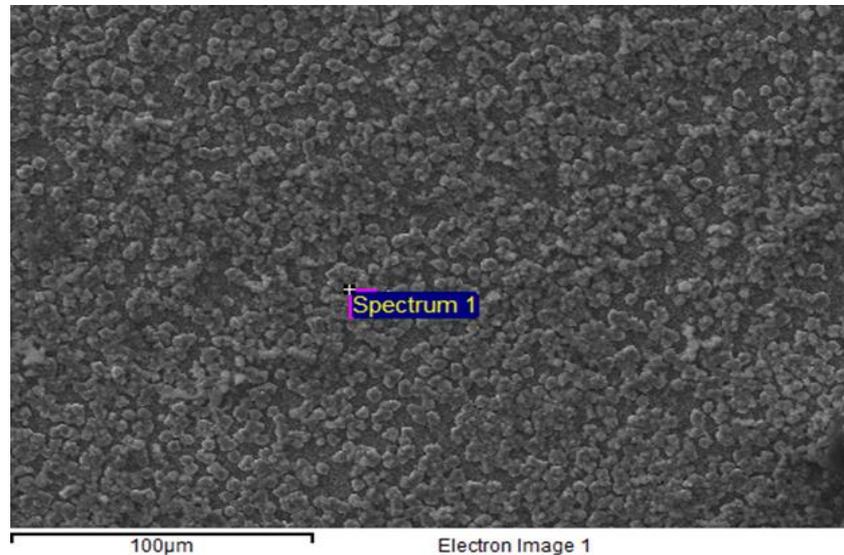
Figure 8-6: SEM images of samples from 4hrs pre-corrosion.

In other to verify the thickness of the film the cross-section of the carbon steel after corrosion test was examined and is shown in Figure 8-7. The result of the SEM shows that the thickness of the film was not quite uniform. The thickness varies along the surface of the metal. This may be due to the deposition rate not being uniform in all part of the metal. This is expected as there is no special control for the deposition on the surface metal. Since the reaction is a chemical process the reactions may not be uniform as it may be affected by the availability of corrosion species on the different parts of the surface. This competition likely leaves the surface with different layers at difference point. The thickness of the corrosion product film was between 2.9µm and 4.9µm. The thickness may mean that the corrosion species are able to penetrate the film and reach the bare steel.

The rate of deposition of iron carbonate on the surface of the carbon steel can be calculated. From calculation it shows that the deposition rate for iron carbonate on the surface is 0.72 µm/hr (i.e. 2.9µm thickness) – 1.2 µm/hr (4.9µm thickness). The average rate of iron carbonate deposition will be less than the maximum rate and will be in the lesser region of 0.72µm because the majority of the films formed were

approximately 3μm thickness. The image also shows iron carbide which forms an anchor for some of the crystalline corrosion product. This film thickness will be compared to the film thickness for 24hrs pre-corrosion to determine the effect of corrosion product thickness on the corrosion resistance of the carbon steel.
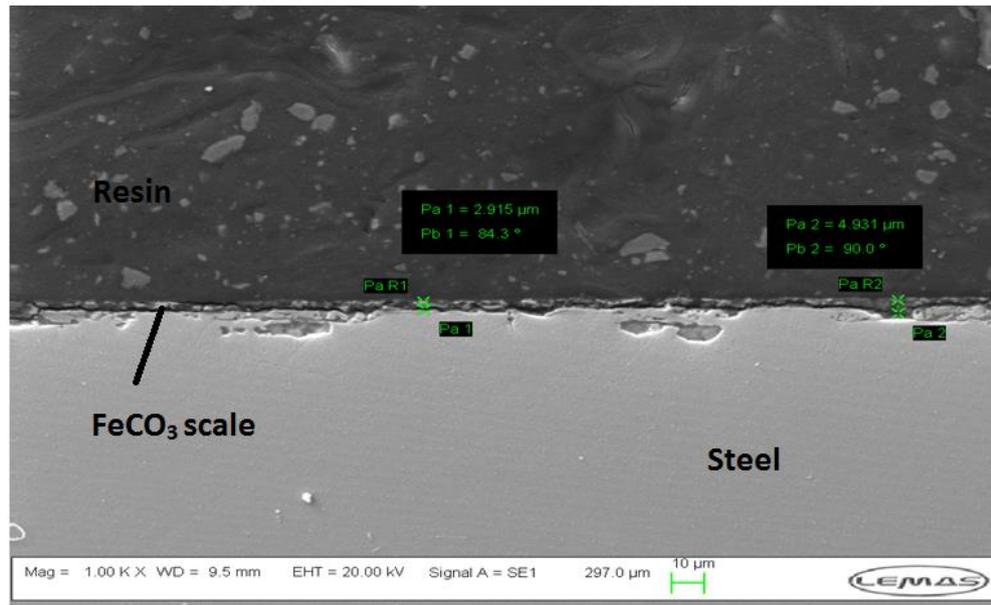
Figure 8-7 : SEM corrosion product (i.e.$FeCO_3$) thickness measurement for 4hrs pre-corrosion test

EDX analysis of the surface of the carbon steel was performed for the pre-corroded sample. This is to understand the type of corrosion product that is formed on the surface of the metal. EDX may not be a confirmatory method to understand the corrosion product formed on the surface of the carbon steel. However it can still give an idea of the corrosion product that is mostly formed on the surface of the carbon steel. The EDX measurement result for the 4hrs pre-corrosion test is shown below in Table 8-1. The analysis from the EDX shows that the crystals formed on the surface of the carbon steel are mostly made of Fe, C, and O. with an increase in the atomic percentage of C and O and a decrease in the Fe atomic %. This is an indication of the formation of iron carbonate, Iron carbide and other oxides of iron on the surface. To confirm the corrosion product formed on the surface additional test may be required. This may mean the use of other surface analysis technique.

Further analysis using FTIR was used to test the corrosion product formed on the surface and is presented later in this section.

Table 8-1 : EDX on 4hrs pre-corroded carbon steel surface showing the composition of the crystals for 4hrs pre-corrosion.

Element %	Atomic %
C	19.33
O	63.08
Fe	17.59

The result of the SEM image for the 24 hours test is shown in Figure 8-8. The SEM image for the test for 24hrs pre-corrosion shows a well compact film layer. The film is presumably made of iron carbonate crystals particles which are cubical in shape. The iron carbonate crystals were smaller in size compared to the size formed by the 4hrs test. This is due to competition of the crystal particles and increase in crystal stability with time. This makes the particles to cluster together and formed a well packed film layer. This layer has less gap in-between particles due to the competition on space between the crystal particles as they grow. This also makes the crystal particles to look more cubical in shape. The formation of this type of film improves the barrier against the corrosion species. This is reflected in the large reduction of the corrosion rate after the 24hrs test on the LPR measurement. This gives the carbon steel good protection against general corrosion.

The thickness of the corrosion film on surface of 24hrs pre-corroded carbon steel gave another insight into the low corrosion rate obtained. The measured thickness is shown in Figure 8-9. The SEM was used in determining the thickness of the film the same way it was used for the 4hrs pre-corroded carbon steel sample. The result from the SEM shows a very thick film was formed on the surface of the pre-corroded carbon steel. The measurement showed a maximum film thickness of 13.5μm. This thick film formed on the surface of the pre-corroded sample after 24hrs serves as a bigger barrier to corrosion species in reaching the bare carbon steel. This gives a

very high reduction in the anodic corrosion reaction and contributes to slight increase in a higher OCP at the end of the 24hrs reaction as compared to the 4hrs corrosion reaction. The rate of deposition of the iron carbonate on the surface of the 24hrs pre-corroded samples is calculated to be 0.56μm (i.e. 13.5μm thickness) at maximum showing a reduction in deposition rate with time.
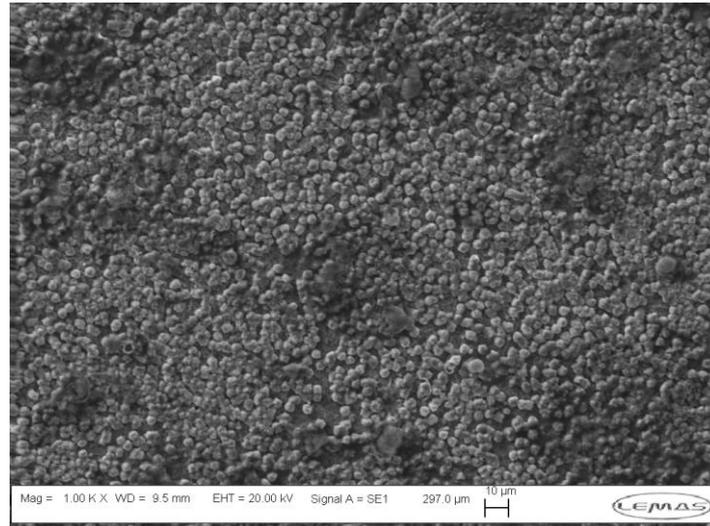
Figure 8-8 : SEM images of samples from 24hrs pre-corrosion showing closely packed iron carbonate crystals.
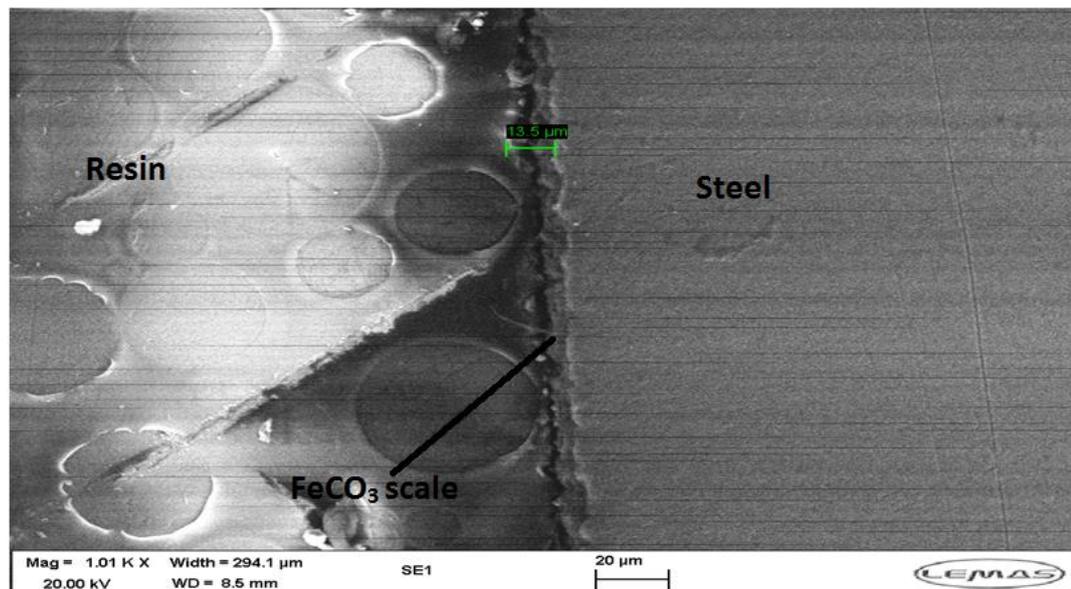
Figure 8-9 : SEM corrosion product (i.e.$FeCO_3$) thickness measurement for 24hrs pre-corrosion test.

Table 8-2 shows the EDX surface composition for the 24hrs pre-corroded carbon steel. EDX on the surface of the 24hrs pre-corrosion shows element of Fe, C, and O are also predominant on the spectrum on the crystals surface as seen for the 4 hours pre-corrosion. This is an indication that what is composed on the surface of the sample is mainly iron carbonate and iron carbide or iron oxides. But since the pre-corrosion process was conducted in an oxygen free environment, the predominant scale on the surface of the metal will be that of iron carbonate.

Table 8-2 : EDX on X65 carbon steel surface showing the composition of the crystals for 24hrs pre-corrosion

Element %	Atomic %
C	25.48
O	60.24
Fe	14.29

8.4.2. Fourier Transform Infrared Spectrometry (FTIR)

Having identified the elements that are present on the surface of the pre-corroded samples by EDX analysis, the FTIR results can be used to substantiate the fact that iron carbonate is formed on the surface of the pre-corroded sample. A sample of the 24hrs-precorroded sample was used for FTIR analysis. The test result is shown in Figure 8-10. The result shows the presence of CO_3 at the wavenumber of 1480 and 862. This is an indication that carbonates are formed on the surface of the carbon steel sample [134, 155]. As the iron ions were predominately present in the solution through addition of 250ppm iron ions and from the anodic corrosion process, it may be right to confirm that the carbonate present was that of iron carbonate on the sample surface. This is in line with studies by Akbar et al. [155] which showed that this carbonate formed was that of iron carbonate through FTIR and X-ray diffraction analysis.
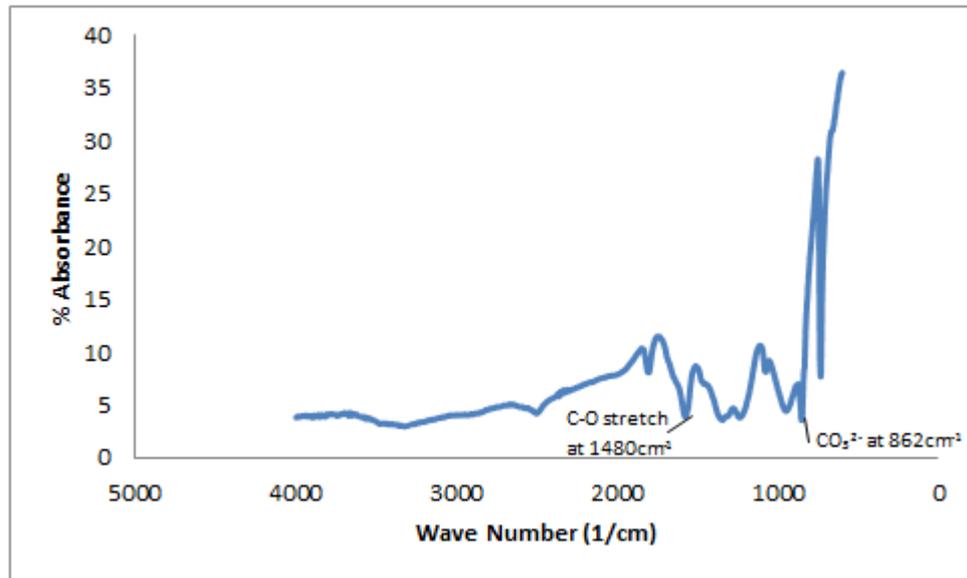
Figure 8-10 : FTIR spectrum for a 24hrs pre-corrosion sample

8.4.3. Interferometry

Interferometry was used to determine the surface topography of the samples after pre-corrosion test. This is just a way to know what happens to the surface of the sample when corrosion products are formed on the surface. Studies shows that the iron carbonate films formed on the surface of the sample becomes cathodic to bare steel [190]. The presence of bare steel (ferrite) in the presence of iron carbonate can lead to localised corrosion. This localised corrosion can even grow further if there is no formation of iron carbonate in the localised area to stop further corrosion. In this test, the profilometer were used to measure the depth of the surface and determine under scale localised corrosion.

The Profilometry measurements after iron carbonate scale was removed from the 4hrs pre-corroded carbon steel surface showed that the maximum depth to be 1.5µm. Figure 8-11 shows the measurement of the 4hr pre-corroded carbon steel after the surface scale had been removed. The pit growth rate using this maximum depth was calculated as 0.4µm/hr.
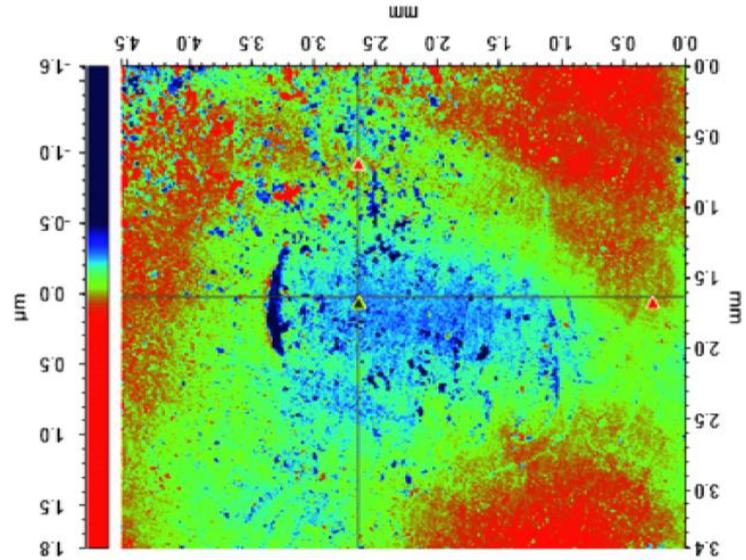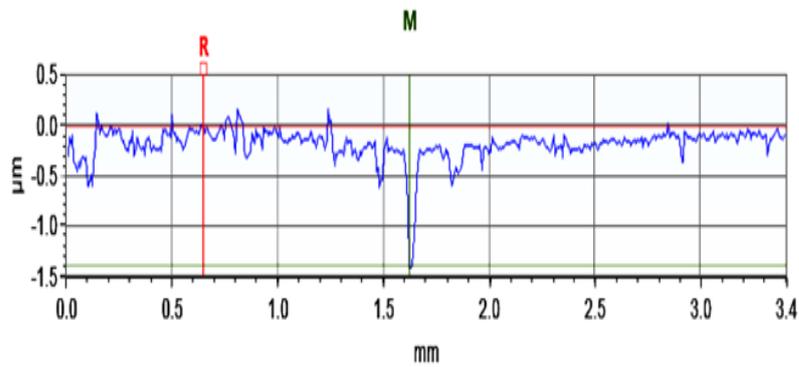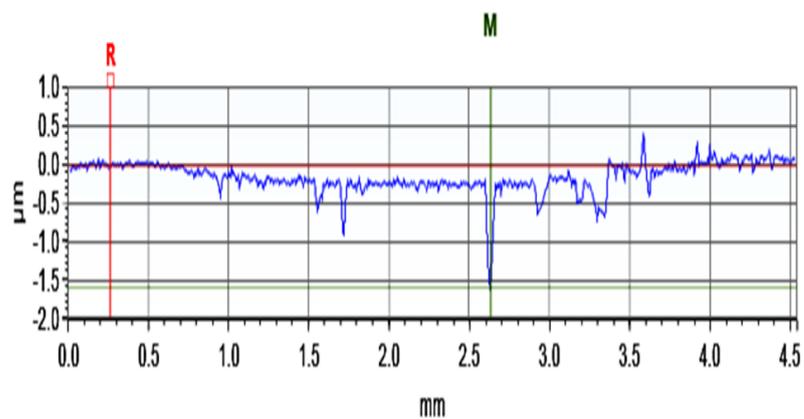
Figure 8-11 : Typical Pit Measurement of pre-corroded sample after 4 hours at 80°C showing maximum pit depth.
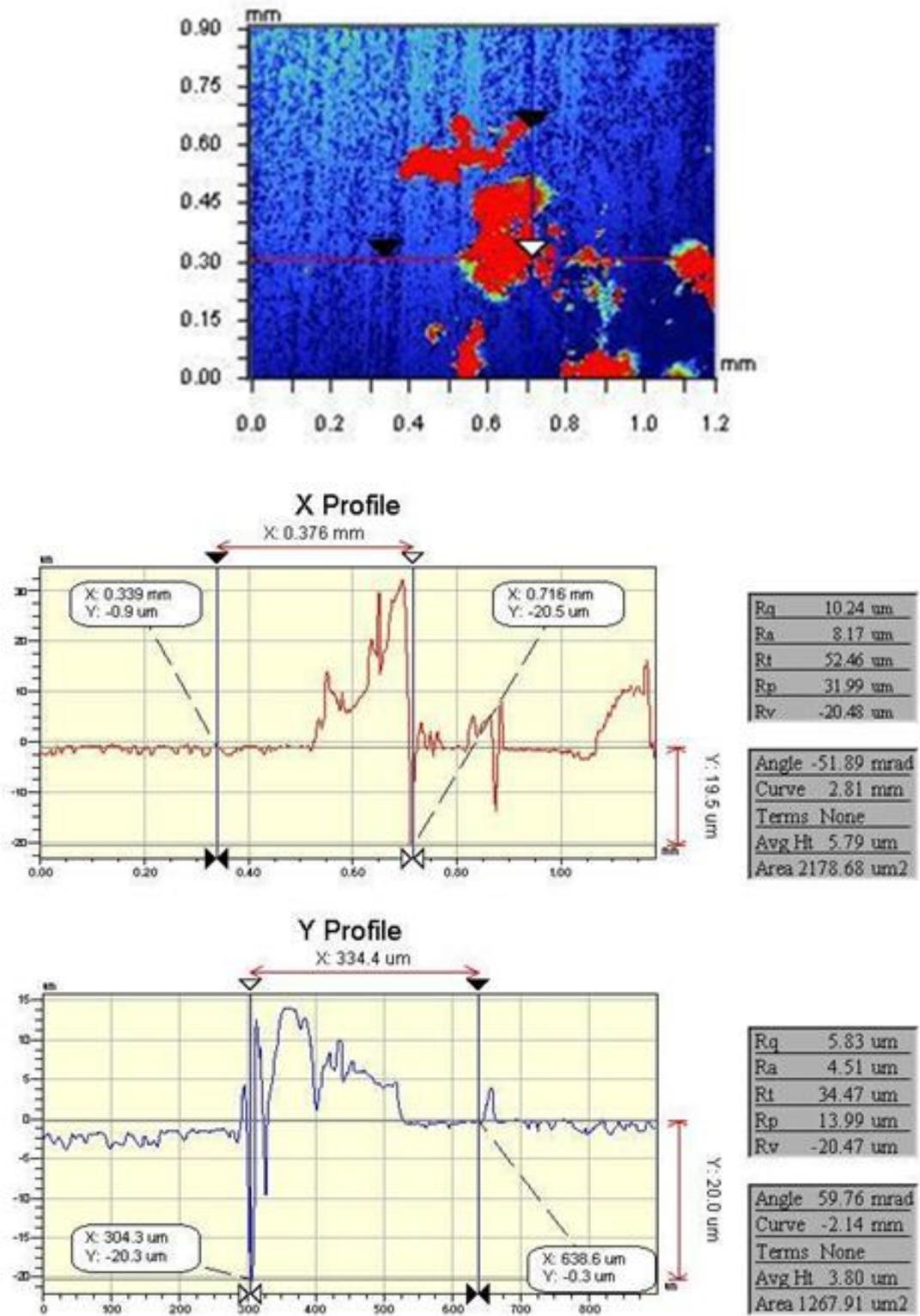
Figure 8-12 : Typical Pit Measurement of pre-corroded sample after 24 hours at 80°C showing maximum pit depth.

The result of the 24hrs pre-corrosion test still had localised corrosion under the iron carbonate scale after cleaning the surface with Clarke solution. The maximum pit that was seen in all samples tested was 20μm. The pit was observed beside areas with well form iron carbonate film. The shape of the pit tends to thin down the depth which may indicate filling up due to the formation of more corrosion product on that area. The pit growth rate was calculated to be 0.83μm/hr. The rate was approximately the same as the 0.8μm/hr derived from the general corrosion rate. The pit growth rate was however higher than that for the 4hrs pre-corrosion even as the corrosion rate was much lower.

8.5. Summary of result of corrosion process in the presence of iron carbonate scale (Pre-corrosion)

This chapter described the result of the pre-corrosion of carbon steel. It can be summarised as follows

- The formation of iron carbonate is achieved at high iron concentration, pH and high temperature of 80°C.

- The formation of protective $FeCO_3$ scale at 80°C depends on the thickness, shape, packing and size of the crystals.

- Longer tests of 24 hours gave a more protective iron carbonate scale of up 13.5μm as compared to the less protective iron carbonate formed for 4 hours period.

- There may be formation of under scale corrosion on the surface of the pre-corroded carbon steel. This occurs more when protective thick films are formed on the surface.

Chapter 9. CORROSION ASSESSMENT IN THE PRESENCE OF IRON CARBONATE SCALE (PRE-CORROSION), MONOETHYLENE GLYCOL AND ORGANIC CORROSION INHIBITORS

9.1. Introduction

The formation of iron carbonate scale on the surface of carbon steel pipeline occurs under certain conditions. In the transportation of natural gas from a remote source to the process area, iron carbonate can formed on the surface of the pipeline with high temperature and pH. In the North Sea and in Norwegian natural gas pipeline transportation, pH stabilization has been used to prevent corrosion along pipeline [77, 108, 114, 117, 122]. This encourages the formation of iron carbonate on the surface of the pipeline at high temperature areas of the transport system and relies on this to reduce corrosion. In some situations the formation of other scales like calcium carbonate ($CaCO_3$) may occur in the presence of formation water. This may lead to undesirable scale formation and problems for the operation of the pipeline. If scaling by $CaCO_3$ is very severe the pH stabilization method can be inadequate for preventing corrosion. The introduction of organic corrosion inhibitors are often used as a more reliable means of managing corrosion.

This chapter will look at the corrosion processes in the presence of iron carbonate, MEG and corrosion inhibitor. The first section will look at the corrosion process of iron carbonate scale and MEG alone and the second section will then look at the corrosion process in the presence of iron carbonate, MEG and inhibitor. This will give an idea of the effect of MEG on the formation of iron carbonate scale in MEG-containing systems. The introduction of MEG may increase the tendency of iron carbonate scaling in the system which may be beneficial in some aspects. The effect of inhibitor in the presence of iron carbonate scale and MEG-containing system will be assessed. The inhibitor could potentially affect both MEG and iron carbonate formation and may destroy the existing protective iron carbonate film.

9.2. Open Circuit Potential (OCP) measurement for pre-corroded carbon steel in MEG solution

The OCP measurements for pre-corroded steel samples in the presence of MEG were performed. These measurements were achieved by using duplicates of pre-corroded samples from previous section 8-2 to 8-3 and testing them in a solution of MEG. The test was conducted at concentrations of 50% MEG and 80% MEG as described in chapter 4. The OCP results are shown in Figure 9-1. The results of the OCP for the 4 hour pre-corroded carbon steel sample at 20°C shows a massive increase in the OCP immediately the pre-corroded samples were introduce into the MEG solution. For the 50% MEG solution, the OCP increased to -455mV as compared to polished samples in blank solution represented as blank in Figure 9-1. This is an indication that there is a formation of protective layer on the surface of the pre-corroded sample. The combination with the MEG solution makes the OCP to be very high at the initial point. This gives rise to high OCP at the initial time. For the 80% MEG solution, the OCP was even higher than that of the 50% MEG solution at the initial point. The value of the OCP from the result was -242mV. As the corrosion test time increases, the OCP of both the 50% MEG solution and the 80% MEG starts to decrease. After the 4 hour test, the OCP values of the pre-corroded sample stabilized in both solutions.
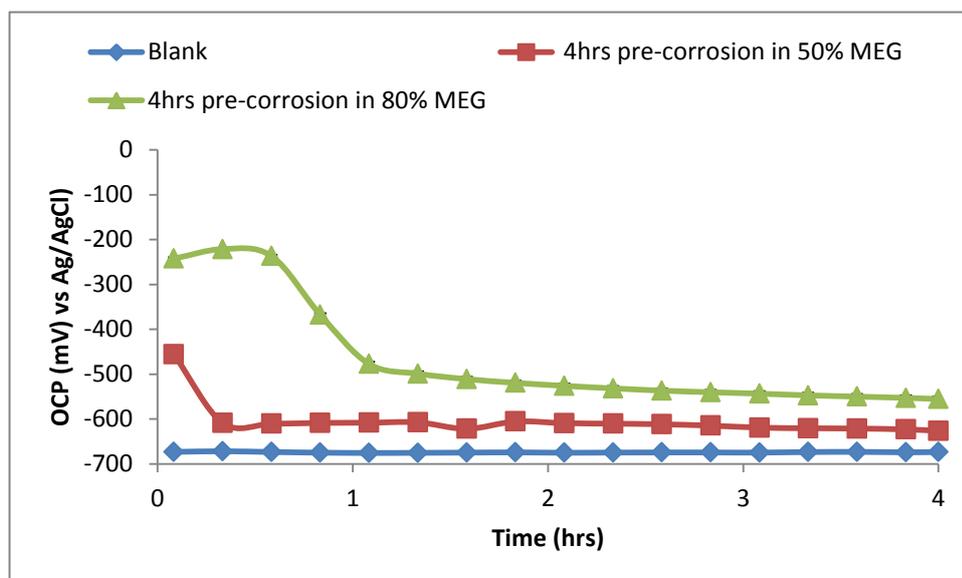
Figure 9-1 : OCP measurement for blank (i.e. polished sample), 4hrs pre-corroded sample in the presence of 50% MEG solution and 80% MEG solution at 20°C.

For the 4 hours pre-corroded test with MEG solution at 80°C, the OCP values also increase at the initial point. The increases were not as much as the increase with the OCP values at 20°C. The value for the OCP in 50% MEG solution at the initial point was -648mV. This shows that at high temperature the corrosion species easily penetrate the film formed on the surface of the sample. This is expected as corrosion species are more active at high temperature as compared to the low temperature. For the 80% MEG solution the OCP did not increase much at the initial point as compared to the OCP for the low temperature of 20°C. This is also due to the corrosion species being active at this temperature. The value at the initial point for the OCP in 80% MEG solution is -613mV. This may explain why high corrosion rate may be obtained at high temperature than at lower temperature for the MEG solution. This will be investigated further using other electrochemical test and surface analysis.
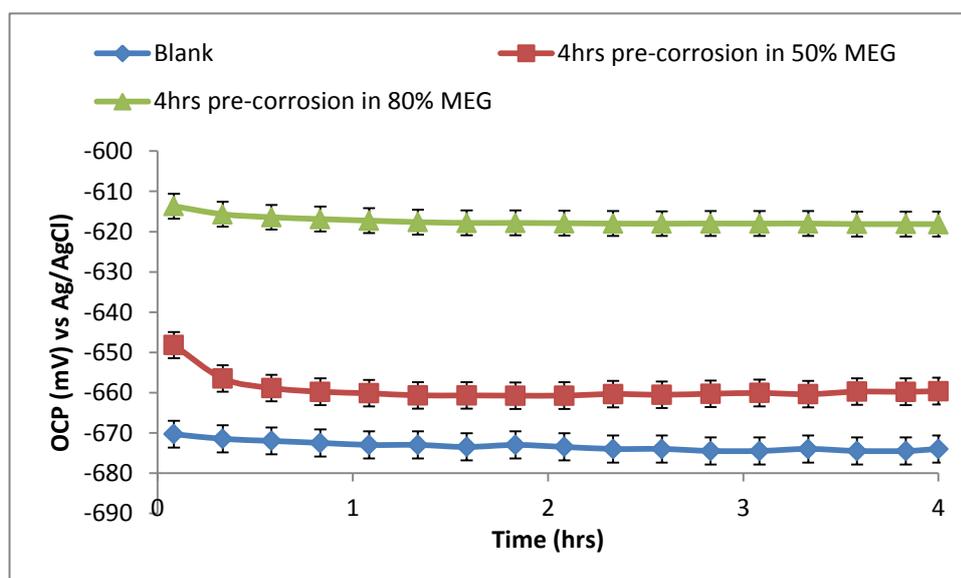
Figure 9-2 : OCP measurement for blank (i.e. polished sample), 4hrs pre-corroded sample in the presence of 50% MEG solution and 80% MEG solution at 80°C.

Similar trends of OCP results were obtained for the 24hrs pre-corroded carbon steel tested in 50% MEG and 80% MEG solution. For tests at 20°C, the OCP increased at the starting point of the test for the 50% MEG solution. The value for the OCP was -

598mV. This is an indication of the slow diffusion of the corrosion species to the pre-corroded sample bare metal surface. These also occur for the 80% MEG solution at the same temperature. The OCP value for the sample at the starting point was -218mV.The value of the OCP at the starting point for the 80% MEG is higher than that of the 50% MEG solution as seen for the result of the 24hrs pre-corrosion. This shows that the corrosion rate in 80% MEG may be lower than the corrosion rate in the 50% MEG solution even for pre-corroded carbon steel. The value of the OCP for both test samples in the MEG solutions reach a stable value as the test proceeded. The end OCP value for the test samples in 50% MEG solution was -605mV, while that for the test samples in 80% MEG solution was -552mV.

More tests using other electrochemical methods were done to verify this as OCP values are semi-quantitative at the best [17].
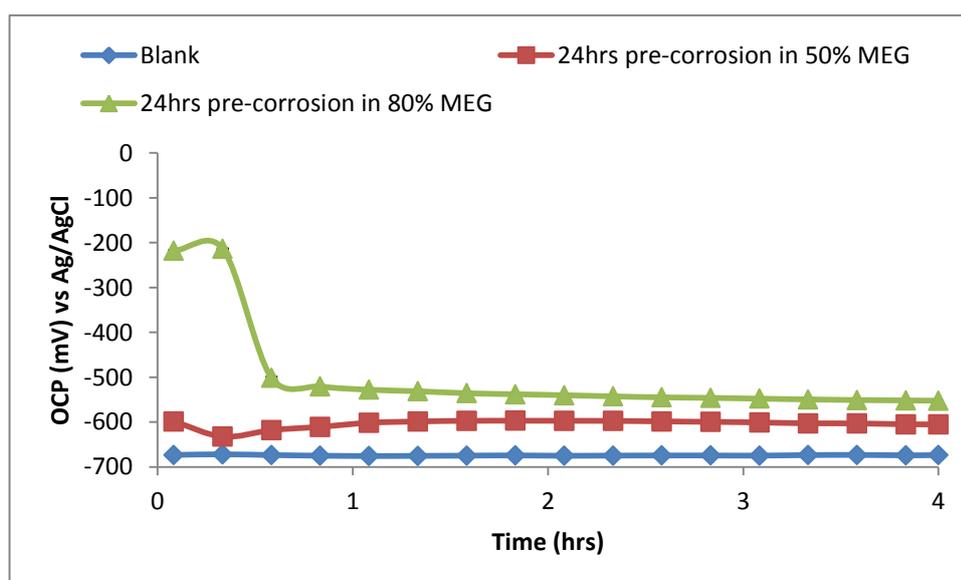
Figure 9-3 : OCP measurement for blank (i.e. polished sample), 24hrs pre-corroded sample in the presence of 50% MEG solution and 80% MEG solution at 20°C.

The result for test at higher temperature of 80°C for the 24 hours pre-corroded carbon steel in MEG show that the OCP values did not increase very much compared to the values for the blank. The value for the OCP of test sample in 50% MEG solution were -594mV at the starting point. This does not show much increase as compared to the increase for the lower temperature of 20°C at the starting point.

This again may be an indication of higher corrosion rate at high temperature of 80°C for this test. The OCP value for test sample in 80% MEG solution was -514mV at the starting point. This was less than the OCP value for the same test at lower temperature of 20°C as described previously. The OCP values for tests in 80% MEG were higher than those for tests in 50% MEG at this temperature.
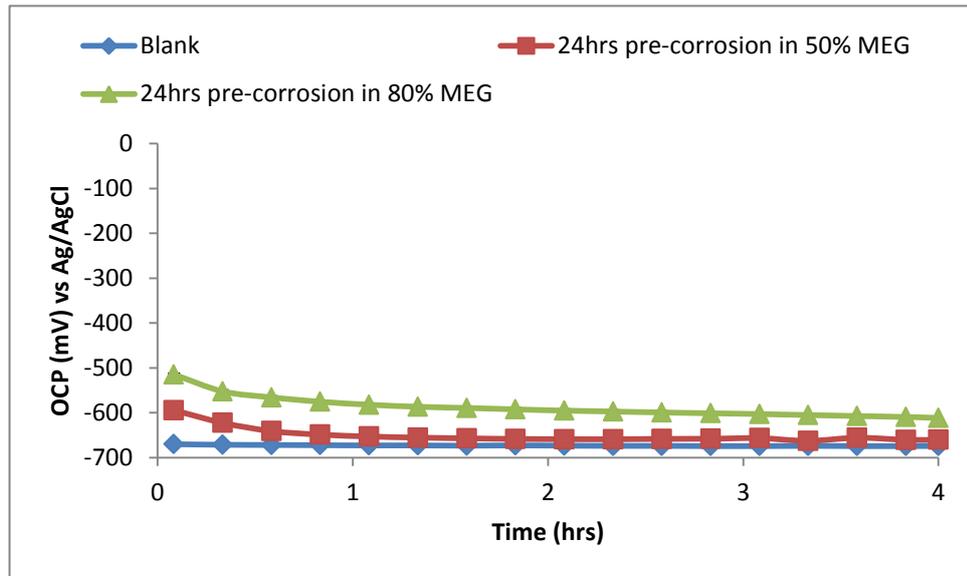
Figure 9-4 : OCP measurement for blank (i.e. polished sample), 24hrs pre-corroded sample in the presence of 50% MEG solution and 80% MEG solution at 80°C.

9.3. Linear Polarization Resistance (LPR) measurement for pre-corroded sample in MEG

The results from the linear polarisation measurement for the 4hrs pre-corroded carbon steel in MEG solution are shown in Figure 9-5 and Figure 9-6. The results for the 4hrs pre-corroded carbon steel in MEG show that the presence of the iron carbonate on the surface helps in the reduction of the final corrosion rate in the presence of 50% MEG. The final corrosion rate for the tested 4hrs pre-corroded sample in the 50% MEG solution averaged 0.35mm/y. The corrosion rate did not reduce drastically as expected since the initial corrosion rate of the pre-corroded carbon steel was already low. This may be that there is not much support from the

MEG solution in retaining the iron carbonate crystals already formed on the surface of the pre-corroded sample.

On the other hand, the result for the 4hr pre-corrosion test in the presence of 80% MEG shows a higher reduction in the corrosion rate. The average corrosion rate achieved in presence of 80% MEG was 0.06mm/y. This was lower than half of the corrosion rate achieved for the 4hr test in the presence of MEG alone on polished samples. This reduction in corrosion rate may give an idea of the interaction of the high concentration MEG on the pre-corroded sample. The increase in the resistance of the pre-corroded sample is also expected as higher concentration of MEG at low temperature gives a corresponding low corrosion rate on polished samples as compared to lower MEG concentration [53, 77, 87, 108]. The much higher resistance achieved with the 4hrs pre-corroded sample in 80% MEG as compared to the resistance of polished samples in 80% MEG may be due to lower solubility of the iron carbonate at 80% MEG solution.
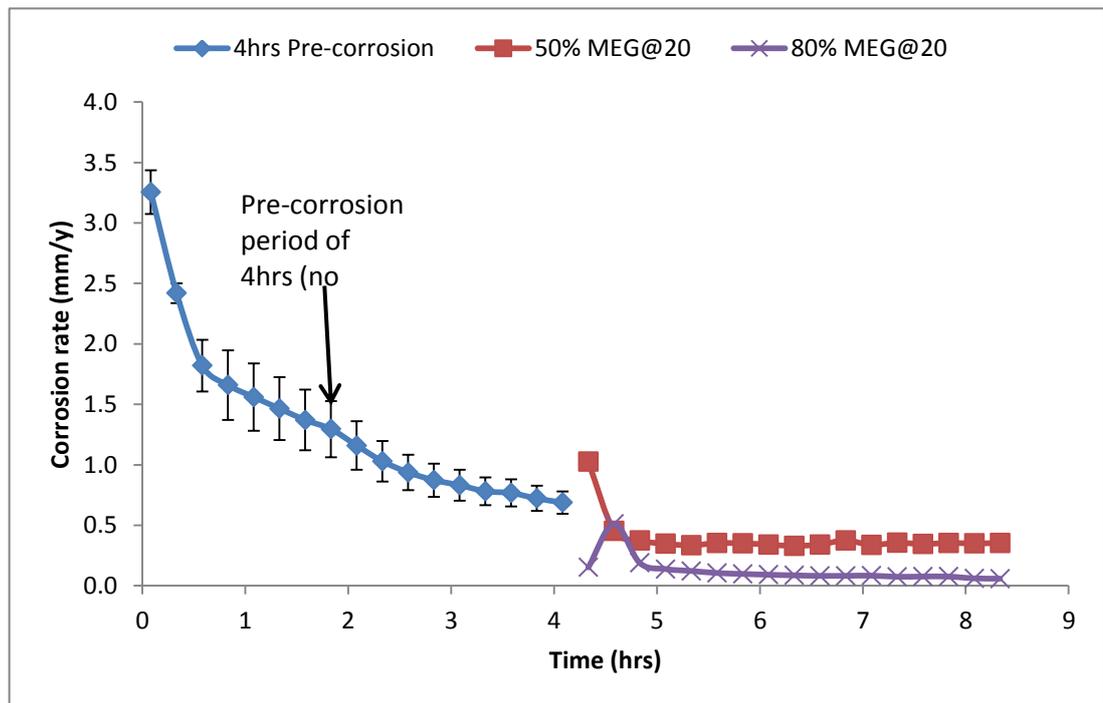
Figure 9-5 : Results of corrosion rate of 4hrs pre-corrosion at 80°C and of 4hrs pre-corroded sample in the presence of 50% MEG and 80% MEG at 20°C.

The results for the 4hrs pre-corroded at 80°C in the presence of MEG for 4hrs shows that the presence of iron carbonate on the surface helps in the reduction of the final corrosion slightly. The corrosion rate for test of the 4hrs pre-corroded carbon steel 50% MEG solution shows a final average value of 1.75mm/y. This high corrosion rate is attributed to high corrosion rate of carbon steel in 50% MEG solution as was observed for polished carbon steel in MEG in chapter 5. The lack of adequate protective iron carbonate film on the surface was critical to the high corrosion rate. Generally high temperature always gives higher corrosion rate where no protective iron carbonate is formed.

The corrosion rate for 4hrs pre-corroded samples in 80% MEG solution at 80°C had an average final corrosion rate of 0.44mm/y. The final corrosion rate was almost the same with the final corrosion rate of the polish samples in 80% MEG solution at 80°C. It shows that reduction of corrosion rate at high temperature in the presence of MEG may not be achieved without forming a protective iron carbonate film on the surface.
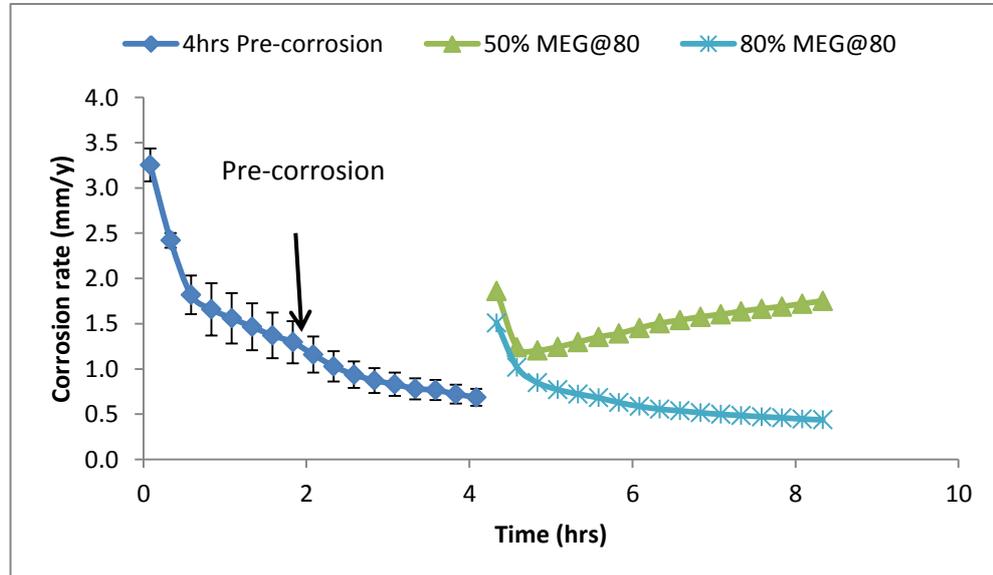
Figure 9-6 : Results of corrosion rate of 4hrs pre-corroded at 80°C and of 4hrs pre-corroded sample in the presence of 50% MEG and 80% MEG at 80°C.

The comparison of results as shown in Figure 9-7 shows that 4hrs pre-corroded samples tested at 20°C were all lower than the 4hrs pre-corroded samples tested at

80°C. This is an indication that the presence of iron carbonate on the surface of the sample at this condition is not enough to reduce the corrosion rate at 80°C when compared to the corrosion rate at 20°C. The reduction in corrosion rate is attributed mostly to the concentration of MEG at lower temperature. The effect of MEG on the iron carbonate crystals formed on the pre-corroded surface needs to be examined to understand more on this area. A discussion of this point will be made further in the discussion chapter of the work.
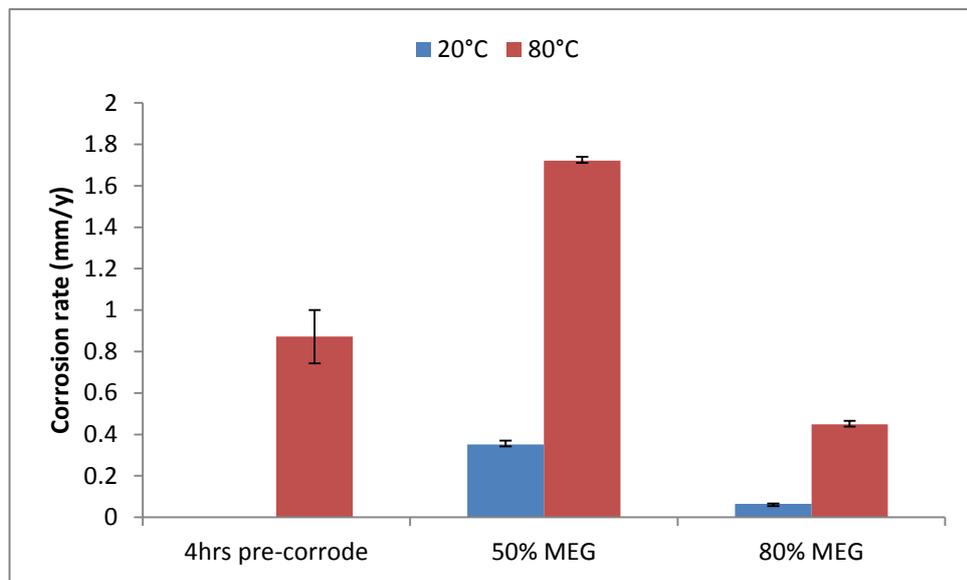
Figure 9-7 : Comparison of corrosion rate of 4hrs pre-corrosion at 80°C and 4hrs pre-corroded sample in the presence of 50% MEG and 80% MEG at 20°C and 80°C.

Tests for the 24hrs pre-corroded samples were also performed in the presence of MEG of different concentration and at different temperature. The results of the test for the 24hrs pre-corroded samples and 50% MEG solution at low temperature of 20°C shows an increase in the resistance of the pre-corroded sample. The average final corrosion rate of the 24hrs pre-corroded samples was 0.06mm/y. This was a massive increase compared to the result for the 4hrs pre-corroded samples test. This may be due to the more protective layer of iron carbonate formed after the 24hrs test as compared to the 4hrs test pre-corrosion.

Results for the 24hrs pre-corroded carbon steel samples in the presence of 80% MEG at 20°C showed also an increase in the resistance of the carbon steel. This increase in the resistance was observed in the corrosion rate of the 24hrs pre-corroded carbon steel sample that reduces to a final average rate of 0.04mm/y. The reduction in the corrosion rate is an indication of the contribution from the protective iron carbonate coverage and the effect of MEG concentration on the solution.
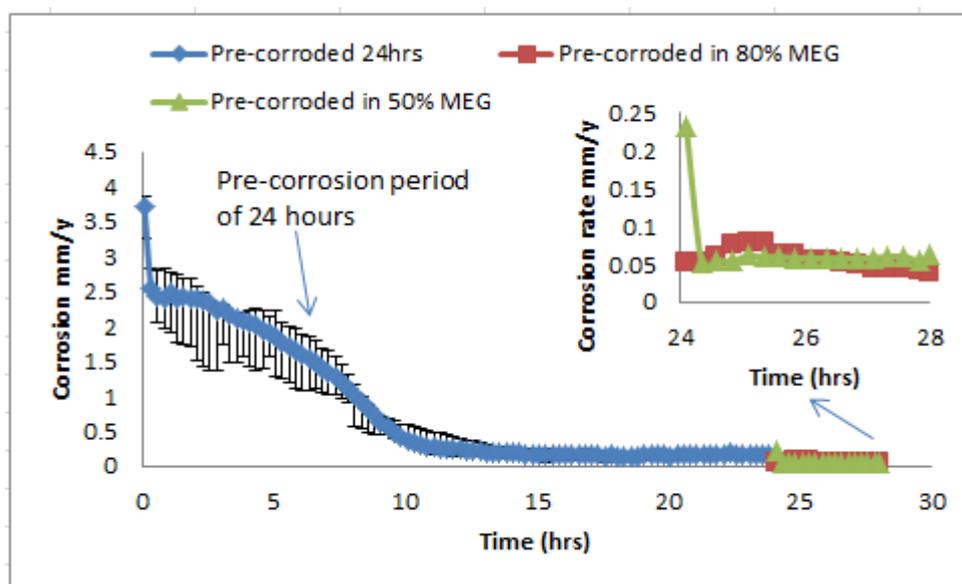
Figure 9-8 : Results of corrosion rate of 24hrs pre-corrosion at 80°C and 24hrs pre-corroded sample in the presence of 50% MEG and 80% MEG at 20°C

The results for test on 24hrs pre-corroded carbon steel samples in MEG solution at 80°C is shown in Figure 9-9. At higher temperature of 80°C, the results for the 24hrs pre-corroded carbon steel sample in 50% MEG and 80% MEG both gave a corrosion rate which was low compared to the corrosion rate of polished samples in MEG shown in chapter 5. At 80°C The average final corrosion rate for the 24hrs pre-corroded carbon steel sample in 50% MEG solution was 0.82mm/y while the corrosion rate of the 24hrs pre-corroded carbon steel sample in 80% MEG was 0.35mm/y. The result also highlighted the contribution of the protective iron carbonate scale in the reduction of corrosion rate in the presence of MEG.
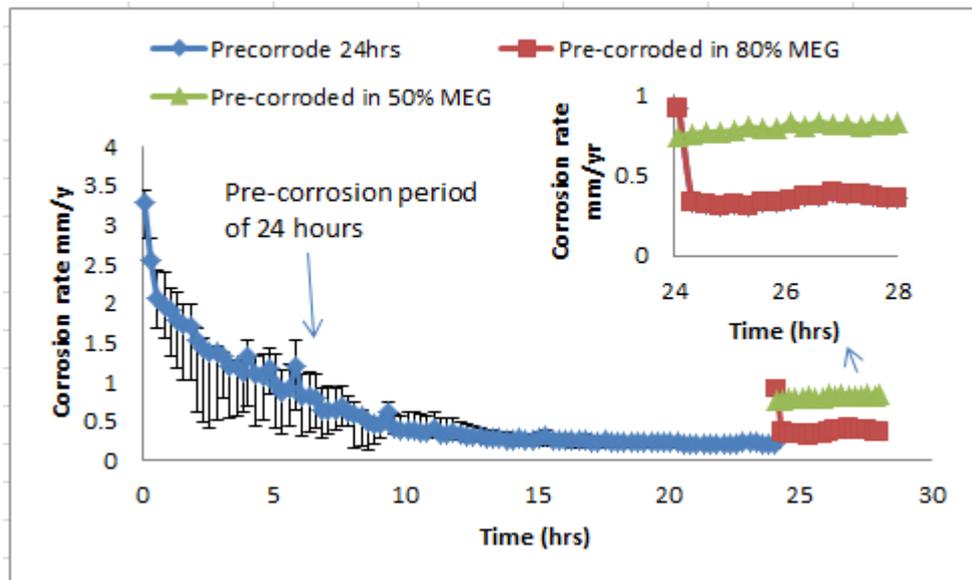
Figure 9-9 : Results of corrosion rate of 24hrs pre-corrosion at 80°C and 24hrs pre-corroded sample in the presence of 50% MEG and 80% MEG at 80°C.

A comparison of the corrosion rate of the 24hrs pre-corroded carbon steel sample in high and low temperature is shown below in Figure 9-10. At low temperature of 20°C, the corrosion rate of the 24hrs pre-corroded carbon steel samples for both MEG concentration tested were lower than that at high temperature of 80°C. This shows that the corrosion rate at high temperature in the presence of MEG does not decrease below the values at low temperature even in the presence of pre-corroded carbon steel with protective iron carbonate film. The high increase shows that if there is no formation of iron carbonate film the corrosion rate of carbon steel in the presence of MEG solution is likely to be high.

Another important observation from the result is that the corrosion rate of the higher MEG concentration of 80% is always less than that of the 50% MEG corrosion rate. These result support the result of the 4hrs pre-corrosion that shows that the test with 50% MEG solution has a higher corrosion rate compared to the test with 80% MEG solution. This value is in line with the results of the corrosion rate for polished carbon steel samples in the presence of MEG concentration where the corrosion rate of the polished carbon steel samples reduces at higher MEG concentration. The use of higher MEG concentration at high temperature also showed that the corrosion rate was lower compared to lower MEG concentration for the 24hrs pre-corrosion. This

214

result is also in line with the results from the 4hrs pre-corrosion test with 50% MEG solution and 80% MEG solution. The polished samples corrosion rate as seen in the previous chapter also shows the same trend when 50% and 80% MEG solution were used.
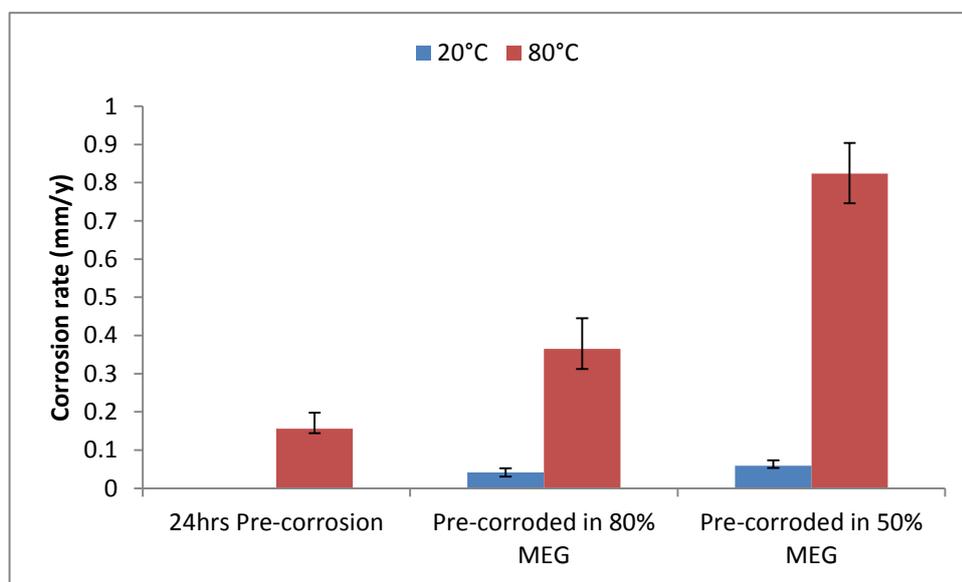
Figure 9-10 : Comparison of corrosion rate of 24hrs pre-corrosion at 80°C and 24hrs pre-corroded sample in the presence of 50% MEG and 80% MEG at 20°C and 80°C.

9.4. Surface analysis

As previously discussed, the electrochemical measurements usually give an idea of the corrosion rate on the carbon steel sample. The use of scanning electron microscopy (SEM) was employed to identify the possible mechanism involved in the corrosion of pre-corroded carbon steel in the presence of MEG. Formation of protective corrosion product such as iron carbonate can easily be determined by the use of SEM.

9.4.1. Scanning Electron Microscopy (SEM)

The tested samples from the 4hrs pre-corroded test in 50% MEG solution and 80% MEG solution were all kept in the desiccators prior to the surface analysis. For the SEM test, the first part of the pre-corroded carbon steel samples used for the SEM

test were those carbon steel pre-corroded for the 4 hour in the 50% and 80% MEG. The results for all the 4hrs pre-corroded sample in both 50% and 80% MEG at 20°C and 80°C are shown in Figure 9-11. The SEM results for the 4hrs pre-corroded carbon steel sample tested in 50% MEG solution at 20°C shows that the corrosion products previously formed on the surface of the samples had a change in morphology. The $FeCO_3$ crystals shape which was previously spherical and rounded was observed to be changing to a distorted and fluffy shape on the surface of the carbon steel. This may be that the crystals particles are dissolving in the presence of the new solution it was tested on (i.e. MEG solution without pH increase). Likewise, the lowering of the initial temperature for the formation of the iron carbonate in the 4hrs pre-corrosion was also another factor which may also increase the solubility. As describe by de Waard et al. [67] the formation of iron carbonate on the surface of the carbon steel is made possible at scaling temperature which are always very high. Bearing in mind that the 20°C is below the scaling temperature, the formation of iron carbonate scale can only be possible if the MEG solution encourage the build-up of this crystal at this low temperature condition. From the results shown, it can be deduced that the 50% MEG solution has little contribution in promoting the growth of the formed iron carbonate crystal at this condition.

SEM image results for the 4hrs pre-corroded carbon steel sample in 80% MEG at 20°C shows also a distorted corrosion product on the surface of the carbon steel. The distorted crystals were less fluffy than those of the 4hrs pre-corroded carbon steel sample in 50% MEG test. This may be an indication of a slower increase in the solubility and dissolution of the iron carbonate in the presence of 80% MEG. This may mean that this concentration of MEG at low temperature does not increase the solubility of the iron carbonate very quickly. It does not however mean that the MEG helps in build-up of the structure and shape of the iron carbonate effectively. At this lower temperature condition, the lack of well-formed iron carbonate crystal on the surface of the 4hrs pre-corroded carbon steel in MEG means that MEG has less influence on the growth of the formed iron carbonate crystal at this condition.

The reduction in the stability and crystallization of the iron carbonate on the surface of the 4hrs pre-corroded carbon steel in the presence of MEG may be an indication that the presence of MEG at these concentrations may not be enough to encourage

the growth of iron carbon crystals. This observation was pronounced in the presence of 50% MEG solution as compared to the 80% MEG solution where the protective iron carbonate was less distorted.
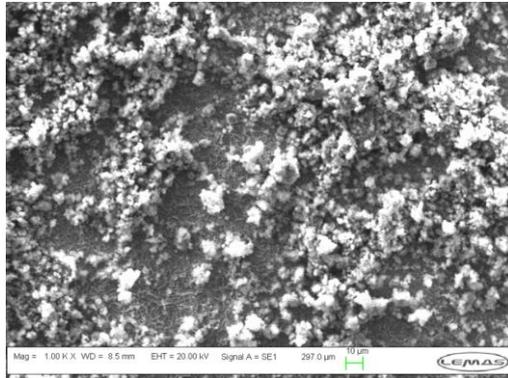
(a)
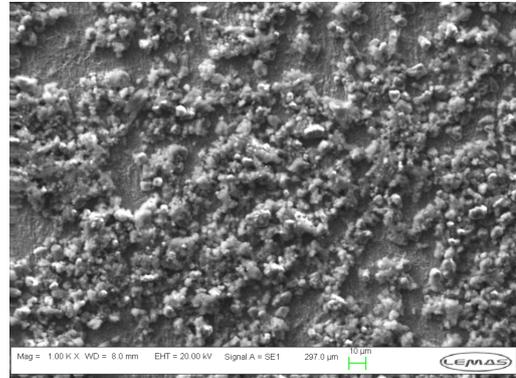
(c)
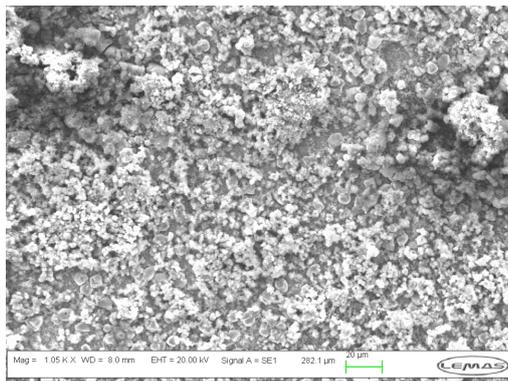
(b)
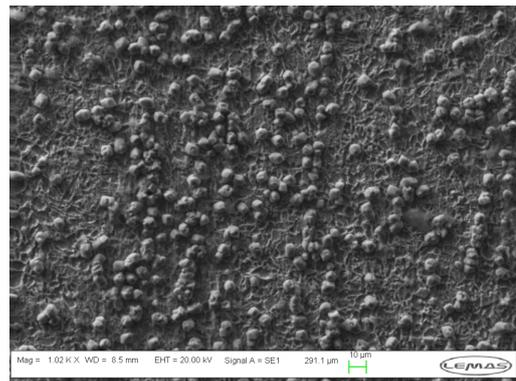
(d)
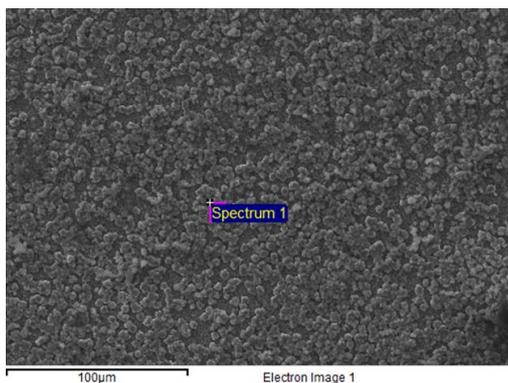
(e)

Figure 9-11 : SEM images of 4hrs pre-corroded carbon steel sample after 4 hours test in (a) 50% MEG (b) 80% MEG at 20°C and (c) 50% MEG (d) 80% MEG and (e) 4hrs pre-corroded carbon steel at 80°C.

This may be one of the reasons why the 4hrs pre-corroded carbon steel tested in the presence of 80% MEG solution had a higher resistance to corrosion than that tested in the presence of the 50% MEG solution.

The SEM image for the 4hrs pre-corroded carbon steel sample in 50% MEG at high temperature of 80°C shows little or no distortion on the corrosion product on the surface of the carbon steel. This maybe that the 50% MEG at this high temperature were able to support the stabilization of the corrosion product (i.e. iron carbonate) on the surface of the 4hrs pre-corroded sample.

The SEM image for the 4hrs pre-corroded carbon steel sample in 80% MEG at high temperature of 80°C shows even no distortion on the corrosion product on the surface of the carbon steel except for lesser iron carbonate coverage on the surface as compared to the original 4hrs pre-corroded carbon steel sample. The iron carbonate crystals were all in shape and a bit larger than the initial iron carbonate crystals formed on the surface carbon steel sample.

Furthermore, SEM result also indicates that the growth and stabilization of the iron carbonate on the surface of the 4hrs pre-corroded samples in the presence of MEG solution is enhanced by higher concentration of MEG. The higher the concentration the more likely iron carbonate crystals will grow and be stabilized on the surface of the 4hrs pre-corrosion carbon steel. This is in agreement with the result of LPR since the growth and stabilization of the iron carbonate results in less corrosion rate.

The SEM image for the 24hrs pre-corroded carbon steel sample in 50% MEG and 80% MEG are shown in Figures 9-12. The SEM for the 24hrs pre-corroded carbon steel sample in 50% MEG at high temperature of 80°C shows no distortion on the corrosion product (i.e. iron carbonate) on the surface of the carbon steel. The surface though had less iron carbonate on the surface as compared to the 24hrs pre-corrosion test surface shown in the previous chapter. This stability and growth of the iron carbonate on the surface indicates that the solubility of the iron carbonate does not reduce at this temperature and MEG concentration. There may be lack of formation of more iron carbonate as the pH and iron concentration is lower in the solution with 50% MEG as compared to initial solution for pre-corrosion. The crystals on the surface increased in sized as compared to the crystals on the surface of the initial pre-corrosion without MEG. This indicates that there may be less nucleation

occurring in the presence of MEG within the stated condition. The stability of this iron carbonate crystal may lead to better protection due to coverage of the carbon steel from corrosion species. This surface coverage contribution by the iron carbonate film is seen in the reduction of the corrosion rate of pre-corroded carbon steel in MEG as compared to corrosion rate of polished samples in MEG where there was no iron carbonate coverage on the surface. The MEG solution encourages the growth and stability of the iron carbonate at this temperature and hence a better protection of the carbon steel.
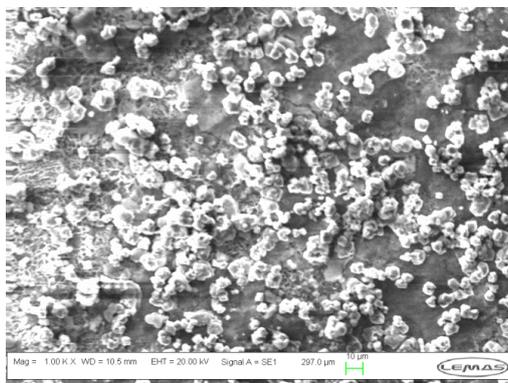
(a)
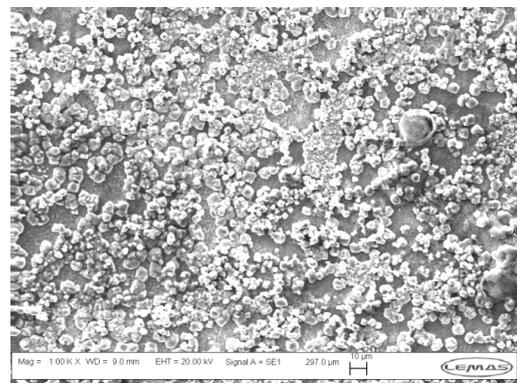
(b)
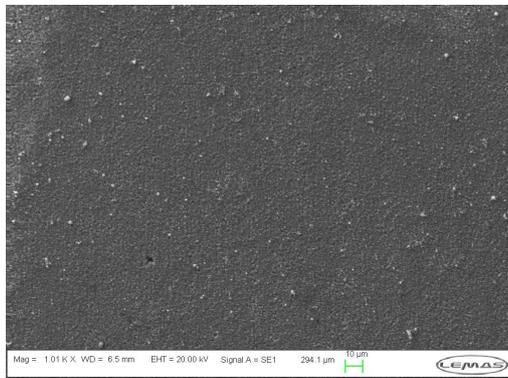
(c)

Figure 9-12 : SEM images of 24hrs pre-corroded carbon steel sample after 4 hours test in (a) 50% MEG (b) 80% MEG and (c) 24hrs pre-corroded carbon steel sample at 80°C .

SEM image for the 24hrs pre-corroded carbon steel sample in 80% MEG at 80°C shows no distortion on the corrosion product (i.e. iron carbonate) on the surface of

the carbon steel except for lesser corrosion product on the surface as compared to the previous 24hrs pre-corrosion test on the carbon steel alone. The iron carbonate crystal size increased as compared to the size of iron carbonate crystal on the initial carbon steel. This may be as a result of less nucleation occurring at this condition. The crystals tend to merge together to form larger crystals on the surface of the carbon steel as larger crystals are observed. This stability and growth of the iron carbonate leads to the preservation of most of the iron carbonate covering to reduce corrosion rate in the presence of 80% MEG solution.

9.5. Open Circuit Potential (OCP) measurement for pre-corroded carbon steel in the presence of MEG and corrosion inhibitors

The result of some selected OCP measurement for pre-corroded steel samples in the presence of MEG and the inhibitors are presented here. Figure 9.13 and Figure 9.14 shows the OCP changes for the test of pre-corroded sample in the presence of MEG and the inhibitors. The result of the OCP for the 4hrs pre-corroded carbon steel sample at 20°C shows a massive increase in the OCP immediately the pre-corroded samples were introduced into the MEG solution and inhibitors. The increase was more for the 10ppm inhibitor 2 than for 10ppm inhibitor 1. Both results showed an increase as compared to samples in blank solutions which were higher. This is an indication that there is a formation of protective layer on the surface of the pre-corroded sample [8].

The combination of the inhibitor with the MEG solution ennobles the OCP at the initial point and this later drop to a more active value which was still higher than the pre-corroded sample OCP. For the 80% MEG solution and inhibitor, the OCP was even higher than that of the 50% MEG solution with inhibitor at the initial point. The final average value of the OCP from the result shows a value more than -500mV for both concentrations of inhibitors and 80% MEG. On the other hand the final average value of the OCP for 50% MEG and the inhibitor 1 was lower than -600mV but the OCP value was higher than -600mV for the inhibitor 2. The higher increase in OCP for the inhibitor 2 may suggest that the corrosion rate will be lower

at 20°C.   It may be that the inhibitor 2 is quite efficient at lower temperature in the presence of MEG even for pre-corroded sample.
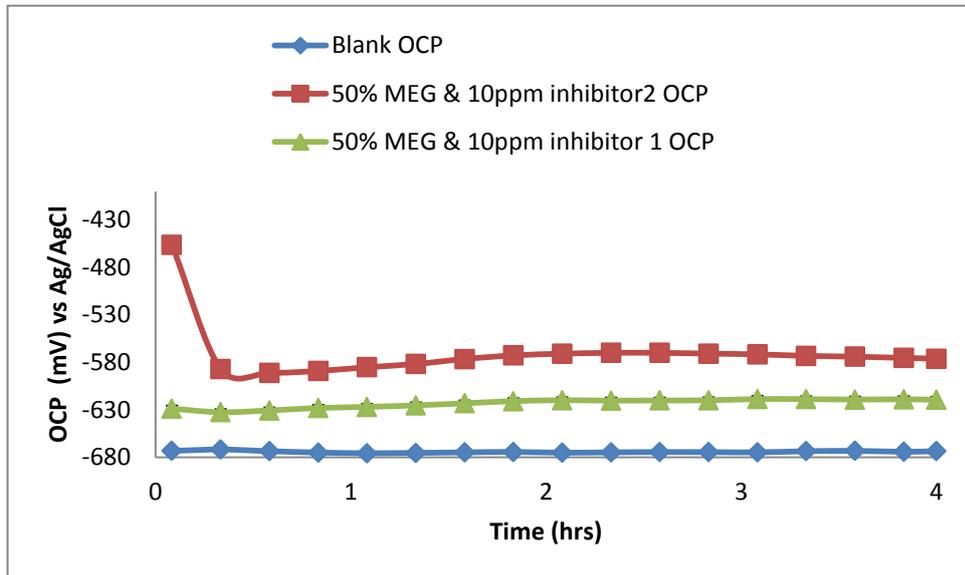
Figure 9-13 : OCP measurement for blank solution (i.e. polished sample), and for 4hrs pre-corroded sample in the presence of 50% MEG solution with 10ppm inhibitor 1 and 10ppm inhibitor 2 at 20°C.
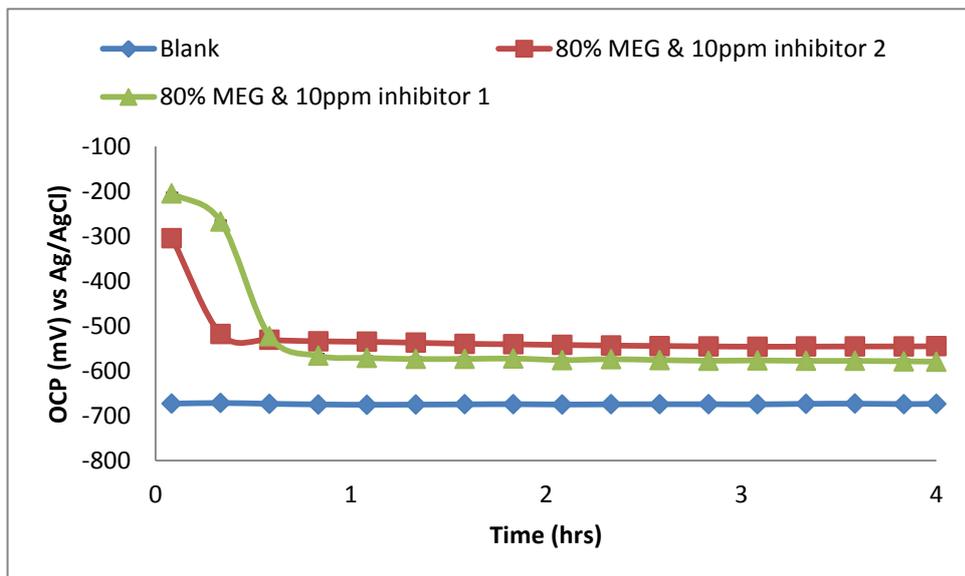
Figure 9-14 : OCP measurement for blank solution (i.e. polished sample) and for 4hrs pre-corroded sample in the presence of 80% MEG solution with 10ppm inhibitor 1 and 10ppm inhibitor 2 at 20°C.

Figure 9-15 and Figure 9-16 shows the OCP values of the pre-corroded samples in MEG and the inhibitors at 80°C
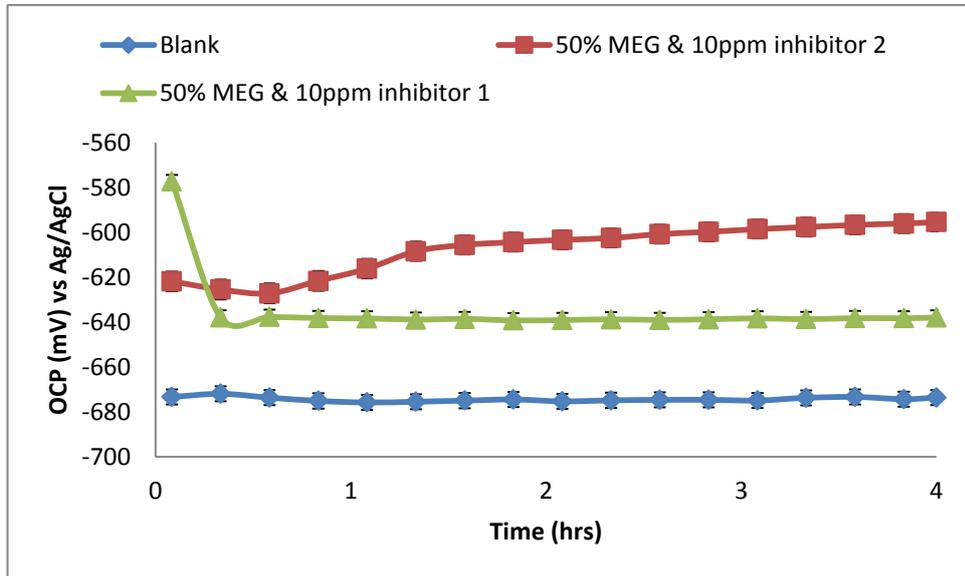
Figure 9-15 : OCP measurement for blank solution (i.e. polished sample) and for 4hrs pre-corroded sample in the presence of 50% MEG solution with 10ppm inhibitor 1 and 10ppm inhibitor 2 at 80°C.
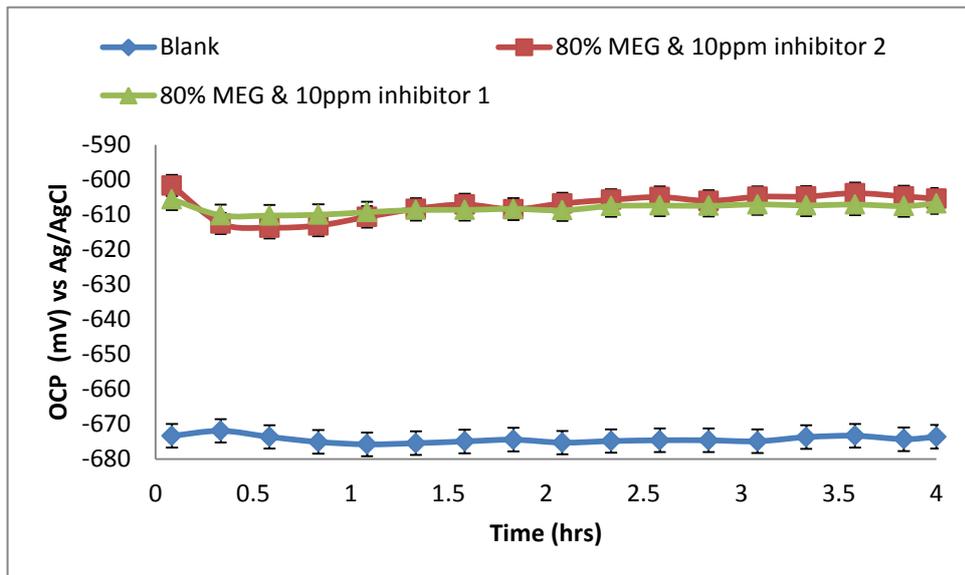
Figure 9-16 : OCP measurement for blank solution (i.e. polished sample) and for 4hrs pre-corroded sample in the presence of 80% MEG solution with 10ppm inhibitor 1 and 10ppm inhibitor 2 at 80°C.

For higher temperature, the result of the OCP value showed the same trend with that of the lower temperature. There was a reduction though in the OCP values for that at higher temperature compared to that at lower temperature

9.6. Linear Polarization Resistance (LPR) measurement for pre-corroded sample in MEG and inhibitor

The results for the 4hrs pre-corrosion in the presence of MEG and inhibitor 1 for 4hrs at 20°C and 80°C is shown in Figure 9-17. The results showed a reduction of the corrosion rate of the pre-corroded sample in the presence of MEG and inhibitor 1 at 20°C was more than the reduction in corrosion rate at 80°C. All the corrosion rate with the use of inhibitor 1 showed were lower than the corrosion rate obtained for pre-corrosion alone.

The results for the 4hrs pre-corrosion in the presence of MEG and inhibitor 2 for 4hrs at 20°C and 80°C is shown in Figure 9-18. The use of MEG and inhibitor 2 on the other hand showed more reduction in the corrosion rate of the pre-corroded sample at both high and lower temperature as compared to that of MEG and inhibitor 1 on the pre-corroded sample. This reduction is attributed mainly to the MEG and inhibitor at low temperature since no further iron scale was formed at that condition in this test.

The results for the 24hrs pre-corrosion in the presence of MEG and inhibitor 1 for 4hrs at 20°C and 80°C are shown in Figure 9-19. The results surprisingly showed a reduction of the corrosion rate of the pre-corroded sample in the presence of MEG and inhibitor 1 at 80°C was more than the test result at 20°C. This is an indication that the reduction is due to the presence of a protective and well-formed iron carbonate scale, MEG and the inhibitor rather the MEG and inhibitor alone. It may also be an indication that the inhibitor 1 may also be very efficient at high temperature and in the presence of iron carbonate film.
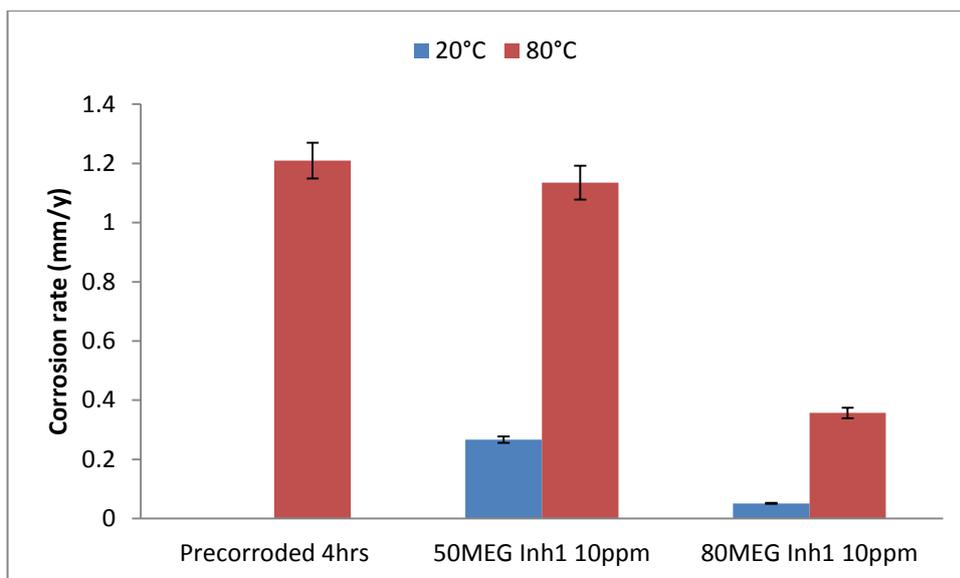
Figure 9-17 : Final corrosion rate measurement for 4hrs pre-corroded sample in 50% MEG and 80% MEG solution with 10ppm inhibitor 1 at 20°C and 80°C.
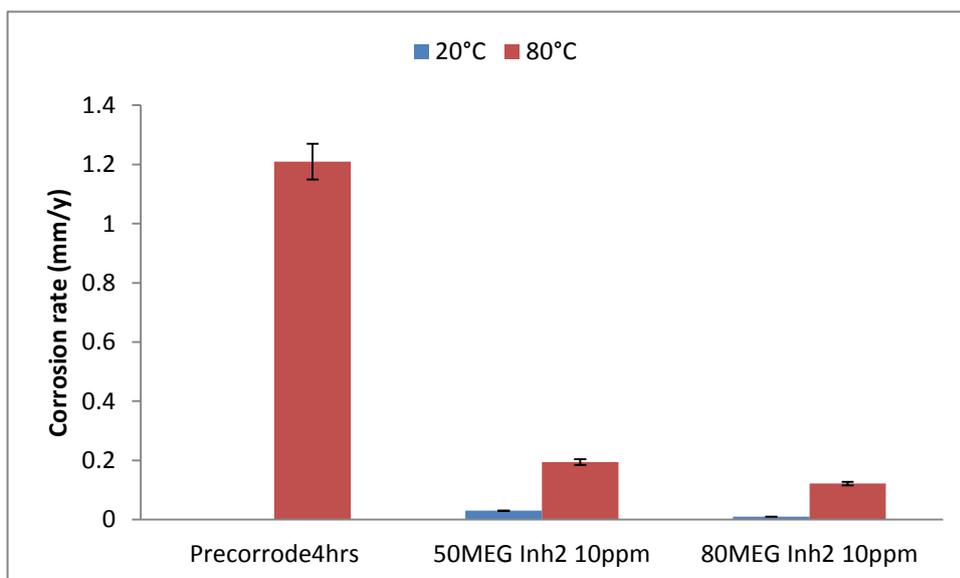
Figure 9-18 : Final corrosion rate measurement for 4hrs pre-corroded sample in 50% MEG and 80% MEG solution with 10ppm inhibitor 2 at 20°C and 80°C.

The results for the 24hrs pre-corrosion in the presence of MEG and inhibitor 2 for 4hrs at 20°C and 80°C are shown in Figure 9-20. The result also showed a reduction in the corrosion rate of the pre-corroded sample at lower temperature and high temperature. This is an indication that the reduction is due to the presence of a

protective and well-formed iron carbonate scale, MEG and the inhibitor rather the MEG and inhibitor alone. It was observed though that the reduction in corrosion rate at 20°C was lower than that at 80°C with the use of MEG and inhibitor 2. The reduction in corrosion rate was also higher at 80% MEG than at 50% MEG.
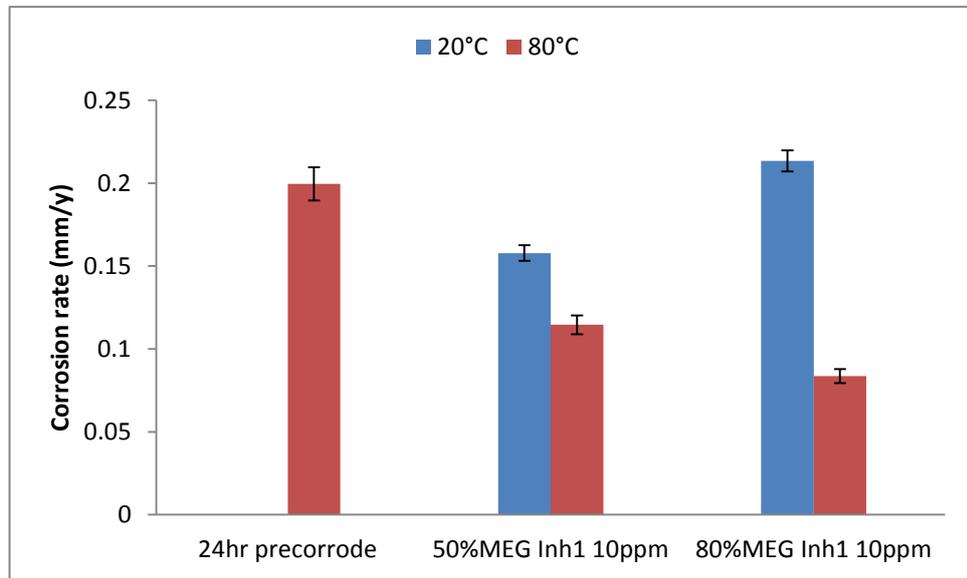
Figure 9-19 : Final corrosion rate for 24hrs pre-corroded sample in 50% and 80% MEG solution with 10ppm inhibitor 1 at 20°C and 80°C.
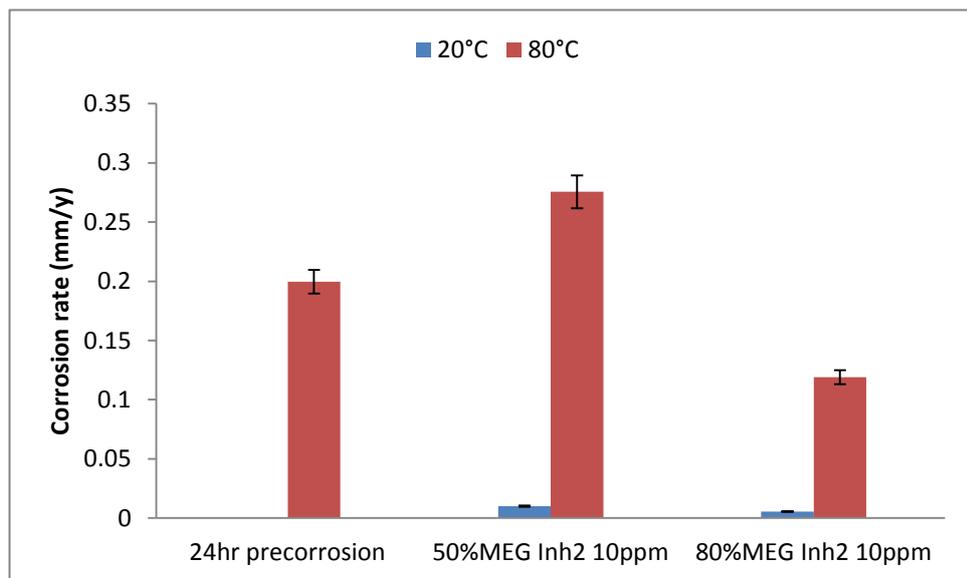
Figure 9-20 : Final corrosion rate for 24hrs pre-corroded sample in 50% and 80% MEG solution with 10ppm inhibitor 2 at 20°C and 80°C.

A further test at 20°C and 80°C with 100ppm inhibitor 1 were performed for 24hrs pre-corroded sample. These tests were performed to determine if the synergist effect of iron carbonate and inhibitor 1 are consistence for pre-corroded carbon steel with iron carbonate. Previously presented results of lower concentrations of inhibitor 1 suggested a synergist effect with pre-corroded carbon steel unlike the antagonist effect observed for polish carbon steel. The results are shown in Figure 9-21. The results showed that at low and high temperature, 100ppm inhibitor1 was able to reduce the corrosion rate below 0.1mm/y for both MEG concentrations.
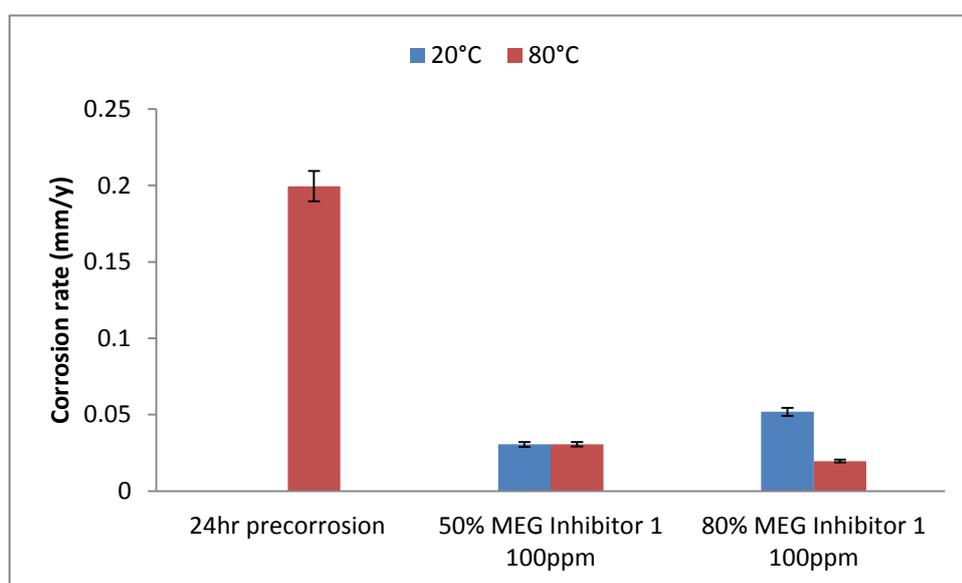
Figure 9-21: Final corrosion rate for 24hrs pre-corroded sample in 50% and 80% MEG solution with 100ppm inhibitor 1 at 20°C and 80°C.

9.7. Surface analysis

The surface analysis was carried on the pre-corroded samples tested in the presence of MEG and inhibitor to determine how the all affect the carbon steel sample. It may also give an idea on possible formation of localised corrosion on the surface of the pre-corroded sample. The effect of the MEG and inhibitor on the formation and stability of the iron carbonate was also observed using this surface analysis.

9.7.1. Scanning Electron Microscopy (SEM)

The SEM image of some of the tested pre-corroded samples in the presence of MEG and the inhibitors are shown in Figure 9-22. The results from the SEM images at low temperature of 20°C showed that the use of MEG and 10ppm inhibitor 1 had most of the iron carbonate still on the surface with a few point of detachment which may lead to localised corrosion especially in the presence of 80% MEG. The use of 10ppm inhibitor 1 may not be able to prevent localised corrosion on the surface of the pre-corroded sample. The SEM image for 10ppm inhibitor 2 was also able to prevent localised corrosion on the surface of the pre-corroded sample even as there were fewer iron carbonate crystals on the surface of the pre-corroded sample. This may mean a good combination of MEG and 10ppm inhibitor 2 but also a negative effect on the formation iron carbonate film.

(a) (c)

(b) (d)
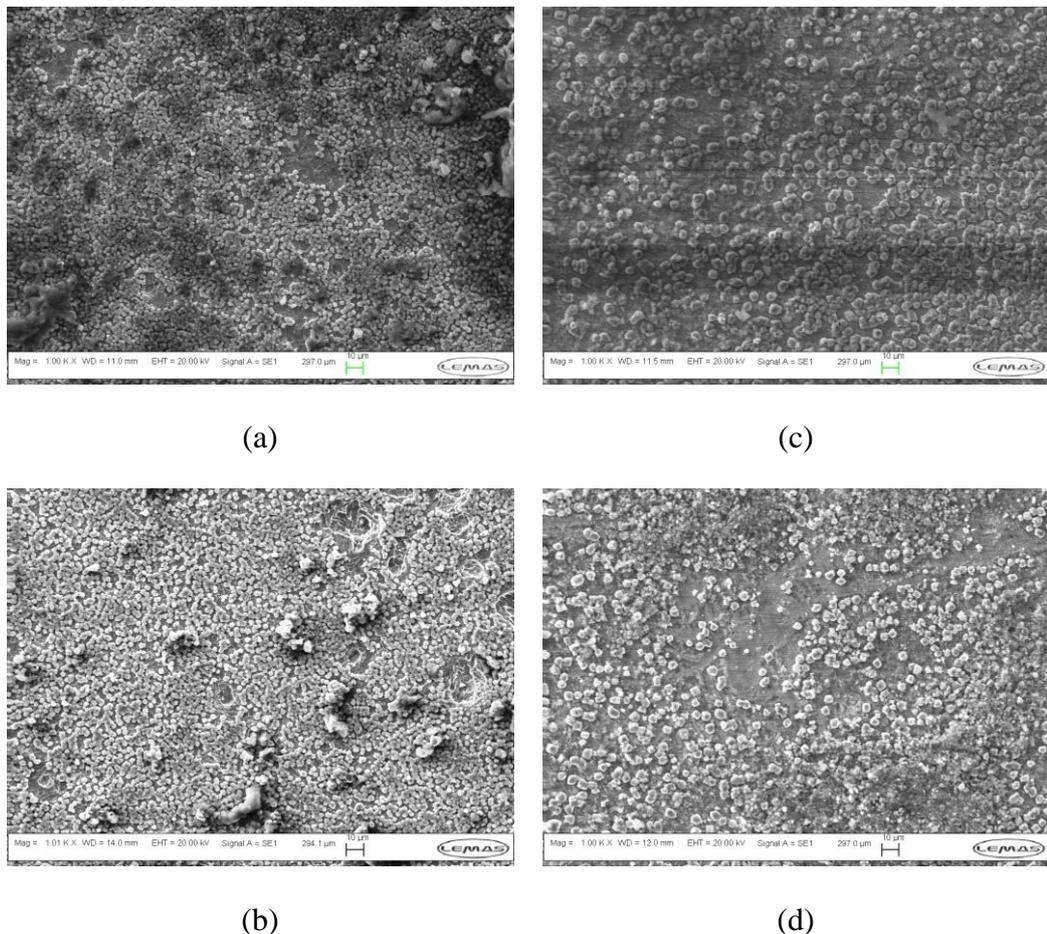
Figure 9-22 : SEM images of 24hrs pre-corroded carbon steel sample after 4 hours test in (a) 50% MEG with 10ppm inhibitor 1 (b) 80% MEG with 10ppm inhibitor 1 at 20°C and (c) 50% MEG with 10ppm inhibitor 2 (d) 80% MEG with 10ppm inhibitor 2 at 20°C.

The results for the SEM image at 80°C are shown in Figure 9-23. The results from the SEM images at this high temperature of 80°C showed that the use of MEG and 10ppm inhibitor 1 may not be able to prevent localised corrosion. The results showed that the iron carbonate may have detached in some point on the surface of the carbon steel. This may again lead to possible localised corrosion on the surface even as the general corrosion rate is being reduced. The same was also seen for MEG and 10ppm inhibitor 2 at the high temperature where the iron carbonate may have also detached with some sign of localised corrosion on the surface of the pre-corroded sample.


(a)

(c)

(b)

(d)
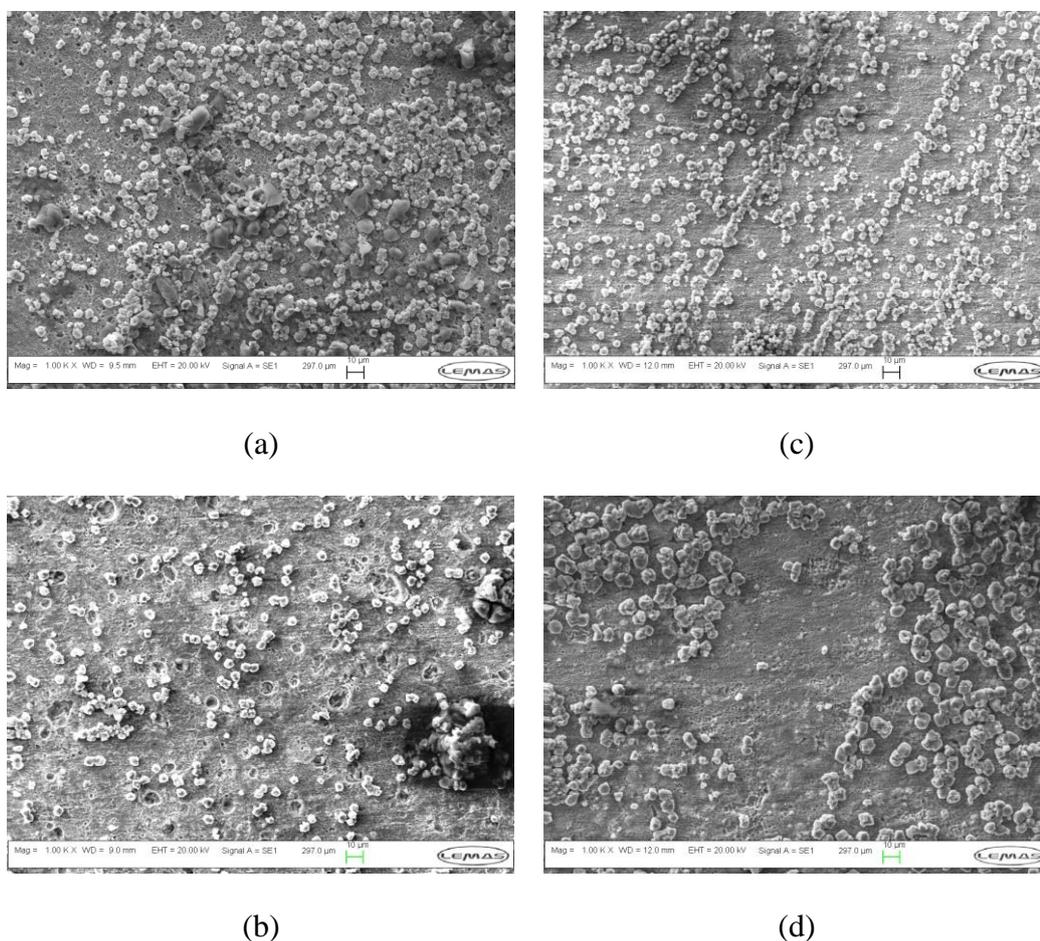
Figure 9-23 : SEM images of 24hrs pre-corroded carbon steel sample after 4 hours test in (a) 50% MEG with 10ppm inhibitor 1 (b) 80% MEG with 10ppm inhibitor 1 at 80°C and (c) 50% MEG with 10ppm inhibitor 2 (d) 80% MEG with 10ppm inhibitor 2 at 80°C

At this temperature the concentration of the inhibitors is not enough to protect the carbon steel from localised corrosion due to possible change in minimum inhibitor concentration with temperature. Higher concentration of both inhibitors may be required to prevent localised corrosion at this temperature. Although the corrosion rate may have gone down, the surface of the carbon steel still was not adequately protected from localised corrosion.

SEM results for 100ppm inhibitor 1 are shown in Figure 9-24. The image showed that the inhibitor was able to stabilize the iron carbonate in 50 % and 80% MEG for both low and high temperature.

(a)   (c)

(b)   (d)
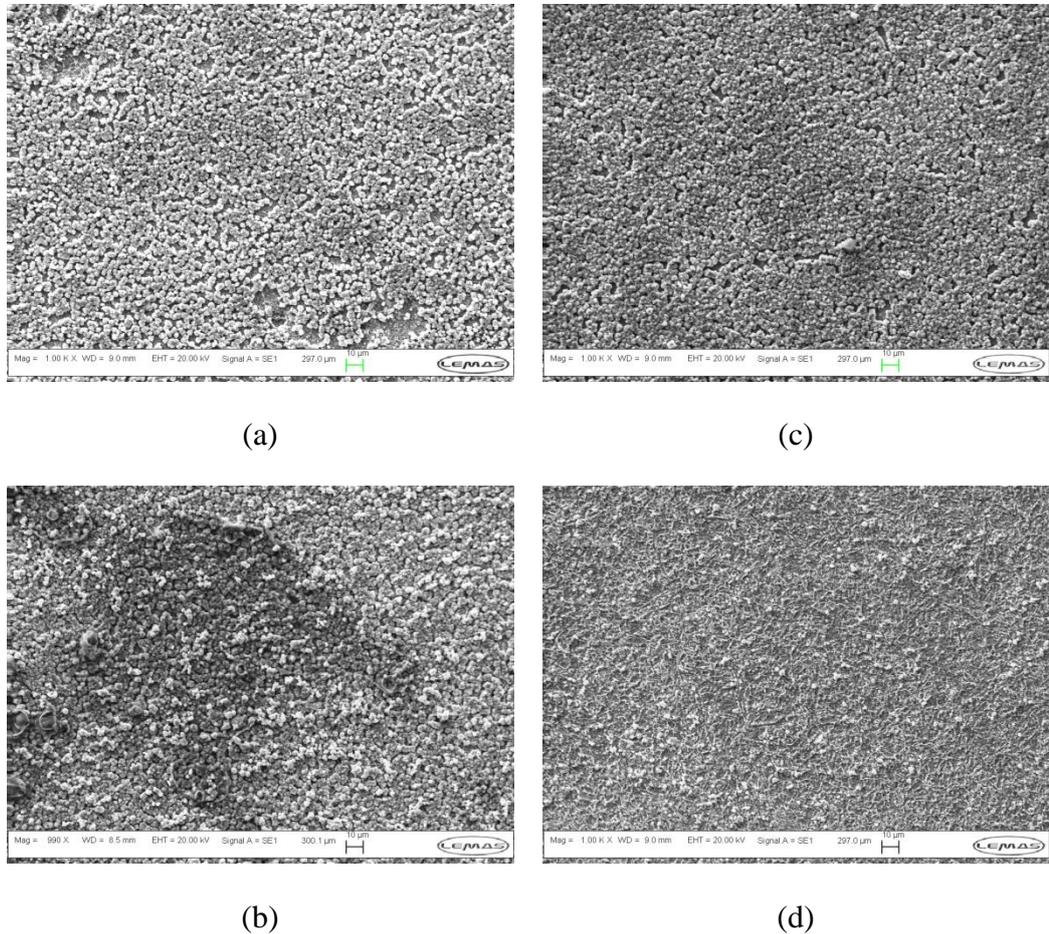
Figure 9-24 : SEM images of 24hrs pre-corroded carbon steel sample after 4 hours test in (a) 50% MEG with 100ppm inhibitor 1 (b) 80% MEG with 100ppm inhibitor 1 at 20°C and (c) 50% MEG with 100ppm inhibitor 1 (d) 80% MEG with 100ppm inhibitor 1 at 80°C.

The 50% MEG and 100ppm inhibitor 1 showed more stability of the iron carbonate crystals. There were no sign of localised corrosion as seen for the lower concentration of 10ppm inhibitor 1 and MEG. This shows that 100ppm inhibitor is able to protect the surface of the pre-corroded carbon steel in the presence of both MEG concentrations. This is in line with the electrochemical test results that showed very low corrosion rate for 100ppm inhibitor 1 with different MEG concentration for the pre-corroded carbon steel.

9.8. Summary of result and discussion of corrosion process in the presence of iron carbonate scale (pre-corrosion), MEG and organic corrosion inhibitors

This chapter described the result of pre-corroded carbon steel in the presence of MEG with the two inhibitors used. It can be summarised as follows

- The formation of protective $FeCO_3$ scale/film helps to reduce the corrosion rate in the presence of MEG at high temperature.

- MEG influences the growth of iron carbonate scale/film at 80 °C with more influence at higher concentration of MEG.

- MEG does not encourage the growth of iron carbonate scale at 20 °C as irregular shape and fluffy crystals of $FeCO_3$ scale are formed.

- The use of adequate inhibitor can reduce the corrosion of carbon steel in the presence of iron carbonate and MEG

- The presence of protective & thick iron carbonate will further reduce the corrosion rate of carbon steel in the presence of MEG with inhibitor (i.e. 24hrs test).

- Inhibitor 2 in general performs better with MEG than inhibitor 1 both at high and low temperature and can effectively reduce the corrosion rate.

- Surface analysis showed that there may be formation of pits with inhibitor 1 and MEG on pre-corroded sample at high temperature and low concentration of 10ppm.

- 100ppm inhibitor 1 in MEG solution was able to protect the pre-corroded carbon steel at both high and low temperature.

Chapter 10. GENERAL DISCUSSION

10.1. Introduction

The study has been carried out in order to investigate corrosion of carbon steel in the presence of MEG at both high and low temperature. The tests carried out were for both polished and pre-corroded carbon steel. DC and AC electrochemical methods were employed to derive information regarding the corrosion mechanisms and the corrosion rate. Surface analysis was also used to aid the determination of the mechanism of corrosion involve in the presence of MEG. The general discussions based on the results presented are given below. The discussions are presented based on the following three major points.

   i.   MEG as a corrosion inhibitor

  ii.   Interactions between MEG and corrosion inhibitors and

 iii.   Industrial relevance

10.2. MEG as a corrosion inhibitor

10.2.1. Effect of concentration

Results presented in chapter 5 have shown that MEG concentration plays a major role in the corrosion of carbon steel. From the results, it was seen that the OCP of both polished and pre-corroded carbon steel in the presence of MEG solution showed an increase compared to the OCP of blank solution. The increase was more for higher mass concentration of 80% MEG than that of 50% MEG. This is an indication that higher concentration of MEG will reduce the iron activities and, hence, corrosion rate of carbon steel.

If the change in potential is assumed to be due to a change in the activity of the iron, the change in potential in the presence of MEG is given as the change in the half-cell potential as

$$\Delta \emptyset = \emptyset°_{corr} MEG - \emptyset°_{corr} Blank = \Delta \emptyset_{Fe^{2+}/Fe} \qquad \text{10-1}$$

Where $\emptyset°_{corr}MEG$ and $\emptyset°_{corr}Blank$ is the OCP for the MEG and blank solution respectively and $\Delta\emptyset_{Fe^{2+}/Fe}$ is the change in the potential of the anodic half-cell.

Using the Nernst equation modified to calculate the potential of a cell as presented in equation 2-19, then Equation 10-1 will become

$$\Delta\emptyset_{Fe^{+2}/Fe} = [\emptyset°_{Fe^{2+}/Fe} + \frac{RT}{nF} \ln \frac{(Fe^{2+})}{(Fe)_{MEG}}] - [\emptyset°_{Fe^{2+}/Fe} + \frac{RT}{nF} \ln \frac{(Fe^{2+})}{(Fe)_{Blank}}] \qquad \text{10-2}$$

Where (Fe_{MEG}) and (Fe_{Blank}) is the activity of iron in MEG solution and activity of iron in blank solution respectively. Equation 10-2 can be express further as

$$\Delta\emptyset = \frac{RT}{nF} \ln \frac{(Fe)_{Blank}}{(Fe)_{MEG}} \qquad \text{10-3}$$

If $(Fe)_{Blank}$ activity is taken to be 1 and n the number of electrons participating in the corrosion reaction of Fe involves 2 electrons, then equation 10-2 is simplified to:

$$\Delta\emptyset = \frac{RT}{2F} \ln \frac{1}{(Fe)_{MEG}} \qquad \text{10-4}$$

Deriving $\Delta\emptyset$ from the result of the OCP of MEG and blank, the activity of iron in the presence of MEG is calculated and presented in Table 10-1.

Table 10-1 : Iron activity in the presence of MEG

	Temperature (°C)	50% MEG	80% MEG
$(Fe)_{MEG}$	20	0.0678	0.0013
$(Fe)_{MEG}$	80	0.2063	0.0373

The table showed that as the concentration of MEG increased from 50% to 80% MEG, the iron activity is reduced from 0.0678 to 0.0013 at 20°C. Similar reduction

was also observed at 80°C. The reduction in the iron activity is taken as a reduction in the anodic reaction and hence the corrosion rate [8]. Figure 10-1 shows a schematic description of the change in the OCP in the presence of MEG.
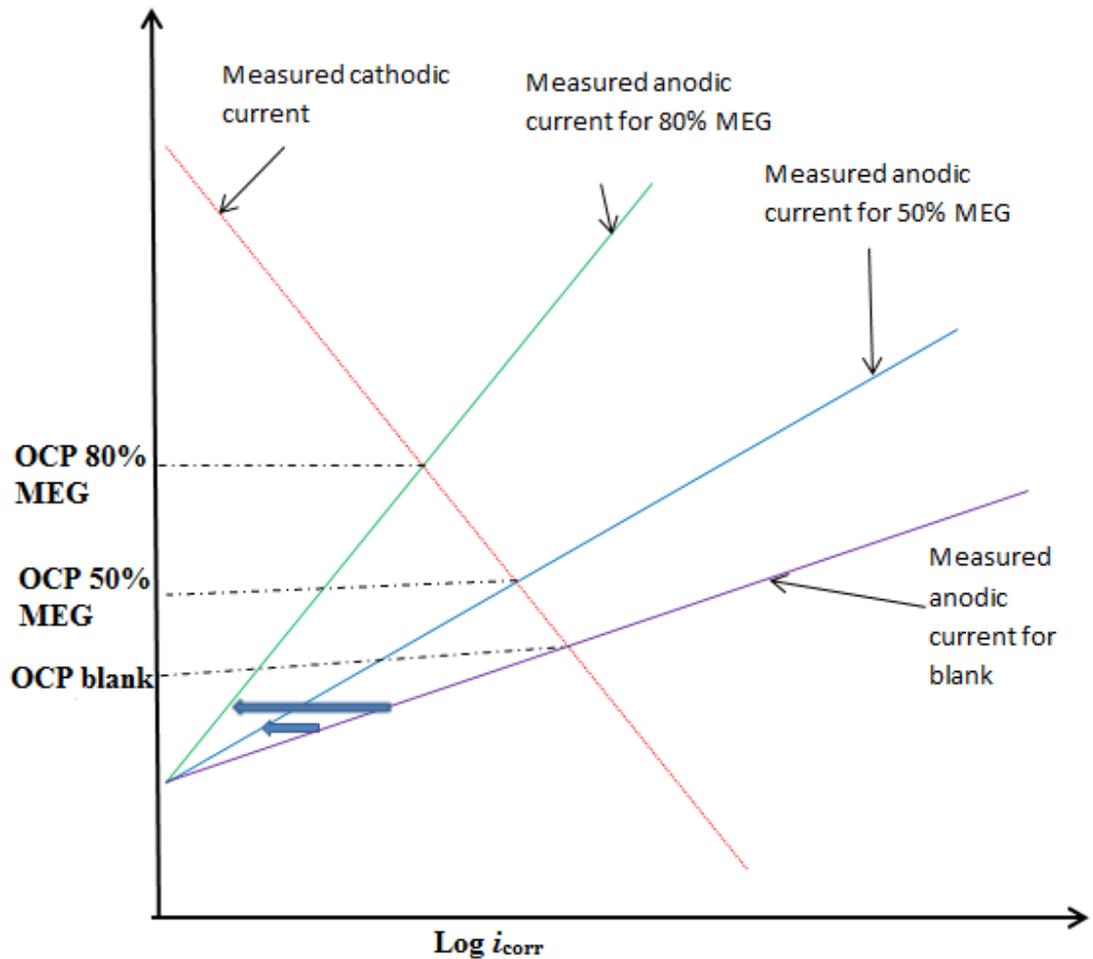
Figure 10-1 : Schematic diagram representing change in the OCP of blank to a nobler OCP in the presence of 50% MEG and 80% MEG due to reduction of the anodic current in both MEG solutions.

AC impedance measurement also showed the effect of concentration of MEG on the corrosion of carbon steel. The corrosion impedance for 80% MEG was much higher than that of 50% MEG concentration at both low and high temperature. This shows that concentration has a lot of influence on MEG as a corrosion inhibitor. Higher MEG concentration will always give a higher reduction in the corrosion rate of carbon steel. This is in line with studies by de Waard et al [53, 67] that gave a relationship where higher concentration of MEG reduces the corrosion rate. Other

Authors [77, 87, 112] also had similar relation where higher concentration of MEG gave a higher reduction in corrosion rate.

The LPR results showed higher reduction in the corrosion rate of the carbon steel in the presence of the 80% MEG than the 50% MEG content. This is in line with the reduction effect of the OCP. Test with 20% MEG concentration as seen in Figure 5-14 through Figure 5-17, showed reduction in the corrosion rate was less than that for 50% MEG and 80% MEG concentration. It can also be seen from the results that the efficiency for lower concentrations of MEG was very low compared to higher mass concentration. This effect is observed more at higher temperature where the corrosion inhibition efficiency of the 20% MEG was around 14% while that of 40% MEG mass was around 64% at the same high temperature of 70°C. The efficiency of MEG in reducing corrosion rate at lower concentration reduces drastically. Consequently, lower concentration of MEG can be said to be inactive as a corrosion inhibitor and may function only as a hydrate inhibitor. In order to achieve a corrosion inhibition of 50% or more at temperature higher than 20°C, A minimum concentration of 30% MEG is required in the system. It then means that concentration below 30% MEG may not be sufficient in reducing the corrosion rate of carbon steel at temperature above 20°C although they may serve as hydrate inhibitor in the system.

10.2.2. Effect of pre-corrosion

The effect of MEG on corrosion inhibition can be influenced by pre-corrosion where iron carbonate films are formed on the surface of the sample. Corrosion control by MEG has been shown to be more effective at lower temperature with polished samples as can be seen from results of the AC impedance and LPR measurement. This trend also is seen for corrosion rate in the presence of pre-corroded carbon steel where iron carbonate films are already formed on the surface. The presence of iron carbonate however affects the corrosion inhibition of MEG in low and high temperature as well.

OCP results for the pre-corroded sample in the presence of MEG at low temperature were high at initial point as seen in Figure 9-1 and Figure 9-3. This is an illustration that there is non-conductive layer coverage on the metal surface which does not

allow for a full spontaneous contact of the electrolyte to the surface. These always give a potential difference nobler than the potential difference for polished carbon steel electrode. With the viscosity of MEG obviously higher than water [87, 101], the solution species are bound to move slowly towards the metal surface. After a 4 hour period, the OCP value fluctuated to a lower value than the initial start value. This value was still higher than the OCP value of the blank solution. The 50% MEG test record a final average of -626mV while the 80% MEG test recorded a final average of -556mV. This higher OCP values shows that there is reduction in the anodic reaction due to the additional influence of iron carbonate. This reduction in the OCP was more than the reduction of OCP for polished samples. This indicates an additional influence due to the iron carbonate formed on the surface. The OCP results at a higher temperature of 80°C showed that there was also an increase in the OCP values for both 50% MEG and 80% MEG solution as compared to the blank OCP. This increase showed that there was also a reduction in the activities of iron in the presence of MEG. The reduction in the iron activities at this temperature is expected to be lower as the OCP increase was not as large compared to the OCP increase at 20°C temperature. This was also seen for the polished samples where the OCP for MEG solution did not increase much compared to the OCP of blank solution. The increase in OCP of MEG solution in the presence of pre-corrosion was however more than that for MEG solution in the presence of polished sample. This again may be an indication that corrosion inhibition of MEG increases in the presence of iron carbonate.

Results for the LPR measurement for 4hrs pre-corrode carbon steel in the presence of MEG shown in Figure-9-5 and Figure 9-6 showed that the corrosion rate is reduced more due to the additional effect of the iron carbonate on the surface. This reduction is more noticeable for higher temperature test where the corrosion rate reduces more. This shows a synergistic effect with the iron carbonate on the surface of the carbon steel. Dugstad and Dronen [86] in their study used sodium bicarbonate to increase the pH of MEG containing solution to 6.5. They argued that formation of iron carbonate on X65 carbon steel surface reduces the corrosion below 0.1mm/y for test above 40°C. The reduction in the corrosion however was not observed at 20°C due to lack of protective iron-carbonate film on the X65 carbon steel at that low

temperature. 24hr pre-corrosion samples tested in the presence of MEG at both low and high temperature showed reduction in corrosion rate due to protective iron carbonate formation. The corrosion rate at both low and high temperature for both 50% MEG and 80% MEG was higher for polished carbon steel as compared with that on 24hr pre-corroded carbon steel in the presence of MEG. A description of the effect of pre-corrosion on the reduction of corrosion is shown in Figure 10-2 with more reduction in corrosion achieved in the presence of iron carbonate through pre-corrosion.
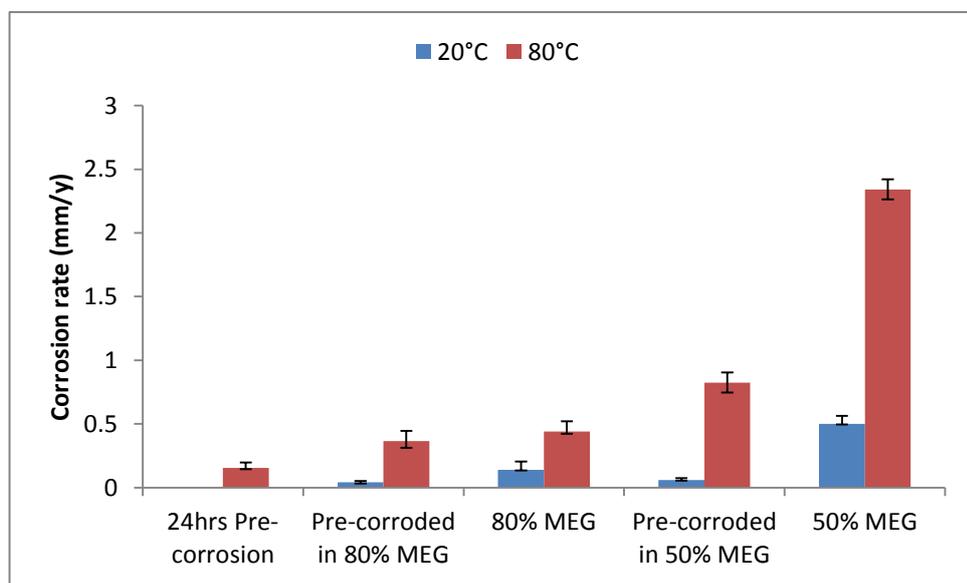
Figure 10-2 : Comparison of corrosion rate for polished samples in MEG and 24hrs pre-corroded samples in MEG.

In this study, corrosion rate for the 24hrs pre-corrosion alone was, lower than that for all tests conducted with pre-corroded carbon steel in the presence of MEG at 80°C. This may be due to lack of additional initiation and formation of more iron carbonate layer on the surface of the pre-corroded sample in the presence of MEG. The solution for tests on the pre-corroded carbon steel in the presence of MEG had a reduce pH of 4.2 to 4.6 with no additional Fe^{2+} to increase the super-saturation of iron carbonate in the solution, while during the 24hr pre-corrosion, there was addition of Fe^{2+} and the pH increased to around 7. This may have led to the increased corrosion rate at 80°C. Another reason is the reduced efficiency of MEG at

237

high temperature which made the corrosion rate at that point to be less than that for pre-corrosion alone.

SEM images for the pre-corroded samples tested in the presence of MEG at lower temperature of 20°C showed that the iron carbonates were still present after the 4 hours test, but the crystal shape had become fluffy. The change in shape of the crystal was due to the decrease in the pH and temperature, thereby, making the iron carbonate crystals more soluble in the solution. The dissolution process changes the shape of iron carbonate crystals in a certain order, where the appearance of a fluffy shape indicates instability of the crystals as described by Shindo and Kwak [191]. Watterud et al. [116] observed that iron carbonate solubility reduces 1.5 times more at higher MEG concentration as previously described in chapter 3. They showed that the solubility product (K_{sp}) of iron carbonate in the presence of MEG decreases with temperature. However, the presence of the iron carbonate on the surface may have contributed to the reduction of the corrosion at the lower temperature, even as the crystal shape was changing. There was no sign of localised corrosion on visual inspection of the SEM image which was also the case on the polished sample. It may then mean that at lower temperature the pre-corroded carbon steel helps form a more protective surface with MEG as compared to polished carbon steel in the presence of MEG.

For a high temperature of 80°C, it was seen that iron-carbonate crystals formed for the 4hr pre-corroded carbon steel in MEG grew and were stable. This may mean that at this temperature MEG may be encouraging the growth of the crystal. The growth however did not prevent the surface from exhibiting general and localised corrosion which also occurred for the polished. This indicates that the reduction of corrosion in the presence of such film may lead to pitting if the surface is not well protected.

For the 24hrs pre-corroded carbon steel sample tested in MEG, the surface showed iron carbonate crystals also grew and were stable. The surface did not show signs of localised corrosion rather, it showed signs of general corrosion. This means that a thicker protective iron carbonate film will reduce the corrosion rate of the carbon steel more in the presence of MEG. This in line with LPR results that showed that 24hrs pre-corroded carbon steel led to more resistance to corrosion in the presence of MEG. It may be inferred that the formation of protective iron carbon during pre-

corrosion will reduce the corrosion rate more in the presence of MEG than for polished carbon steel. However, non-protective iron carbonate formed for pre-corroded surface may lead to the formation of localised corrosion in the presence of MEG.

10.2.3. Effect of temperature

Temperature plays a major role in the corrosion of carbon steel. At very high temperature, corrosion rate of carbon steel is generally high. This is because the corrosion species becomes more active and diffuses to the steel surface faster thereby, increasing the corrosion reaction at the surface [32, 34]. The use of MEG at different temperature is obviously affected by temperature. From the results presented for 50% MEG and 80% MEG at 20°C and 80°C, it was observed that the OCP value reduced at higher temperature of 80°C as compared to that at lower temperature 20°C. The effect of temperature on test in MEG was for all concentrations of MEG. The lower concentration of MEG was affected more by increase in temperature. This lower OCP value indicates that the corrosion activities increased at high temperature in the presence of MEG.

AC impedance results for both 50% MEG and 80% MEG showed that reduction in corrosion rate at 80°C was less than the reduction in the corrosion rate for 20°C. The reduction may be attributed to the increase in the diffusion of the corrosion species and also the increase in the conductivity of the MEG solution at higher temperature as seen from the conductivity result in Figure 5-8. AC impedance results showed that the solution resistance, which is an indication of the resistance to electron flow in the solution, was high at 20°C. Although at higher temperature of 80°C the solution resistance of the same solution reduces to more than a quarter of the value at 20°C. This is likely an indication that more electrons flows at higher temperature than at a lower temperature. Since the corrosion of the carbon steel involves oxidation of iron to produce electron, the flow of electron at higher temperature will likely increase the rate at which electrons are released from the iron as long as every other variable remain constant [24, 36, 67, 166].

The results of the conductivity test showed that the 50% MEG concentration solution had the highest conductivity of 8300 μS/cm at high temperature of 80°C

which reduces to 2350 µS/cm at lower temperature of 20°C. This shows how temperature can affect the conductivity in a solution of MEG. The reduction at low temperature indicates that the solution resistance which is inversely proportional to the conductivity will be affected with change in temperature. This will then cause an increase in the corrosion rate at higher temperature. The increase in the carbon steel corrosion for 50% MEG from 0.44mm/y at 20°C to 2.48mm/y at 80°C was quite high for it to be attributed mostly to increase in the conductivity. As can be seen from the results of conductivity in Figure 5-8, the conductivity of 50% MEG increase to about 8300 µS/cm which was still half the conductivity (i.e. 16000 µS/cm) for the blank solution at 20°C with a corrosion rate of 2.23mm/y. The conductivity of 80% MEG did not increased up to that for 50% MEG at 20°C, but still had a corrosion rate of up to 0.42mm/y that was similar to the corrosion rate of 50% MEG at 20°C (i.e. 0.44mm/y).   The increase in corrosion with temperature in the presence of MEG must not then be attributed only to the increase in the conductivity with temperature, but in addition to another mechanism of reaction.

The linear polarisation results also showed that increase in the temperature increases the corrosion rate in the presence of MEG. The corrosion resistance at 50% MEG and 80% MEG reduces at high temperature of 80°C as compared to that at 20°C. This increase was also seen for the LPR measurements results for lower concentration of MEG tested. The reduction in the efficiency of MEG from 20°C to 70°C for lower MEG concentration tested showed that MEG has a lower effect on corrosion rate as the temperature increase. This effect was even more with very low concentration of 20% MEG, where the efficiency of the MEG reduces from 48% at 20°C through to 14% at 70°C as shown in Table 5-3 through to Table 5-6. This reduction in the efficiency of the MEG shows that high temperature affects the ability of MEG to inhibit corrosion. The lesser the amount of MEG in the solution, the more temperature will impact negatively to the corrosion of the carbon steel.

SEM image for all the carbon steel samples at the high temperature of 80°C showed higher general corrosion than carbon steel samples at lower temperature. The SEM image for the sample tested in MEG solution showed general corrosion which indicates that MEG does not inhibit corrosion of the carbon steel effectively at a high temperature of 80°C. This shows that MEG does not form a permanent

protective film on the surface of the carbon steel at this high temperature. Carbon steel pipeline at high temperature need to be protected more from corrosion in the presence of MEG using additional means.

10.2.4. Mechanism of corrosion inhibition

The increase in OCP of the carbon steel in the presence of 50% MEG and 80% MEG at low temperature of 20°C showed that the use of MEG increases the resistance of MEG by mostly affecting the anodic reaction. The introduction of MEG at low temperature increased the OCP immediately. This means that MEG is surface active. Gulbrandsen and Morard [87] suggested that the reduction in the anodic current in the presence of MEG is due to changes in solution properties and to MEG adsorption. The use of MEG reduces the surface tension of the total solution, thereby, encouraging immediate film formation and adherence to the surface. This layer may be in the form of electrostatic attraction due to the OH group from MEG. It does not require high activation energy to form this type of film. The OCP for test with MEG reduces quickly showing that the reaction is very fast and instantaneous. This means that the activation energy for MEG to form a barrier over the carbon steel is low. This indicates a type of physical reaction or exothermic reaction which does not require input of energy [17, 24, 192]. The same result where the corrosion rate in MEG reduces rapidly was observed when LPR measurements were taken. This also confirms that MEG is surface active, with the effect seen more at lower temperature and higher concentration. This is similar to the work done by Wong and Park [157] with phosphate ester base inhibitor. This inhibitor had a rapid reduction effect on the corrosion rate of the carbon steel immediately it was introduce into the system.

The results from the AC impedance did not give any sign of formation of strong film on the surface of the carbon steel. The Nyquist plot in the presence of both 50% MEG and 80% MEG showed a single time constant in the exception of the unusual time constant due to high solution resistance. This means that any formation of film on the surface by MEG is porous and still allows corrosion species to proceed to the surface of the metal easily as described by Hong et al. [193] for porous film formation. The reduction in the corrosion resistance for MEG at higher temperature as seen from the AC impedance results in Figure 5-3 and Figure 5-5 means that

241

higher temperature reduces any protective coverage formed by MEG at high temperature. This indicates that the formation of film by MEG is through physical adsorption to the surface, which does not require high activation energy by increase temperature.

FTIR spectra at high temperature of 80°C did not detect any formation of films on the surface of the carbon steel after test with 50% MEG or 80% MEG. There was a lack of the OH group on the surface of the tested carbon steel which indicates a lack of strong chemical bond between MEG and the tested carbon steel. It is likely that MEG forms a protective layer through physical adsorption to the steel surface.

From the results of the enthalpy of adsorption of MEG, it was seen that MEG fits the adsorption isotherm of Temkin. In order to understand the mechanism behind the film formation, further results from the adsorption isotherm gave a heat of adsorption which was negative. The low values of the activation corrosion energy in the range of 25kJ/mol and 22kJ/mol is evidence of physical interaction with the carbon steel. This confirms that the film formed on the surface of the carbon steel was typical of a physical process and does not require high activation energy. The mechanism of formation of film on the surface of the carbon steel may be concluded to be through physisorption process rather than chemisorption process [138, 142]. Figure 10-3 describes the formation of film on the surface of carbon steel by MEG.
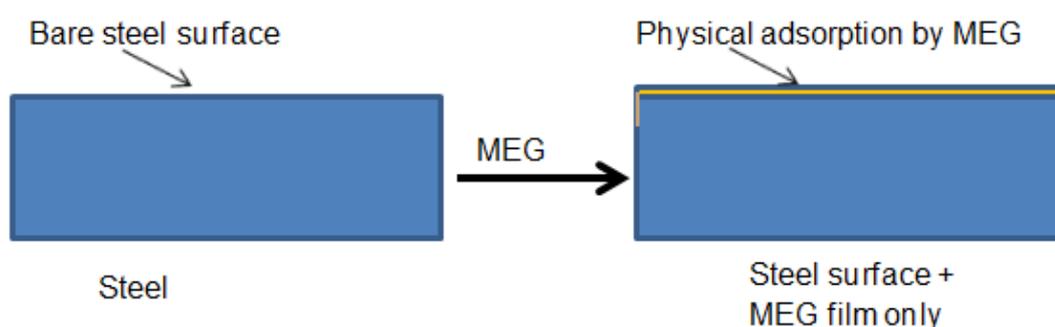
Figure 10-3 : Schematic description of physical adsorption by MEG on the surface of carbon steel.

This may be another reason why the efficiency of MEG reduces with increase in temperature. A combination of low solution polarity in the presence of MEG,

physical film barrier, and surface active nature of MEG and other properties of MEG, such as high viscosity, contribute to the reduction of corrosion rate of carbon. This corrosion inhibition character is prominent at higher concentrations and lower temperatures. At higher temperature however the corrosion rate in the presence of MEG tends to increase as the physical barrier becomes less effective since more corrosion species are able to penetrate the surface of the carbon steel.

10.2.5. de Waard's Model

The studies of de Waard et al. [53] were the first popular corrosion model to put the effect of MEG into consideration   [53]. Their studies used mostly data from corrosion rate performed at lower temperature of 20°C and 40°C by Veritec [53]. They developed an equation (i.e. equation 3-14) which has a satisfactory fit on the data from the Veritec report. The equation which was described in literature review chapter gave a correction factor which is used to multiply the corrosion rate derived from their model (nomogram). The result from the multiplier gave a worse case corrosion rate scenario for the system with MEG. Works on MEG by other authors [77, 87, 112] also were in agreement with de Waard correction factor, with most of them giving a corrosion rate just less than the corrosion rate from de Waard correction factor. This shows that the case for de Waard [53] was for a worst case scenario.

This study for low temperature also gave satisfactory results when compared with the results from the correction factor of de Waard et al. [53]. The results here all gave corrosion rate which were within range but lower than that of de Waard et al. This also makes the results of this particular study less conservative like those of the results of the other aforementioned authors. The worst case approach for de Waard is good for modelling situation where other variables and real field experience may change the actual corrosion rate. An example of a graph showing a comparison of de Waard correction factor and this study results for lower concentration of MEG at a low temperature of 20°C is shown in Figure 10-4. The results showed clearly that the corrosion rate for this studies were in line and less conservative than that of de Waard [53].
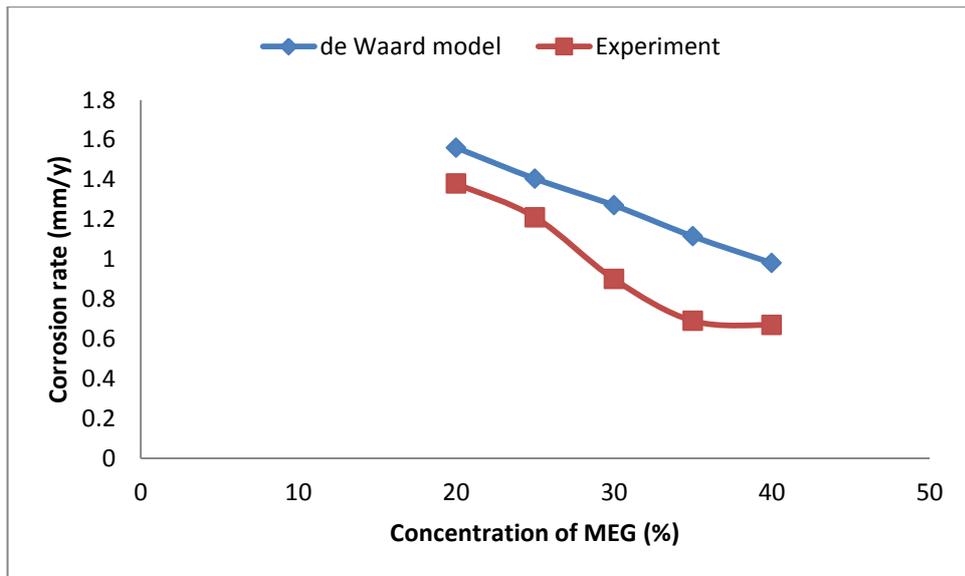
Figure 10-4 : Comparison of experimental corrosion rate results and de Waard correction corrosion value for different concentrations of MEG at 20°C.

For high temperature of 70°C and above, the results of this study has shown that some of the corrosion rate was higher than that derived from de Waard correction. A graph derived from the results previously presented is shown in Figure 10-5. The graph gave a comparison of de Waard correction factor and this study results for lower concentration of MEG at a higher temperature of 70°C. From the comparison it is clearly seen that at high temperature the corrosion rate increases in the presence of MEG. This is even more noticeable at lower concentration of 20% MEG where the corrosion rate was much higher than that for de Waard corrosion factor at that temperature. The increase in the corrosion rate as temperature increases clearly showed that higher temperature reduces the efficiency of MEG in reducing corrosion rate in a system. This increase in corrosion rate was not taken into consideration by de Waard et al. in deriving the equation for the correction factor. This is understandable, as most of the data used to derive the equation for correction factor was obtained at lower temperature below 40°C. Base on this fact, it may be concluded that the use of the de Waard corrosion factor should be applied for temperature of 40°C and below to still maintain the worst case approach of the correction factor in the model.
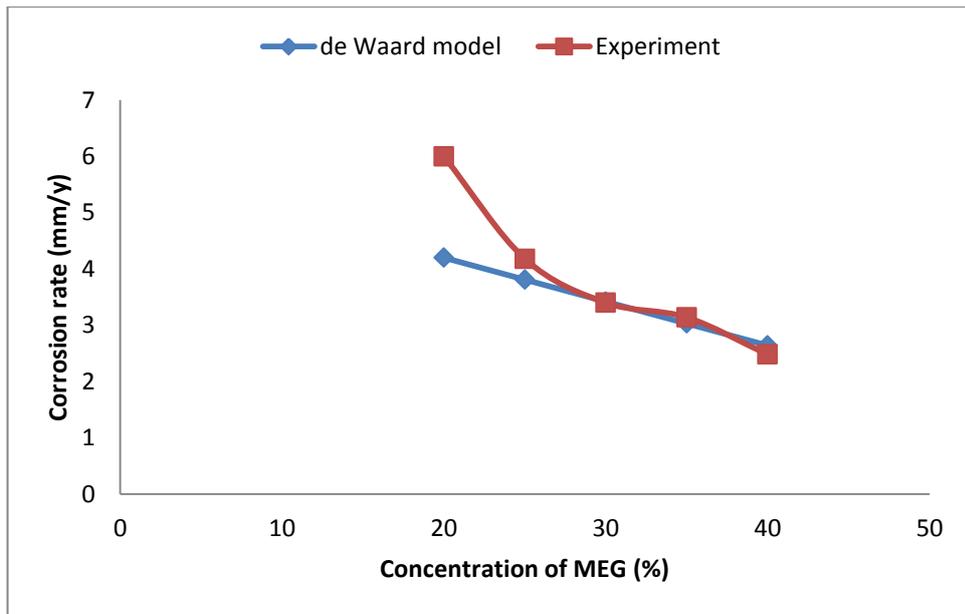
Figure 10-5 : Comparison of experimental corrosion rate results and de Waard correction corrosion value for different concentrations of MEG at 70°C

Results for higher temperature above 70°C are expected to give higher corrosion with the effect being more at lower concentrations. This effect tends to increase with temperature. The higher temperature gives more deviation from the corrected corrosion rate using de Waard correction factor result. Results for the 50% MEG and 80% MEG are also in agreement with the de Waard at lower temperature as previously described. These results also showed an increase in corrosion rate at higher temperatures of 80°C which were more for the 50% MEG concentration. Table 10-2 gives a comparison of the experimental corrosion rate results from this study with that of MEG at 50% and 80% concentration.

Table 10-2 : Comparison of the experimental corrosion rate value and the de Waard corrected corrosion rate for 50% MEG and 80% MEG solution

	50% MEG		80%MEG	
Temperature of Experiment	20°C	80°C	20°C	80°C
Experimental corrosion rate	0.44	2.40	0.14	0.48
de Waard Corrected corrosion rate	0.66	1.96	0.15	0.45

245

10.3. Interactions between MEG and corrosion inhibitors

10.3.1. Polished samples with no pre-corrosion

LPR measurement results in the presence of MEG and corrosion inhibitors showed that there was synergistic and antagonistic effect of adding an inhibitor to a MEG solution. The results showed that the corrosion resistance of 10ppm inhibitor 1 was adversely affected in the presence of MEG at low temperature. Adverse effect was observed with the use of inhibitor 1 in the presence of MEG. There was an increase in the corrosion rate for 10ppm inhibitor 1 with 50% MEG compared to the use of only 10ppm inhibitor 1. The corrosion rate for the carbon steel in 10ppm inhibitor 1 with MEG was more than the corrosion rate for 10ppm inhibitor 1 without MEG as previously shown in Figure 6-7. The reduction in the efficiency for the 10ppm inhibitor 1 in the presence of 50% MEG is calculated to be 36% even as the corrosion rate was lower than that for 50% MEG. The presence of MEG in the solution has hindered the inhibitor working effectively at that low concentration [124, 159]. The MEG forms a barrier which may not give access to the 10 ppm inhibitor 1 to reach the carbon steel surface since the concentration is low. Figure 10-6 and 10-7 shows the comparison of the final corrosion rate of both inhibitors with 50% MEG and 80% MEG concentration at 20°C derived from the result previously presented.
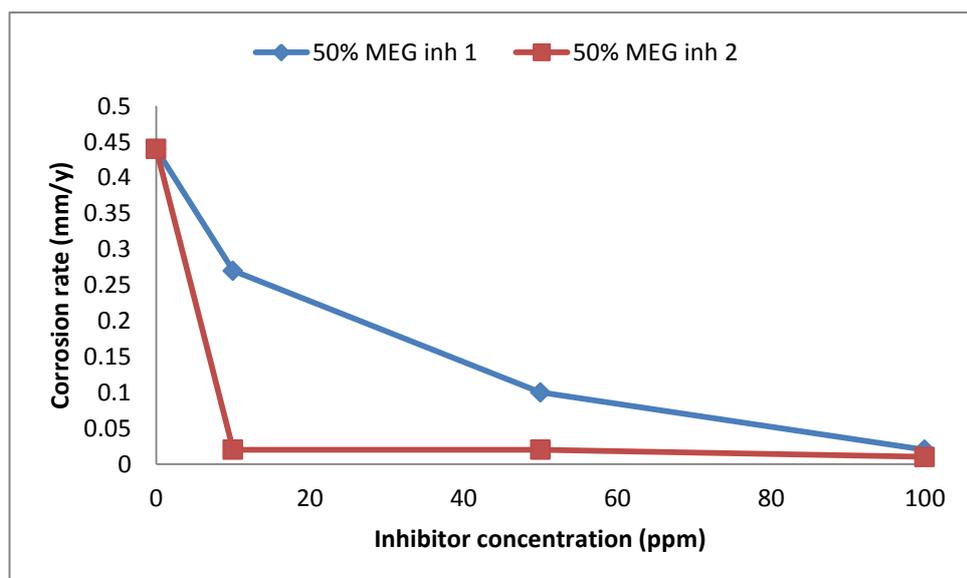
Figure 10-6 : Comparison of the final corrosion rate of different combination of inhibitor 1 with 50% MEG and inhibitor 2 with 50% MEG at 20°C.
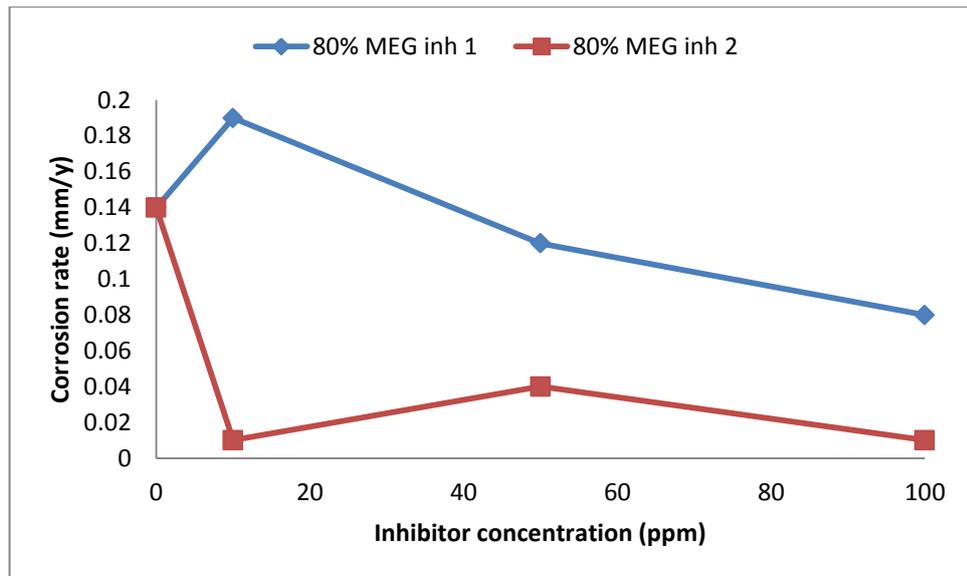
Figure 10-7 : Comparison of the final corrosion rate of different combination of inhibitor 1 with 80% MEG and inhibitor 2 with 80% MEG at 20°C.

It is seen clearly that a combination of MEG and inhibitor 1 at low concentration gave a higher corrosion rate than a combination of MEG with inhibitor 2 at all concentration except for 100ppm Inhibitor 1 with 50% MEG. This shows that the MEG helps in reducing corrosion rate in the presence of inhibitor 2 but does the opposite for inhibitor 1. Riggs [132] presented results which shows that the addition of ethylene oxide help to improve the efficiency of some corrosion inhibitor of N-hexadecylpropylene diamine. The effect however was shown to increase with the concentration of ethylene oxide to a peak and then reduce even to a very low efficiency.

The addition of MEG has the same effect of increasing the inhibition efficiency with inhibitor 2 but not with inhibitor 1. The reduction in the efficiency was not observed with increase in the concentration of MEG from 50% MEG to 80% MEG at this temperature. However it was also seen from the result that, the corrosion rate in the presence of 10ppm inhibitor with 80% MEG was less than the corrosion rate in the presence of 80% MEG without the inhibitor. The difference in the corrosion rate was around 35%. The huge difference shows that there was no need to add inhibitor 1 at 10ppm concentration in the presence of MEG. The corrosion rate of the carbon steel in the presence of MEG was better without inhibitor 1 at that concentration. This is similar to studies by Kvarekval et al. [111] where the addition of pH

stabilizer in the presence of MEG for sour systems led to formation of localised corrosion as compared to the use of MEG only where general corrosion was observed. This indicates antagonistic behaviour with the MEG and pH stabilizer for that system [110].

Higher concentration of inhibitor 1 had a lower corrosion rate but did not perform well in the presence of MEG at 20°C as the corrosion rate was less than expected. On the other hand, the inhibitor 2 had more favourable corrosion resistance which was more prominent at a higher concentration of MEG. The presence of MEG in the systems increased the solubility of inhibitor 2 and makes it to form a more protective film. This is so because inhibitor 2 is an ester base inhibitor as describe in chapter 4. Esters are less polar organic compounds than amine and their solubility increase in the presence of MEG [96]. The increase in the solubility occurs because a mixture of MEG and water changes the thermodynamics and kinetics of the systems making the solution less polar and less conductive. This enables less polar soluble substances to dissolve more than polar substances [110]. Inhibitor 1 which is made up of quaternary ammonium chloride will have its solubility reduce in the presence of MEG and water mixture. In the presence of a more polar solution such as NaCl solution the solubility of quaternary ammonium chloride is usually high and this will increase their inhibition efficiency. Meakins [133] was able to show that the increase in the corrosion efficiency of quaternary ammonium chloride was due to the increase in their solubility as compared to primary amine. The quaternary ammonium chloride is polar than their primary amine counterpart and hence is more soluble in solution with high polarity. It then means that any reduction in the solubility of the quaternary ammonium chloride will reduce its efficiency as seen in the test of inhibitor 1 with MEG that was prominent at higher MEG concentration of 80% MEG.

Gulbrandsen and Morard [194] also showed that addition of corrosion inhibitor can be used to improve the corrosion rate of carbon steel in the presence of MEG and DEG. They were able to show that with the addition of 0.5ppm sodium thiosulphate to 10% MEG at pH 5 and 25°C. This is similar to the observation made in this study with inhibitor 2. A comparison of both results is shown in Figure 10-8.

(a)   (b)
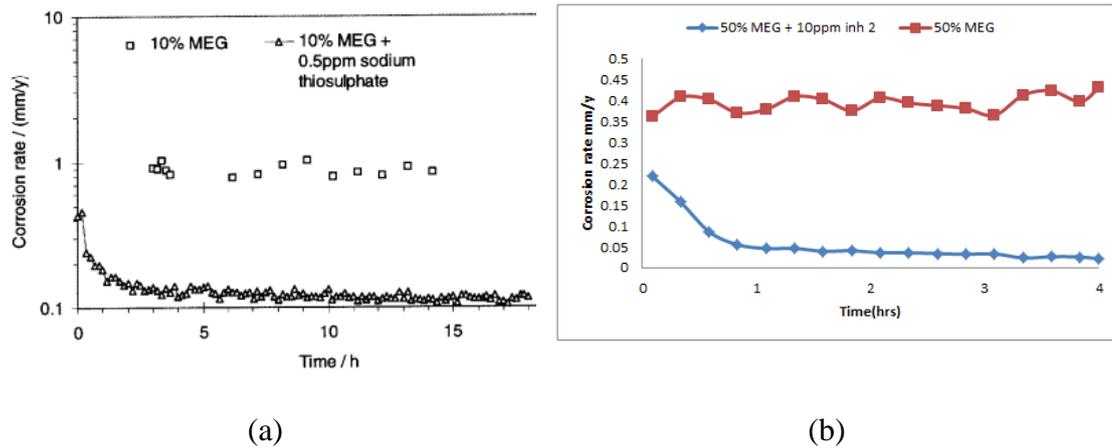
Figure 10-8 : Comparison of the effect of corrosion inhibitor with MEG on corrosion rate of carbon steel (a)10% MEG and 10% MEG with 0.5ppm sodium thiosulphate at pH 5 and 25°C [87] (b) 50% MEG and 50% MEG with 10ppm inhibitor 2 at 4.2 and 20°C.

MEG as a precursor to ester formation will help to stabilize the ester base inhibitor 2 in the system. It has been shown that the formation of ester during esterification process is a reversible reaction [96, 195]. This process of ester formation is favoured by addition of excess OH group such as those from MEG. The presence of MEG with inhibitor 2 which is an ester base inhibitor will not only increase its solubility but also increase its stability. This will lead to the formation of more protective film and reduction in the corrosion rate as seen in all the test with inhibitor 2 and MEG.

High temperature of 80°C did not favour inhibitor 1 and MEG mixtures as the corrosion resistance of the carbon steel in the presence of the inhibitor 1 was hampered by MEG. However, synergistic effect of MEG and inhibitor 2 at high temperature was observed where the corrosion resistance of carbon steel in inhibitor 2 and MEG was very high compared to the any of the corrosion resistance achieved by either of them. Figure 10-9 and 10-10 shows the comparison of the final corrosion rate of both inhibitors with 50% MEG and 80% MEG concentration at 80°C in the presence of MEG as derived from the result previously presented.
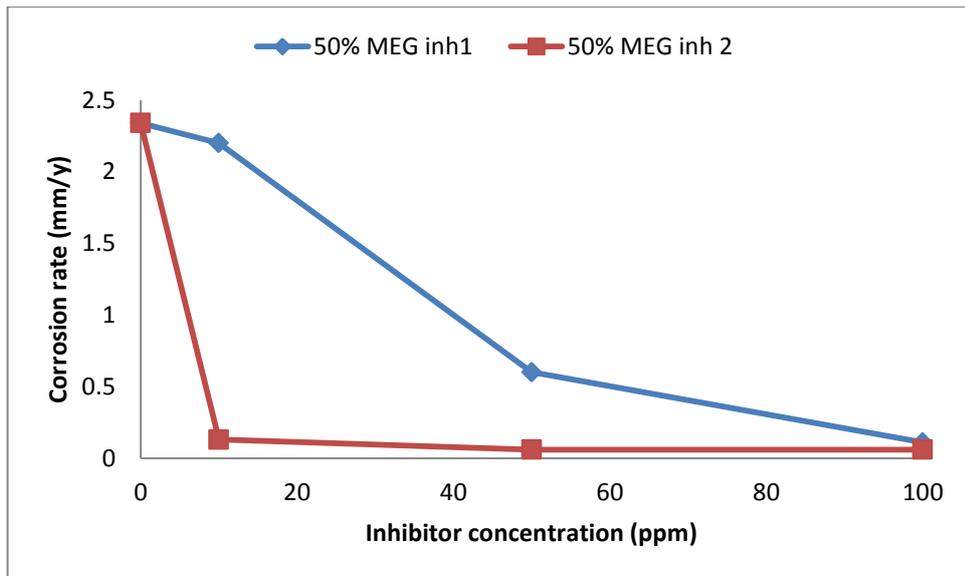
Figure 10-9 : Comparison of the final corrosion rate of different combination of inhibitor 1 with 50% MEG and inhibitor 2 with 50% MEG at 80°C.
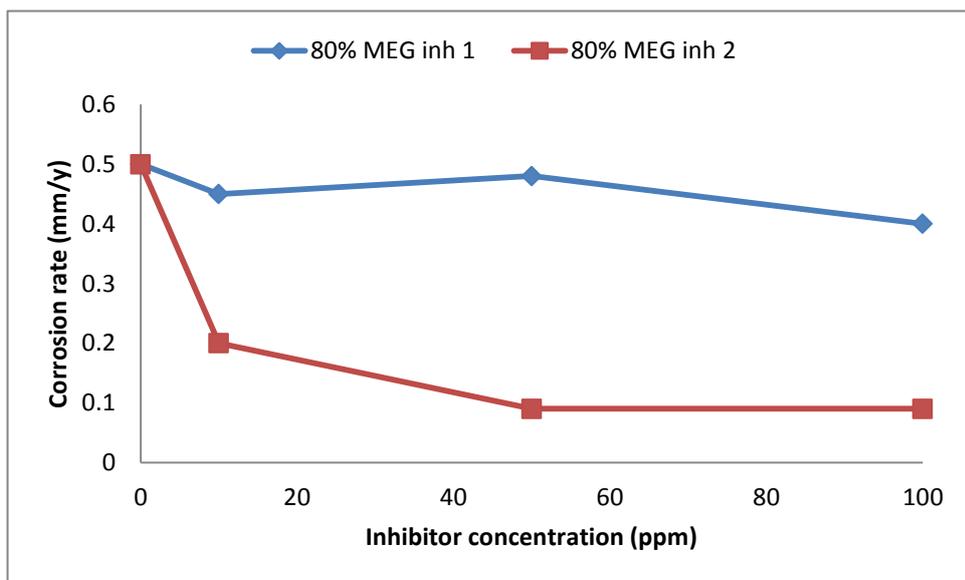
Figure 10-10 : Comparison of the final corrosion rate of different combination of inhibitor 1 with 80% MEG and inhibitor 2 with 80% MEG at 80°C.

It is seen clearly that a combination of MEG and inhibitor 1 at low concentration gave a higher corrosion rate than with inhibitor 2 at all concentration and combination. This also shows that the higher concentration of MEG may be hindering the effectiveness of inhibitor 1 at a high temperature of 80°C. The

corrosion rate for 100ppm inhibitor 1 with 50% MEG showed the lowest corrosion rate for the combination of inhibitor 1 and MEG.

10.3.2. Temperature

The effect of temperature on the corrosion of carbon steel in the presence of the inhibitors and MEG can be seen from the results presented in chapter 6 and chapter 7. At low temperature of 20°C the corrosion rate of the carbon steel in the presence of inhibitor 1 and MEG was lower than the corrosion rate at higher temperature of 80°C. The same was seen for corrosion rate of carbon steel in the presence of inhibitor 2 and MEG where the corrosion rate were all lower than that at a higher temperature of 80°C. This shows that at higher temperature the corrosion rate increase as expected as there was no formation of protective iron carbonate scale [32, 53, 160, 166].

On the other hand, the corrosion of carbon steel in the presence of inhibitor 1 and MEG showed higher corrosion rate compared with the corrosion of inhibitor 1 in the absence of MEG for high temperature of 80°C. This increase in corrosion at higher temperature is likely due to low solubility of inhibitor 1 in the presence of MEG. This reduction in solubility reduces the adsorption of inhibitor 1 on the carbon steel surface in forming a protective film. It then means that the reduction in the corrosion rate was mostly from the effect of the MEG and not the inhibitor. This is evident since a higher concentration of 80% MEG affects the corrosion rate more at the high temperature. As MEG is not very efficient at high temperature, the corrosion rate of inhibitor 1 in the presence of MEG will be high as seen from Figure 7-6.

The increase in temperature also affects the corrosion rate of carbon steel in the presence of inhibitor 2 and MEG but to a less extent. This is attributed mostly to the compatibility nature of inhibitor 2 with MEG. It was seen that the corrosion rate in the presence of inhibitor 2 and MEG was lower than the corrosion rate in the presence of either MEG or inhibitor alone. This shows that the presence of MEG allows the inhibitor 2 to form a more protective surface than the inhibitor 1 alone at this high temperature. From Figure 6-12 it is shown clearly that the corrosion rate of inhibitor 1 was lower for higher concentration than for inhibitor 2 at 80°C. This was not the case when both are compared in the present of MEG as seen in Figure 10-9

and Figure 10-10 previously presented in this chapter. The result showed that at this high temperature and in the presence of MEG, the inhibitor 2 performed better than inhibitor 1. This shows that the presence of MEG boost the performance of inhibitor 2 while hindering or having no positive effect on the performance of inhibitor 1 at high temperature.

10.3.3.Surface analysis

SEM image for test at 20°C showed the cluster of shallow pit on the tested carbon steel surface of 10ppm inhibitor 1 and 80% MEG mixture. This was not seen of inhibitor 2 and any of the MEG mixture. This means that the low concentration of inhibitor 1 in the presence of high concentration of MEG may lead to porous film formation by the inhibitors. This has occurred because the low concentration of 10ppm inhibitor 1 was not able to penetrate the barrier posed in the presence of MEG to form a very protective inhibitor film. This will then generate localised corrosion on the surface of carbon steel through micro-galvanic interaction of well cover inhibitor film areas and the bare steel. Higher concentration of MEG (i.e. 80% MEG) made it even more difficult for the inhibitor to penetrate to the surface. The use of higher concentration of inhibitor 1 with MEG did not show signs of localised corrosion on the surface. This maybe that higher concentration of inhibitor 1 was able to penetrate to the surface of the carbon steel to form a less porous film than the 10ppm inhibitor 1 film. The formation of pit on the surface of inhibitor 1 with MEG shows the importance of surface analysis in complementing the LPR result. LPR results may not be able to show where there are formations of localised corrosion on the surface of the carbon steel.

Interferometer measurement results complemented the SEM results and the LPR results and showed the presence of pit for the 10ppm inhibitor 1 and 80% MEG. The results showed that corrosion rate may be lower from LPR result but may still have formation of pit at that low corrosion rate when the inhibitor film are poorly formed or damaged. It is then necessary to test an inhibitor in the presence of MEG in order to understand the synergistic or antagonistic effect of MEG on the inhibitor efficiency. A summary of the interaction of MEG with the inhibitors as derived from the result is shown in Table 10-3 and Table 10-4.

Table 10-3 : Summary of the interaction of MEG with the inhibitors at 20°C (Here (+) = positive interaction and (-) = negative interaction)

Inhibitor 1	10ppm	50ppm	100ppm
50% MEG	-	+	+
80% MEG	- - -	+	+
Inhibitor 2	10ppm	50ppm	100ppm
50% MEG	+	+	+
80% MEG	+	+	+

Table 10-4 : Summary of the interaction of MEG with the inhibitors at 80°C (Here (+) = positive interaction and (-) = negative interaction)

Inhibitor 1	10ppm	50ppm	100ppm
50% MEG	- - -	- -	-
80% MEG	- -	- -	- - -
Inhibitor 2	10ppm	50ppm	100ppm
50% MEG	+	++	++
80% MEG	+	++	++

10.3.4. Localised/general corrosion

The use of corrosion inhibitor in the presence of MEG has been shown to produce either an antagonistic and synergistic effect. From the result of LPR measurement, it has been shown that general corrosion rate for 10ppm inhibitor 1 with 80% MEG increases when compared with 80% MEG alone. The increase in corrosion rate showed the inability of lower concentration of inhibitor to penetrate through the viscous less polar MEG and form a very protective film against corrosion. The reduction in general corrosion rate for the combination improved at higher concentration of inhibitor 1 but was still lower than expected. The higher the

concentration the more the corrosion rate reduces at both low and high temperature. This means that in the presence of MEG the concentration of inhibitor 1 to reduce corrosion may be higher as compared to that without MEG. This reduction in the efficiency of the inhibitor in the presence of MEG showed that the inhibitors may function differently at difference system. This effect of environment factor was also observed for n-hexadecyl propylene diamino salicylate which was very effective at lower sulphate environment but ineffective at higher sulphate environment [132].

SEM image showed that the presence of a high concentration of MEG and lower concentration of inhibitor 1 may even lead to localised corrosion. The localised corrosion may have generated from the inability of the inhibitor 1 to form a good protective film when less inhibitor reaches the carbon steel surface in the presence of MEG. It has been shown that poorly formed films by inhibitor may lead to micro-galvanic corrosion between the bare steel and the film covered region that will generate localised corrosion [173]. Riggs and Hurd also showed that some corrosion inhibitor may increase the general corrosion at lower limiting concentration [132]. This is the case of 10ppm inhibitor 1 concentration which may be below the limiting concentration in a MEG environment as shown in Figure 10-11.
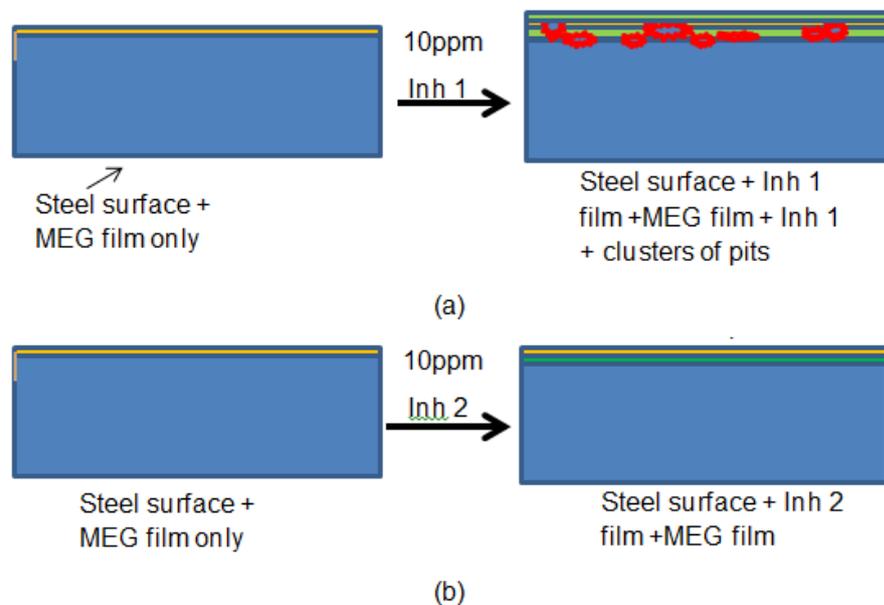
Figure 10-11 : Schematic description of (a) formation of porous film with cluster of pits by inhibitor 1 due to under-dose and poor solubility in MEG and (b) formation of non-porous protective inhibitor 2 film directly on the steel surface.

The use of inhibitor 2 with MEG showed a rather improved general corrosion rate at both low and high temperature. The general corrosion rate from the LPR measurement showed that there was an improvement in all the concentration tested. This shows a synergistic effect between inhibitor 2 and MEG. It should be seen that for lower temperature of 20°C, the difference corrosion rate were not much from the lowest concentration 10ppm through to the highest concentration of 100ppm. This may mean that at this lower temperature and concentration of 10ppm the inhibitor 2 has reach its optimum concentration. Additional increase in the concentration of inhibitor 2 did not have any big effect on the general concentration. This type of observation was made by Wong et al.[157]. They observed that the effect of increase in concentration of phosphate ester after the minimum concentration level showed little effect on the corrosion rate. Ismail [196] also had the same result where no further improvement was seen after optimal concentration of phosphate ester based inhibitor was added. The use of inhibitor 2 which is an ester base inhibitor as previously described follows the same process as the phosphate ester base inhibitor even in the presence of MEG. At 80°C it was observed that the concentration of inhibitor 2 in the presence of MEG required in reducing the corrosion rate below 0.1mm/y increased above 10ppm. This indicates that temperature plays a large role in the manner in which inhibitor 2 behaves. Minimum inhibitor concentration for inhibitor 2 is temperature dependent. This type of observation was made by Alink et al. [197] while studying the mechanism of corrosion inhibition of phosphate ester. The concluded that critical micelle concentration (CMC) of nonylphenol phosphate is strongly dependent on temperature.

The SEM image for the samples showed good protection between the MEG and inhibitor 2 as no localised corrosion rate was observed. This shows that inhibitor 2 and MEG can be applied together without any localised corrosion occurring.

10.3.5.Pre-corroded surfaces

The effect of pre-corrosion on the corrosion of carbon steel for solution of MEG and the inhibitor 1 was observed in the reduction of the corrosion rate. At lower concentration of 10pppm inhibitor 1, it was seen that the corrosion rate reduces for lower concentration of inhibitor 1 in the presence of MEG. At lower temperature of 20°C, The reduction was not below 0.1mm/y but was lower than corrosion rate with

polished sample. This reduction may be attributed to the protective iron carbonate formed on the surface of the carbon steel. It contributed in the reduction of the corrosion rate as the iron carbonate were still much present as previously shown in Figure 9-22. There may be possible localised corrosion if there is a detachment of the iron carbonate on the surface of the carbon steel. This was seen for the 10ppm inhibitor 1 and 80% MEG concentration. The same type of localised corrosion behaviour was observed for the polish sample in the presence of MEG at the same concentration. This may then mean that the 10ppm inhibitor 1 may be under dosed at this concentration in the presence of MEG. Hu et al. [173] argued that under dosing of inhibitor may accelerate the formation of localised corrosion on the surface of the carbon steel. Higher concentration of 100ppm inhibitor 1 and MEG show a massive reduction in the corrosion rate of the pre-corroded carbon steel. The SEM image showed that there was a large amount of iron carbonate present on the surface which helps in the prevention of corrosion. At this concentration, there were no detachments of iron from the surface which may lead to localised corrosion on the surface. It may be that at this concentration, there is a synergist effect between the iron carbonate and the inhibitor 1 which helps to reduce the corrosion more than for only polished samples. This synergistic effect between the iron carbonate was observe by Wong et al [156] on test with quaternized amine during iron carbonate scale formation. They were able to show the presence of well-formed iron carbonate on the surface of the carbon steel in the presence of the inhibitor. The inhibitor was assumed to adsorb on the surface of the iron carbonate forming a well protective layer. Tsui et al. [158] also showed that alkyl pyridine quaternary amine when added to pre-corroded scaled surfaces were able to reduces the corrosion rate effectively while still retaining the iron carbonate scale surface. The effect for the inhibitor and the corrosion scaled surface were assumed to complement one another.

The SEM image results for Wong et al. [156] and Tsui et al. [158] are compared with the results of this study in Figure 10-12. Table 10-5 also show a comparison of the reduction in corrosion rate of the inhibitors due to the presence of iron carbonate scale. The results of this study highlight clearly how the retention of a compact iron carbonate scale by inhibitor 1 improved the corrosion rate below 0.1mm/y.
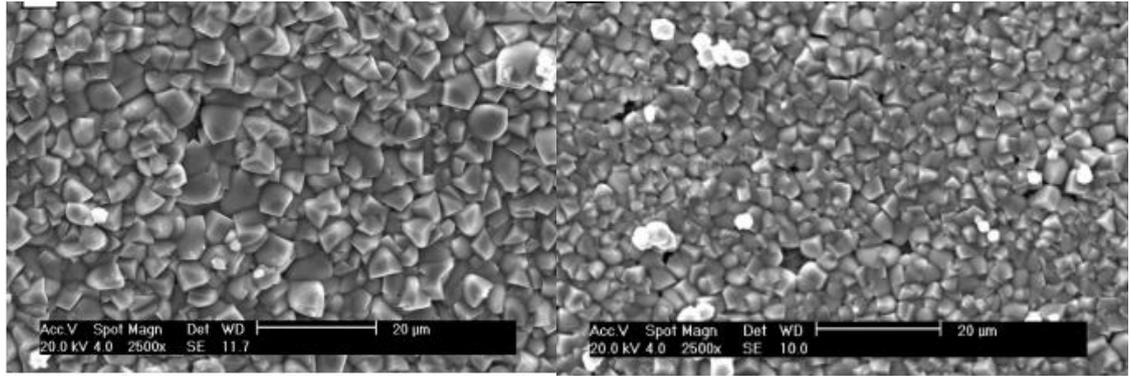
<div align="center">(a)</div>

<div align="center">(b)</div>
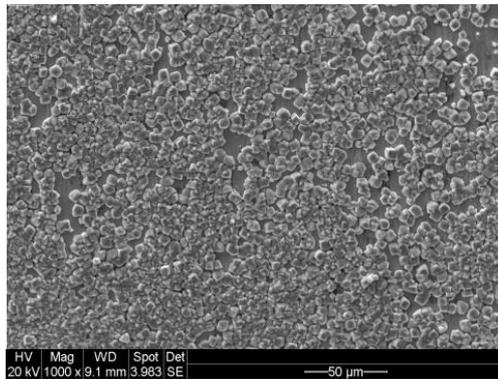
<div align="center">(c)</div>
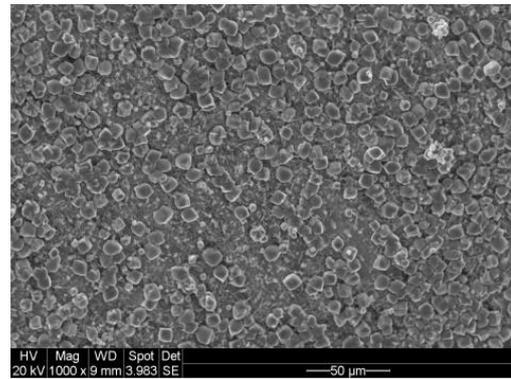
<div align="center">(d)</div>
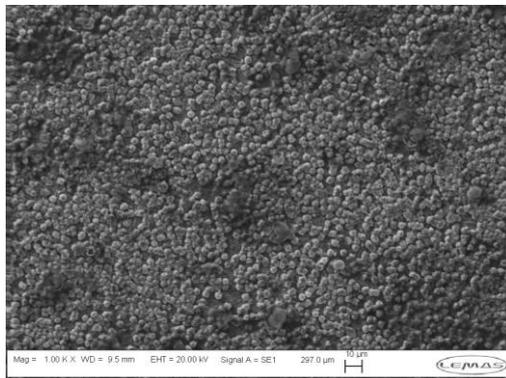
<div align="center">(e)</div>
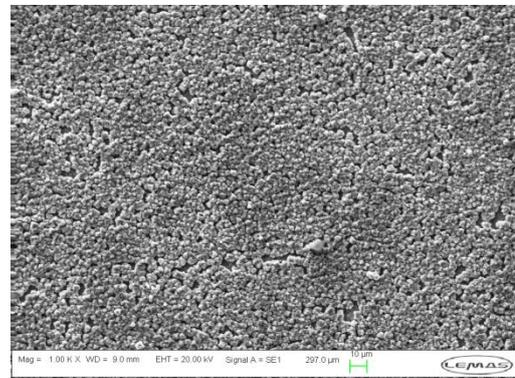
<div align="center">(f)</div>

Figure 10-12 : SEM image at 80°C ((a) pre-corrosion at pH 6.5 (b) pre-corrosion + 50ppm quaternized amine inhibitor at pH 6.5 [156]) ((c) pre-corrosion at 6.5 (d) pre-corrosion + 50ppm alkyl pyridine quaternary amine at pH 6.5 [158]) (e) pre-corrosion at pH 7 (f) pre-corroded at pH 7 + 100ppm inhibitor 1 + 50% MEG at pH 4.3

Table 10-5 : Effect of pre-corroded scale on corrosion rate of carbon steel in the presence of different type of inhibitors at 80°C (i.e. scale retention inhibitors).

Experiment (4 hours test)	Initial Pre-corrosion conditions at 80°C	Initial corrosion rate(mm/y) after pre-corrosion	Final corrosion rate after 4hrs (mm/y)	Comments
50ppm quaternized amine at pH 6.5 [156]	250ppm Fe^{2+} + 0hr Pre-corrosion, pH 6.5	2.0	0.09	Compact iron carbonate scale formed
100ppm alkyl pyridine quaternary amine at pH 6.5 [158]	100ppm Fe^{2+} + 24hrs Pre-corrosion, pH 6.5	0.9	0.5	Compact iron carbonate scale formed
100ppm Inhibitor 1 + 80% MEG at pH 4.6	250ppm Fe^{2+} + 24hrs Pre-corrosion, pH 7	0.16	0.02	Compact iron carbonate scale formed
100ppm Inhibitor 1 + 80% MEG at pH 4.6	No pre-corrosion	0.50	0.40	No iron carbonate scale formed

Pre-corrosion also showed an improvement in the corrosion rate in condition where the iron carbonate formed already on the carbon steel were protective with addition of inhibitor 2. The reduction of corrosion rate was mostly seen at 20°C where the general corrosion rate was low.

At 80°C, the reduction in the corrosion rate was not pronounces at this concentration for inhibitor 2. This means pre-corrosion may not contribute much to the protection of carbon steel in the presence of inhibitor 2 and MEG at high temperature. SEM images showed that in the presence of inhibitor 2 there was less formation of iron carbonate on the surface of the pre-corroded carbon steel compared to the amount formed in the presence of inhibitor 1. This indicates that iron carbonate is not encouraged in the presence of inhibitor 2. The appearance of iron carbonate on the surface may mostly be from the effect MEG has on solubility of iron carbonate which encourages the growth of iron carbonate at the right conditions. At high temperatures 10ppm inhibitor 2 does not perform better on pre-corroded surface when compared with polished sample. This is mostly due to less protective iron carbonate on the pre-corroded carbon steel tested in 10ppm inhibitor 2 and MEG at 80°C.

Wong et al. [157] has shown that phosphate ester may not contribute to the formation of iron carbonate on the surface as the formed complex with the iron ions (Fe^{2+}). Sun et al. [198] also showed that imidazoline acetate salts based inhibitors does not promote the formation of iron carbonate on the surface of pre-corroded carbon steel. This makes the inhibitor and the pre-corroded surfaces to have a lesser complementary effect as expected. This is the reason why there was less iron carbonate film present in the SEM image of inhibitor 2 an ester base inhibitor than inhibitor 1 a quaternary amine base inhibitor. Inhibitor 1 on the hand encourage the formation of iron carbonate especially at the tested condition since the amount of iron carbonate on the surface of the pre-corroded tested samples was still high.

Figure 10-13 compares the results of inhibitor 2 and MEG on pre-corroded carbon steel surface with that of Wong et al. [157] and Sun et al. [198]. Table 10-6 also show a comparison of the reduction in corrosion rate of the inhibitors due to the presence of iron carbonate scale. The results of this study highlight clearly how non-retention of a compact iron carbonate scale by inhibitor 2 may not improve the corrosion rate below 0.1mm/y as expected.
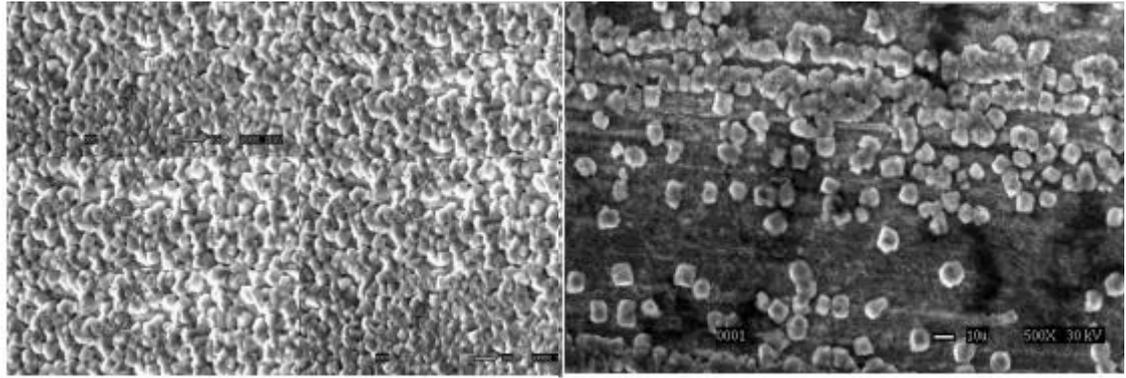
(a)   (b)
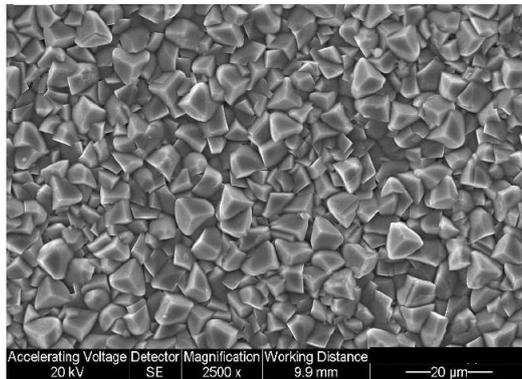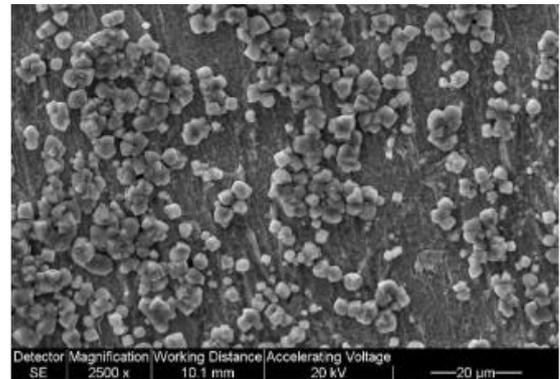
(c)   (d)
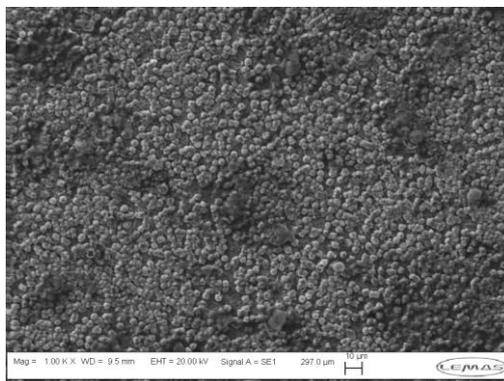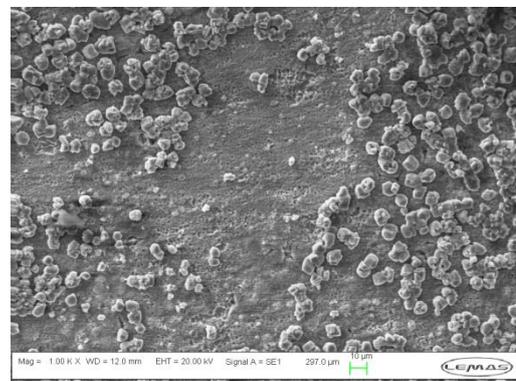
(e)   (f)

Figure 10-13 : SEM image at 80°C ((a) pre-corrosion at pH 6.6 (b) pre-corrosion +
50ppm imidazoline acetate salts at pH 6.6 [156, 198]) ((c) pre-corrosion at 6.5 (d)
pre-corrosion + 10ppm phosphate ester at pH 6.5 [157]) (e) pre-corrosion at pH 7 (f)
pre-corroded at pH 7 + 10ppm inhibitor 2 + 80% MEG at pH 4.6

Table 10-6 : Effect of pre-corroded scale on corrosion rate of carbon steel in the presence of different type of inhibitors at 80°C (i.e. non-scale retention inhibitors).

Experiment (4 hours test)	Initial Pre-corrosion conditions at 80°C	Initial corrosion rate(mm/y) after pre-corrosion	Final corrosion rate after 4hrs (mm/y)	Comments
25ppm Imidazoline acetate salts at pH 6.6 [198]	50ppm Fe^{2+} + 0.5hrs Pre-corrosion, pH 6.6	1.2	0.1	Less iron carbonate scale formed
25ppm Imidazoline acetate salts at pH 6.6 [198]	50ppm Fe^{2+} + 47hrs Pre-corrosion, pH 6.6	0.2	0.06	Porous iron carbonate scale formed
10ppm phosphate ester inhibitor at pH 6.5 [157]	50ppm Fe^{2+} + 0hrs Pre-corrosion, pH 6.5	3.0	0.5	Less iron carbonate scale formed
10ppm Inhibitor 2 + 80% MEG at pH 4.6	250ppm Fe^{2+} + 24hrs Pre-corrosion, pH 7	0.16	0.13	Less iron carbonate scale formed
10ppm Inhibitor 2 + 80% MEG at pH 4.6	No pre-corrosion	0.45	0.24	No iron carbonate scale formed

10.4. Industrial relevance

10.4.1. Pre-corrosion

The formation of corrosion product on the surface of most carbon steel pipe used in the oil and gas industry is common even before they are used for multiphase transportation. These corrosion products such as rust and mill scale are common from production plant and storage area. [33, 194, 199]. The formation of this product may or may not contribute positively in the reduction of the corrosion rate. In the industry MEG is applied as hydrate inhibitor for the prevention of hydrate in the system. At higher temperature region of the pipeline, there are possibilities for the formation of iron carbonate [115, 121, 200, 201]. When this occurs, the corrosion rate is affected.

The results for the formation of iron carbonate have shown that the formation of protective iron carbonate scales takes time. 250ppm of iron was introduced into the system to form a slightly protective iron carbonate scale in 4 hours. The corrosion rate for this time was down to approximately 1mm/y. The corrosion rate later reduces to approximately 0.15mm/y within 24 hours. The 24hrs test formed a very protective iron carbonate film. The formation of this protective iron carbonate is time dependent with more iron carbonate deposited on the carbon steel surface. It also depends on the amount of iron in the system. From industrial point of view, it means that the formation of iron carbonate on the pipeline can only occur with the presence of iron ions in the system. As this is not possible unless through corrosion of the carbon steel pipeline itself. There is probably an initial high corrosion of the carbon steel pipeline which will then lead to the formation of iron carbonate. This iron carbonate can only be protective in a system where iron concentration is high to form a super-saturated iron carbonate. The result here presented uses 250ppm amount of iron to produce a very protective film of around 13μm. This may mean a corrosion rate of 6mm/y at 80°C for 30 days. Farelas et al. [62] showed that the formation of protective iron carbonate on carbon steel X65 took several days of massive corrosion of the carbon steel before it was achieve. They also mentioned that some of the iron ions may not take part in the formation of the protective iron carbonate as the calculated iron loss from the corrosion rate was higher than the

actual film formed on the surface of the carbon steel. This iron ions that were not involve in iron carbonate formation may have been washed away from the surface to the bulk solution.

A pipeline with protective iron carbonate formed on the surface means that the corrosion rate of the system may have been high. It also means that other favourable conditions for the formation of iron carbonate are in place. These conditions are high temperature and higher surface pH which encourages iron carbonate formation [70, 188, 202]. Nesic et al. [187, 203] showed that the formation of protective iron carbonate occurs at very high temperature and high pH. de Waard et al. [53] proposed that the formation of iron carbonate occur at scaling temperature which is as high as 80°C. It is then important to know that the formation of iron carbonate on the surface of carbon steel pipeline will occur in a system with initial high corrosion and high temperature.

SEM images for the 24hrs pre-corrosion showed formation of protective iron carbonate. The removal of this film using Clark's solution showed under film localised corrosion/pit which was prevalent near very strong protective iron carbonate film. This may mean that even as iron carbonate is formed, there is still the possibility of formation of localised corrosion underneath the film. This is possible as the formation of iron carbonate is a chemical process which is not highly controlled. The random formation of this iron carbonate crystals may lead to sites where there are bare iron uncover by the film. This will generate micro galvanic corrosion between the iron carbide or corrosion film [57]. From the result of this study, the formation of under-film corrosion can be as high as the general corrosion in the absence of protective iron carbonate scale. This may mean that dependence of iron carbonate as a means of controlling corrosion of pipeline may not be satisfactory at all times. Any conditions within the system such as change in flow that will remove the protective iron carbonate can lead to the exposure of pits on the carbon steel surface. These pits, if exposed can accelerate fast due to galvanic interaction between the bare carbon steel and the protected region [65, 190, 204]. Changes in the condition of pipeline should be viewed with care as this can lead to pipe damage due to localised under film corrosion.

The introduction of MEG in a multiphase pipeline system is often done at high concentration and high temperature [3]. The high concentration of MEG and temperature from the results has been shown to favour the growth of iron carbonate crystal in the presence of MEG. Higher quantity of MEG (i.e. 80% MEG) has more effect on the solubility and growth of iron carbonate. It reduces the solubility of iron carbonate and produces a less polar solution that increase and stabilizes the iron carbonate. This condition will lead to iron carbonate film formation on the pipeline at this high temperature region. This will reduce the high corrosion rate at this point as the protective iron carbonate will form a barrier against the corrosion species. On the other hand large formation of iron carbonate may form thick films which can reduce the flow size of the pipeline. This condition need to be control to minimum to avoid reduction in flow pressure.

As natural gas flows along the pipeline, there is a massive temperature drop which can lead to the condensation of more water to the bottom of the pipeline. The increase in water content due to condensation along the pipeline will lead to the reduction in the MEG concentration. Dugstad et al. [77] and Seiersten et al. [118] has shown that the concentration of MEG decreases to about 50% MEG mass. At low temperature (i.e. 20°C or less), iron carbonate may not form on the surface of the carbon steel as low temperature does not favour iron carbonate crystal formation. Experimental results here have shown that at lower temperature and lower concentration of 50% MEG, the iron carbonate crystal becomes unstable and loses its crystalline cubic shape. Berntsen et al. [205] showed that at low temperature the formation of iron carbonate may not be possible even at super-saturation condition for iron carbonate. This is in line with this studies which shows that at lower temperature and lower concentration of MEG, iron carbonate will not be stable in the presence of MEG only. This may mean that the protection of the pipeline at this point will only depend mainly on MEG corrosion inhibition and not on the formation of iron carbonate formation. Additional corrosion protection method will have to be introduced if the pH is kept at normal. The increase in pH may however reduce the corrosion rate of the carbon steel.

10.4.2. Application of inhibitors

The use of inhibitors as an additional protection for the pipeline will become necessary when pH stabilization causes large deposition of unwanted scale [117, 121, 123]. These inhibitors must be compatible with the MEG system. The presence of MEG in a system changes the kinetics and thermodynamic of the system. de Waard et al.[53] concluded that reduction in the corrosion rate of carbon steel can be attributed partly to reduction in the polarity of MEG/water mixture. This reduction in polarity may affect the solubility of water base inhibitors such as the quaternary ammonium chloride base inhibitor used in this study. The reduction in the solubility of the inhibitor in the presence of MEG reduces the penetration of inhibitor to the carbon steel pipeline surface. This will lead to reduction in the efficiency of the inhibitor. It has also be shown that at very low concentration of the inhibitor, and high MEG concentration localised corrosion may even occur with this type of inhibitor.

More so the use of both water and oil base inhibitor such as ester base inhibitors may result in a synergist effect with MEG. The reduction in the polarity of the multiphase natural gas fluid with MEG will lead to an increase in the solubility of less polar base inhibitors. This will lead to good surface penetration and formation of inhibitor film on the surface. This study shows that ester base inhibitors will be more compatible with MEG. MEG also being a precursor to ester may encourage the stability of the ester when it is supplied in excess.

The application of the inhibitors at higher temperature where iron carbonate film are formed may also affect the performance of the inhibitors. Results from this studies showed that the formation of protective iron carbonate may favour the use of quaternary base inhibitor. This is possible due to the synergistic effect of the iron carbonate film with the inhibitor in the presence of MEG. The inhibitor at high concentration forms a very protective film on the surface of carbon steel which protects the iron carbonate. This shows that some inhibitors function very well in the presence of MEG when iron carbonate film is present. These conditions may be present in high temperature area of the pipeline where pH stabilization is being applied or has previously been applied.

Figure 10-14 shows a schematic description of the behaviour of the two inhibitors tested in this study in the presence of already formed protective iron carbonate steel surface.
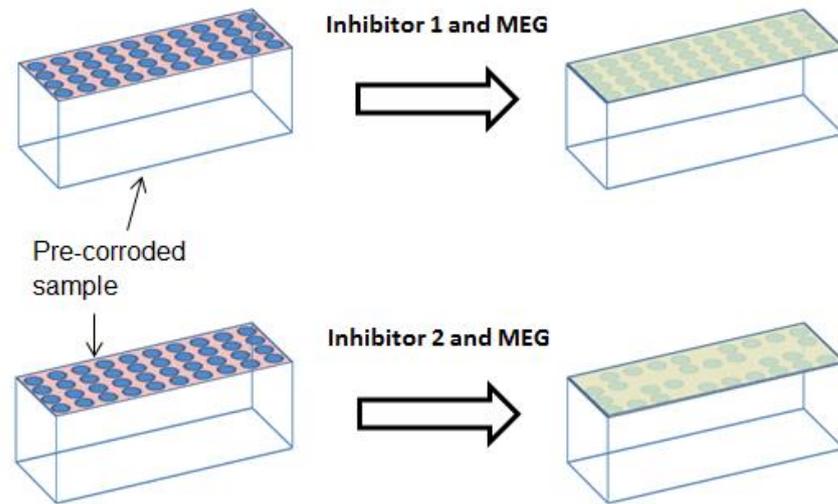
Figure 10-14: Schematic diagram showing the complementary effect of inhibitor 1 and MEG leading to the retention of iron carbonate on pre-corroded and the non-complementary effect of inhibitor 2 and MEG causing reduction of iron carbonate on pre-corroded sample.

The presence of iron carbonate may not have much effect with the use of ester base inhibitors this is possible as ester base inhibitor may not encourage the formation of iron carbonate. As described Wong et al. [157], these inhibitors tend to form complexes with the iron ions. This may mean a lack of iron ion for the nucleation or growth of the iron carbonate film. The lack of growth and stability of the iron carbonate at high temperature may mean lack of additional protection from iron carbonate. This means that at this high temperature regions iron carbonate formation may be hindered by the presence of ester base corrosion inhibitor. This may have a positive impact where too much of the iron carbonate film is detrimental to the flow assurance of the pipeline.

10.4.3. Process condition

From an industrial view of point, MEG is used as a thermodynamic hydrate inhibitor. The use of MEG can also have an effect on the corrosion of carbon steel. This effect can be seen to be pronounced in areas with lower temperature along the

pipeline. Higher temperature increases the corrosion rate in the presence of MEG and reduces the efficiency of MEG in reducing the corrosion rate of carbon steel. This may lead to under estimation of corrosion rate in the presence of MEG at higher temperature area where protective iron carbonate film does not form. Models like de-Waard [53, 67] have given a worst case value for corrosion rate in the presence of MEG. This worst case value does not hold for areas along the pipeline where the pipeline temperature is very high. Areas such as the injection point of MEG or for high temperature producing offshore pipeline. For this high temperature condition, additional control measure may be required.

The study also showed that at high concentration and high temperature of 80°C, there is the possibility of MEG reducing the solubility of iron carbonate while promoting the growth of the iron carbonate. These conditions may have two major effects on the injection part of MEG. The first is that at those point along the pipeline where temperatures are high and MEG concentration are also high, The formation of iron carbonate film will be high as well. This iron carbonate films will grow thicker and help to protect the pipeline along this area. The corrosion rate will be low as long as under film corrosion does not occur.

The second major effect is the formation of too much iron carbonate film along the pipeline which may reduce the internal diameter of the pipeline. This may then reduce the flow of the natural gas along the pipeline. Additional effect may occur if the production line produces water with calcium ion. This will lead to the formation of calcium carbonate scale along the pipeline which may also affect the flow rate. If this occurs the pH of the solution may have to be reduced with the addition of corrosion inhibitor or combine scale and corrosion inhibitor.

When necessary the use of inhibitor must be compatible with MEG. From the study so far, it has been seen that quaternary base inhibitors can be very strong inhibitors at both high and low temperatures. The increased inhibition property is mostly due to its solubility in polar solutions such as salt water. Meakins et al. [133] showed that quaternary ammonium based inhibitors performed better that other amines inhibitors because of their increase solubility. The reduction in the polarity by MEG at high concentration may mean that the quaternary ammonium base inhibitor and other polar soluble inhibitor may not function effectively in a MEG system. This

study showed that inhibitor 1 performed better than inhibitor 2 at higher temperature and higher concentration. However in high concentration of MEG inhibitor 1 efficiency reduces drastically while inhibitor 2 efficiency in reducing corrosion increases. This antagonistic and synergistic effect in MEG means that if an inhibitor is to be applied in a MEG system, the effect of MEG on the inhibitor must be considered.

Chapter 11. CONCLUSIONS AND FUTURE WORK

The conclusion of the studies as described below highlighted the major summary of the whole studies. It shows how the studies and results were used to achieve the aims and objectives which were stated at the beginning of this work.

11.1. Conclusion from results of corrosion assessment in the presence of MEG

- OCP measurements results showed that the use of MEG will increase the OCP state to a noble state. This is an indication that MEG reduces the corrosion rate of carbon steel by reducing the anodic reaction on the surface. The higher the concentration of MEG, the lower the corrosion rate of the carbon steel.

- Conductivity test shows that MEG containing solution has low conductivity. This low conductivity makes it difficult to measure the exact corrosion resistance of carbon steel in the presence of MEG using LPR method. The conductivity of MEG solution reduces with the concentration of MEG while increasing with temperature. Corrosion rate can be inaccurately low in the presence of MEG when measured using LPR unless the solution resistance is used to compensate the polarization resistance from the LPR measurements. This solution resistance can be determined using AC impedance method.

- AC impedance measurement on carbon steel in the presence of MEG showed that the corrosion rate of carbon steel reduces with the concentration of MEG. 80% MEG gave the lowest corrosion rate when compared to 50% MEG at both low and high temperature.

- AC and DC measurements show that efficiency of MEG in reducing the corrosion rate of carbon steel reduces with increase in temperature. This reduction is very significant for very low concentration of MEG.

- The reduction in the corrosion rate of carbon steel in the presence of MEG at 20°C is in agreement with the correction factor proposed by de Waard et al. However, at higher temperatures, the efficiency of MEG reduces. This reduction in efficiency causes a deviation in the correction factor proposed

by de Waard et al. As the temperature increases, de Waard et al. correction factor gives a lower corrosion rate than the actual corrosion rate in the presence of MEG.

- SEM characterization on electrochemically tested carbon steel samples showed lower general corrosion in the presence of MEG as compared to carbon samples tested in blank solution. Lower general corrosion was more in carbon steel tested at a lower temperature of 20°C and with higher MEG concentration. At a higher temperature of 80°C the surface showed a combination of general corrosion and shallow localized corrosion mostly at lower MEG concentration. This is an indication of the reduction in the efficiency of MEG in reducing the corrosion rate of carbon.

- The minimum effective concentration of MEG to give a corrosion inhibition efficiency of 50% at both low and high temperature is derived to be 30% MEG. Below this concentration, MEG may not act as an effective corrosion inhibitor rather it will act more as a hydrate inhibitor.

- FTIR results did not detect the presence of any film by MEG. The analysis suggests that MEG does not reduce corrosion by the formation of a strong chemical interactive film on the surface of the carbon steel. The lack of tenacious film on the surface of carbon steel tested in the presence of MEG means that the reduction of corrosion by MEG is likely through physic-sorption.

- Derivation of adsorption properties of MEG in carbon steel corrosion showed that MEG can fit into the Temkins adsorption isotherm. The negative isosteric enthalpy of adsorption (ΔH_{ad}°) describes the adsorption process as exothermic. This also confirms that MEG adsorbs on the surface of carbon steel through physical process rather than chemisorption. Other properties of MEG such as reduction of solution polarity and pH of the solution do contribute to the corrosion inhibition by MEG.

- Low activation energies (E_a) below 80kJ/mole achieved for the different concentrations of MEG tested inferred physisorption. This is in support of the results of FTIR and the negative isosteric enthalpy of adsorption(ΔH_{ad}°).

11.2. Conclusion from results of corrosion processes in the presence of organic corrosion inhibitors

- OCP measurements gave a semi-quantitative behavior of both inhibitors and showed that both inhibitors can reduce the anodic reaction. Linear polarization method was able to show the reduction in the corrosion in the presence of the two inhibitors but not the mechanism involved.

- The AC results showed that both inhibitors reduce corrosion rate by the formation of thin film layer. Adequate concentration of inhibitor 1 performed very well at both low and high temperature by forming persistence non-porous film. Low concentration of 10ppm inhibitor 1 creates porous film on the carbon steel surface which may lead to shallow localized corrosion. This means that the minimum concentration of inhibitor 1 should be above 10ppm.

- Inhibitor 2 forms thin film layers at very low concentration of 10ppm to protect the carbon steel surface. This thin film layer degrades at high temperature of 80°C for the ester base inhibitor thereby developing localized corrosion of the surface and poor corrosion resistance.

- Surface analysis of SEM and interferometer showed that inhibitor 1 protects the carbon steels at high concentrations of 50ppm and 100ppm at all the tested temperature. At low concentration of 10ppm inhibitor 1 forms localized corrosion and high corrosion rate on the surface of the carbon steel at both low and high temperature. Inhibitor 2 also protects the carbon steel surface at a low temperature of 20°C even at 10ppm concentration. At a high temperature of 80°C the pits are visible on the surface for 10ppm inhibitor 2 suggesting the formation of porous film on the surface.

- FTIR results showed that inhibitor 1 forms a very strong film at the surface of the carbon steel even at high temperatures unlike inhibitor 2 which does not show the formation of strong film at high temperature of 80°C.

- Inhibitor 1 at high concentration of 50ppm and 100ppm can be applied for both low and high temperature using any of the three methods of

inhibitor applications (i.e. continuous application methods, squeeze methods or batch methods) since the films formed by the inhibitors are quite persistence. Inhibitor 2 on the other hand will be suitable for low temperature applications and the inhibitor 2 may also be suitable for high temperature application using higher concentration of up to 100ppm in a continuous application method.

11.3. Conclusion from results of corrosion rates and processes in the presence of MEG and organic corrosion inhibitors

- AC impedance measurements showed that the presence of the inhibitor in MEG solution does not remove the solution resistance due to MEG. This solution resistance needs to be compensated for all LPR measurements in the presence of MEG and inhibitor so as not to underestimate the corrosion rate.

- The LPR and AC impedance results showed that the use of adequate concentration of both corrosion inhibitors in the presence of MEG reduces the corrosion rate of carbon steel further at low temperatures. However, Inhibitor 1 shows reduction in efficiency in the presence of MEG while inhibitor 2 mostly showed increase in efficiency in the presence of MEG.

- At 20°C and higher concentration of MEG (i.e. 80% MEG) and lower concentration of inhibitor 1 (i.e.10 ppm) interacts negatively giving a reduction in the corrosion rate of the carbon steel when compared to 80% MEG solution. This reduction in corrosion rate means that under-dosing of inhibitor 1 will be detrimental to the function of MEG or the inhibitor.

- At high temperatures, the efficiency of inhibitor 2 increases in the presence of MEG while the efficiency of inhibitor 1 decreases in the presence of MEG.

- The reduction in the efficiency of inhibitor 1 can be attributed to the reduction of the polarity of the solution in the presence of MEG. This reduction in polarity reduces the solubility of inhibitor 1 which is a quaternary ammonium chloride base inhibitor. The reduction in the solubility

reduces the ability of the inhibitor to reach the bare steel surface and form a non-porous thin film layer as would have been in the presence of a blank solution.

- The increase in the efficiency of inhibitor 2 can be attributed to its increase in solubility. This increase in solubility is achieved because the ester base inhibitor becomes more soluble in less polar solution like that of MEG. This increases the amount of the inhibitor that reaches the surface of the carbon steel to form a non-porous protective thin film layer.

- It is postulated that additional increase in efficiency of inhibitor 2 is achieved through the stability of the ester base inhibitor 2. This is so because MEG is a pre-cursor to ester and when in excess helps to stabilize the ester inhibitor even at high temperature of 80°C.

- SEM and white light interferometer reveals that under-dosing/low concentration of inhibitor 1 at 10ppm can cause localized corrosion in the presence of high concentration of MEG.

- Inhibitor 2 is suitable for application in the presence of MEG at low temperature and may also serve for higher temperature applications at higher concentrations of 50ppm and above.

11.4. Conclusion from results of corrosion in the presence of iron carbonate scale (Pre-corrosion)

- The formation of iron carbonate is achieved at a high temperature of 80°C when the concentration of iron in the solution is very high. Higher pH is also required for iron carbonate scale to crystallize spontaneously.

- The formation of protective iron carbonate scale is a time-dependence process due to the slow chemical reaction involved. Formation of protective iron carbonate depends on the thickness, packing, shape and size of the iron carbonate crystals.

- LPR results showed that the formation of 13µm thick film with small compact cubical shape gives a very low corrosion rate. This can be achieved within 24 hours under the conditions used in this study.

- Formation of protective iron carbonate scale may not eliminate under-scale corrosion on the surface of the carbon. The study showed that localized corrosion occur which was equivalent to the general corrosion of carbon steel with no protective iron carbonate on the surface. Any exposure or damage to the protective iron carbonate will expose this under-scale localized corrosion.

11.5. Conclusion from results of corrosion assessment in the presence of iron carbonate scale (pre-corrosion), MEG and organic corrosion

- The formation of protective iron carbonate scale helps to reduce the corrosion rate in the presence of MEG both at high and low temperature while non-protective iron carbonate may not reduce the corrosion rate of carbon steel at high temperature.

- At a lower temperature of 20°C images from SEM showed irregular and fluffy shaped iron carbonate crystals on the surface of the carbon steel. This indicates that MEG has less influence on the growth of iron carbonate crystals at a lower temperature of 20°C.

- The higher the concentration of MEG, the more it influences the growth and stability of iron carbonate crystals. The influence is due to the reduction of the solubility of iron carbonate in the presence of MEG.

- MEG has considerable influence on the growth of iron carbonate scale at high temperature of 80°C. The iron carbonate crystal was stable at this temperature and help in the reduction of corrosion rate of the carbon steel.

- The use adequate concentration of inhibitor can reduce the corrosion rate of pre-corroded carbon steel in the presence of MEG and inhibitor. In all concentrations tested inhibitor 2 showed more compatibility with MEG at lower temperature for pre-corroded carbon steel than inhibitor 1.

- SEM image for samples tested in inhibitor 2 with MEG at 20°C showed protection of the surface from both general and localized corrosion at a low concentration of 10ppm.

- At high temperatures SEM images for samples tested in inhibitor 2 with MEG showed the presence of shallow pits. This indicates that higher temperatures of 80°C may require higher concentration of inhibitor 2. The same behavior was observed in carbon steel samples tested in inhibitor 1 with MEG.

- Adequate concentration of inhibitor 1 with MEG can protect the surface of carbon steel with protective iron carbonate scale at both 20°C and 80°C. This is quite different from carbon steel with non-protective iron carbonate where inhibitor 1 does not protect the carbon steel at high temperature. The presence of iron carbonate forms a synergy with inhibitor 1 to form a very protective film. This occurs because inhibitor 1 encourages the formation of iron carbonate scale at the tested condition.

- Inhibitor 2 does not encourage the formation of iron carbonate scale even in the presence of MEG as the SEM image showed less iron carbonate on the surface of pre-corroded carbon steel. This indicates that there is no synergy between inhibitor 2 and iron carbonate in the presence of MEG. However the synergy between MEG and inhibitor 2 is enough to protect the pre-corroded carbon steel.

11.6. Future work

The works carried out in this study have tried to meet with the objective of this study. It is however not exhausted as there are varying conditions which are encountered in the oil and gas operations. Future work will look at some of the possible conditions that can be encountered when using MEG as a hydrate inhibitor and in the presence of other chemicals.

- Experiment will be done on the corrosion of carbon steel in the presence of MEG in flowing condition using a rotating cylinder electrode. The effect of flow will be determined. The mechanism involve during flow condition will

be compared to the mechanism derived in this work. The test will be performed for longer period (i.e. up to 7 days) to see if there will be changes in the corrosion resistance and also the mechanism for reduction of corrosion.

- Sour conditions have posed a great problem in the use of pH stabilization technique in mitigating and controlling corrosion of multiphase natural gas pipeline with MEG as a hydrate inhibitor. There have been issues of formation of pits in highly sour condition when pH stabilization technique is applied. The use of two or more corrosion inhibitors to mitigate corrosion in the presence of MEG for sour condition will be tested. Formation of pit due to sour conditions will be controlled by using the inhibitors at both high and low temperatures. It will be expected that the inhibitors will form a protective film on the surface of the carbon steel. This will help to prevent any localized corrosion.

- The use of inhibitor in the presence of MEG will be done also for pre-corroded sample to identify the effect of formation of iron sulphide layer in sour condition after iron carbonate has already been formed. This will be relevant for sweet well production that may later turn sour.

- Another area of future interest will be the testing of carbon steel in the presence of MEG, acetic acid and organic corrosion inhibitor. This will also be relevant for transportation of oil and gas from wells that have acetic acid.

- The use of surface analysis techniques of SEM, Interferometer, FTIR, XRD and XPS post experimental analysis samples after corrosion will also be applied. The films and corrosion products formed on the surface of both polished and pre-corroded carbon steel in sweet and sour conditions will help to identify the mechanism of corrosion on the tested carbon steel surface. The surface analysis will also help identify the type of corrosion that occurs during the electrochemical test.

Reference

1.   Christof, R. *BP Energy Outlook 2035* 2014 [cited 2014 21/03/2014]; 4th edition:[Available from: http://www.bp.com/en/global/corporate/about-bp/energy-economics/energy-outlook.html?gclid=CMWg5YyXpL0CFS7MtAodiVIAKg.

2.   Brustad, S., K.-P. Løken, and J.G. Waalmann, *Hydrate Prevention using MEG instead of MeOH: Impact of experience from major Norwegian developments on technology selection for injection and recovery of MEG*, in *Offshore Technology Conference*. 2005: Houston, Texas.

3.   L.Fosb, P., K. Thomsen, and E. H.Stenby, *Improving Mechanistic CO_2 Corrosion Models* in *CORROSION 2009*. 2009, NACE International: Atlanta, GA.

4.   Revie, R.W., Uhlig H. Herbert, *Corrosion and Corrosion Control : An Introduction to Corrosion Science and Engineering*. 4th ed. 2008, Hoboken, N.J.: J. Wiley.

5.   G.H.Koch, M.P.H.B., N.G.Thompson,Y.P.Virmani, and J.H.Payer, *Corrosion Cost and Preventon Strategies in the United States,*. 2002, Federal highway administration, U.S. Department of Transportation: McLean VA.

6.   Papavinasam, S., *Corrosion Control in the Oil and Gas Industry*. 2014, London, UK: Elsevier Inc.

7.   *Utility Board (ERCB) 91-G Report* 2007, Alberta Energy Regulator (AER): 250-5th street SW, Calgary, Alberta, Canada,.

8.   Wang, C., *Erosion-Corrosion Mitigation Using Chemicals*, in *School of Mechanical Engineering*. 2007: University of Leeds.

9.   Barker, R.J., *Erosion-Corrosion of Carbon Steel Pipework on an Offshore Oil and Gas facility*, in *School of Mechanical Engineering*. 2012, University of Leeds: University of Leeds.

10.   R.A.Buchanan, E.E.S.a., *Fundamentals of Electrochemical Corrosion*. 2000, Ohio: ASM International.

11.   Tait, W.S., ed. *An Introduction to Electrochemical Corrosion Testing for Practicing Engineers and Scientists*. 1994, Racine, WI: Pair O Docs Publications.

12.   Ren, C.Q., et al., *Corrosion Behavior of Oil Tube Steel in Simulant Solution with Hydrogen Sulfide and Carbon Dioxide.* Materials Chemistry and Physics, 2005. **93**(2-3): p. 305-309.

13.   ; Available from: http://chemwiki.ucdavis.edu/Analytical_Chemistry/Analytical_Chemistry_2.0/11_Electrochemical_Methods/11B_Potentiometric_Methods.

14.   Sastri, V.S., *Corrosion Prevention and Protection : Practical Solutions*. 2007, Chichester: Wiley.

15.   Revie, R.W., *Uhlig's Corrosion Handbook*. 2nd ed. 2000, New York: Wiley.

16. Thomas, J., *The Mechanism of Corrosion Prevention by Inhibitors*, in *Corrosion Control*, L.L.Shreir, Editor. 1979, Newnes-Butterworths: Uk.

17. Sastri, V.S., *Corrosion Inhibitors : Principles and Applications* 1998, Chichester ; New York :: Wiley.

18. Denzine, A.F. and M.S. Reading, *A Critical Comparison of Corrosion Monitoring Techniques used in Industrial applications*, in *Corrosion97*. 1997, NACE International: New Orleans, LA.

19. Scully, J.R., *The Polarization Resistance Method for Determination of Instantaneous Corrosion Rates: A Review*, in *CORROSION 98*. 1998, NACE International: San Diego Ca.

20. Scully, J.R., *Polarization Resistance Method for Determination of Instantaneous Corrosion Rates.* Corrosion, 2000. **56**(2): p. 199-218.

21. Nesic, S., *Key Issues Related to Modelling of Internal Corrosion of Oil and Gas Pipelines - A Review.* Corrosion Science, 2007. **49**(12): p. 4308-4338.

22. Sun, W., S. Nesic, and R.C. Woollam, *The Effect of Temperature and Ionic Strength on Iron Carbonate (FeCO3) Solubility limit.* Corrosion Science, 2009. **51**(6): p. 1273-1276.

23. Wang, X., et al., *Comprehensive Study of the Hydration and Dehydration Reactions of Carbon Dioxide in Aqueous Solution.* The Journal of Physical Chemistry A, 2009. **114**(4): p. 1734-1740.

24. Alberty, R., *Physical Chemistry.* 1983: John Wiley and Sons

25. Bruno, J., *The Influence of Dissolved Carbon dioxide on Trace Metal Speciation in Seawater.* Marine Chemistry, 1990. **30**(0): p. 231-240.

26. Palmer, D.A. and R. Van Eldik, *The Chemistry of Metal Carbonato and Carbon dioxide Complexes.* Chemical Reviews, 1983. **83**(6): p. 651-731.

27. Nesic, S., et al., *An Open Source Mechanistic Model for CO_2/H_2S Corrosion of Carbon Steel*, in *CORROSION 2009*. 2009, NACE International: Atlanta, GA.

28. Schmitt, G. and M. Horstemeier, *Fundamental Aspects of CO_2 Metal Loss Corrosion - Part II: Influence of Different Parameters on CO_2 Corrosion Mechanisms*, in *Corrosion 2006*. 2006, NACE International: San Diego Ca.

29. J. O'M. Bockris, N.B., F. Gutmann, *An Introduction to Electrochemical Science* 1974, London Wykeham Publications.

30. J.O.M. Bockris, D.D., A.R. Despic, , *The Electrode Kinetics of the Deposition and Dissolution of iron.* Electrochemica acta, 1965. **4**: p. 325-361.

31. J.O.M. Bockris, D.M.D., *Electro-Chemical Science*. 1972, Taylor and Francis: London.

32. Nesic, S., J. Postlethwaite, and S. Olsen, *An Electrochemical Model for Prediction of Corrosion of Mild Steel in Aqueous Carbon Dioxide Solutions.* Corrosion, 1996. **52**(04).

33. Dugstad, A., *Mechanism of Protective Film Formation During CO₂ Corrosion of Carbon Steel*, in *CORROSION 98*. 1998, NACE International: San Diego Ca.

34. Nyborg, R., *Overview of CO₂ Corrosion Models for Wells and Pipelines*, in *CORROSION 2002*. 2002, NACE International: Denver, Co.

35. Kermani, M.B. and A. Morshed, *Carbon Dioxide Corrosion in Oil and Gas ProductionA Compendium*. Corrosion, 2003. **59**(08).

36. de Waard, C. and D.E. Milliams, *Carbonic Acid Corrosion of Steel*. Corrosion, 1975. **31**(5): p. 177-181.

37. Hurlen, T., *Corrosion of Iron-Effect of pH and Ferrous Ion Activity* Acta Chemica Scandinavica, 1960. **14**(7): p. 1555-1563.

38. L.G.S. Gray, B.G.A., M.J. Danysh, P.G. Tremaine, , *Mechanism of Carbon Steel Corrosion in Brines Containing Dissolved Carbon Dioxide at pH 4*, in *Corrosion89*. 1989, NACE: Houston Tx.

39. L.G.S. Gray, B.G.A., M.J. Danysh, P.R. Tremaine, , *Effect of pH and Temperature on the Mechanism of Carbon Steel Corrosion by Aqueous Carbon dioxide*, in *NACE International*. 1990, NACE: Houston Tx.

40. Nesic, S., et al., *Electrochemical Properties of Iron Dissolution in the Presence of CO₂ - Basics Revisited*, in *CORROSION 96*. 1996, NACE International: Denver, Co.

41. Dewaard, C. and D.E. Milliams, *CARBONIC-ACID CORROSION OF STEEL*. Corrosion, 1975. **31**(5): p. 177-181.

42. Schmitt, G. and B. Rothmann, *Investigations into Corrosion Mechanism of Unalloyed Steel in Oxygen-Free Carbonic-Acid Solutions .1. Kinetics of Hydrogen Evolution*. Werkstoffe Und Korrosion-Materials and Corrosion, 1977. **28**(12): p. 816-822.

43. Schmitt, G. and B. Rothmann, *Investigations into Corrosion of Mild-Steel in Oxygen-Free Carbon-dioxide Solutions.2. Kinetic of Iron Dissolution*. Werkstoffe Und Korrosion-Materials and Corrosion, 1978. **29**(2): p. 98-100.

44. Schmitt, G. and B. Rothmann, *Corrosion of Unalloyed and Low Alloyed Steels in Carbonic-Acid Solutions*. Werkstoffe Und Korrosion-Materials and Corrosion, 1978. **29**(4): p. 237-245.

45. Ogundele, G.I. and W.E. White, *Some Observations on Corrosion of Carbon-Steel in Aqueous Environments Containing Carbon-dioxide*. Corrosion, 1986. **42**(2): p. 71-78.

46. Mora-Mendoza, J.L. and S. Turgoose, *Influence of Turbulent Flow on the Localized Corrosion Processes of Mild Steel With Inhibited Aqueous CO₂ Systems*, in *CORROSION 2001*. 2001, NACE International: Houston, Tx.

47. Postlethwaite, J. and D. Wang, *Modeling Aqueous CO₂ Corrosion of Iron in Turbulent Pipe Flow*, in *Corrosion 2001*. 2001, NACE International: Houston, Texas.

48.   Nesic, S., G.T. Solvi, and J. Enerhaug, *Organic Materials Generally are Recognized as Effective Inhibitors of the Corrosion of Many Metals and Alloys.* Corrosion, 1995. **51**(10).

49.   Videm, K. and A.M. Koren, *Corrosion, Passivity, and Pitting of Carbon-Steel in Aqueous-Solutions of HCO₃⁻, CO₂, and Cl⁻* Corrosion, 1993. **49**(9): p. 746-754.

50.   K.Videm, A.D., *Corrosion of Carbon Steel in an Aqueous Carbon dioxide Environment. Part 2. Film Formation,.* material Performance, 1989. **28**: p. 46-50.

51.   Ikeda, A., S. Mukai, and M. Ueda, *Relationship Between Environmental-factors and Corrosion Product on CO₂ Corrosion.* Transactions of the Iron and Steel Institute of Japan, 1984. **24**(12): p. B401-B401.

52.   Ikeda, A., *CO₂ Corrosion of Iron and Steel in Oil and Gas Production.* Journal of the Japan Petroleum Institute, 2002. **45**(2): p. 55-69.

53.   de Waard, C., U. Lotz, and D.E. Milliams, *Predictive Model for CO₂ Corrosion Engineering in Wet Natural Gas Pipelines.* Corrosion, 1991. **47**(12): p. 976-985.

54.   Palacios, C.A.a.S., J.R., *Characteristics of Corrosion Scales on Steel in a CO₂-Saturated NaCl Brine.* Corrosion, 1991. **47**(2): p. 122-127.

55.   Papavinasam, S., A. Doiron, and R.W. Revie, *Effect of Surface Layers on the Initiation of Internal Pitting Corrosion in Oil and Gas Pipelines.* Corrosion, 2009. **65**(10): p. 663-673.

56.   Papavinasam, S., A. Doiron, and R.W. Revie, *Model to Predict Internal Pitting Corrosion of Oil and Gas Pipelines.* Corrosion, 2010. **66**(3).

57.   Nyborg, R. and A. Dugstad, *Understanding and Prediction of Mesa Corrosion Attack*, in *CORROSION 2003*. 2003, NACE International: San Diego Ca.

58.   Schmitt, G.A., et al., *Understanding Localized CO2 Corrosion of Carbon Steel from Physical Properties of Iron Carbonate Scales*, in *Corrosion99*. 1999, NACE International: San Antonio, Texas.

59.   Heuer, J.K. and J.F. Stubbins, *An XPS Characterization of FeCO₃ Films from CO₂ Corrosion.* Corrosion Science, 1999. **41**(7): p. 1231-1243.

60.   John, R.C., et al., *SweetCor: An Information System for the Analysis of Corrosion of Steels by Water and Carbon Dioxide*, in *CORROSION 98*. 1998, NACE International: San Diego Ca.

61.   Xia, Z., K.C. Chou, and Z. Szklarskasmialowska, *Pitting Corrosion of Carbon-Steel in CO₂-Containing Nacl Brine.* Corrosion, 1989. **45**(8): p. 636-642.

62.   Farelas, F., B. Brown, and S. Nesic, *Iron Carbide and its Influence on the Formation of Protective Iron Carbonate in CO₂ Corrosion of Mild Steel*, in *Corrosion 2013*. 2013, NACE International: Orlando, Florida.

63.   J-L.Crolet and M.R.Bonis, *Alogorithm of the Protectiveness of Corrosion Layers 1-Protectiveness Mechanism and CO_2 Corrosion Prediction*, in *Corrosion 2010*. 2010, NACE International: San Antonio, Texas.

64.   Crolet, J.L., N. Thevenot, and S. Nesic, *Role of Conductive Corrosion Products in the Protectiveness of Corrosion Layers.* Corrosion, 1998. **54**(03).

65.   Crolet, J.L., S. Nesic, and N. Thevenot, *Role of Conductive Corrosion Products on the Protectiveness of Corrosion Layers*, in *CORROSION 96*. 1996, NACE International: Denver, Co.

66.   De Waard, C., U. lotz, and A. Dugstad, *Influence of Liquid Flow Velocity on CO_2 Corrosion: A Semi-Emprical Model*, in *Corrosion 95*. 1995, NACE USA.

67.   De Waard, C. and U. lotz, *Prediction of CO_2 Corrosion of Carbon Steel*, in *Corrosion 93*. 1993, NACE: USA.

68.   Harris, M.G., M.C.D. Adams, and D.J.D. Garber, *Use of a Corrosion Prediction Program as an Engineering Tool*, in *Corrosion97*. 1997, NACE International: New Orleans, LA.

69.   Woollam, R.C. and S. Hernandez, *Assessment and comparison of CO2 corrosion predicition models*, in *SPE International Oilfield Corrosion Symposium*. 2006: Aberdeen, UK.

70.   Hunnik, E.V., B.F.M. Pots, and E.L.J.A. Hendriksen, *The Formation of Protective Fe_3CO_2 Corrosion Product Layers in CO Corrosion*, in *Corrosion96*. 1996, NACE International: Denver, Colorado.

71.   Pots, B.F.M., *Mechanistic Models for the Prediction of CO_2 Corrosion Rates Under Multi-Phase Flow Conditions*, in *CORROSION*. 1995, NACE.

72.   Nyborg, R., A. Dugstad, and L. Lunde, *Corrosion and Glycol Distribution in a Large Wet-Gas Pipeline.* Materials Performance, 1993. **32**(9): p. 57-61.

73.   Ayello, F.x.o., et al., *Determination of Phase Wetting in Oil-Water Pipe Flows* in *CORROSION 2008*. 2008, NACE International: New Orleans LA.

74.   M. Wicks, J.P.F.M., Material Performance, 1975. **9**.

75.   Halvorsen, A.M. and T. Sontvedt, *CO2 Corrosion Model for Carbon Steel Including Wall Shear Stress Model for Multiphase Flow and Limits for Production Rate to Avoid Mesa Attack*, in *CORROSION 99*. 1999, NACE International: San Antonio, Tx.

76.   Adams, C.D., et al., *Computer Modeling to Predict Corrosion Rates in Gas Condensate Wells Containing CO_2*, in *CORROSION 96*. 1996, NACE International: Denver, Co.

77.   Dugstad, A., M. Seiersten, and R. Nyborg, *Flow Assurance of pH Stabilized Wet Gas Pipelines*, in *CORROSION 2003*. 2003, NACE International: San Diego Ca.

78.   Sun, W. and S. Nesic, *Kinetics of Corrosion Layer Formation: Part 1 - Iron Carbonate Layers in Carbon dioxide Corrosion.* Corrosion, 2008. **64**(4): p. 334-346.

79.   Dugstad, A., *Formation of Protective Corrosion Films during CO_2 Corrosion of Carbon Steel.* Advances in Corrosion Control and Materials in Oil and Gas Production, 1999(26): p. 70-76.

80.   J.L.Crolet, S.O., W.Wilhelmsen, *Influence of a Layer of Indissolved Cementite on the Rate of the CO_2 Corrosion of Carbon steel*, in *Corrosion94*. 1994: Houston, Tx.

81.   Seal, S., et al., *The Effect of Flow on the Corrosion Product Layer in Presence of Corrosion Inhibitors*, in *CORROSION 2002*. 2002, NACE International: Denver, Co.

82.   Wang, H., et al., *Why Corrosion Inhibitors Do Not Perform Well in Some Multiphase Conditions: A Mechanistic Study*, in *Corrosion 2002*. 2002, NACE International: Denver, Colorado.

83.   Chen, H.J. and W.P. Jepson, *Inhibition of Slug Front Corrosion in Multiphase Flow Conditions*, in *CORROSION 98*. 1998, NACE International: San Diego Ca.

84.   Al-Hassan, S., et al., *Effect of Microstructure on Corrosion of Steels in Aqueous Solutions Containing Carbon Dioxide.* Corrosion, 1998. **54**(06).

85.   Dugstad, A., H. Hemmer, and M. Seiersten, *Effect of Steel Microstructure on Corrosion Rate and Protective Iron Carbonate Film Formation.* Corrosion, 2001. **57**(04).

86.   Dugstad, A. and P.-E. Dronen, *Efficient Corrosion Control of Gas Condensate Pipelines by pH - Stabilization*, in *Corrosion 99*. 1999, NACE International.

87.   Gulbrandsen, E. and J.H. Morard, *Why Does Glycol Inhibit CO_2 Corrosion?*, in *CORROSION 98*. 1998, NACE International: San Diego Ca.

88.   Garsany, Y., D. Pletcher, and B.M. Hedges, *The Role of Acetate in CO_2 Corrosion of Carbon Steel: Has the Chemistry Been Forgotten?*, in *Corrosion 2002*. 2002, NACE International: Denver, Colorado.

89.   Garsany, Y., et al., *Quantifying the Acetate-Enhanced Corrosion of Carbon Steel in Oilfield Brines, December 2004.* Corrosion, 2004. **60**(12).

90.   Sun, Y., K. George, and S. Nesic, *The Effect of Cl^- and Acetic Acid on Localized CO_2 Corrosion in Wet Gas Flow*, in *Corrosion 2003*. 2003, NACE International: San Diego Ca.

91.   George, K., K.d. Waard, and S. Nesic, *Electrochemical Investigation and Modeling of Carbon Dioxide Corrosion of Carbon Steel in the Presence of Acetic Acid.* 2004, NACE International.

92.   Crolet, J.L., A. Dugstad, and N. Thevenot, *Role of Free Acetic Acid on the CO_2 Corrosion of Steels*, in *CORROSION 99*. 1999, NACE International: San Antonio, Tx.

93.   Gulbrandsen, E. and K. Bilkova, *Solution Chemistry Effects on Corrosion of Carbon Steels in Presence of CO_2 and Acetic Acid*, in *Corrosion 2006*. 2006, NACE International: San Diego, California.

94.   Nafday, O. and S. Nesic, *Iron Carbonate Scale Formation and CO₂ Corrosion in the Presence of Acetic Acid*, in *Corrosion 2005*. 2005, NACE International: Houston, Texas.

95.   Wheeler, P.J., *lntroduction to the Troll Project*, in *OTC 97*. 1997, Offshore Technology Conference: Houston, Texas.

96.   Rebsdat, S. and D. Mayer, *Ethylene Glycol*, in *Ullmann's Encyclopedia of Industrial Chemistry*. 2000, Wiley-VCH Verlag GmbH & Co. KGaA.

97.   Rebsdat, S. and D. Mayer, *ETHYLENE GLYCOL.* Gerhartz, W., Et Al. (Ed.). Ullmann's Encyclopedia of Industrial Chemistry, Fifth Completely Revised Edition, Vol. A 10. Ethanolamines to Fibers, 4. Synthetic Organic. Xv+655p. Vch Publishers, Inc.: New York, New York, USA; Cambridge, England, Uk; Vch Verlagsgesellschaft Mbh: Weinheim, West Germany. Illus. Maps, 1987: p. 101-116.

98.   Boxall, J., et al., *Predicting When and Where Hydrate Plugs Form in Oil-Dominated Flowlines.* SPE Projects, Facilities & Construction, 2009. **4**(3): p. pp. 80-86.

99.   Elhady, A.A.A., *Operating Experiences of DEG and MEG for Hydrate and Dew Point Control in Gas Production Offshore Mediterranean*, in *International Petroleum Technology Conference*. 2005, International Petroleum Technology Conference: Doha, Qatar.

100.   Hopgood, D., *Why Improve Hydrate Predictions for Deepwater Black Oil?*, in *OTC 2001*. 2001, Offshore Technology Conference: Houston, Texas.

101.   MacDonald, A., et al., *Field Application of Combined Kinetic Hydrate and Corrosion Inhibitors in the Southern North Sea: Case Histories*, in *SPE Gas Technology Symposium*. 2006, Society of Petroleum Engineers: Calgary, Alberta, Canada.

102.   Guan, H., *The Inhibition of Gas Hydrates and Synergy of the Inhibiting Molecules*, in *International Oil and Gas Conference and Exhibition in China*. 2010, Society of Petroleum Engineers: Beijing, China.

103.   E.D., S.a.C.A., Koh, *Clathrate Hydrates of Natural Gases*. 2007, USA: CRC Press.

104.   E.D. Sloan, *Fundamental Principles and Applications of Natural Gas Hydrates.* Nature, 2003. **426**(6964): p. 353-363.

105.   Lorenzo, M.D. *The Hydra Flow Loop; A Tool For Testing The Hydrates Behaviour in Gas Pipelines*. in *R & D Seminar* 2009. Australian resources research center building Perth, Australia: National research flagship/Commonwealth scientific and industrial research organization (CSIRO).

106.   Olsen, S., A. Dugstad, and O. Lunde, *pH-Stabilization in the Troll Gas-Condensate Pipelines*, in *Corrosion 99*. 1999, NACE International: San Atonia, Texas.

107.   PAEZ, J.E. and R. BLOK, *Problems in Hydrates: Mechanisms and Elimination Methods*, in *SPE Production and Operations Symposium*. 2001,

Copyright 2001, Society of Petroleum Engineers Inc.: Oklahoma City, Oklahoma.

108. Ramachandran, S., et al., *Inhibition of Acid Gas Corrosion in Pipelines using Glycol for Hydrate Inhibition*, in *CORROSION 2006*. 2006, NACE International: San Diego Ca.

109. *Ethylene Glycol*.

June 2011; Available from: http://en.wikipedia.org/wiki/Ethylene_glycol.

110. J.Kvarekval, A. Dugstad, and M.Seiersten, *Localized Corrosion on Carbon Steel in Sour Glycolic Solutions*, in *Corrosion 2010*. 2010, NACE International: San Antonio, TX.

111. Kvarekval, J. and A. Dugstad, *Pitting Corrosion Mechanisms on Carbon Steel in Sour Glycol Water Mixtures*, in *CORROSION 2004*. 2004, NACE International: New Orleans, La.

112. Gonzalez, J.J., G. Pellegrino, and M.E. Alfonso, *Corrosion of Carbon Steels in Monoethylene Glycol*, in *Corrosion 2000*. 2000, NACE International: Orlando, Fl.

113. Skar, J.I. and A.M.K. Halvorsen, *Corrosion Control in the Vega Gas-Condensate Pipeline*, in *Corrosion 2010*. 2010, NACE International: San Antonio, TX.

114. Kvarekval, J. and A. Dugstad, *Corrosion Mitigation with pH Stabilization in Slightly Sour Gas/Condensate Pipelines*, in *CORROSION 2006*. 2006, NACE International: San Diego Ca.

115. Dugstad, A. and M. Seiersten, *pH-stabilisation, a Reliable Method for Corrosion Control of Wet Gas Pipelines*, in *SPE International Symposium on Oilfield Corrosion*. 2004, Society of Petroleum Engineers: Aberdeen, United Kingdom.

116. Geir Watterud, M.S., Jens-Petter Andreassen. *Iron Carbonate in MEG/Water mixtures*. in *International Oil Field Chemistry Symposium*. 2009. Geilo, Norway.

117. Tobiassen, P. and A.E. Pedersen, *Experience Feedback on the Use of a Carbon Steel Subsea Pipeline For A High Pressure, Sweet Service Gas Field*, in *Corrosion 2004*. 2004, NACE International: New Orleans, Louisiana

118. Seiersten, M., et al., *Development of a Simulator for Ethylene Glycol Loops Based on Solution Thermodynamics and Particle Formation Kinetics*, in *Corrosion 2010*. 2010, NACE International: San Antonio, TX.

119. Sandengen, K., B. Kaasa, and T. Østvold, *pH Measurements in Monoethylene Glycol (MEG) + Water Solutions.* Industrial & Engineering Chemistry Research, 2007. **46**(14): p. 4734-4739.

120. T.berntsen, M.S.a.T.H., *CO_2 Corrosion of Carbon Steel at Lower Temperatures* in *the european corrosion congress (EUROCORR)*. 2008: Edinburg, Uk,. p. 10.

121. Olsen, S., *Corrosion Control by Inhibition, Environmental Aspects, and pH Control: Part II: Corrosion Control by pH Stabilization*, in *Corrosion 2006*. 2006, NACE International: San Diego Ca.

122. Halvorsen, A.M.K., et al., *The Reletionship Between Internal Corrosion Control Method, scale Contol and MEG Handling of a Multiphase Carbon Steel Pipeline Carrying Wet Gas with CO_2 and Acetic Acid*, in *Corrosion 2007*. 2007, NACE International: Nashville, Tennessee.

123. Hagerup, O. and S. Olsen, *Corrosion Control by pH Stabilizer, Materials and Corrosion Monitoring in 160 km Multiphase Offshore Pipeline*, in *Corrosion 2003*. 2003, NACE International: San Diego Ca.

124. Kvarekval, J. and A. Dugstad, *Pitting Corrosion in CO_2/H_2S Containing Glycol Solutions under Flowing Conditions*, in *Corrosion 2005*. 2005, NACE International: Houston, Tx.

125. N.Hackerman, E.S.S.a., *NACE Basic Corrosion Course*. 1970, NACE: Houston, Texas.

126. Vuorinen, E., E. Kálmán, and W. Focke, *Introduction to Vapour Phase Corrosion Inhibitors in Metal Packaging.* Surface Engineering, 2004. **20**(4): p. 281-284.

127. B.Sanyal, *Organic Compounds as Corrosion Inhibitors in Different Environments -A Review.* Progress in Organic Compounds as Corrosion 1981. **9**(2): p. 165-236.

128. E.Hamner, N., ed. *Scope and Importance of Inhibitor Technology*. Corrosion Inhibitors, ed. N. C.C. 1973, NACE: Houston, Texas. 1-6.

129. Rostami, A., *Review and Evaluation of Corrosion Inhibitors Used in Well Stimulation*, in *SPE International Symposium on Oilfield Chemistry*. 2009, Society of Petroleum Engineers: The Woodlands. Texas.

130. Crouse, M., et al., *Evaluation of Potassium Permanganate (KMnO4) as a Green Corrosion Inhibitor/Sealant for Anodized Al 2024 and Al 6061 at Different pH Values*, in *Corrosion 2002*. 2002, NACE International: Denver Co.

131. Okamoto, G., et al., *Effect of Organic Inhibitors on the Polarization Characteristics of Mild Steel in Acid Solution.* Corrosion Science, 1962. **2**(1): p. 21-27.

132. jr, R.l.O., *Theoretical Aspects of Corrosion Inhibitors and Inhibition*, in *Corrosion Inhibitors*, N. C.C., Editor. 1981, NACE: Houston Texas. p. 7-27.

133. Meakins, R.J., *Alkyl Quaternary Ammonium Compounds as Inhibitors of the Acid Corrosion of Steel.* Journal of Applied Chemistry, 1963. **13**(8): p. 339-345.

134. Campbell, S. and V. Jovancicevic, *Corrosion Inhibitor Film Formation Studied by ATR-FTIR*, in *Corrosion 99*. 1999, NACE International: San Antonio, Tx.

135.   Hellberg, P.-E., *Environmentally Acceptable Polymeric Corrosion Inhibitors*, in *SPE International Symposium on Oilfield Chemistry*. 2011: The Woodlands, Texas, USA.

136.   Mackenzie, C.D., et al., *Development of a New Corrosion Management Tool - Inhibitor Micelle Presence as an Indicator of Optimum Dose*, in *SPE International Conference on Oilfield Corrosion*, SPE, Editor. 2010: Aberdeen, UK.

137.   Durnie W., D.M.R., Jefferson A., and Kinsella B., *Development of a Structure-Activity Relationship for Oil Field Corrosion Inhibitor.* The Electrochemical Society, 1999. **146**(5): p. 1751-1756.

138.   De Marco, R., et al., *Persistence of Carbon Dioxide Corrosion Inhibitors.* Corrosion, 2002. **58**(4): p. 354-363.

139.   Vijayalakshmi, P.R. and R. Rajalakshmi, *Inhibition of Mild Steel Corrosion Using Aqueous Extract of Cocos nucifera L. Peduncle in Acidic Solutions and Their Adsorption Characteristics*, in *Corrosion 2013*. 2013: Orlando, Florida.

140.   Leelavathi, S. and R. Rajalakshmi, *Mundulea Sericea Leaves as a Corrosion Inhibitor for Mild Steel in Acidic Solution*, in *Corrosion 2013*. 2013, NACE International: Orlando, Florida.

141.   Nalini, D. and R. Rajalakshmi, *Inhibition of Mild Steel Corrosion in the Presence of p-Nitrophenyl-2-Imidazoline*, in *Corrosion 2013*. 2013, NACE International: Orlando, Florida.

142.   Durnie, W.H., et al., *A Study of the Adsorption Properties of Commercial Carbon Dioxide Corrosion Inhibitor Formulations.* Journal of Applied Electrochemistry, 2001. **31**(11): p. 1221-1226.

143.   Gibson, D.H., *The Organometallic Chemistry of Carbon Dioxide.* Chemical Reviews, 1996. **96**(6): p. 2063-2096.

144.   N.Hackermann, R.M.H., and R.R.Annand, Corrosion, 1962. **18**.

145.   Wang D., L.S., Ying Y.,Wang M, Xiao He and Chen Z., *Theoretical and Experimental Studies of Structure and Inhibition Efficiency of Iimidazoline Derivatives* Corrosion Science, 1999. **41**: p. 1911-1919.

146.   N.Hackerman, K.A.a., *Effect of Molecular Size on Inhibition of Dimethylpolymethylene Ammonium Chloride.* Electrochemical Society, 1969. **116**(5).

147.   Frenier, W.W. and D.G. Hill, *Green Inhibitors - Development and Applications for Aqueous Systems*, in *Corrosion 2004*. 2004, NACE International: New Orleans, La.

148.   Taj, S., R.W. Revie, and S. Papavinasam, *Development of Green Inhibitors for Oil and Gas Applications*, in *Corrosion 2006*. 2006, NACE International: San Diego Ca.

149.   Taj, S., et al., *Some Natural Products As Green Corrosion Inhibitors*, in *Corrosion 2007*. 2007, NACE International: Nashville, Tennessee.

150. E.Schaschl, *Method for Evaluation and Testing of Corrosion Inhibitors*. Corrosion Inhibitors, ed. C.C. Nathan. 1973, Houston, Texas: NACE. 28-41.

151. Bregman, J.I., *Corrosion Inhibitors*. 1963, New York: Macmillan company.

152. Bowman, J.A.K.a.C.W., ed. *The Chemistry of Corrosion Inhibitors used in Oil Production,*. 1984, UK Corrosion: London.

153. Free, M.L., W. Wang, and D.Y. Ryu, *Prediction of Corrosion Inhibition Using Surfactants.* Corrosion, 2004. **60**(09).

154. Mansfeld, F., S.L. Jeanjaquet, and M.W. Kendig, *An Electrochemical Impedance Spectroscopy Study of Reactions at the Metal/Coating Interface.* Corrosion Science, 1986. **26**(9): p. 735-742.

155. Akbar, A., *Understanding the Interactions Between Corrosion Scales and Inhibitor Films in Flow conditions*, in *School of Mechanical Engineering*. 2013, University of Leeds: University of Leeds.

156. Wong, J.E. and N. Park, *Effect of Corrosion Inhibitor Active Components on the Growth of Iron Carbonate Scale under CO_2 conditions*, in *Corrosion 2008*. 2008, NACE International: New Orleans, Louisiana.

157. Wong, J.E. and N. Park, *Further Investigation On The Effect Of Corrosion Inhibitor Actives On The Formation Of Iron Carbonate On Carbon Steel*, in *Corrosion 2009*. 2009, NACE International: Atlanta, Georgia.

158. Tsui, K. and J.E. Wong, *Effect Of Corrosion Inhibitor Active Components On Corrosion Inhibition In A Sweet Environment*, in *Corrosion 2010*. 2010, NACE International: San Atonia, Texas.

159. Bikkina, C., et al., *Development of MEG Regeneration Unit Compatible Corrosion Inhibitor for Wet Gas Systems*, in *SPE Asia Pacific Oil and Gas Conference and Exhibition*. 2012, Society of Petroleum Engineers: Perth, Australia.

160. Olsen, S., et al., *CO2 Corrosion Prediction Model - Basic Principles*, in *CORROSION 2005*. 2005, NACE International: Houston, Tx.

161. Ashton, J.J.B.C. *The Effect of Temperature on Conductivity Measurement*. 2013; Available from: http://www.camlabworld.com/originalimages/sitefiles/Tech_papers/TempCondMeas.pdf.

162. Bevilacqua, D.M.G.a.A.C. *Cation Conductivity Temperature Compensation* in *International Water Conference,*. 1997. Pittsburgh, PA,.

163. Chen, T.-Y., *A Transient Technique to Determine Solution Resistance for Corrosion Rate Measurements in Low-Conductivity Solutions*, in *Corrosion96*. 1996, NACE International: Denver , Co.

164. Waxman, M.H. and E.C. Thomas, *Electrical Conductivities in Shaly Sands-I. The Relation Between Hydrocarbon Saturation and Resistivity Index; II. The Temperature Coefficient Of Electrical Conductivity.* Journal of Petroleum Technology, 1974. **26**(2): p. 213-225.

165.   Tanupabrungsun, T., B. Brown, and S. Nesic, *Effect of pH on CO_2 Corrosion of Mild Steel at Elevated Temperatures*, in *Corrosion 2013*. 2013, NACE International: Orlando, Florida.

166.   Mishra, B., et al., *Development of a Predictive Model for Activation-Controlled Corrosion of Steel in Solutions Containing Carbon Dioxide.* Corrosion, 1997. **53**(11).

167.   Al-Fozan, A.U.M.a.S.A. *Pitting Behaviour of Type 316L S.S in Arabian Gulf Seawater*. 1992; Available from: http://www.swcc.gov.sa/files%5Cassets%5CResearch%5CTechnical%20Papers%5CCorrosion/PITTING%20BEHAVIOUR%20OF%20TYPE%20316L%20S.S%20INARABIAN%20GULF%20SEAWATER.

168.   Azghandi, M., et al., *Corrosion Inhibitive Evaluation of an Environmentally Friendly Water-Base Acrylic Terpolymer on Mild Steel in Hydrochloric Acid Media.* Metallurgical and Materials Transactions A, 2013. **44**(12): p. 5493-5504.

169.   R.H.Petrucci, W.S.H., G.E.Herring and J.Madura, *General Chemistry Principles & Modern Applications*. 2006, New Jersey Prentice Hall.

170.   L.Pacheco, J., F.C. Ibrahim, and R. J.Franco, *Testing Requirements of Corrosion Inhibitor Qualification for Pipeline Applications*, in *Corrosion 2010*. NACE International: San Antonio, TX.

171.   Mok, W.Y., et al., *Control of Localized Corrosion using Green Corrosion Inhibitors*, in *Corrosion 2005*. 2005, NACE International: Houston Texas.

172.   Frenier, W.W., F.B. Growcock, and V.R. Lopp, *Mechanisms of Corrosion Inhibitors Used in Acidizing Wells.* SPE Production Engineering, 1988. **3**(4): p. 584-590.

173.   Hu, X., I.M. Ismail, and A. Neville, *Investigation of Pitting Corrosion and Inhibition in Sweet Conditions*, in *Corrosion 2013*. 2013, NACE International: Orlando, Florida.

174.   Jenkins, A., *Performance of High-Temperature, Biodegradable Corrosion Inhibitors*, in *Corrosion 2011*. 2011, NACE International: Houston, Texas.

175.   Magana-Zavala, C.R., et al., *Electrochemical Impedance Spectroscopy (EIS) Modelling of Different Behaviours of Ni and Ni Oxide Thin Films for Corrosion Prevention in Sour Media.* Anti-Corrosion Methods and Materials, 2010. **57**(3): p. 118-125.

176.   Castaneda, H., E. Sosa, and M.A. Espinosa-Medina, *Film Properties and Stability Influence on Impedance Distribution During the Dissolution Process of Low-carbon Steel Exposed to Modified Alkaline Sour Environment.* Corrosion Science, 2009. **51**(4): p. 799-806.

177.   Lopez, H.C., et al., *Film Stability for API 5L X-52 Line Pipe Steel in CO_2 (aq) and Cl (aq) Solutions in Presence of Amine Based Inhibitor under Hydrodynamic Conditions*, in *Corrosion 2004*. 2004, NACE International: New Orleans, Louisiana.

178. Duval, S., R. Sauvant-Moynot, and F. Ropital, *EIS: A Powerful Tool for In Situ Monitoring Coating Performance*, in *Corrosion 2003*. 2003, NACE International: San Diego, Ca.

179. Wang, H., et al., *Characterization of Inhibitor and Corrosion Product Film Using Electrochemical Impedance Spectroscopy (EIS)*, in *Corrosion 2001*. 2001, NACE International: Houston, Texas.

180. Lillard, R.S., et al., *Using Local Electrochemical Impedance Spectroscopy to Examine Coating Failure.* Corrosion, 1995. **51**(04).

181. Ruedisueli, R.L., A. Sheetz, and A. Field, *Paint Coating Electrical Resistance and Performance in Service Environments*, in *Corrosion 2006*. 2006, NACE International: San Diego, Ca.

182. Torres-Islas, A., et al., *Corrosion Inhibition Efficiency Study in a Microalloyed Steel for Sour Service at 50 degrees C.* Journal of Applied Electrochemistry, 2010. **40**(8): p. 1483-1491.

183. Mansfeld, F., et al., *Analysis of Electrochemical Impedance and Noise Data for Polymer Coated Metals.* Corrosion Science, 1997. **39**(2): p. 255-279.

184. Esih I., S.T.a.P.Z. *Inhibition of Mild Steel Corrosion in CO_2-Saturated Chloride Solutions by Acylated Polyamine Salts.* in *Proceedings of the 8th European Symposium on Corrosion Inhibitors (8 SEIC)*. 1995. Ann, Univ. Ferrara, N.S.

185. Halvorsen, E.N., et al., *Qualification of Scale Inhibitors for Subsea Tiebacks With MEG Injection*, in *SPE International Symposium on Oilfield Chemistry*. 2009, Society of Petroleum Engineers: The Woodlands. Texas.

186. Nesic, S. and K.-L.J. Lee, *A Mechanistic Model for Carbon Dioxide Corrosion of Mild Steel in the Presence of Protective Iron Carbonate FilmsPart 3: Film Growth Model.* Corrosion, 2003. **59**(07).

187. Nesic, S., et al., *A Mechanistic Model for Carbon Dioxide Corrosion of Mild Steel in the Presence of Protective Iron Carbonate Films - Part 2: A Numerical Experiment.* Corrosion, 2003. **59**(6): p. 489-497.

188. Llongueras, J.G., et al., *Mechanism of $FeCO_3$ Formation on API X70 Pipeline Steel in Brine Solutions Containing CO2*, in *Corrosion 2005*. 2005, NACE International: Houston, Texas.

189. Nordsveen, M., et al., *A mechanistic model for carbon dioxide corrosion of mild steel in the presence of protective iron carbonate films - Part 1: Theory and verification.* Corrosion, 2003. **59**(5): p. 443-456.

190. Han, J., et al., *Electrochemical Investigation of Localized CO2 Corrosion on Mild Steel*, in *Corrosion 2007*. 2007, NACE International: Nashville, Tennessee.

191. Hitoshi Shindo, a.M.K., *Stabilities of Crystal Faces of Aragonite (CaCO3) Compared by Atomic Force Microscopic Observation of Facet Formation Processes in Aqueous Acetic acid.* Physical Chemistry Chemical Physics, 2005. **7**(4): p. 691-6.

192.   Ahmad, Z., *Principles of Corrosion Engineering and Corrosion Control*. Materials & Mechanical. 2006: Butterworth-Heinemann. 1-672.

193.   Hong, T., et al., *EIS Study of Corrosion Product Film in Pipelines*, in *Corrosion 2000*. NACE International: Orlando, Florida.

194.   Gulbrandsen, E. and J.H. Morard, *Study of the Possible Mechanisms of Steel Passivation in CO2 Corrosion*, in *Corrosion 99*. 1999, NACE International: San Antonio, Tx.

195.   Riemenschneider, W. and H.M. Bolt, *Esters, Organic*, in *Ullmann's Encyclopedia of Industrial Chemistry*. 2000, Wiley-VCH Verlag GmbH & Co. KGaA.

196.   Ismail, I.M., *Inhibition of Pitting on Carbon Steel*, in *School of Mechanical Engineering*. 2011, University of Leeds: University of Leeds.

197.   Alink, B.A., et al., *Mechanism of CO2 Corrosion Inhibition by Phosphate Esters*, in *Corrosion99*. 1999, NACE International: San Atonia, Texas.

198.   Sun, W., K. Chokshi, and S. Nesic, *Iron Carbonate Scale Growth and the Effect of Inhibition in CO2 Corrosion of Mild Steel*. 2005, NACE International.

199.   Nyborg, R., et al., *Effect of Steel Microstructure and Composition on Inhibition of CO2 Corrosion*, in *Corrosion 2000*. 2000, NACE International: Orlando, Fl.

200.   Kvarekval, J., S. Skjerve, and S. Olsen, *The Effect of O2 on CO2 Corrosion in pH Stabilized Gas/Condensate Pipelines*, in *Corrosion 2005*. 2005, NACE International: Houston, Tx.

201.   Lu, H., A.T. Kan, and M.B. Tomson, *Effects of Monoethylene Glycol on Carbonate Equilibrium and Calcite Solubility in Gas/Monoethylene Glycol/Water/Salt Mixed Systems*, in *SPE International Symposium on Oilfield Chemistry*. 2009, Society of Petroleum Engineers: The Woodlands. Texas.

202.   Vuppu, A.K. and W.P. Jepscm, *Study Of Sweet Corrosion In Horizontal Multiphase, Carbon Steel Pipelines*, in *OTC* 1994, Offshore Technology Conference: Houston, Texas.

203.   Nordsveen, M., S.N.R. Nyborg, and A. Stangeland, *A Mechanistic Model for Carbon Dioxide Corrosion of Mild Steel in the Presence of Protective Iron Carbonate FilmsPart 1: Theory and Verification.* Corrosion, 2003. **59**(05).

204.   Han, J., B.N. Brown, and S. Nesic, *Investigation of the Galvanic Mechanism for Localized Carbon Dioxide Corrosion Propagation Using the Artificial Pit Technique.* Corrosion, 2010. **66**(9).

205.   Berntsen, T., M. Seiersten, and T. Hemmingsen, *Effect of $FeCO_3$ Supersaturation And Carbide Exposure On the CO_2 Corrosion Rate of Carbon Steel*, in *Corrosion 2011*. 2011, NACE International: Houston, Texas.

APPENDIX A

The use of Microsoft Excel in compensation for solution resistance of test in the presence of MEG and derivation of compensated corrosion rate.

Derivation of uncompensated corrosion rate for 80% MEG at 20°C

Time (hrs)	Potential (mV)	LPR (Ohm.cm²)	Tafel slope (B)	uncompensated corrosion rate (mm/y)
0.33	-587.38	2987.4	26	0.101
0.67	-595.04	3226	26	0.093
1	-595.58	3269.7	26	0.092
1.33	-594.81	3110	26	0.097
1.67	-592.67	3307	26	0.091
2	-592.31	3401	26	0.089
2.33	-590.31	3358	26	0.090
2.67	-591.13	3400	26	0.089
3	-590.3	3478	26	0.087
3.33	-588.11	3502	26	0.086
3.67	-586.56	3508	26	0.086
4	-585.48	3523.5	26	0.086

Derivation of compensated corrosion rate for 80% MEG at 20°C

Time (hrs)	Potential (mV)	LPR (Ohm.cm²)	Compensated LPR (Ohm.cm²)	Tafel slope (B)	Corrosion rate (mm/y)
0.33	-587.38	2987.4	1787.4	26	0.169
0.67	-595.04	3226	2026	26	0.149
1	-595.58	3269.7	2069.7	26	0.146
1.33	-594.81	3110	1910	26	0.158
1.67	-592.67	3307	2107	26	0.143
2	-592.31	3401	2201	26	0.137
2.33	-590.31	3358	2158	26	0.140
2.67	-591.13	3400	2200	26	0.137
3	-590.3	3478	2278	26	0.132
3.33	-588.11	3502	2302	26	0.131
3.67	-586.56	3508	2308	26	0.131
4	-585.48	3523.5	2323.5	26	0.130

APPENDIX B

Future Publications relating to this study

- Determination of the adsorption property and enthalpy of adsorption of MonoEthylene Glycol (MEG) in the corrosion of carbon steel.
- Effect of temperature on the corrosion of newly synthesis green inhibitor using Linear Polarization Resistance method (LPR), Electrochemical Impedance Spectroscopy (EIS) and surface analysis technique
- Comparison of commercially available green inhibitor and non-green inhibitor using Linear Polarization Resistance method (LPR), Electrochemical Impedance Spectroscopy (EIS) and surface analysis technique
- The corrosion of carbon steel in the presence of MonoEthylene Glycol (MEG) under protective iron carbonate.
- The corrosion of carbon steel in the presence of MonoEthylene Glycol (MEG) under protective iron carbonate scale
- Dissolution of protective iron carbonate scale under low pH and the influence of MonoEthylene Glycol (MEG) and organic corrosion inhibitor
- Corrosion of carbon steel in the presence of MonoEthylene Glycol (MEG), commercial inhibitor and iron carbonate scale.